A UNITED STATES DEPARTMENT OF COMMERCE PUBLICATION

NBS MONOGRAPH 138

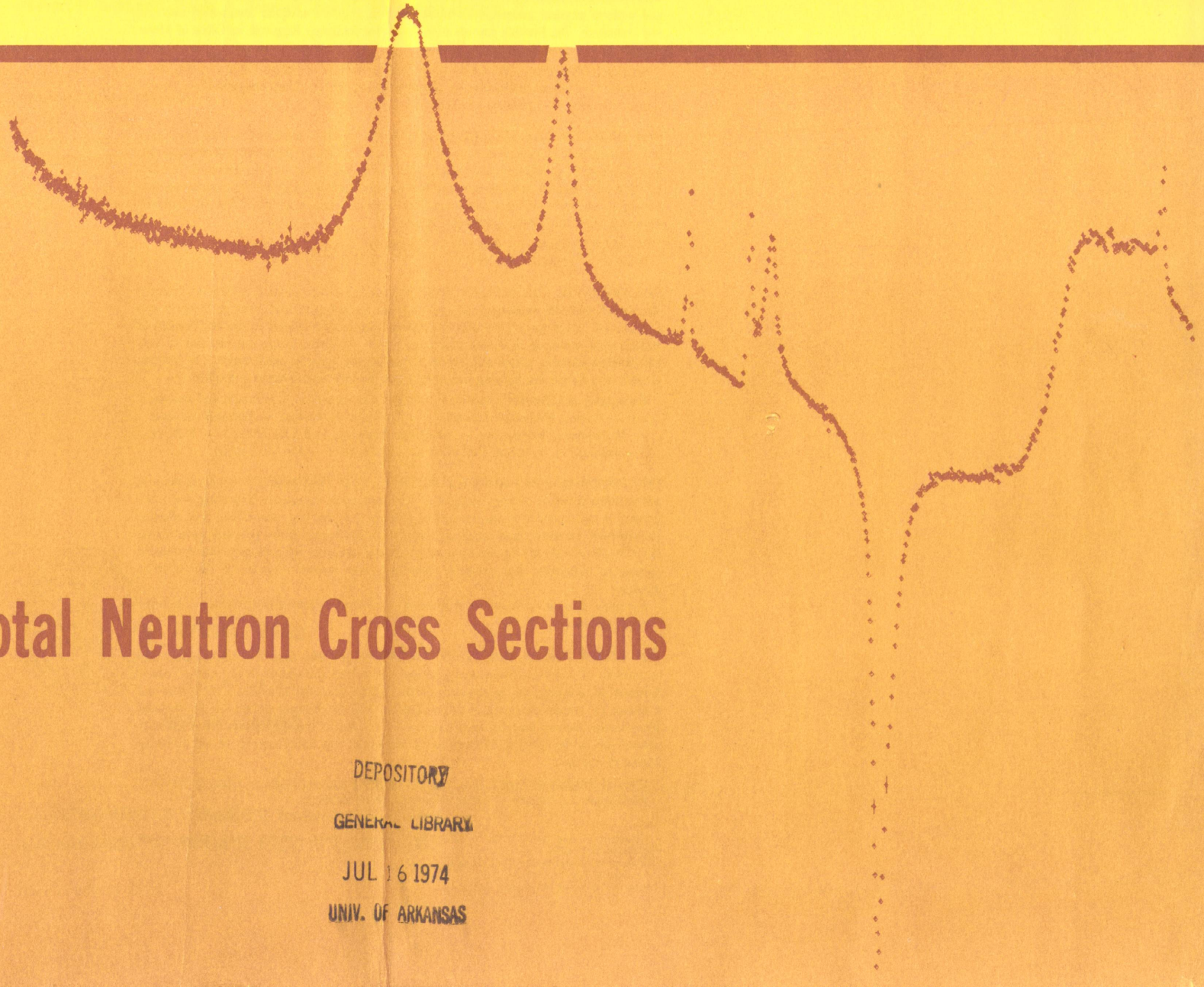

MeV Total Neutron Cross Sections

U.S. DEPARTMENT OF COMMERCE
National Bureau of Standards

NATIONAL BUREAU OF STANDARDS

The National Bureau of Standards [1] was established by an act of Congress March 3, 1901. The Bureau's overall goal is to strengthen and advance the Nation's science and technology and facilitate their effective application for public benefit. To this end, the Bureau conducts research and provides: (1) a basis for the Nation's physical measurement system, (2) scientific and technological services for industry and government, (3) a technical basis for equity in trade, and (4) technical services to promote public safety. The Bureau consists of the Institute for Basic Standards, the Institute for Materials Research, the Institute for Applied Technology, the Institute for Computer Sciences and Technology, and the Office for Information Programs.

THE INSTITUTE FOR BASIC STANDARDS provides the central basis within the United States of a complete and consistent system of physical measurement; coordinates that system with measurement systems of other nations; and furnishes essential services leading to accurate and uniform physical measurements throughout the Nation's scientific community, industry, and commerce. The Institute consists of a Center for Radiation Research, an Office of Measurement Services and the following divisions:

Applied Mathematics — Electricity — Mechanics — Heat — Optical Physics — Nuclear Sciences [2] — Applied Radiation [2] — Quantum Electronics [3] — Electromagnetics [3] — Time and Frequency [3] — Laboratory Astrophysics [3] — Cryogenics [3].

THE INSTITUTE FOR MATERIALS RESEARCH conducts materials research leading to improved methods of measurement, standards, and data on the properties of well-characterized materials needed by industry, commerce, educational institutions, and Government; provides advisory and research services to other Government agencies; and develops, produces, and distributes standard reference materials. The Institute consists of the Office of Standard Reference Materials and the following divisions:

Analytical Chemistry — Polymers — Metallurgy — Inorganic Materials — Reactor Radiation — Physical Chemistry.

THE INSTITUTE FOR APPLIED TECHNOLOGY provides technical services to promote the use of available technology and to facilitate technological innovation in industry and Government; cooperates with public and private organizations leading to the development of technological standards (including mandatory safety standards), codes and methods of test; and provides technical advice and services to Government agencies upon request. The Institute consists of a Center for Building Technology and the following divisions and offices:

Engineering and Product Standards — Weights and Measures — Invention and Innovation — Product Evaluation Technology — Electronic Technology — Technical Analysis — Measurement Engineering — Structures, Materials, and Life Safety [4] — Building Environment [4] — Technical Evaluation and Application [4] — Fire Technology.

THE INSTITUTE FOR COMPUTER SCIENCES AND TECHNOLOGY conducts research and provides technical services designed to aid Government agencies in improving cost effectiveness in the conduct of their programs through the selection, acquisition, and effective utilization of automatic data processing equipment; and serves as the principal focus within the executive branch for the development of Federal standards for automatic data processing equipment, techniques, and computer languages. The Institute consists of the following divisions:

Computer Services — Systems and Software — Computer Systems Engineering — Information Technology.

THE OFFICE FOR INFORMATION PROGRAMS promotes optimum dissemination and accessibility of scientific information generated within NBS and other agencies of the Federal Government; promotes the development of the National Standard Reference Data System and a system of information analysis centers dealing with the broader aspects of the National Measurement System; provides appropriate services to ensure that the NBS staff has optimum accessibility to the scientific information of the world. The Office consists of the following organizational units:

Office of Standard Reference Data — Office of Information Activities — Office of Technical Publications — Library — Office of International Relations.

---

[1] Headquarters and Laboratories at Gaithersburg, Maryland, unless otherwise noted; mailing address Washington, D.C. 20234.
[2] Part of the Center for Radiation Research.
[3] Located at Boulder, Colorado 80302.
[4] Part of the Center for Building Technology.

MeV Total Neutron Cross Sections

Robert B. Schwartz, Roald A. Schrack, and H. Thompson Heaton, II

Nuclear Sciences Division
Institute for Basic Standards
National Bureau of Standards
Washington, D.C. 20234

U.S. DEPARTMENT OF COMMERCE, Frederick B. Dent, *Secretary*
NATIONAL BUREAU OF STANDARDS, Richard W. Roberts, *Director*

Issued January 1974

Library of Congress Catalog Number: 73-600276

National Bureau of Standards Monograph 138

Nat. Bur. Stand. (U.S.), Monogr. 138, 160 pages (Jan. 1974)
CODEN: NBSMA6

U.S. GOVERNMENT PRINTING OFFICE
WASHINGTON: 1974

For sale by the Superintendent of Documents, U.S. Government Printing Office, Washington, D.C. 20402
(Order by SD Catalog No. C13.44:138). Price $3.60
Stock Number 0303-01189

Contents

CROSS SECTION CURVES

APPENDIX – EXPERIMENTAL TECHNIQUES

MeV Total Neutron Cross Sections*

Robert B. Schwartz, Roald A. Schrack, and H. Thompson Heaton, II

This report is a compilation of the MeV neutron total cross section data measured at the National Bureau of Standards over the past several years. The measurements generally span the energy interval from 0.5 to 15 or 20 MeV; data are presented in graphical form for twelve normally occurring elements, plus the separated isotopes ^{235}U, ^{238}U, and ^{239}Pu. An appendix is included which gives complete details of the experimental technique.

Key words: MeV neutrons; neutron time-of-flight; neutron total cross sections.

1. Introduction

This report is a compilation of the MeV Total Neutron Cross Section data measured at the U.S. National Bureau of Standards. The neutron time-of-flight method was used for the measurements, with the NBS electron linear accelerator as the pulsed neutron source. The measurements were made over the energy range 0.5 to 20 MeV (in some cases, only to 15 MeV). Except for the uranium and plutonium isotopes, the measurements were made on the naturally occurring isotopic mixtures of the elements in question. In each case, the data are presented in the form of graphs, both linear and logarithmic. Descriptive notes are also included for each element, giving details concerning the samples.

Most of these data have not as yet been formally published. In most cases, however, the data have been presented orally at various meetings of the American Physical Society. A "Literature Reference" is given which refers to the abstracts for these talks.

Details of the experimental technique are given in the appendix.

1.1. Quality of Data

A. Energy Resolution

At low energies the resolution is largely determined by the neutron detector thickness (12.7 cm); at high energies the electronic response function plays the dominant role. For our 40 m flight path, the resolution varies from 0.2 ns/m at 500 keV to 0.08 ns/m at 15 MeV. The resolution as a function of energy is shown in figure 5 in the appendix.

B. Energy Scale Uncertainty

The energy scale uncertainty is 0.04 ns/m. There is excellent agreement between our energy assignments and, for example, the precision neutron energy determinations of Davis and Noda (Nucl. Phys. **A134**, 361 (1969)).

C. Absolute Accuracy

The absolute accuracy of the data is estimated to be within ± 1 percent. This estimate is based largely on the excellent ($< 1\%$) internal consistency of data taken with different sample thicknesses, and under different experimental conditions, as well as the excellent ($< 1\%$) agreement between our hydrogen data (Schwartz et al., Phys. Letters **30B**, 36 (1969)) and previously measured values, as represented by the shape-independent effective range theory. Detailed comparisons between our data and those from other laboratories will be given in later publications; we simply state here that such comparisons have generally shown good agreement consistent with our estimated 1 percent accuracy.

D. Statistical Precision

The statistical errors are generally 1 percent to 2 percent per point, but somewhat poorer at the extreme high and low energy regions of our data. In any case, the statistical errors are indicated by the usual vertical lines at every tenth point on our curves, except in cases where the error bars are smaller than the points.

1.2. Experimental Technique

A brief account of our experimental setup has been given previously (R. B. Schwartz, H. T. Heaton II, and R. A. Schrack, Proc. Symposium Neutron Standards and Flux Normalization, AEC Conf-701002, Argonne, Illinois, p. 377 (October 21, 1970)). This description is brought up to date, and further details given, in the appendix.

*This work was supported in part by the U.S. Defense Nuclear Agency, Washington, D.C. 20305.

HYDROGEN

Sample material: polyethylene $(CH_2)x$

open: high-purity carbon

Sample diameter: 12.7 cm

Sample thickness: 18.3 cm
$n = 1.438$ atoms/barn of hydrogen

Analysis: polyethylene: stochastic ratio of hydrogen to carbon within 0.04 percent of theoretical value

carbon: Volatile and nonvolatile contamination less than 0.01 percent

Literature Reference: R. B. Schwartz, R. A. Schrack, and H. T. Heaton II, Physics Letters **30B**, 36 (1969); also, Proc. Symp. Neutron Standards and Flux Normalization, AEC CONF-701002, Argonne, Illinois, p. 57 (Oct. 21, 1970).

Comments: Equality of carbon atoms/barn in the carbon and polyethylene samples can be seen from the absence of structure in the observed hydrogen cross section. The statistical precision is degraded where there are large peaks in the carbon cross section (e.g., 2.1 MeV), but there are no net fluctuations.

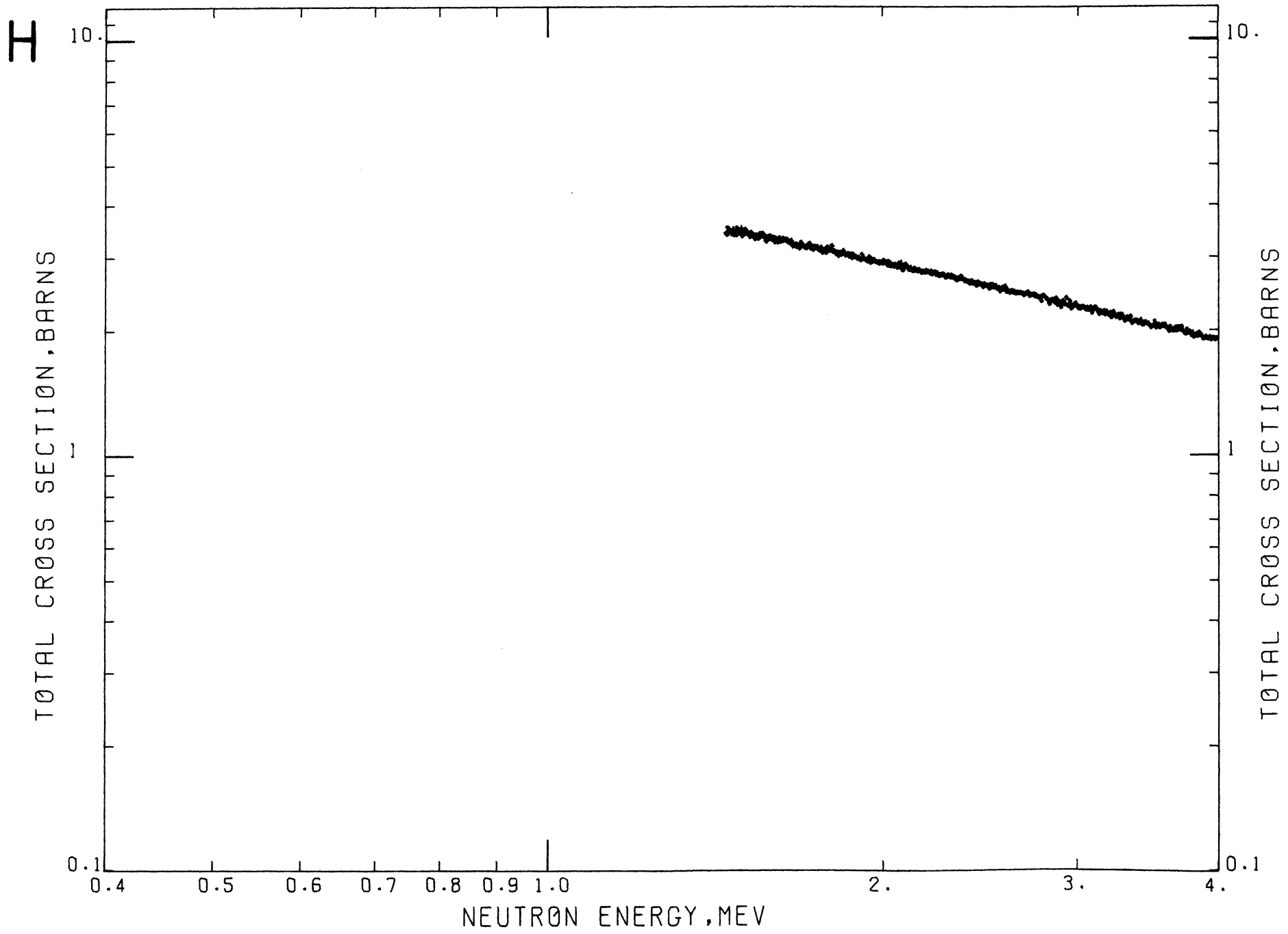
H
10.
1
0.1
TOTAL CROSS SECTION, BARNS
0.4
0.5
0.6
0.7
0.8
0.9
1.0
2.
3.
4.
NEUTRON ENERGY, MEV

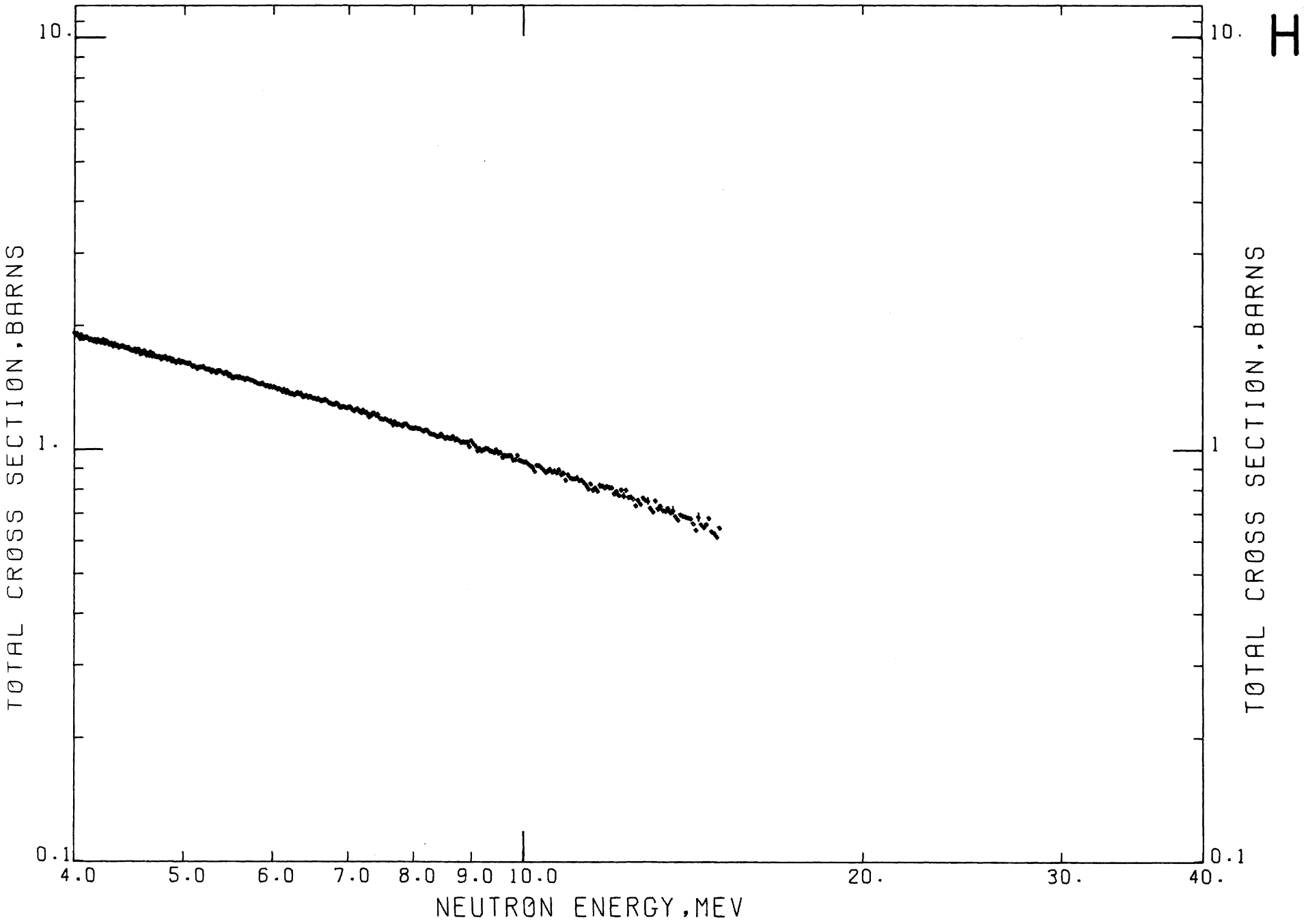
H
10.
1.
0.1
TØTAL CRØSS SECTIØN, BARNS
4.0
5.0
6.0
7.0
8.0
9.0
10.0
20.
30.
40.
NEUTRØN ENERGY, MEV

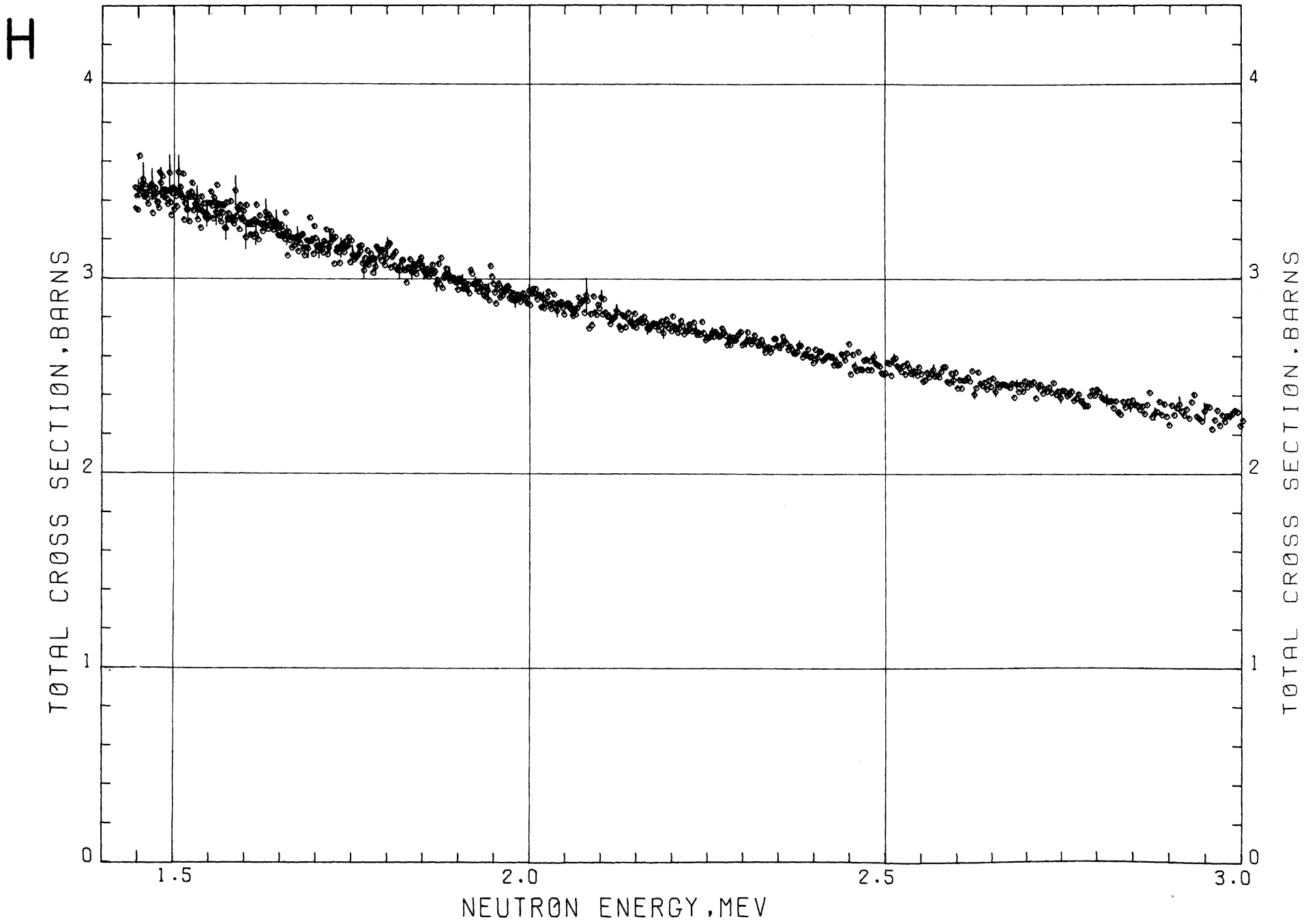
H
TOTAL CROSS SECTION, BARNS
NEUTRON ENERGY, MEV
0
1
2
3
4
1.5
2.0
2.5
3.0

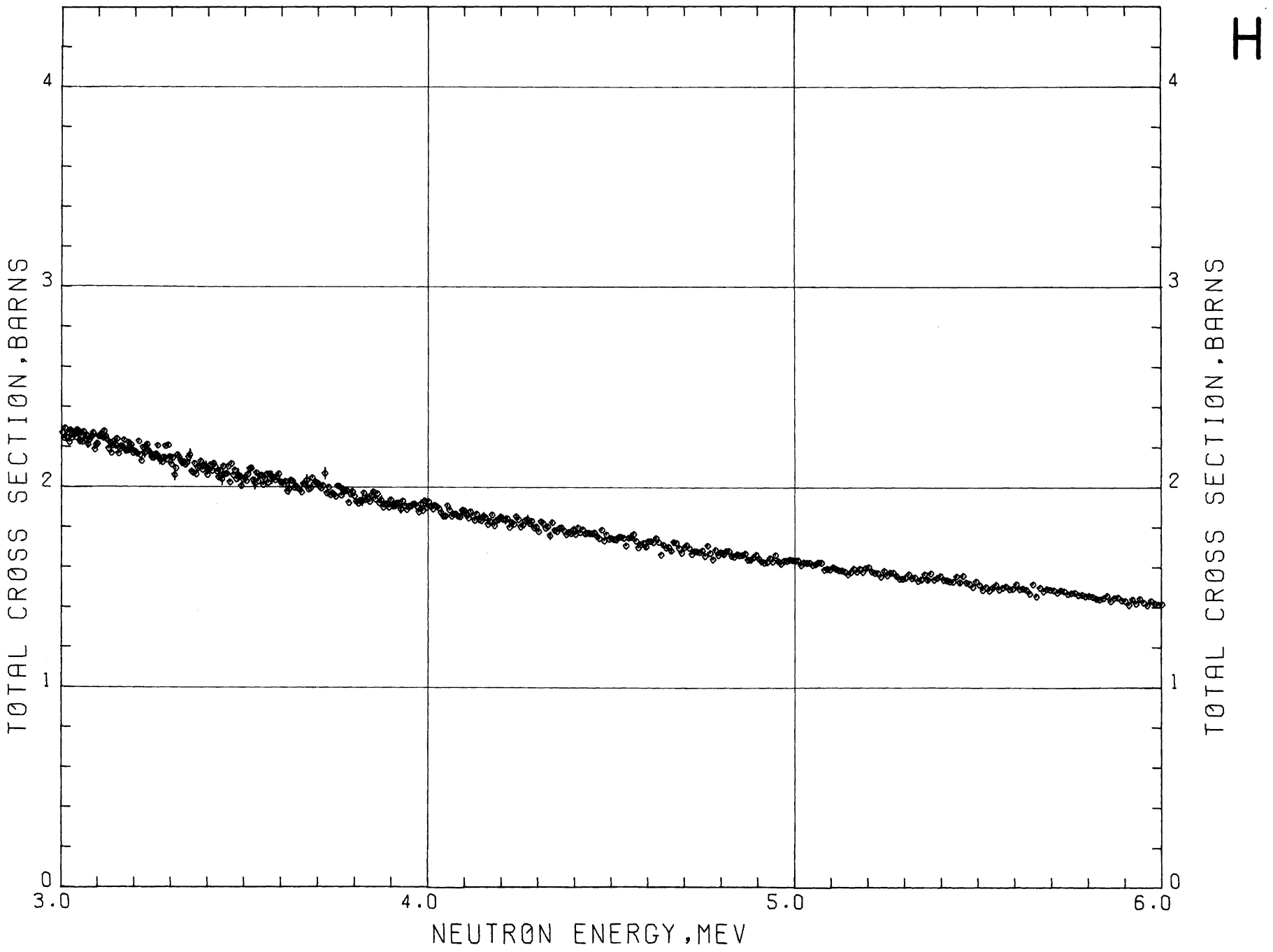
H
TOTAL CROSS SECTION, BARNS
NEUTRON ENERGY, MEV
0
1
2
3
4
3.0
4.0
5.0
6.0

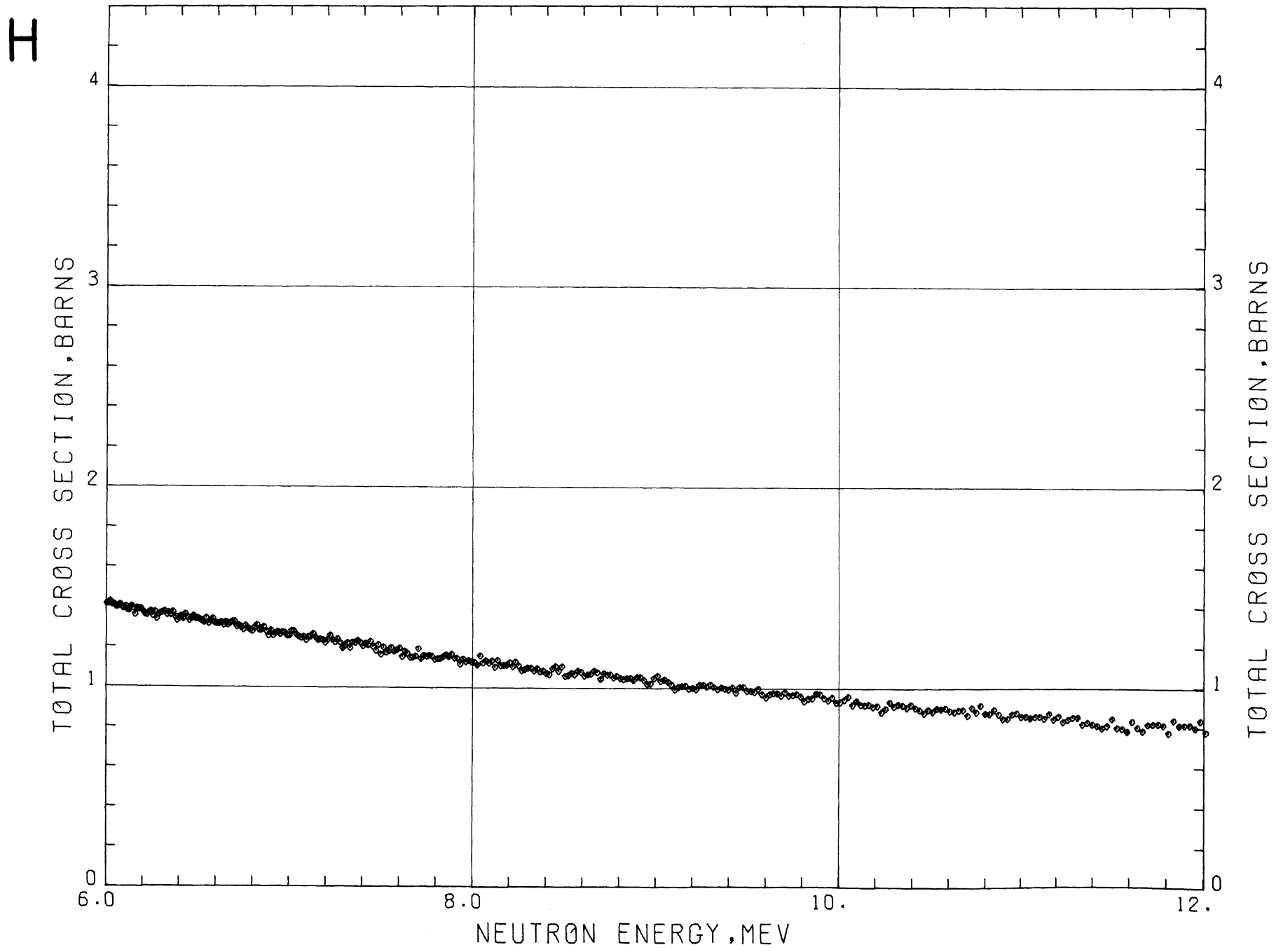
H
TOTAL CROSS SECTION, BARNS
TOTAL CROSS SECTION, BARNS
0
1
2
3
4
6.0
8.0
10.
12.
NEUTRON ENERGY, MEV

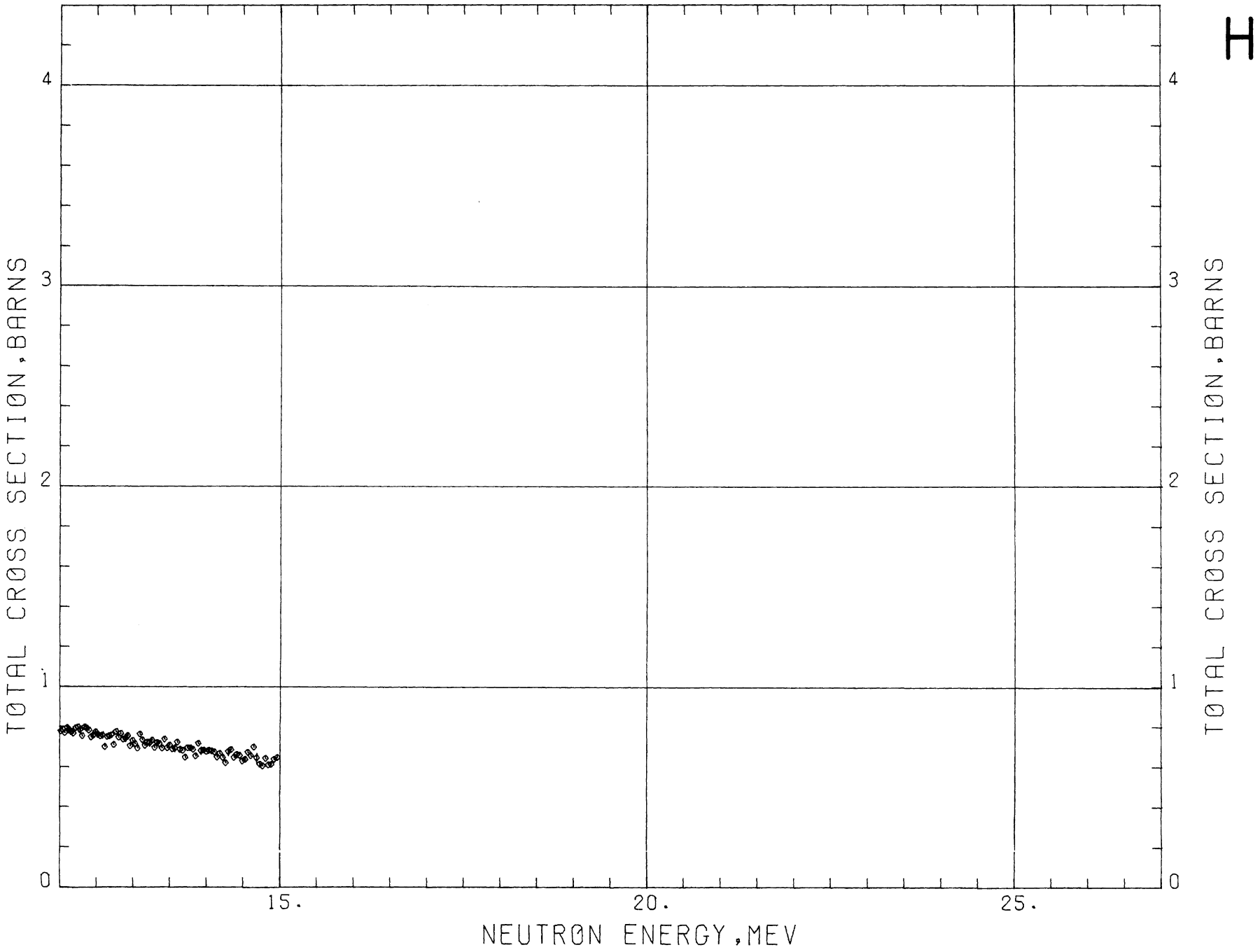
H
TOTAL CROSS SECTION, BARNS
TOTAL CROSS SECTION, BARNS
0
1
2
3
4
15.
20.
25.
NEUTRON ENERGY, MEV

BERYLLIUM

Sample Material: metallic beryllium

Sample Diameter: 12.7 cm

Sample Thicknesses: 3.3 cm; n=0.4069 atoms/barn

7.65 cm; n=0.9447

Analysis: $\geq$ 99.39 percent beryllium

principal impurity: $<$ 0.6 percent oxygen

Literature Reference: R. A. Schrack, R. B. Schwartz, and H. T. Heaton II, Bull. Am. Phys. Soc. **16**, 495 (1971).

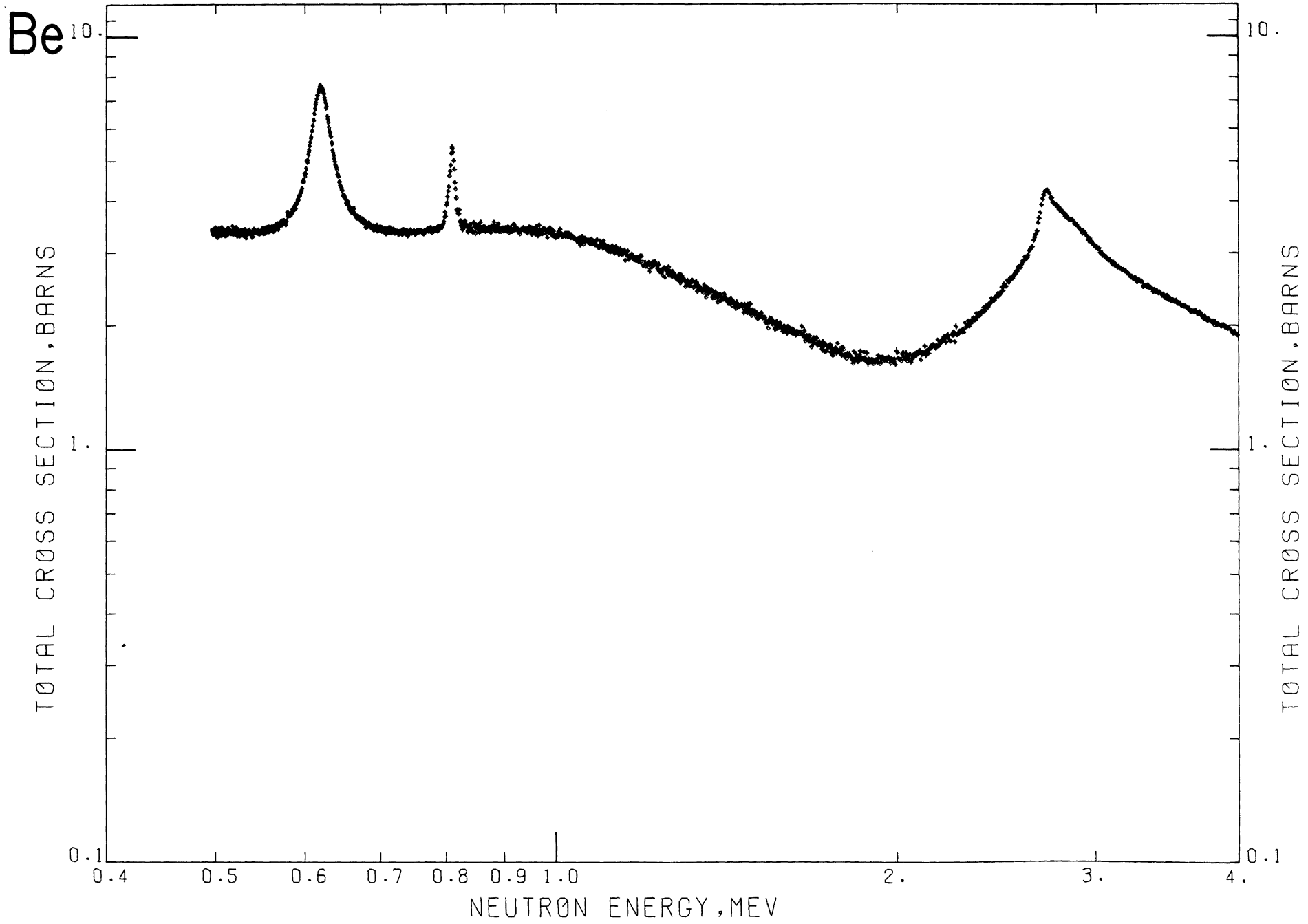
Be
10.
1.
0.1
TOTAL CROSS SECTION, BARNS
0.4
0.5
0.6
0.7
0.8
0.9
1.0
2.
3.
4.
NEUTRON ENERGY, MEV

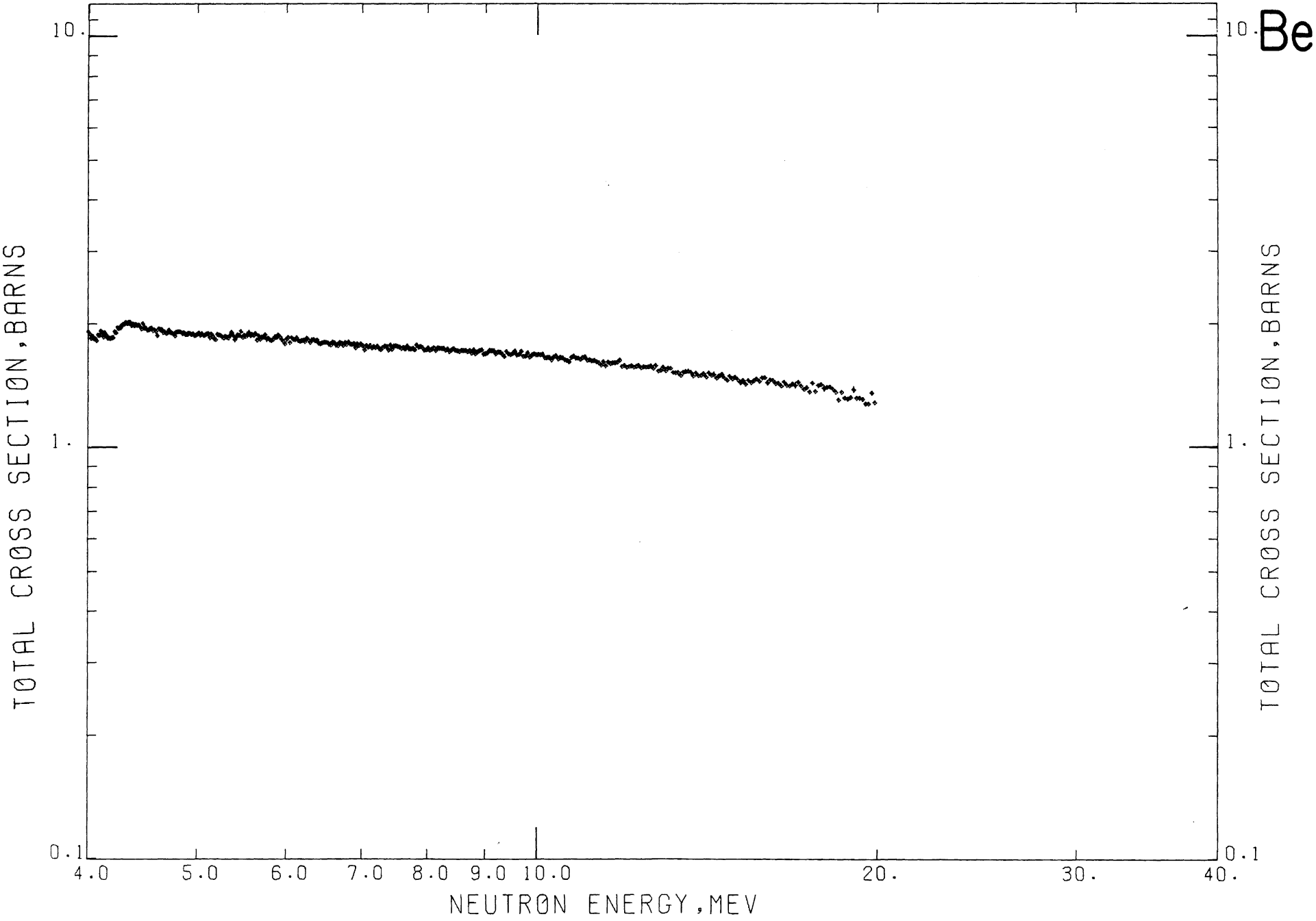
Be
TOTAL CROSS SECTION, BARNS
NEUTRON ENERGY, MEV
10.
1.
0.1
4.0
5.0
6.0
7.0
8.0
9.0
10.0
20.
30.
40.

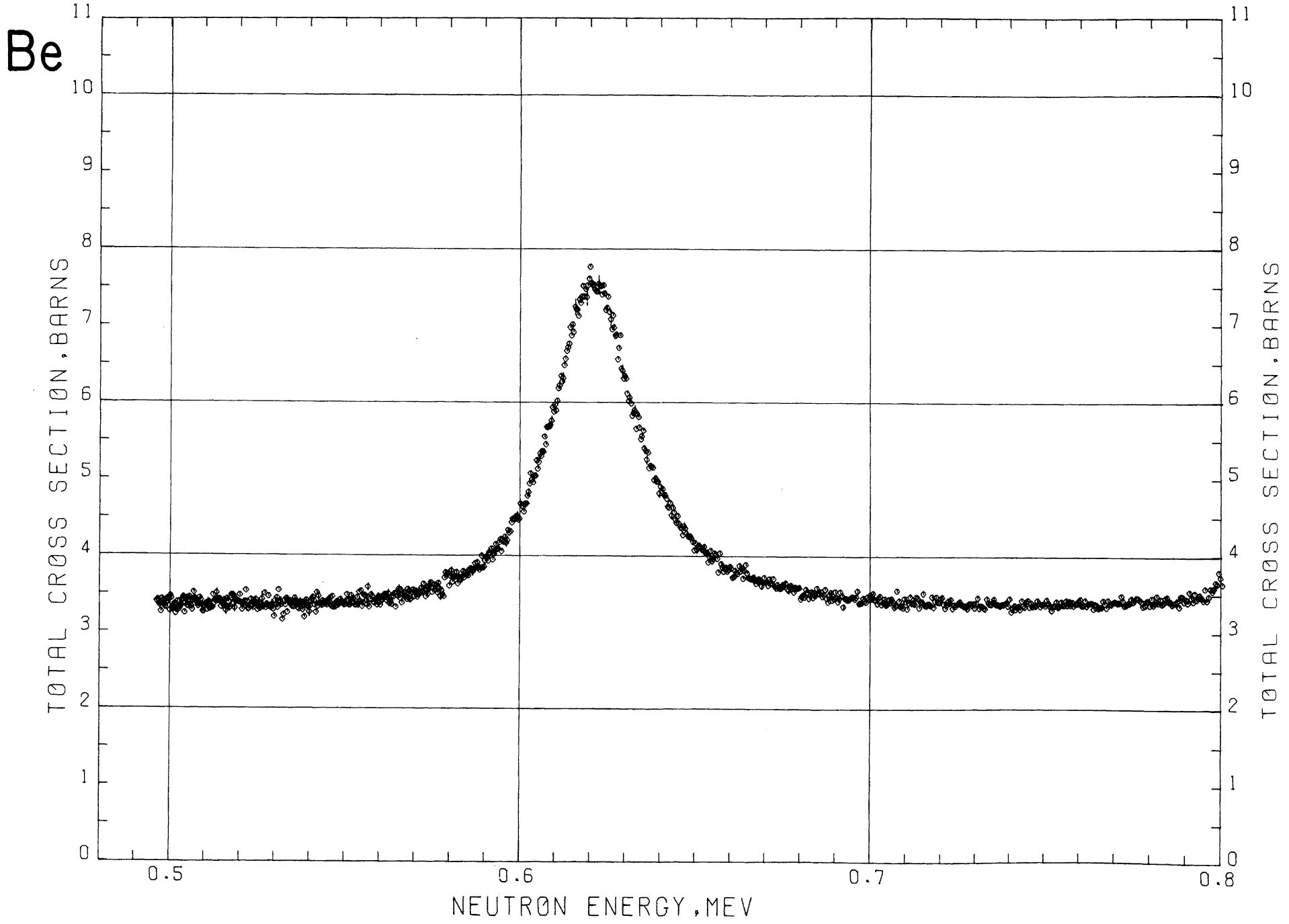
Be
TØTAL CRØSS SECTIØN, BARNS
NEUTRØN ENERGY, MEV
0.5
0.6
0.7
0.8
0
1
2
3
4
5
6
7
8
9
10
11

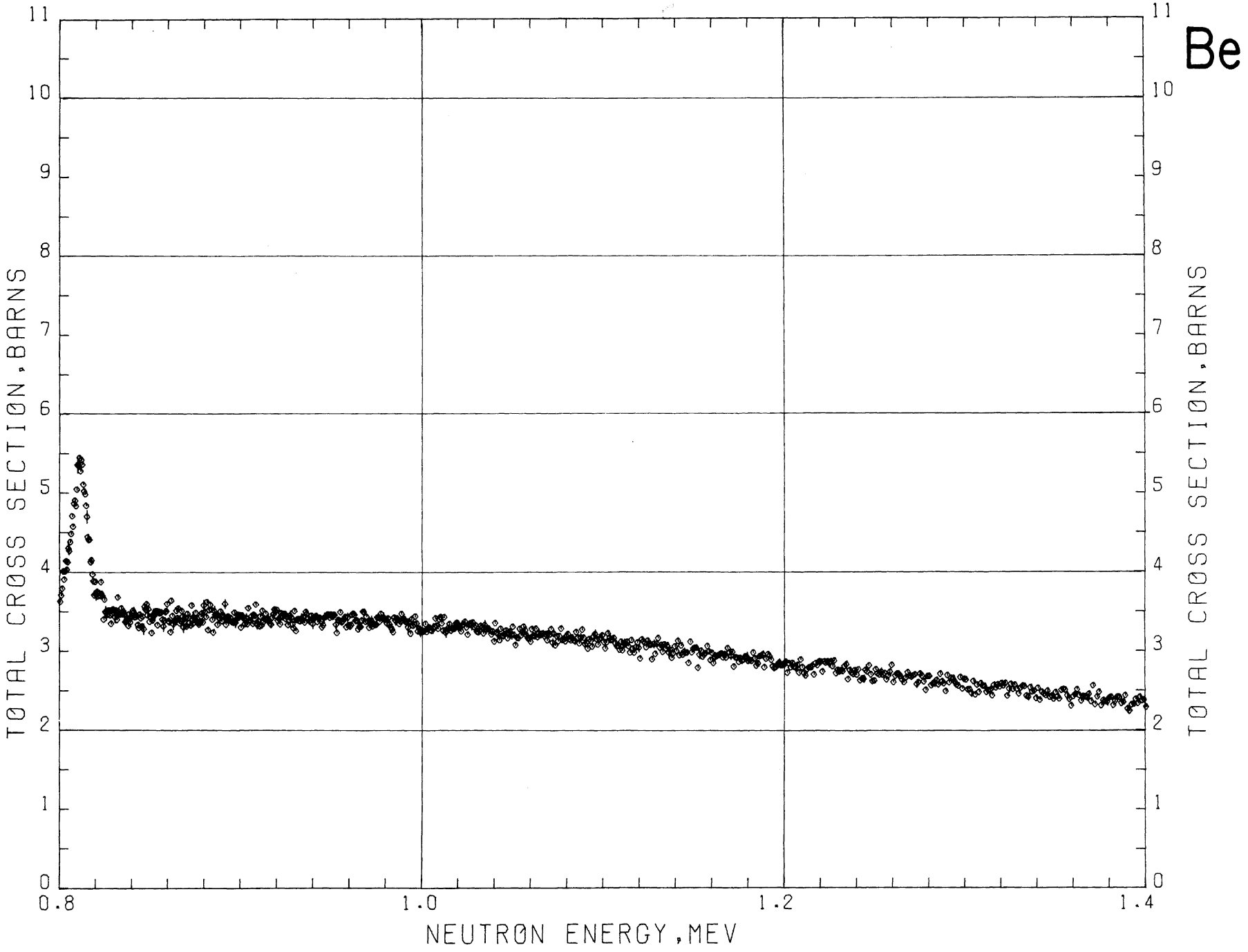
Be
TOTAL CROSS SECTION, BARNS
NEUTRON ENERGY, MEV
0.8
1.0
1.2
1.4
0
1
2
3
4
5
6
7
8
9
10
11

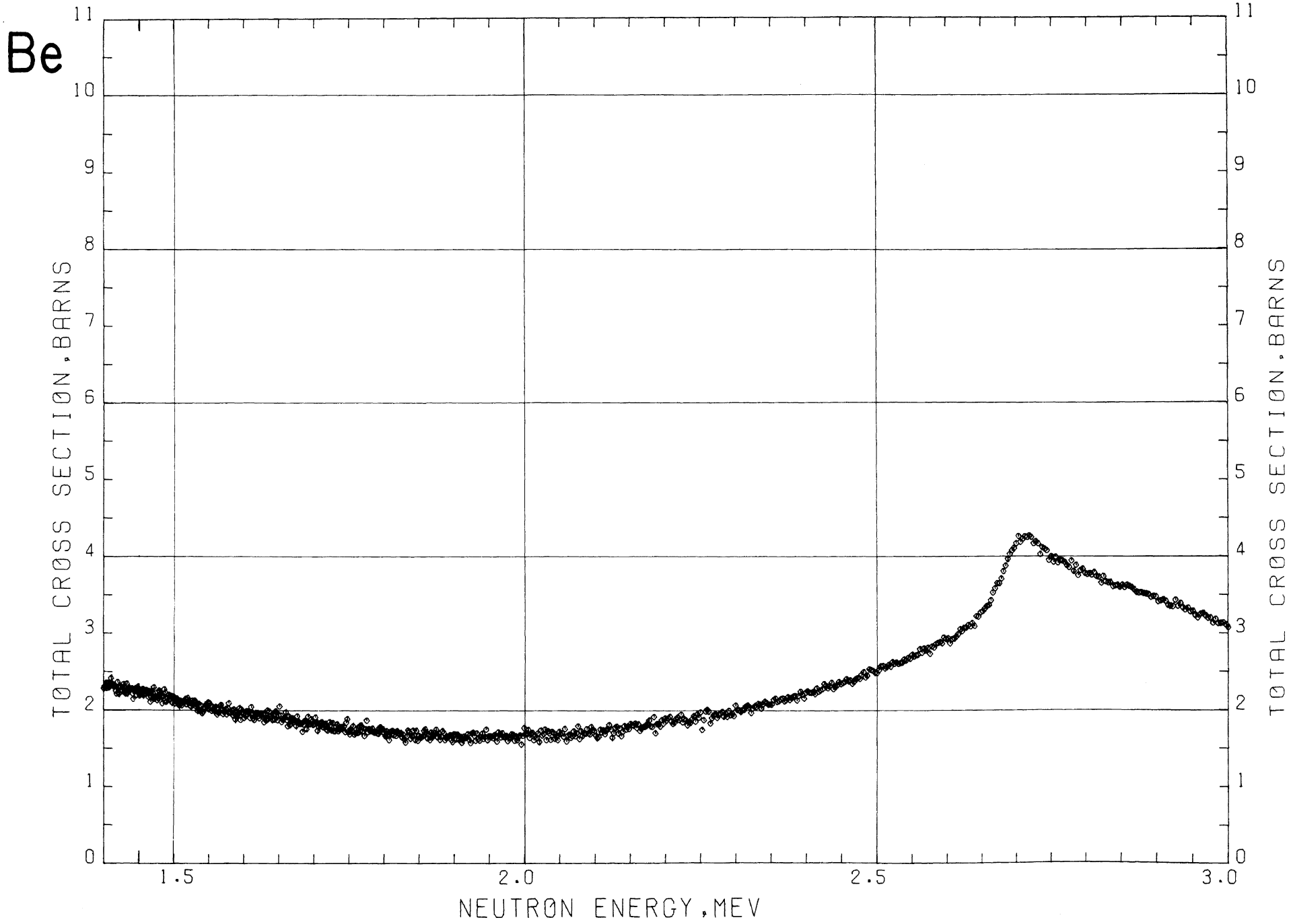
Be
TOTAL CROSS SECTION, BARNS
NEUTRON ENERGY, MEV
0
1
2
3
4
5
6
7
8
9
10
11
1.5
2.0
2.5
3.0

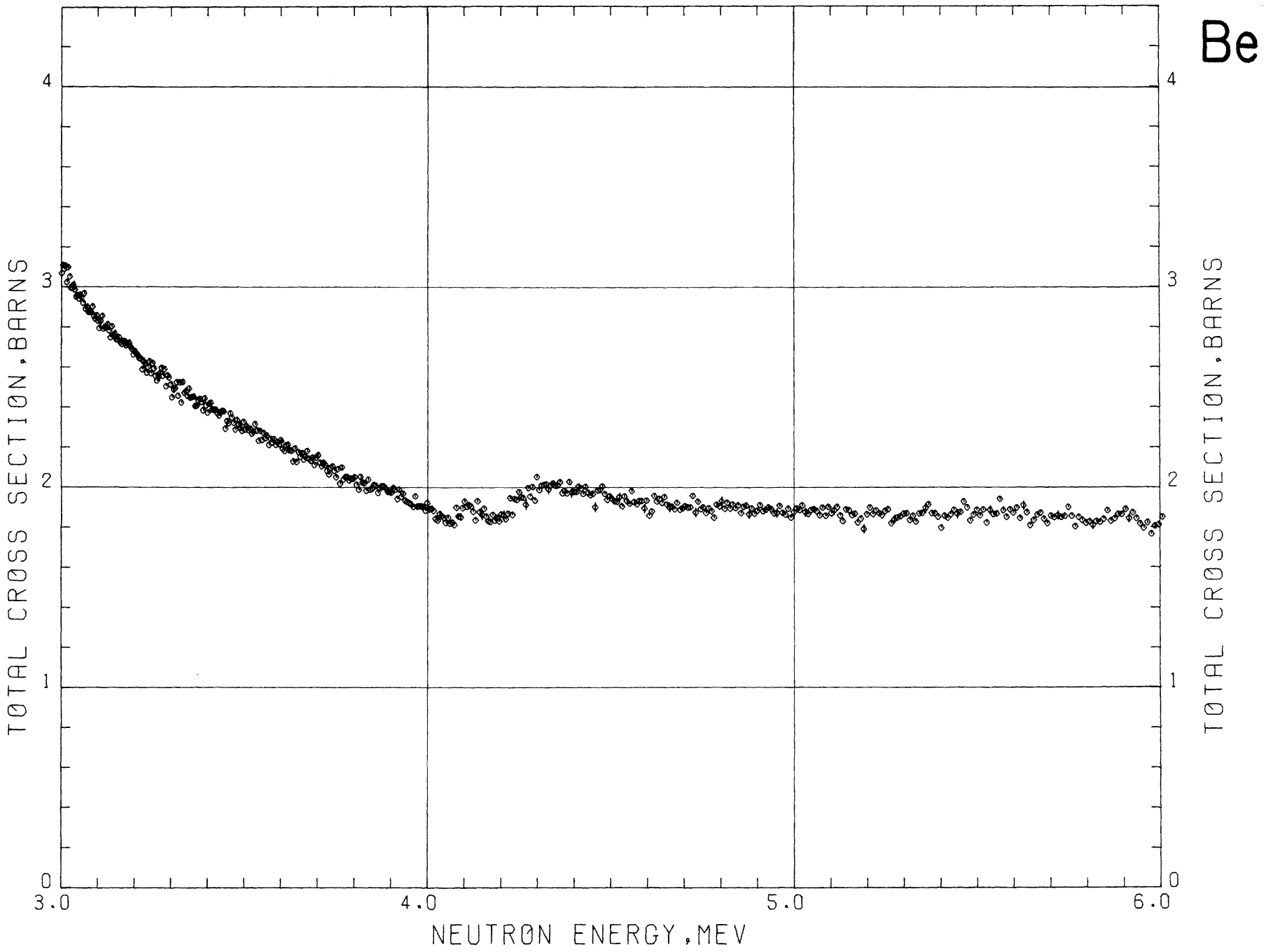
Be
TOTAL CROSS SECTION, BARNS
TOTAL CROSS SECTION, BARNS
0
1
2
3
4
3.0
4.0
5.0
6.0
NEUTRON ENERGY, MEV

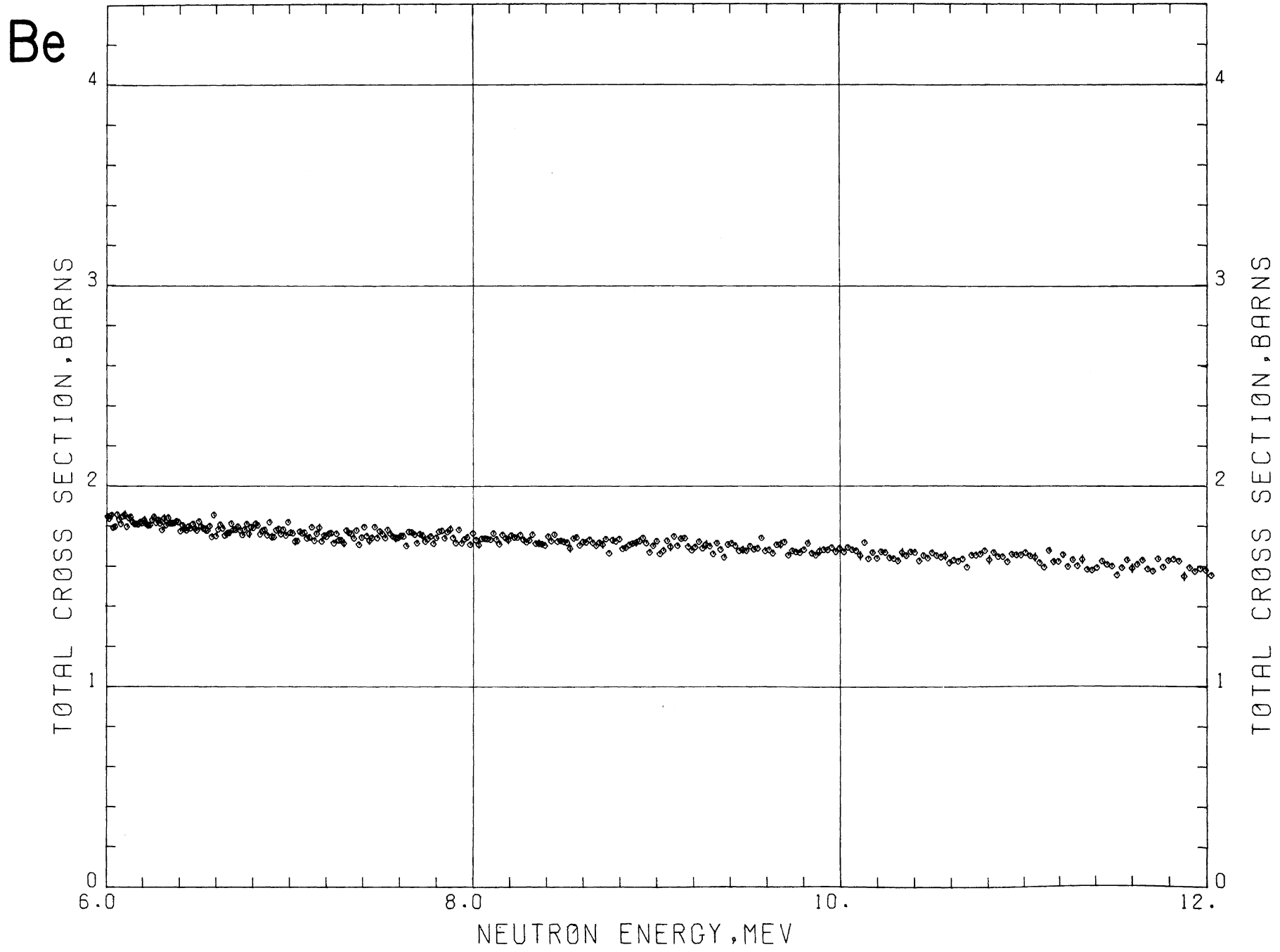
Be
TOTAL CROSS SECTION, BARNS
NEUTRON ENERGY, MEV
0
1
2
3
4
6.0
8.0
10.
12.

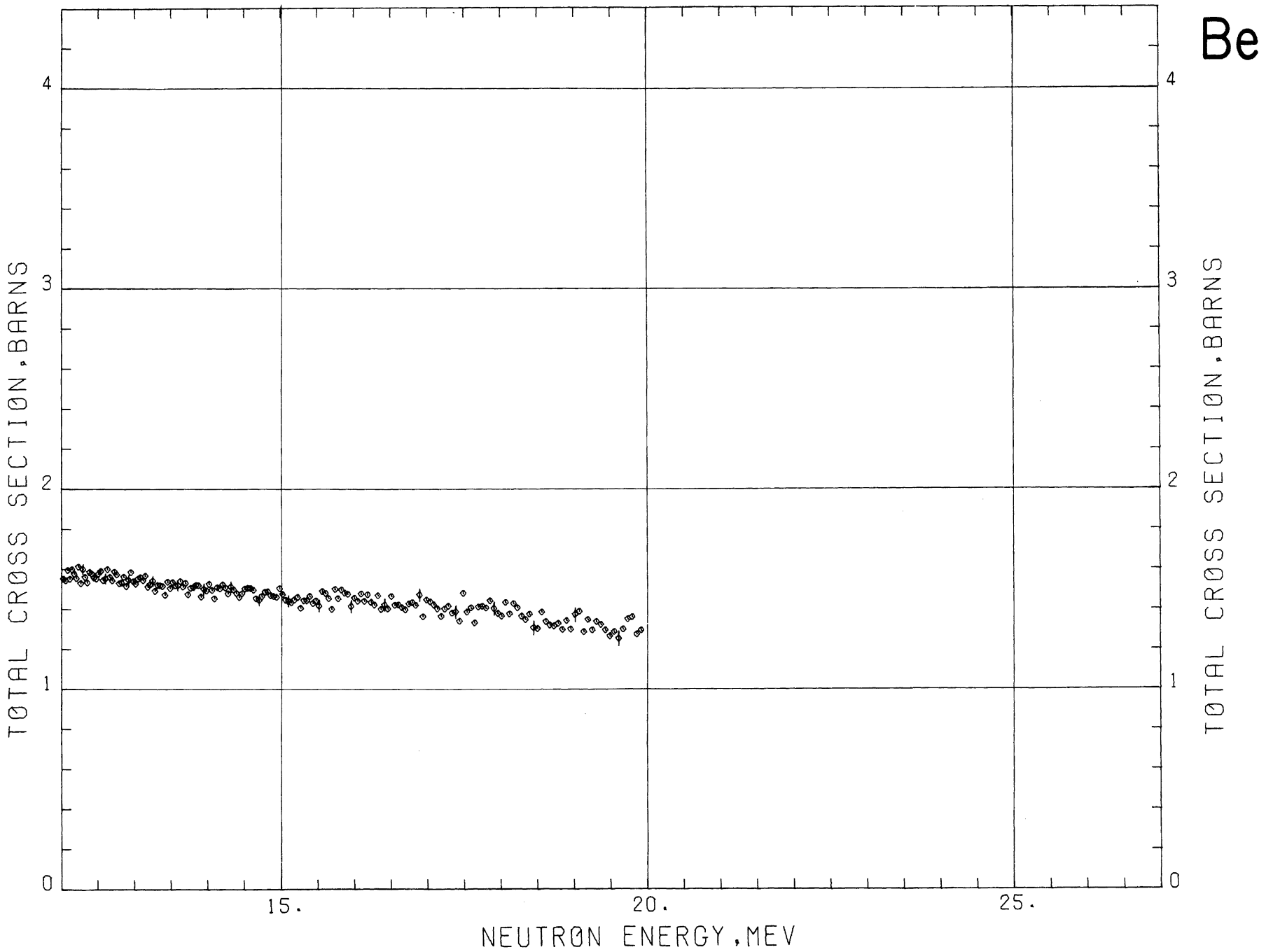
Be
TOTAL CROSS SECTION, BARNS
TOTAL CROSS SECTION, BARNS
0
1
2
3
4
15.
20.
25.
NEUTRON ENERGY, MEV

CARBON

Sample Material: pressed graphite

Sample Diameter: 12.7 cm; 5.08 cm.

Sample Thickness: 5.08 cm $n = 0.4803$ atoms/barn
10.16 cm $n = 0.9557$ atoms/barn
17.78 cm $n = 1.6750$ atoms/barn

Analysis: volatile components < .01 percent

nonvolatile components < .01 percent

Literature Reference: R. B. Schwartz, H. T. Heaton II, and R. A. Schrack, Bull. Am. Phys. Soc. 15, 567 (1970).

Comments: Density fluctuations within a sample are less than 1 percent. There was no evidence of absorption of impurities on exposure to air.

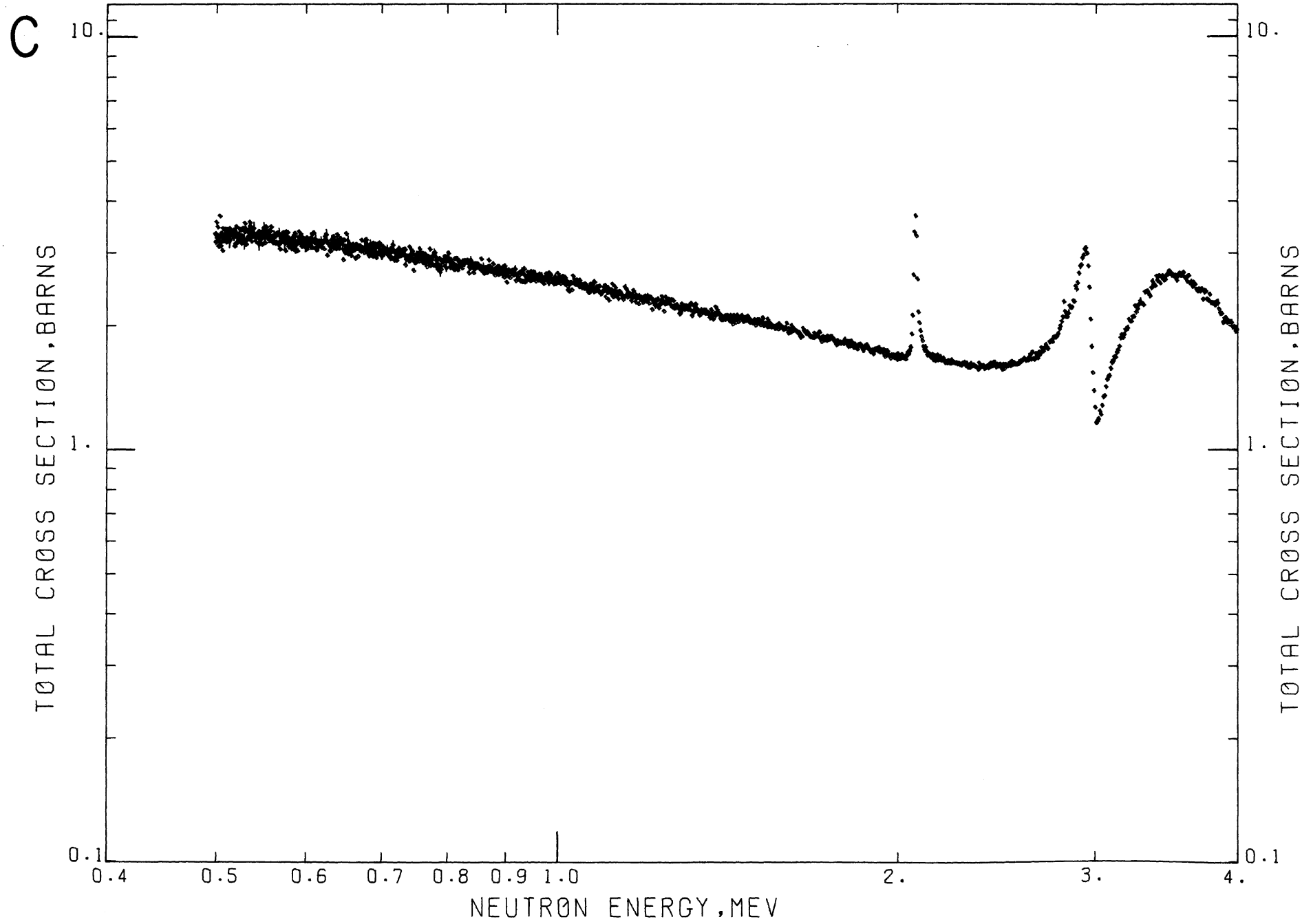
C
10.
1.
0.1
TOTAL CROSS SECTION, BARNS
0.4
0.5
0.6
0.7
0.8
0.9
1.0
2.
3.
4.
NEUTRON ENERGY, MEV

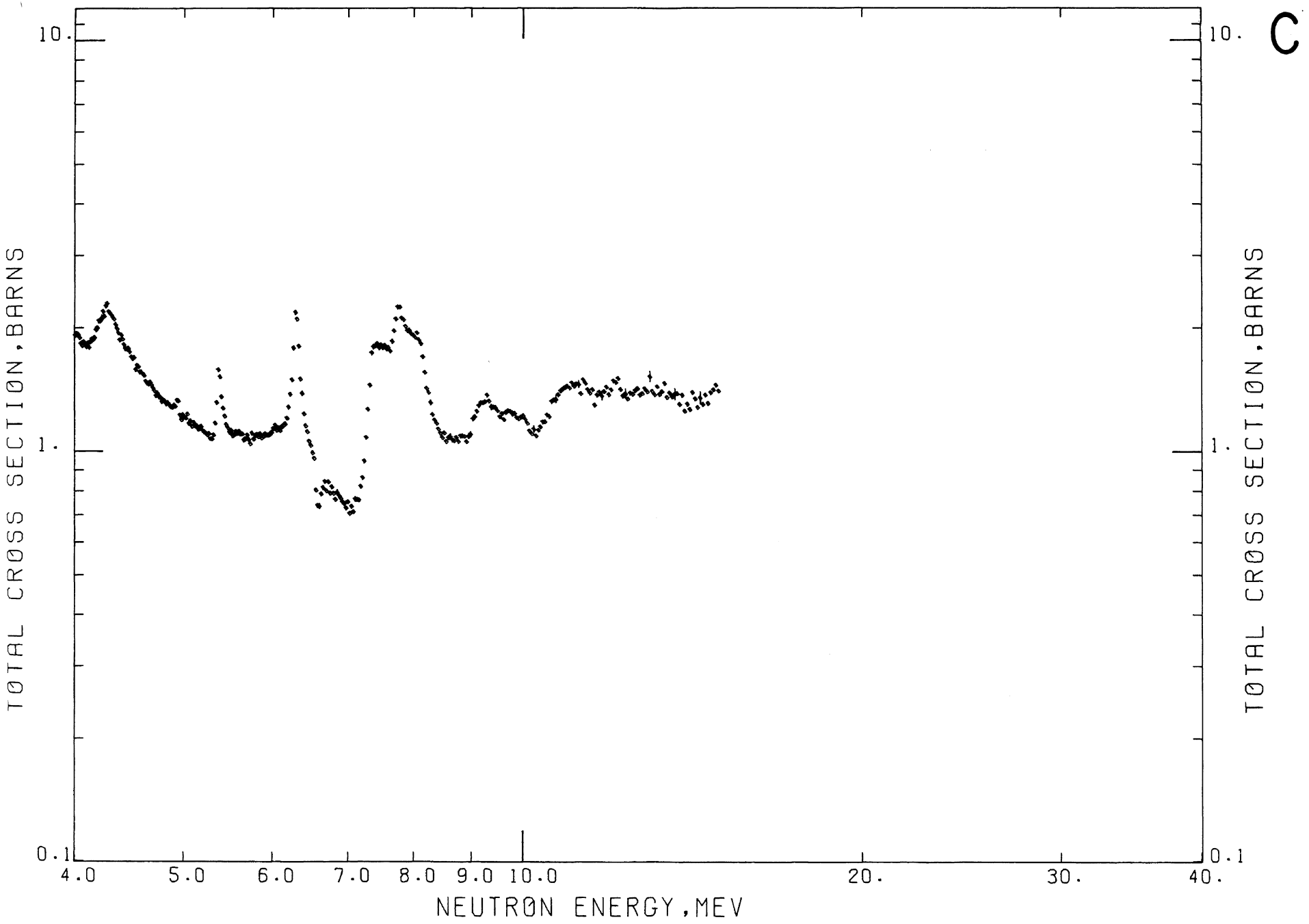
C
10.
1.
0.1
TOTAL CROSS SECTION, BARNS
4.0
5.0
6.0
7.0
8.0
9.0
10.0
20.
30.
40.
NEUTRON ENERGY, MEV

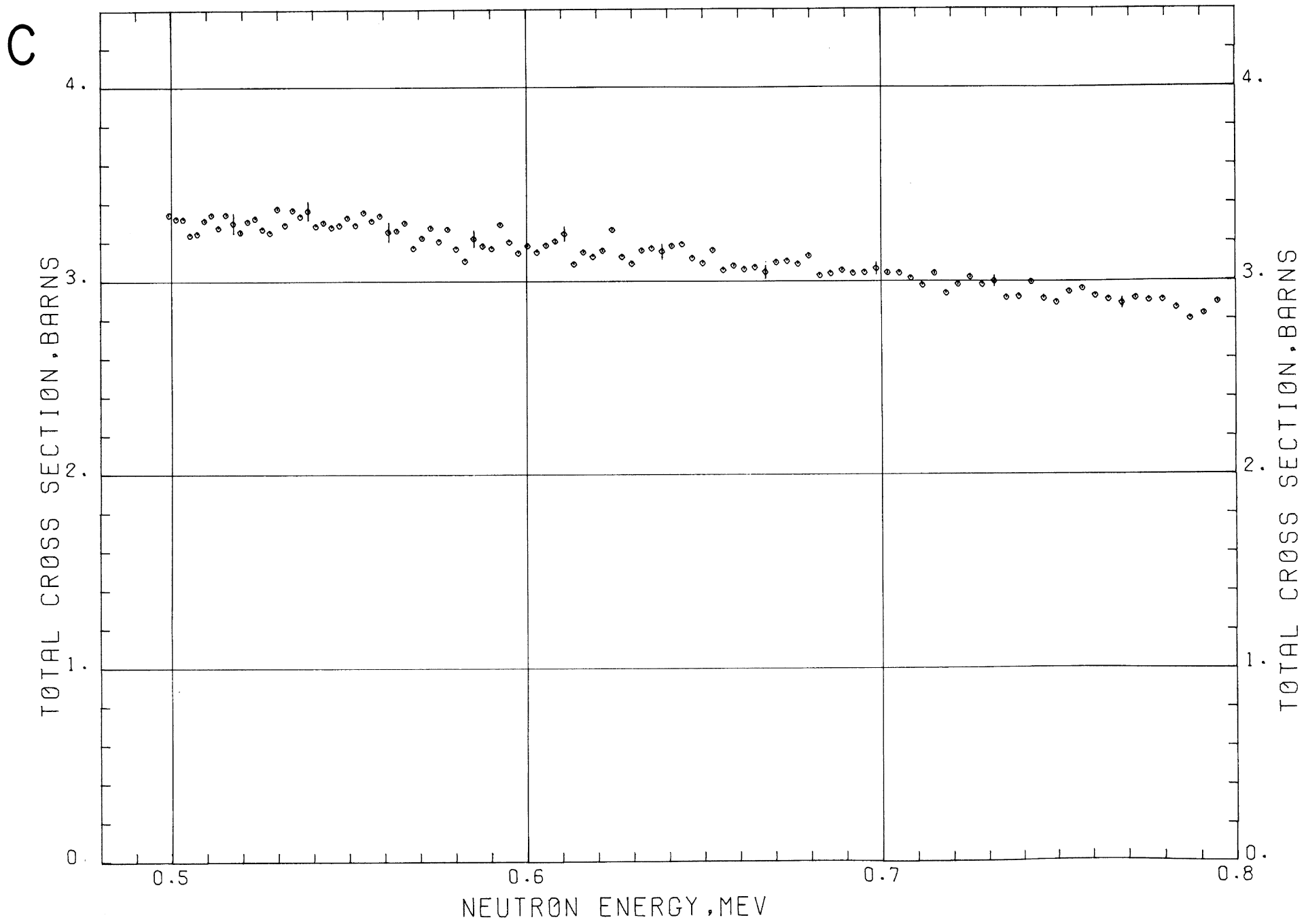
C
TØTAL CRØSS SECTIØN, BARNS
NEUTRØN ENERGY, MEV
0.
1.
2.
3.
4.
0.5
0.6
0.7
0.8

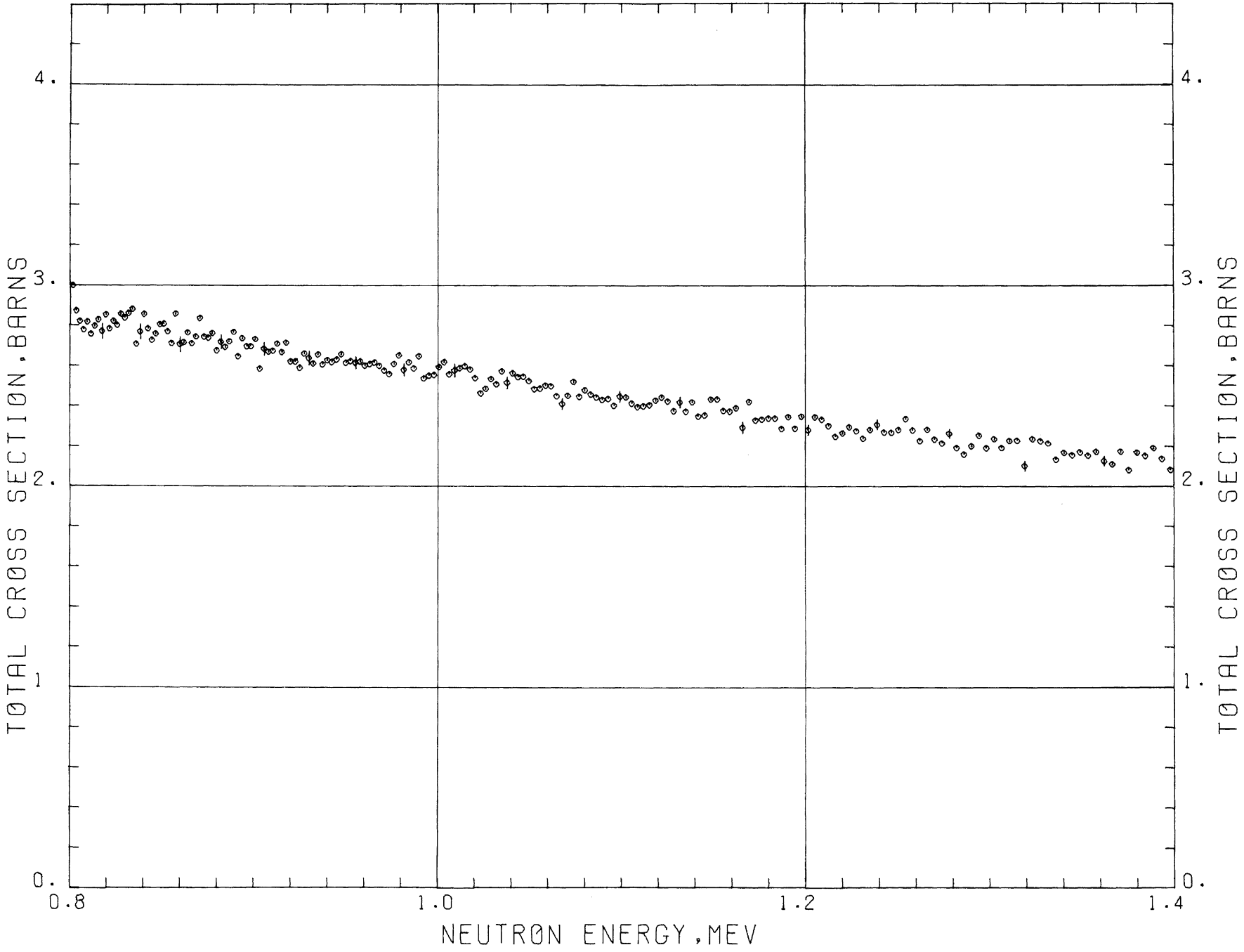
C
TOTAL CROSS SECTION, BARNS
4.
3.
2.
1.
0.
0.8
1.0
1.2
1.4
NEUTRON ENERGY, MEV

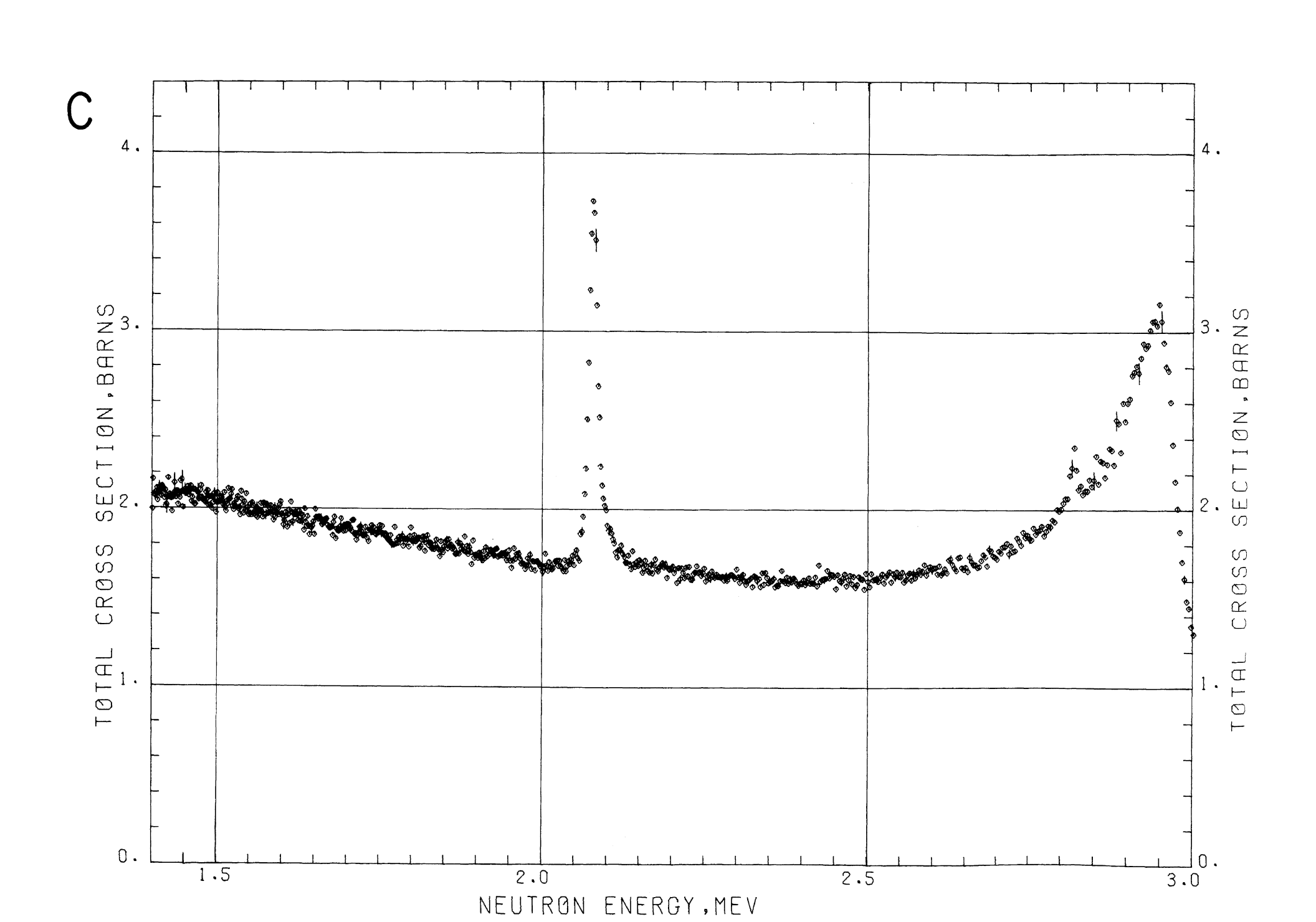
C
TOTAL CROSS SECTION, BARNS
NEUTRON ENERGY, MEV
0.
1.
2.
3.
4.
1.5
2.0
2.5
3.0

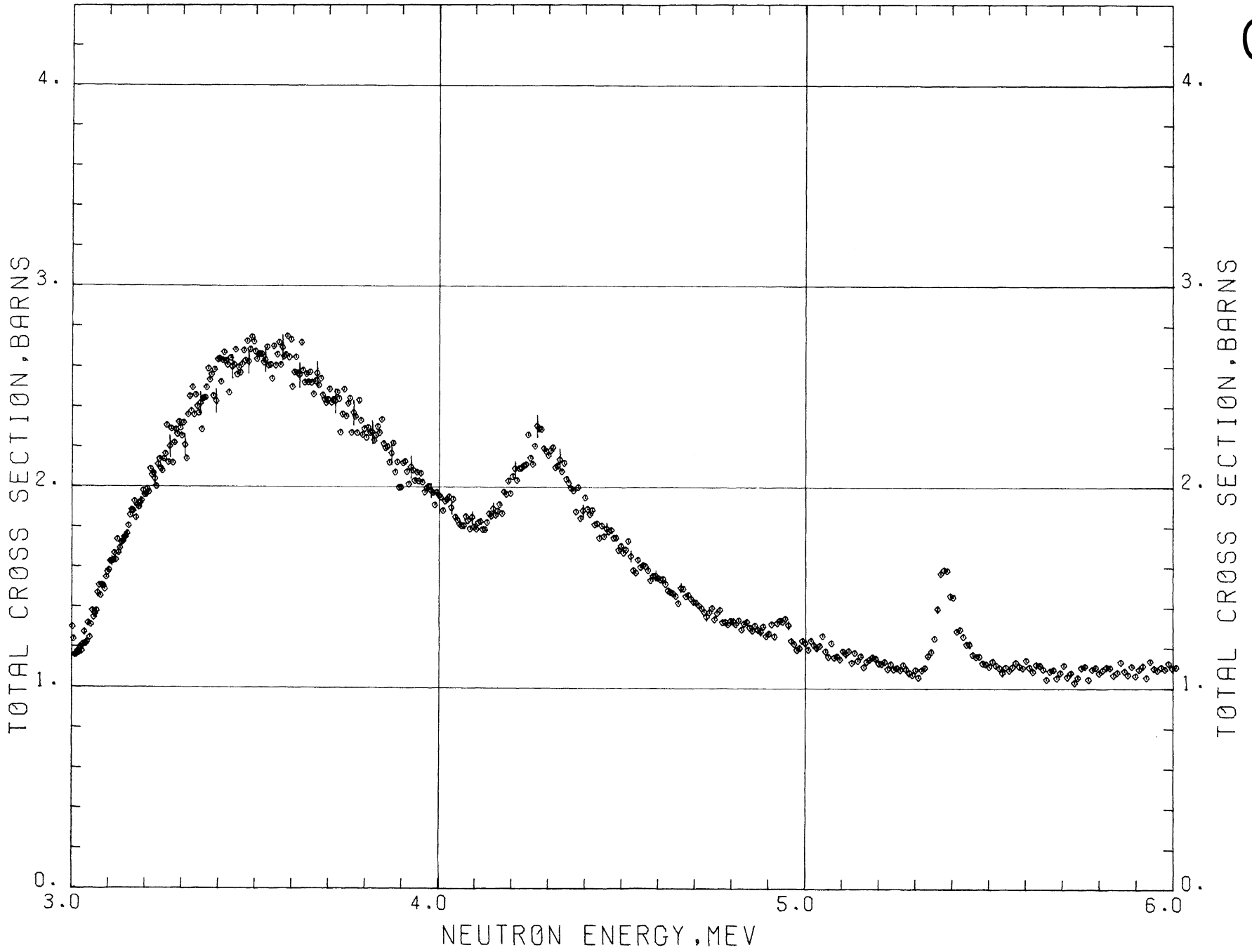
C
TOTAL CROSS SECTION, BARNS
NEUTRON ENERGY, MEV
0.
1.
2.
3.
4.
3.0
4.0
5.0
6.0

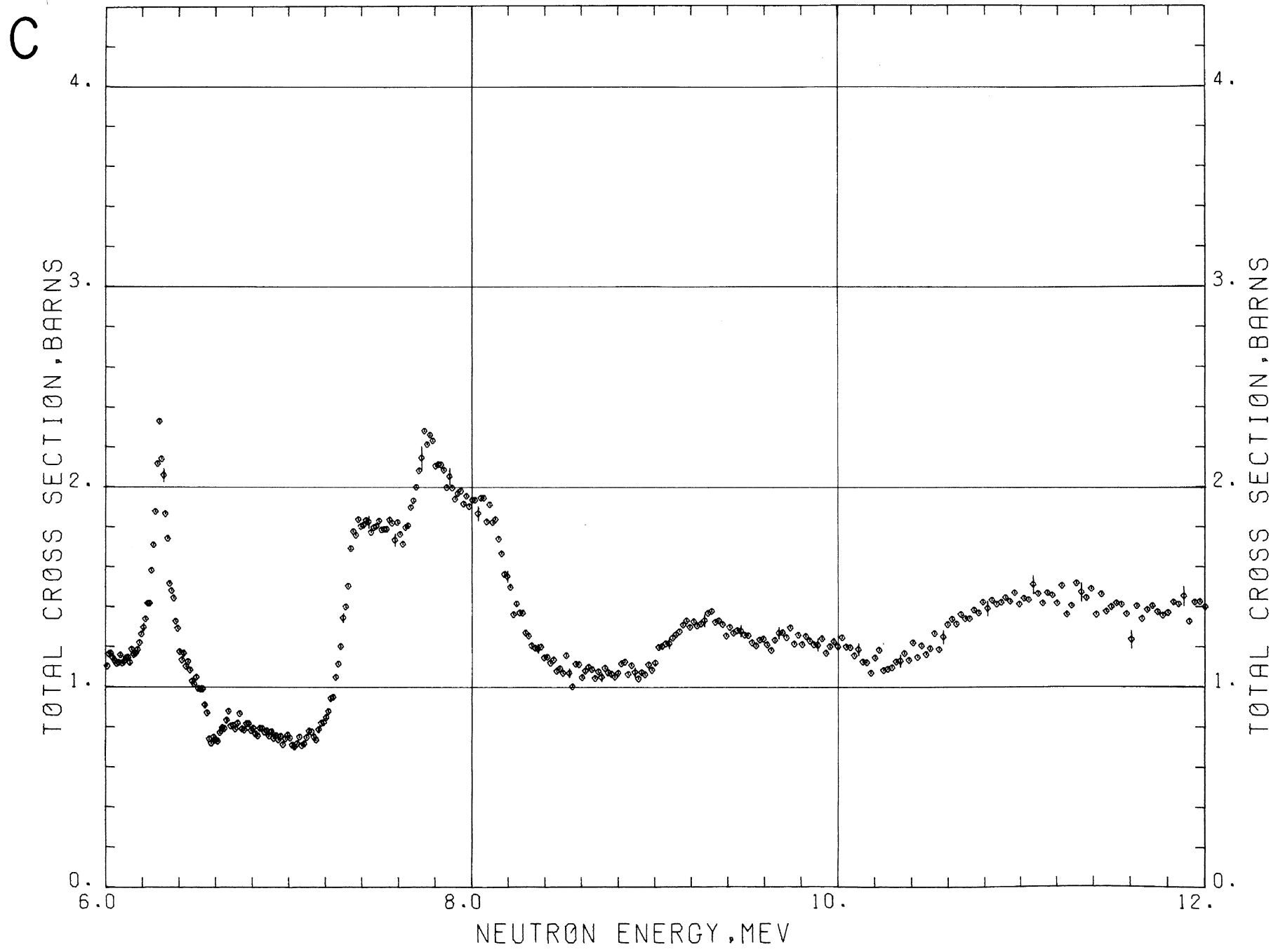
C
TØTAL CRØSS SECTIØN,BARNS
NEUTRØN ENERGY,MEV
0.
1.
2.
3.
4.
6.0
8.0
10.
12.

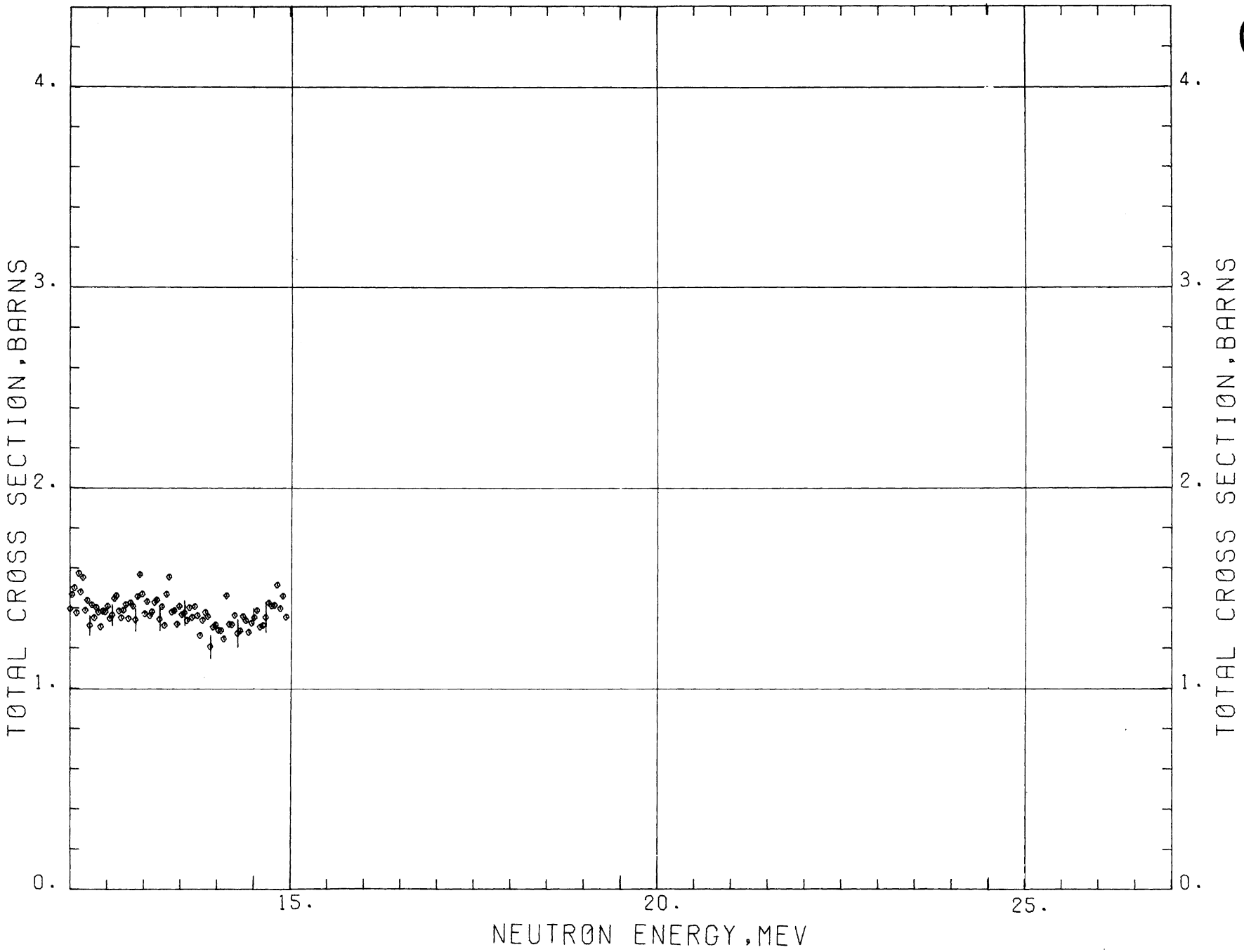
C
TOTAL CROSS SECTION, BARNS
4.
3.
2.
1.
0.
15.
20.
25.
NEUTRON ENERGY, MEV

NITROGEN

Sample Material: liquid nitrogen

Sample Diameter: 12.7 cm

Sample Thickness: 27.9 cm, $n = 0.9684$ atoms/barn

13.5 cm, $n = 0.4683$

Literature Reference: H. T. Heaton II, R. B. Schwartz, and R. A. Schrack, Bull. Am. Phys. Soc. **15**, 568 (1970).

Comments: Special dewars were constructed with end windows of known thickness of pyrex. Open runs were made with duplicates of the end windows in the beam. The nitrogen cross section was also obtained by running melamine (CH_2N_2) against polyethylene (CH_2). A powdered sample of melamine with $n = 0.6756$ atoms/barn of nitrogen was run against a sample of polyethene having the same number of atoms of C and H. Figure A shows the ratio of cross sections obtained using melamine and liquid nitrogen.

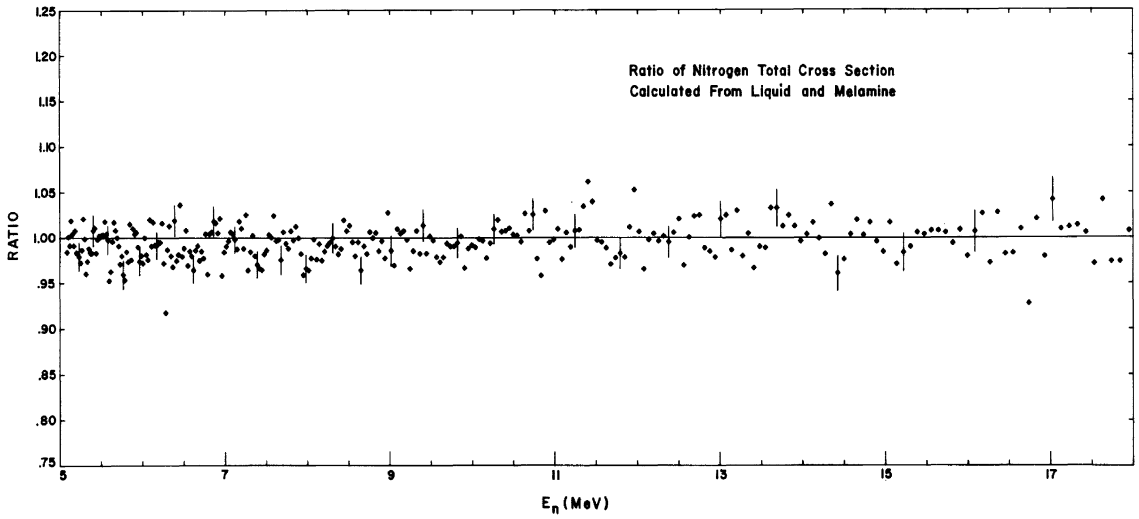

FIGURE A.

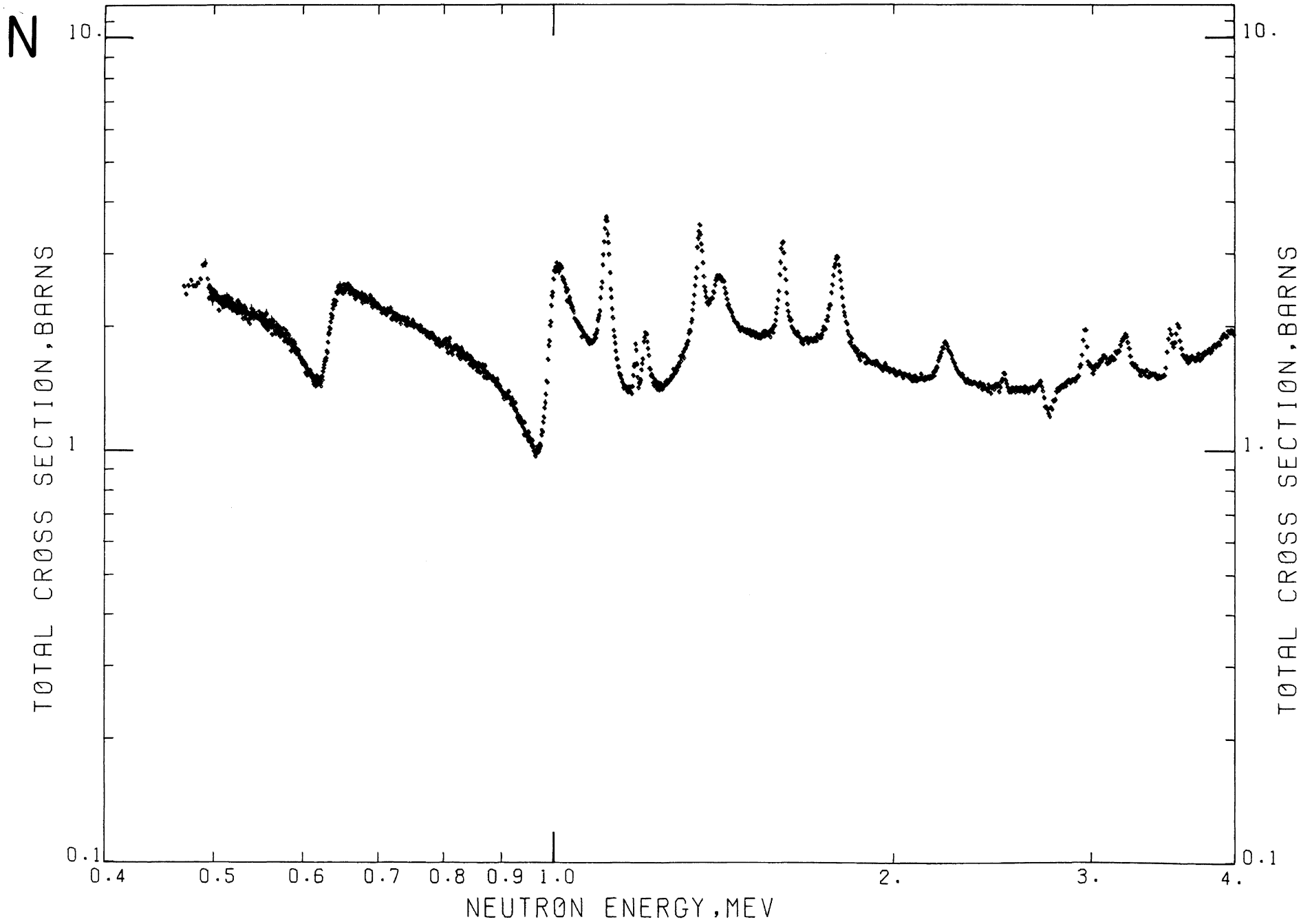
N
10.
1
0.1
TOTAL CROSS SECTION, BARNS
0.4
0.5
0.6
0.7
0.8
0.9
1.0
2.
3.
4.
NEUTRON ENERGY, MEV

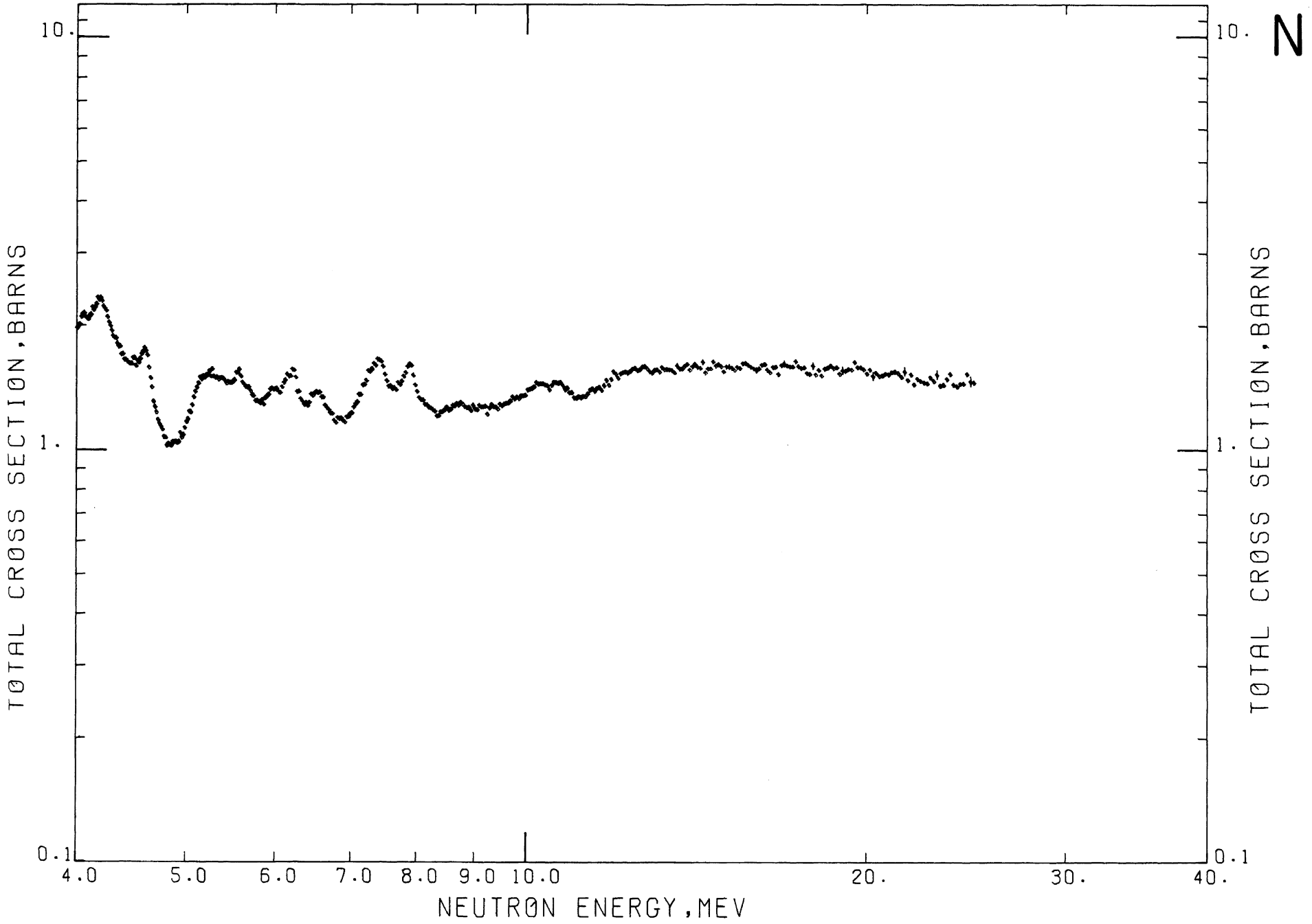
10.
1.
0.1
TØTAL CRØSS SECTIØN,BARNS
4.0
5.0
6.0
7.0
8.0
9.0
10.0
20.
30.
40.
NEUTRØN ENERGY,MEV

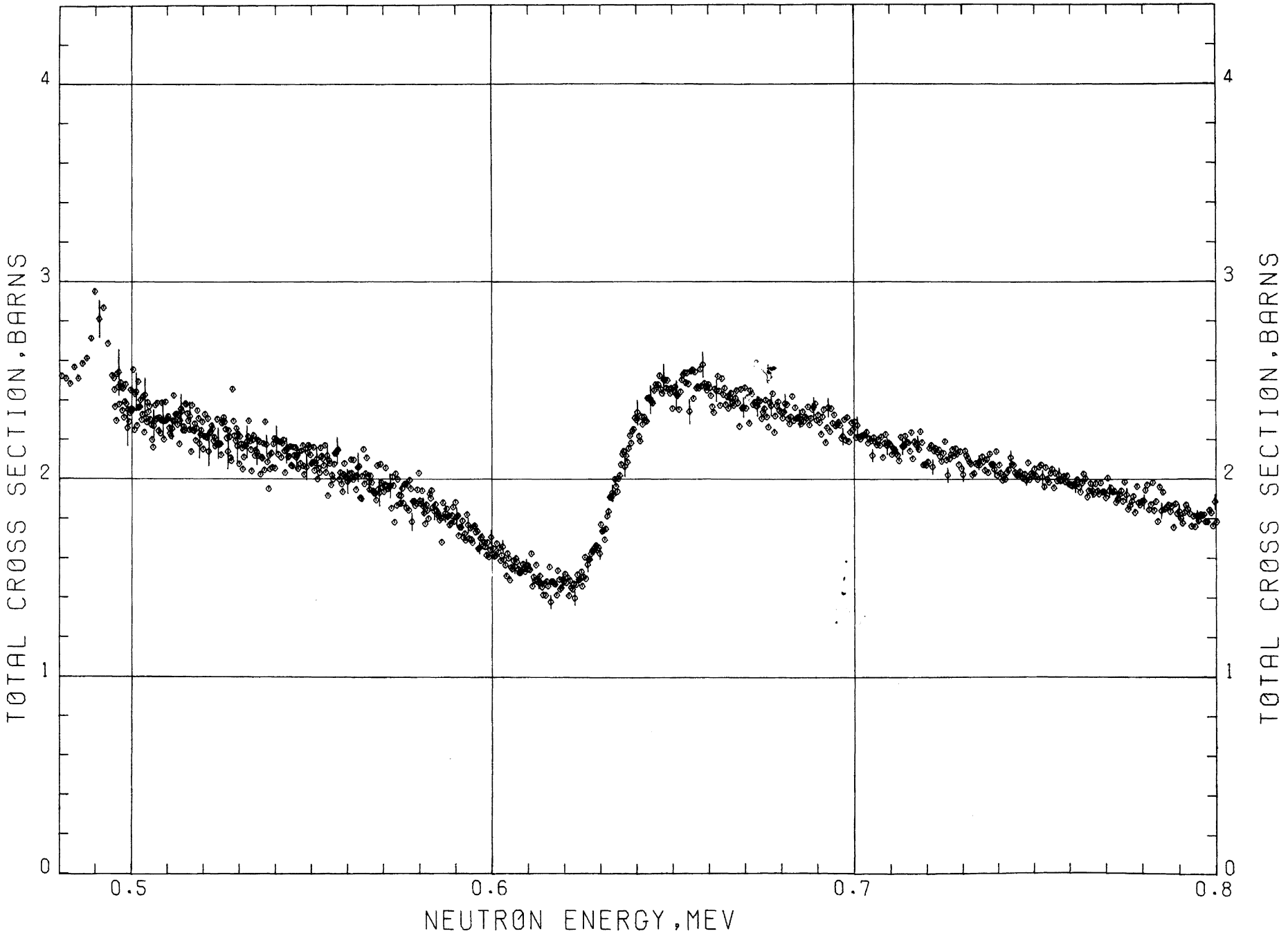
N
TØTAL CRØSS SECTIØN, BARNS
NEUTRØN ENERGY, MEV
0
1
2
3
4
0.5
0.6
0.7
0.8

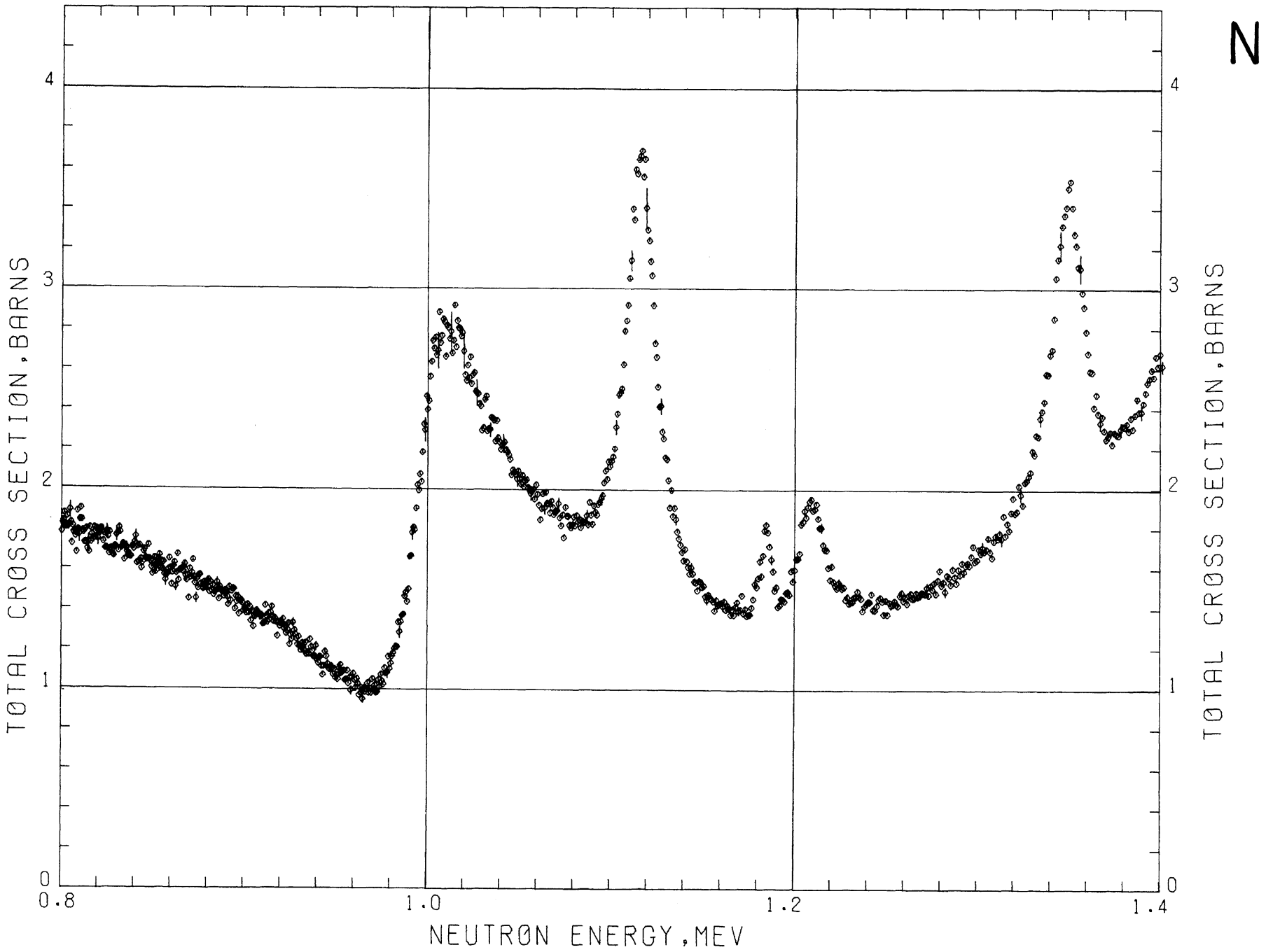
N
TOTAL CROSS SECTION, BARNS
NEUTRON ENERGY, MEV
0
1
2
3
4
0.8
1.0
1.2
1.4

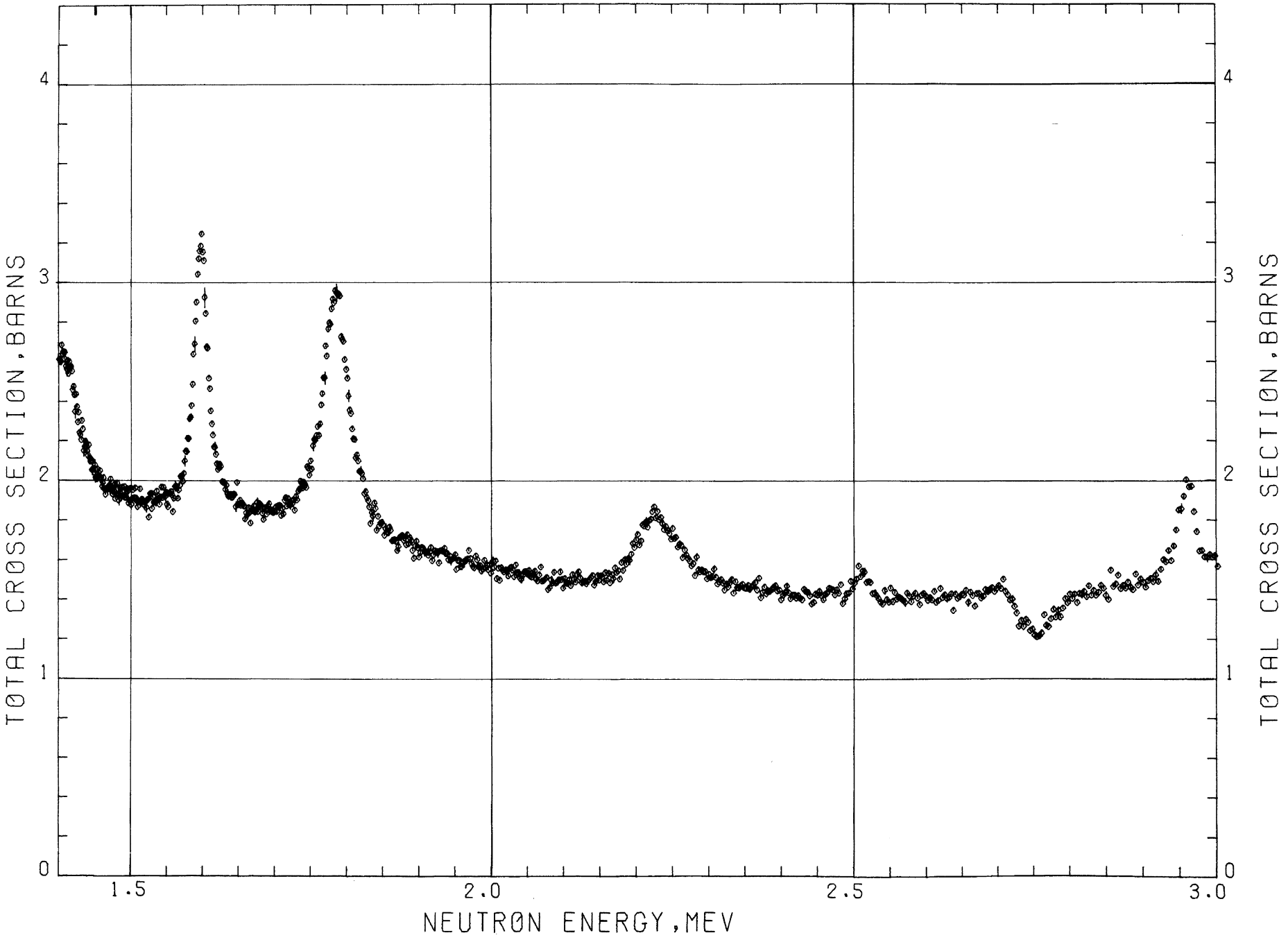
N
TØTAL CRØSS SECTIØN, BARNS
NEUTRØN ENERGY, MEV
0
1
2
3
4
1.5
2.0
2.5
3.0

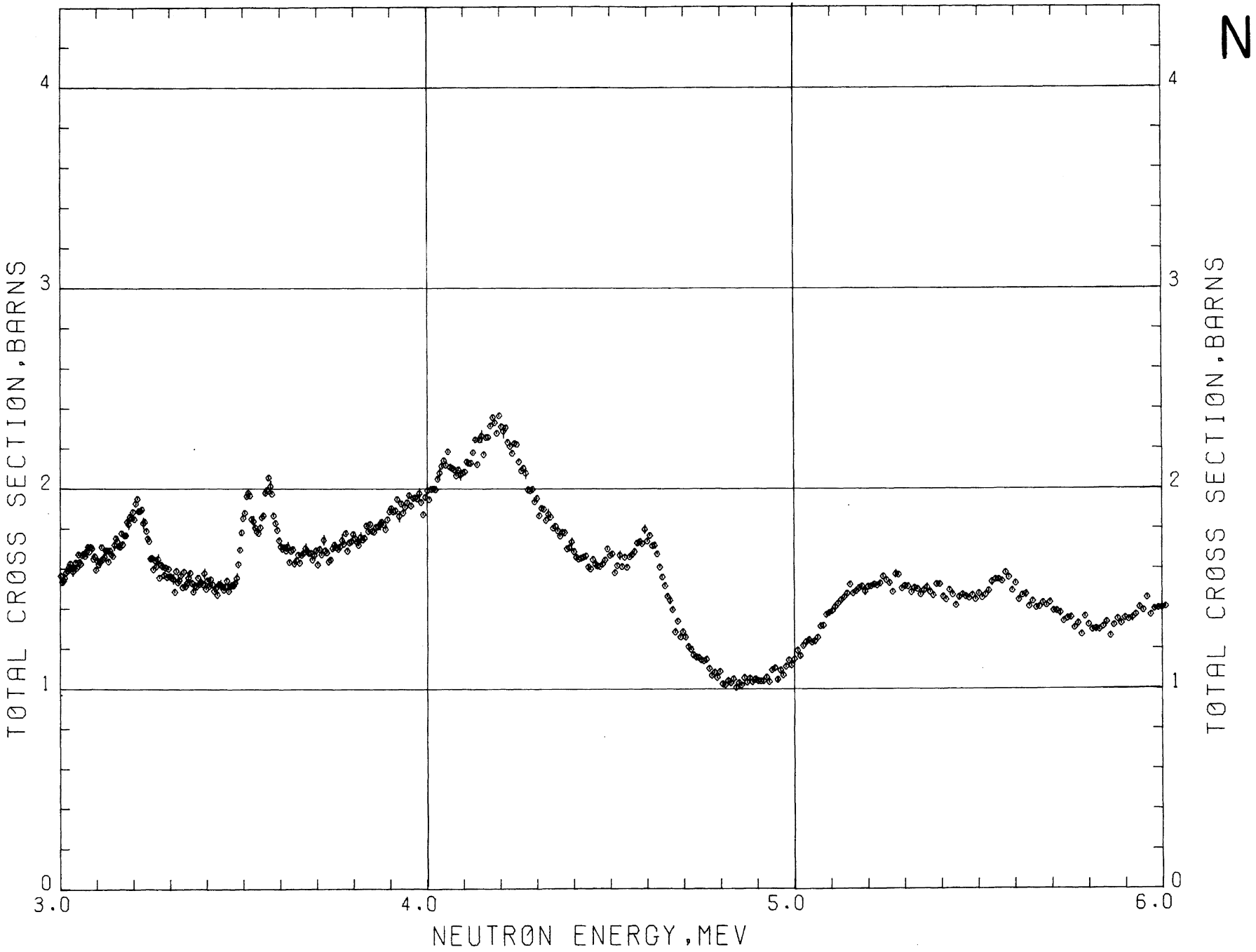
TOTAL CROSS SECTION, BARNS
NEUTRON ENERGY, MEV
3.0
4.0
5.0
6.0
0
1
2
3
4

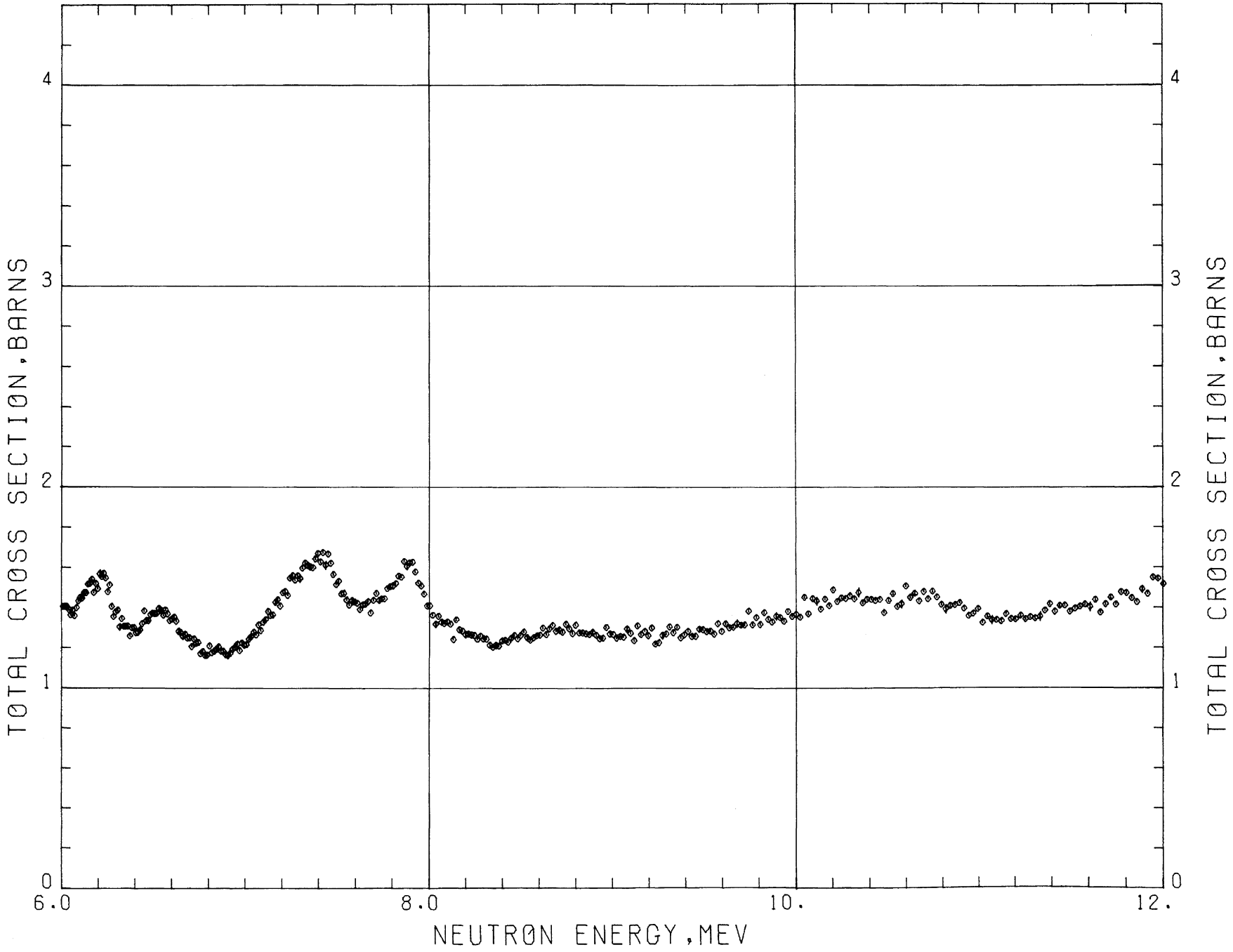
N
TOTAL CROSS SECTION, BARNS
TOTAL CROSS SECTION, BARNS
0
1
2
3
4
6.0
8.0
10.
12.
NEUTRON ENERGY, MEV

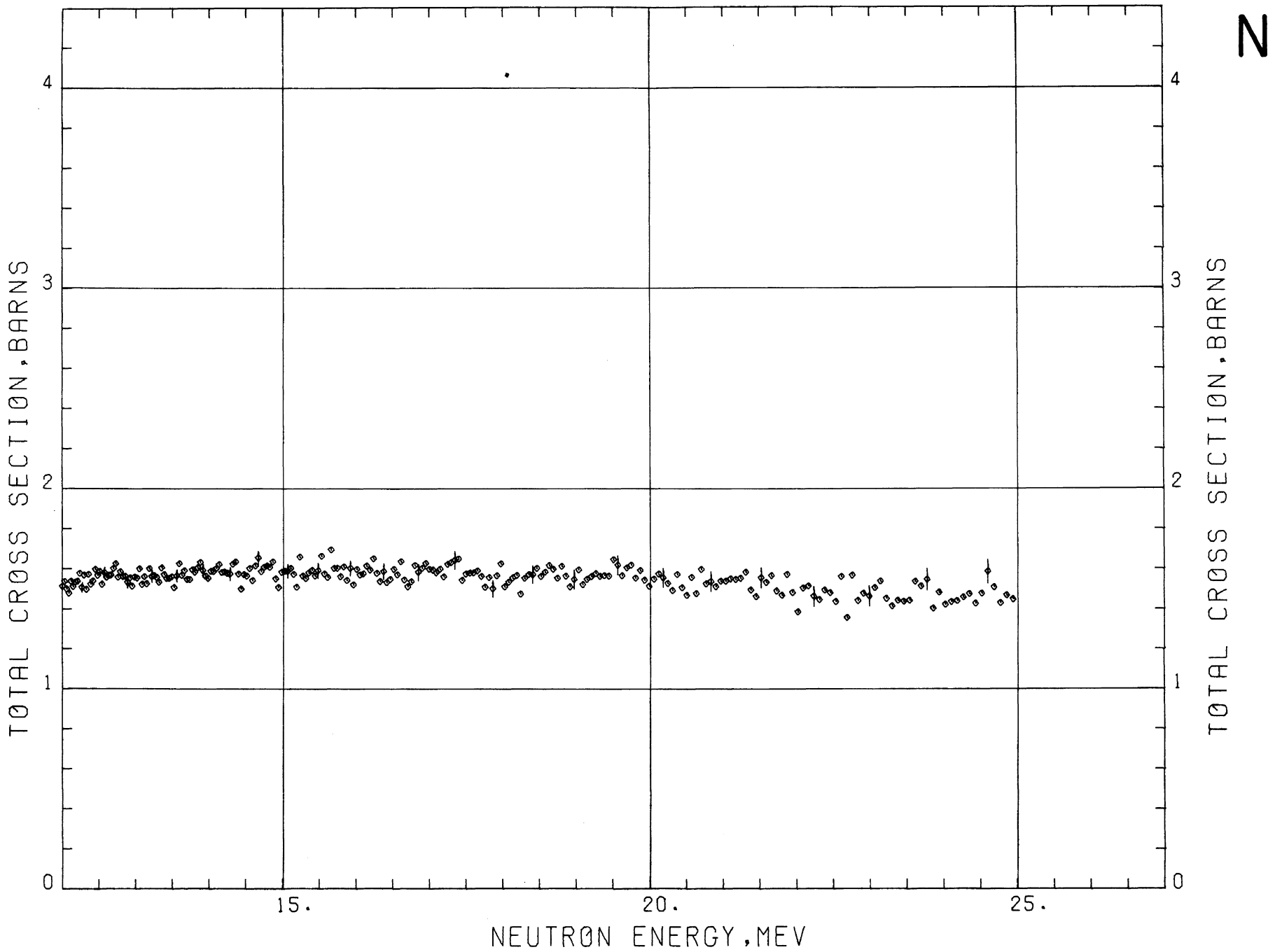
N
TOTAL CROSS SECTION, BARNS
0
1
2
3
4
15.
20.
25.
NEUTRON ENERGY, MEV

OXYGEN

Sample Material: quartz (SiO_2) single crystals

open: semiconductor grade silicon

Sample diameter: 5.08 cm

Sample thickness: 7.54 cm; $n = 0.396$ atoms/barn

29.98 cm; $n = 1.576$ atoms/barn

Literature Reference: R. A. Schrack, R. B. Schwartz, and H. T. Heaton II, Bull. Am. Phys. Soc. 17, 555 (1972).

Comments: Equality of silicon atoms/barn in the quartz and silicon samples can be deduced from the absence of structure due to silicon in the measured oxygen cross section. The statistical precision is degraded where there are large peaks in the silicon cross section (e.g., 570 keV), but there are no net fluctuations.

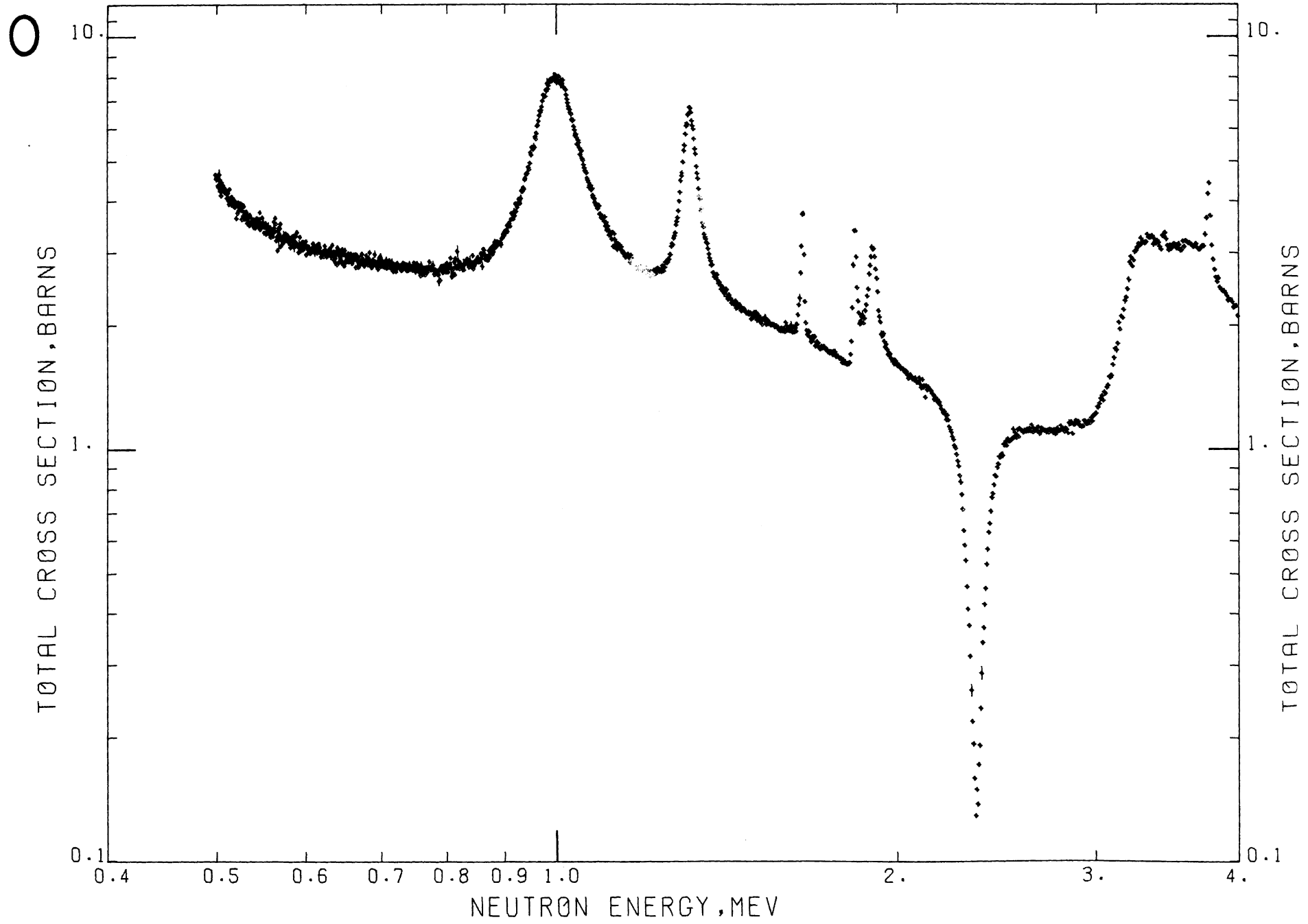
O
10.
1.
0.1
TOTAL CROSS SECTION, BARNS
0.4
0.5
0.6
0.7
0.8
0.9
1.0
2.
3.
4.
NEUTRON ENERGY, MEV

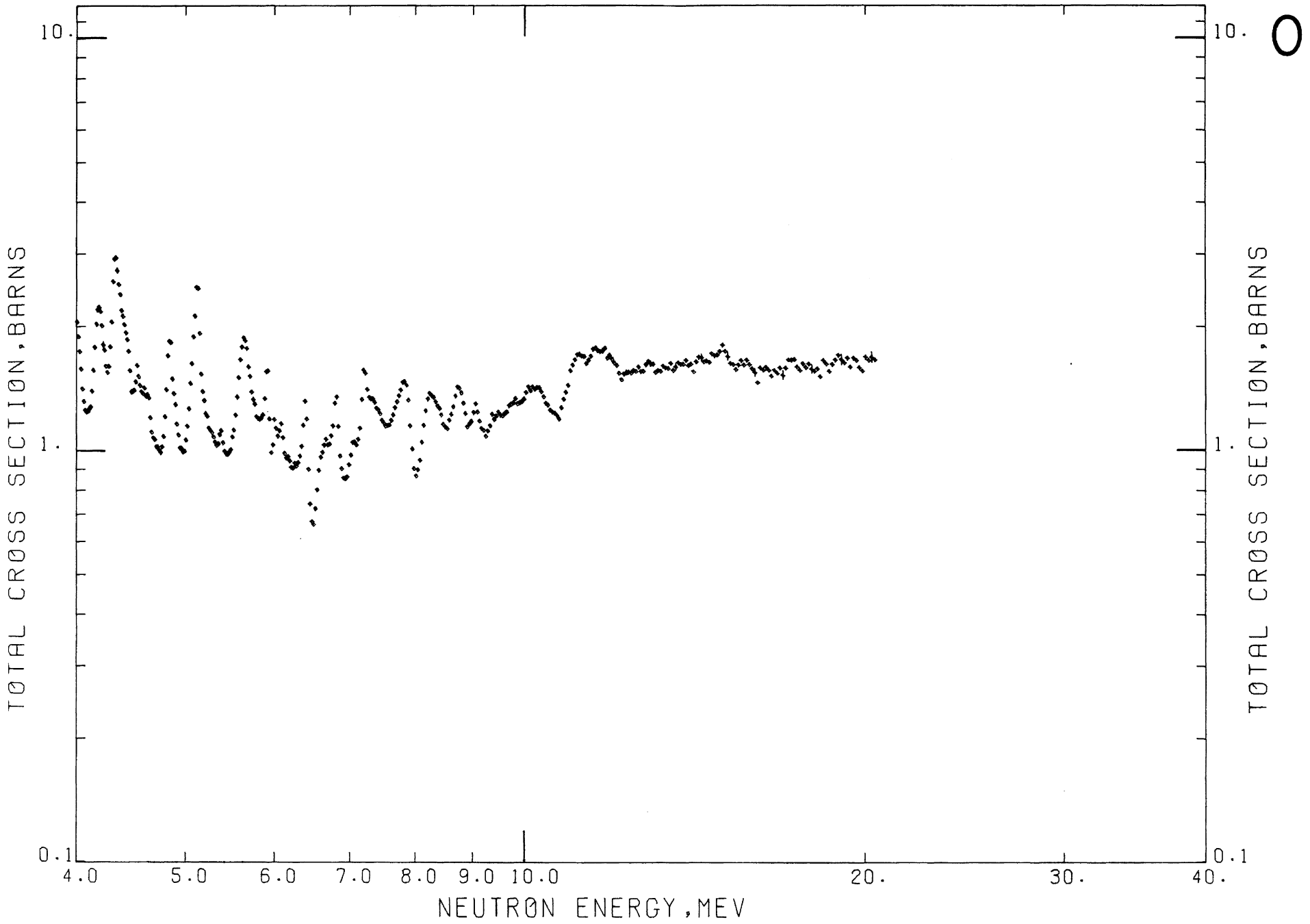
10.
1.
0.1
TOTAL CROSS SECTION, BARNS
4.0
5.0
6.0
7.0
8.0
9.0
10.0
20.
30.
40.
NEUTRON ENERGY, MEV
O

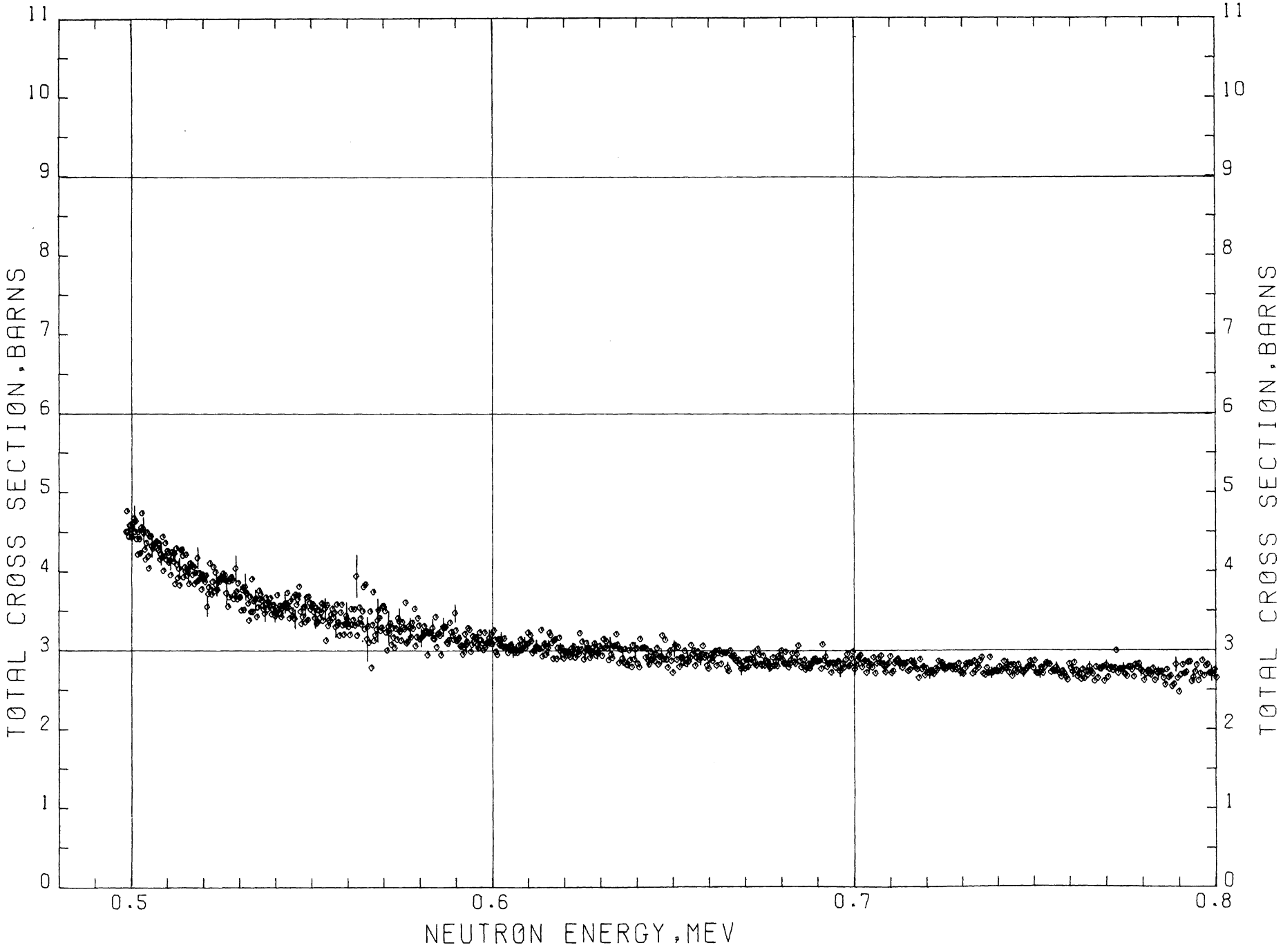
TOTAL CROSS SECTION, BARNS
NEUTRON ENERGY, MEV
0
1
2
3
4
5
6
7
8
9
10
11
0.5
0.6
0.7
0.8

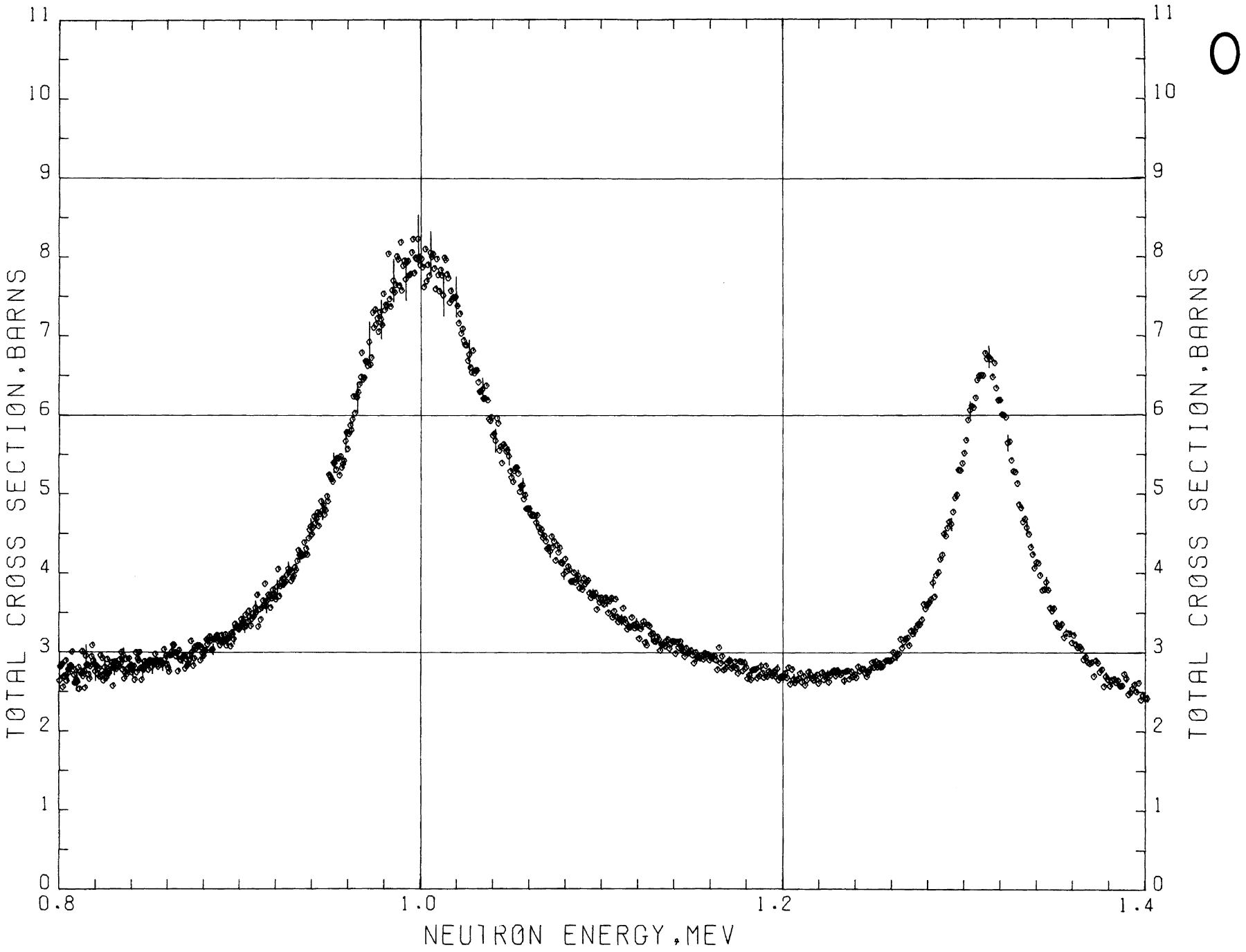
TOTAL CROSS SECTION, BARNS
NEUTRON ENERGY, MEV
0
1
2
3
4
5
6
7
8
9
10
11
0.8
1.0
1.2
1.4

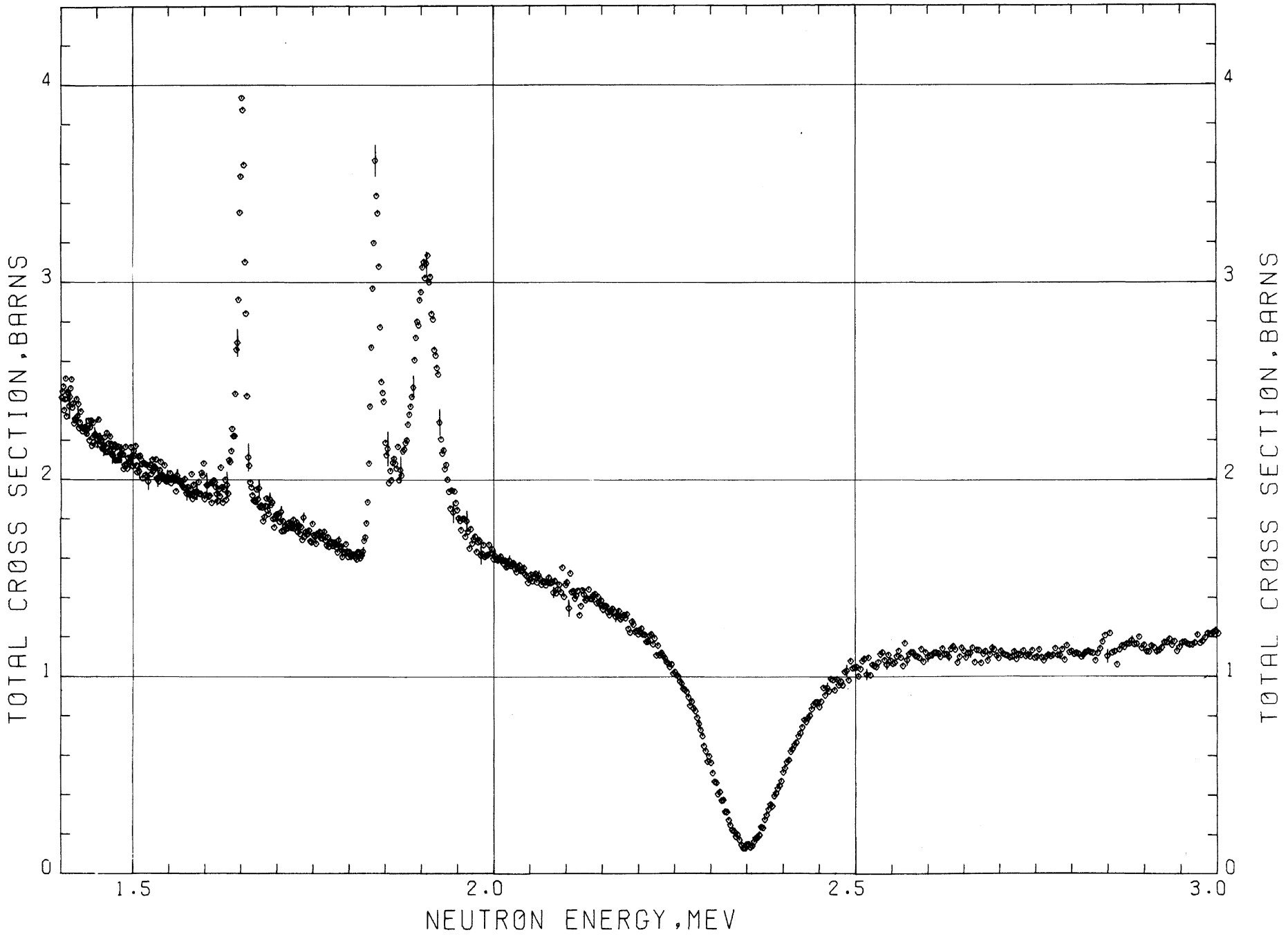
TOTAL CROSS SECTION, BARNS
NEUTRON ENERGY, MEV
0
1
2
3
4
1.5
2.0
2.5
3.0

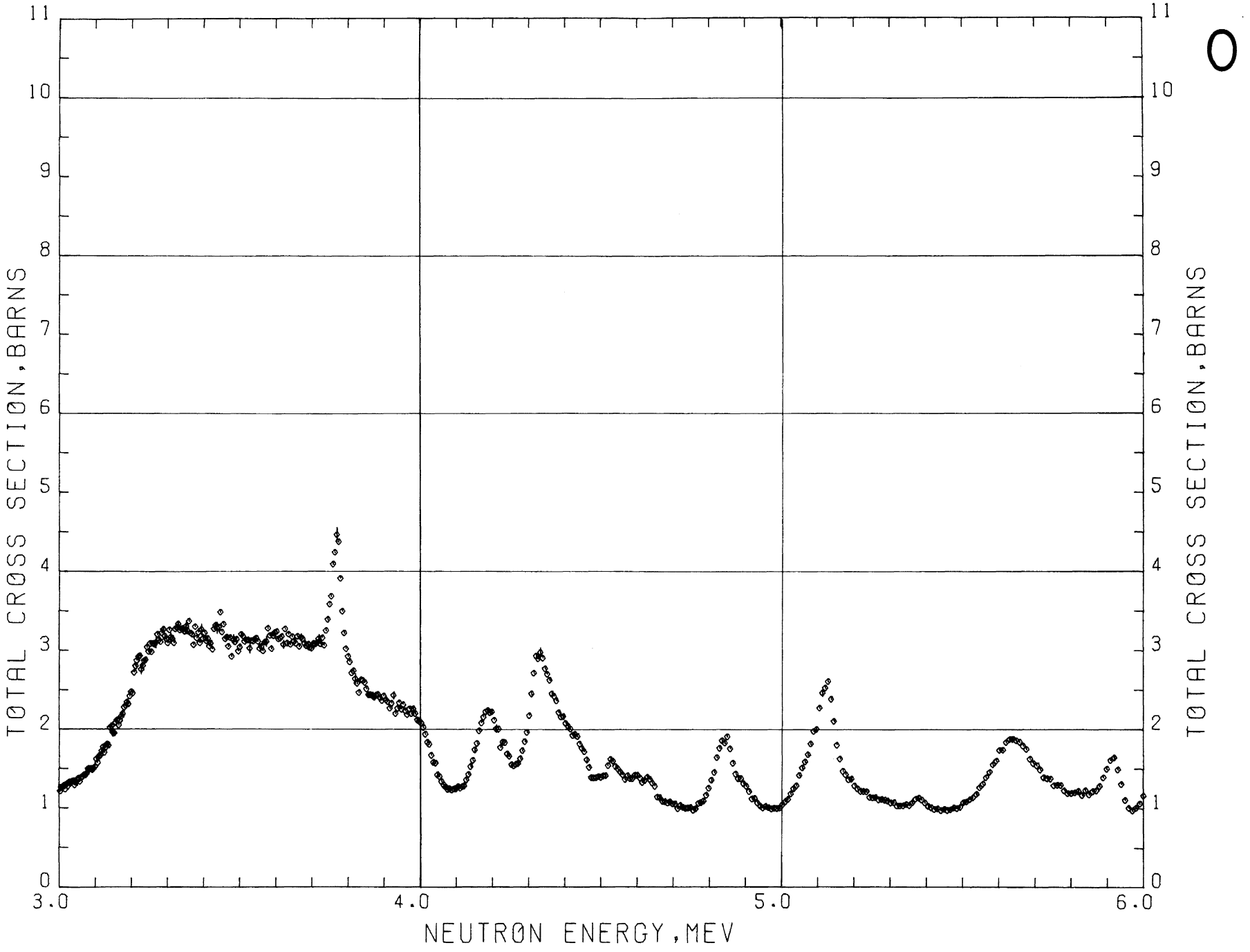
TOTAL CROSS SECTION, BARNS
NEUTRON ENERGY, MEV
0
1
2
3
4
5
6
7
8
9
10
11
3.0
4.0
5.0
6.0

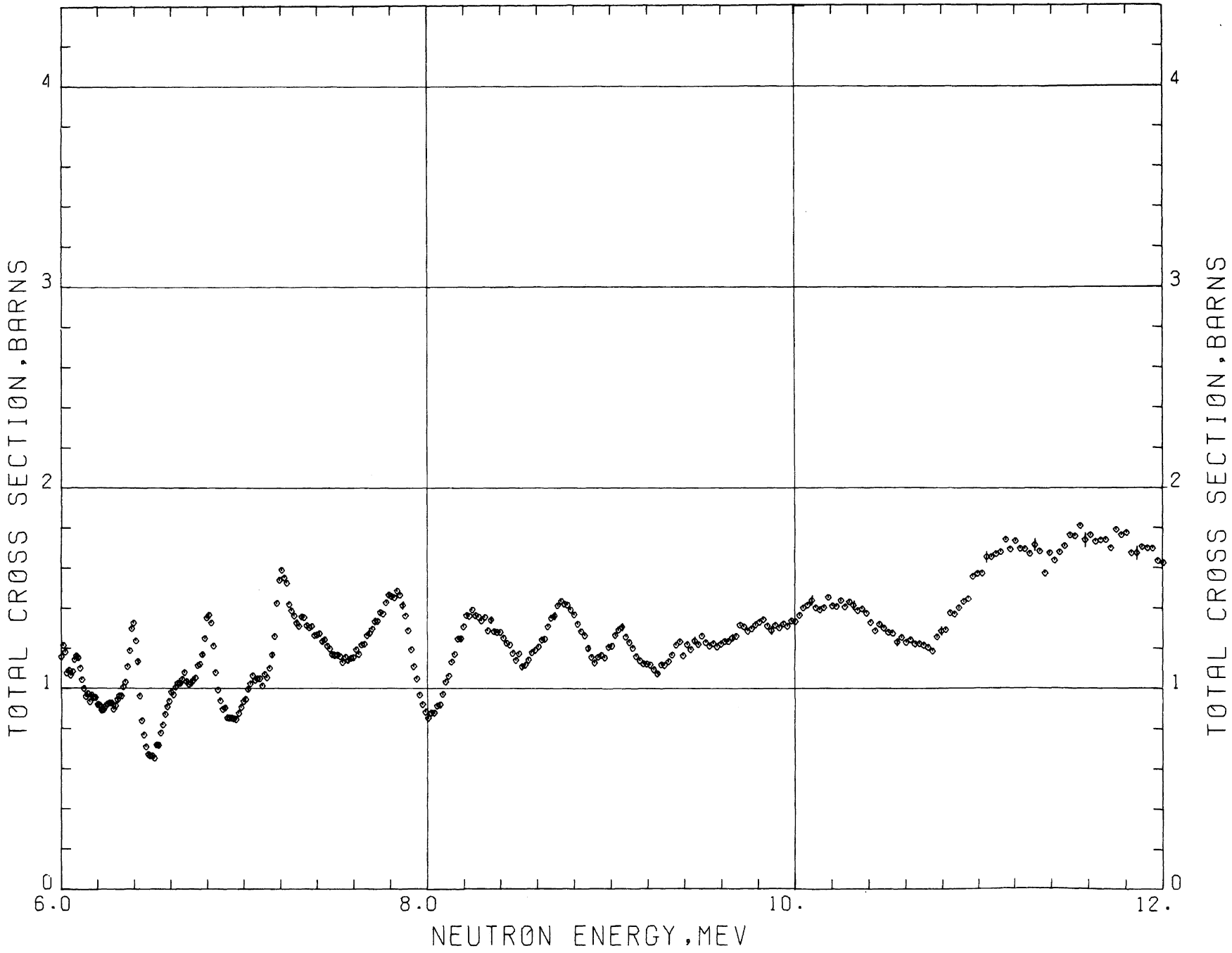
TØTAL CRØSS SECTIØN, BARNS
NEUTRØN ENERGY, MEV
6.0
8.0
10.
12.
0
1
2
3
4

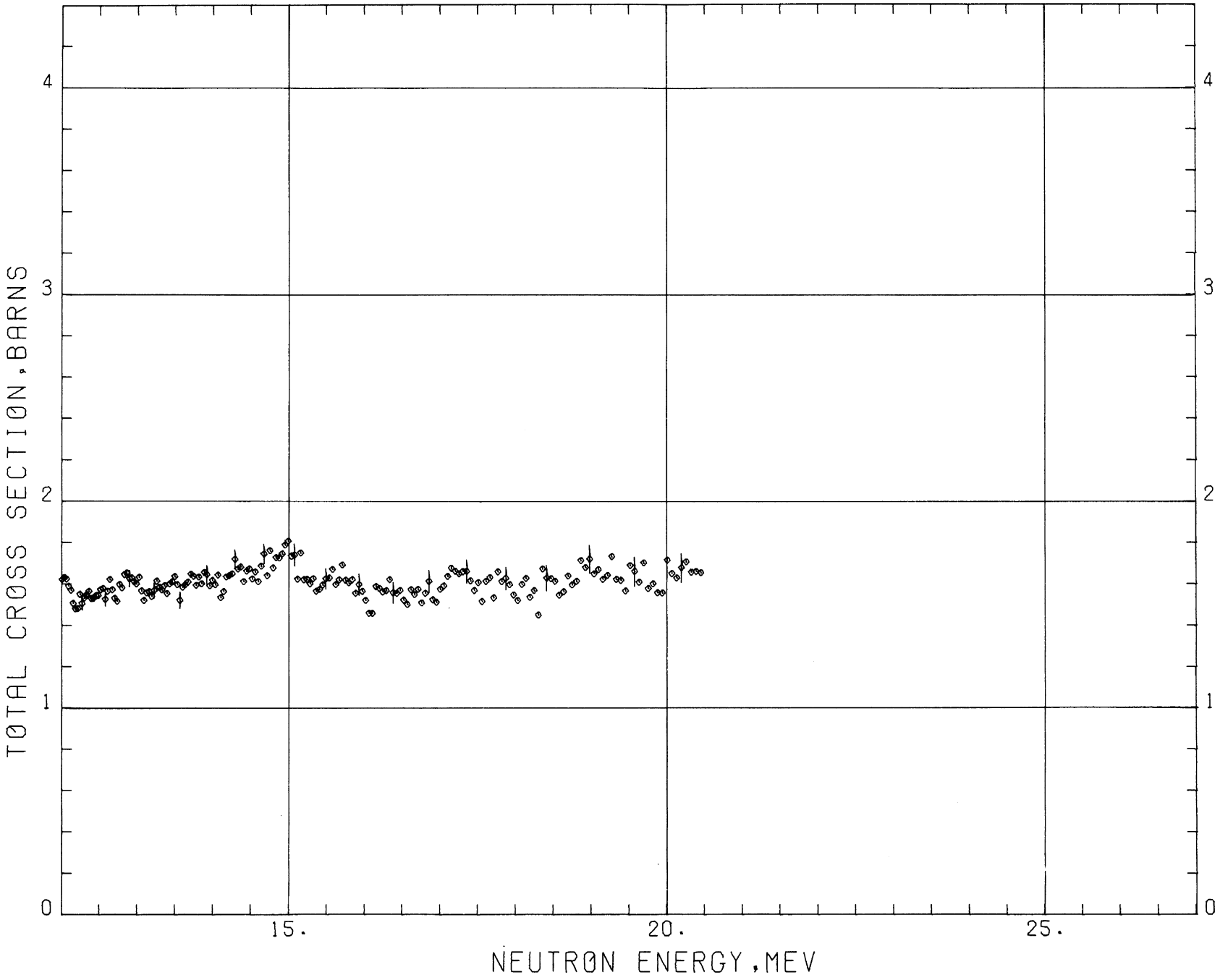
TOTAL CROSS SECTION, BARNS
0
1
2
3
4
15.
20.
25.
NEUTRON ENERGY, MEV

ALUMINUM

Sample Material: metallic aluminum plate

Sample Diameter: 12.7 cm

Sample Thickness: 11.3 cm, $n = 0.6858$ atoms/barn

Analysis: The samples were fabricated from 1100 grade aluminum. The principal impurities were 0.62 percent iron and 0.16 percent copper. All other impurities were less than 0.1 percent.

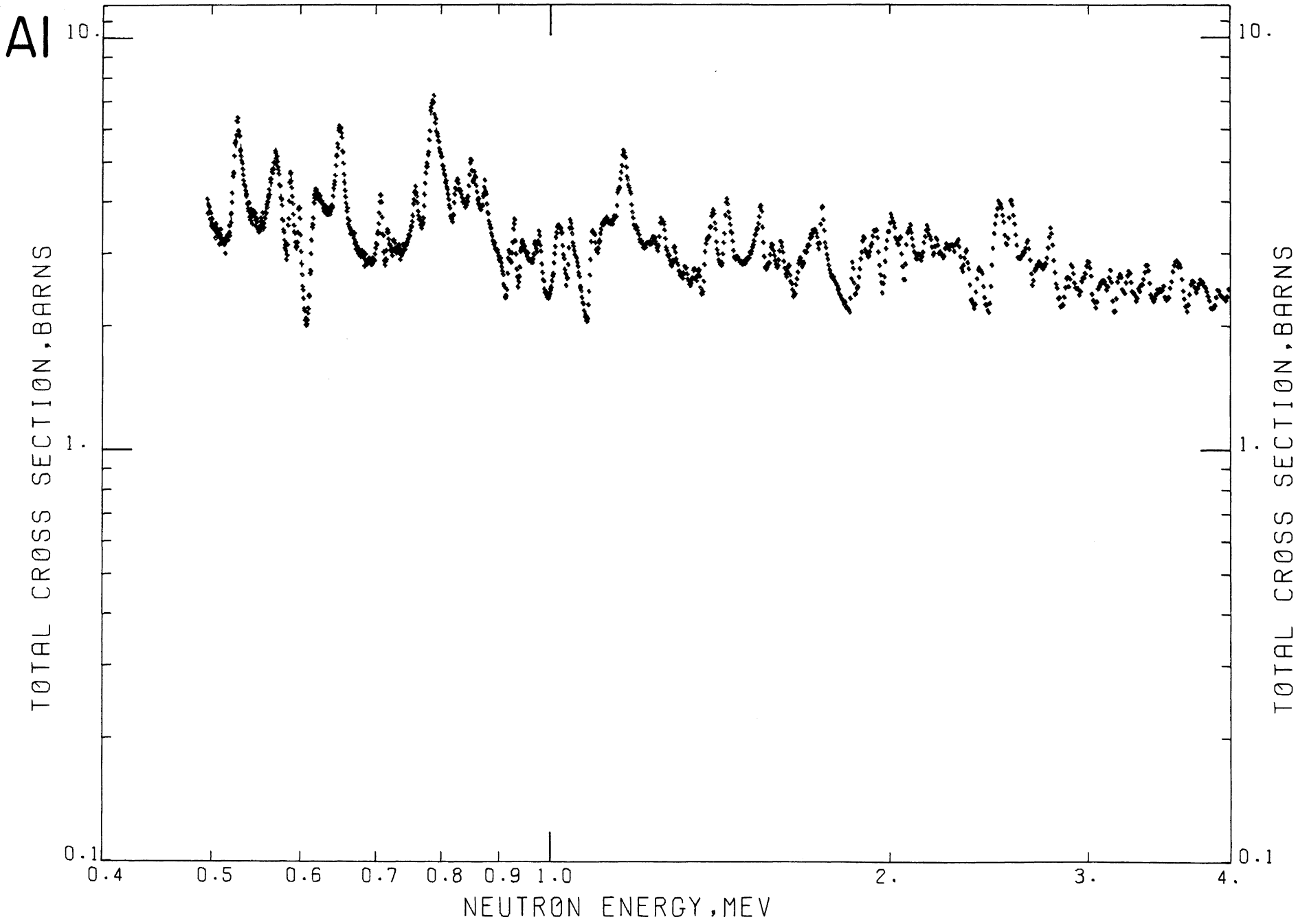
Al
10.
1.
0.1
TOTAL CROSS SECTION, BARNS
0.4
0.5
0.6
0.7
0.8
0.9
1.0
2.
3.
4.
NEUTRON ENERGY, MEV

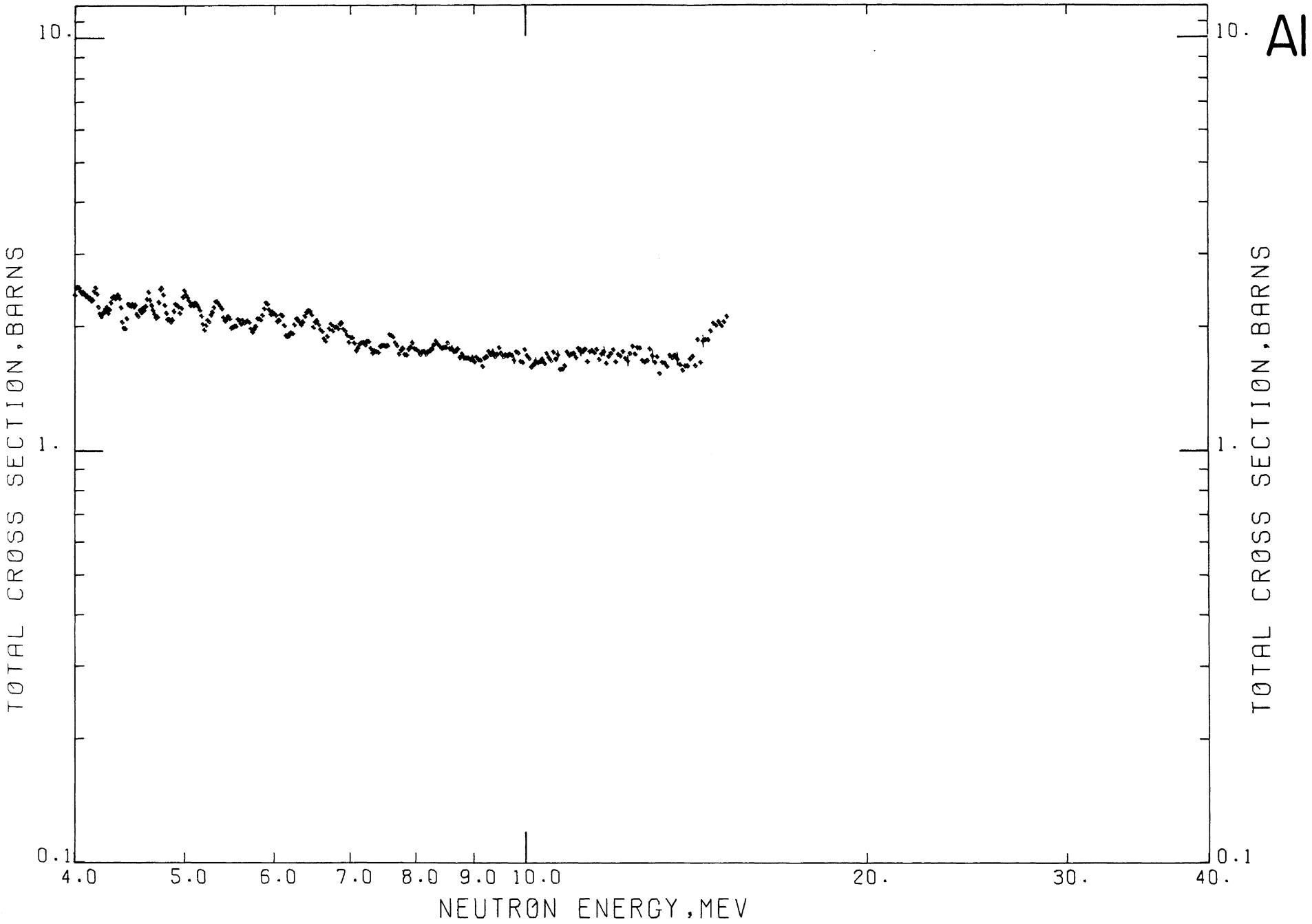
Al
10.
1.
0.1
TØTAL CRØSS SECTIØN,BARNS
4.0
5.0
6.0
7.0
8.0
9.0
10.0
20.
30.
40.
NEUTRØN ENERGY,MEV

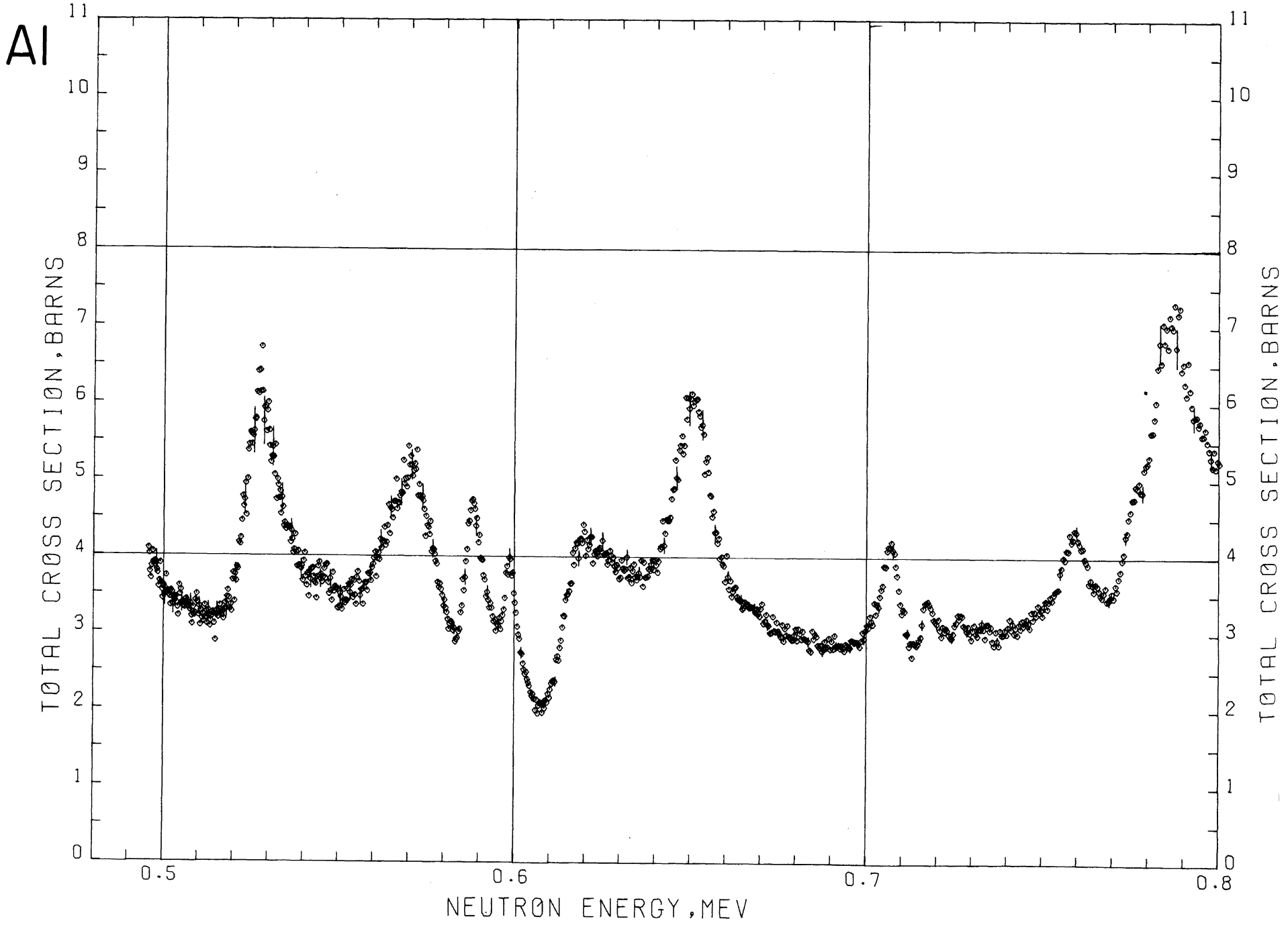
Al
TOTAL CROSS SECTION, BARNS
NEUTRON ENERGY, MEV
0.5
0.6
0.7
0.8
0
1
2
3
4
5
6
7
8
9
10
11

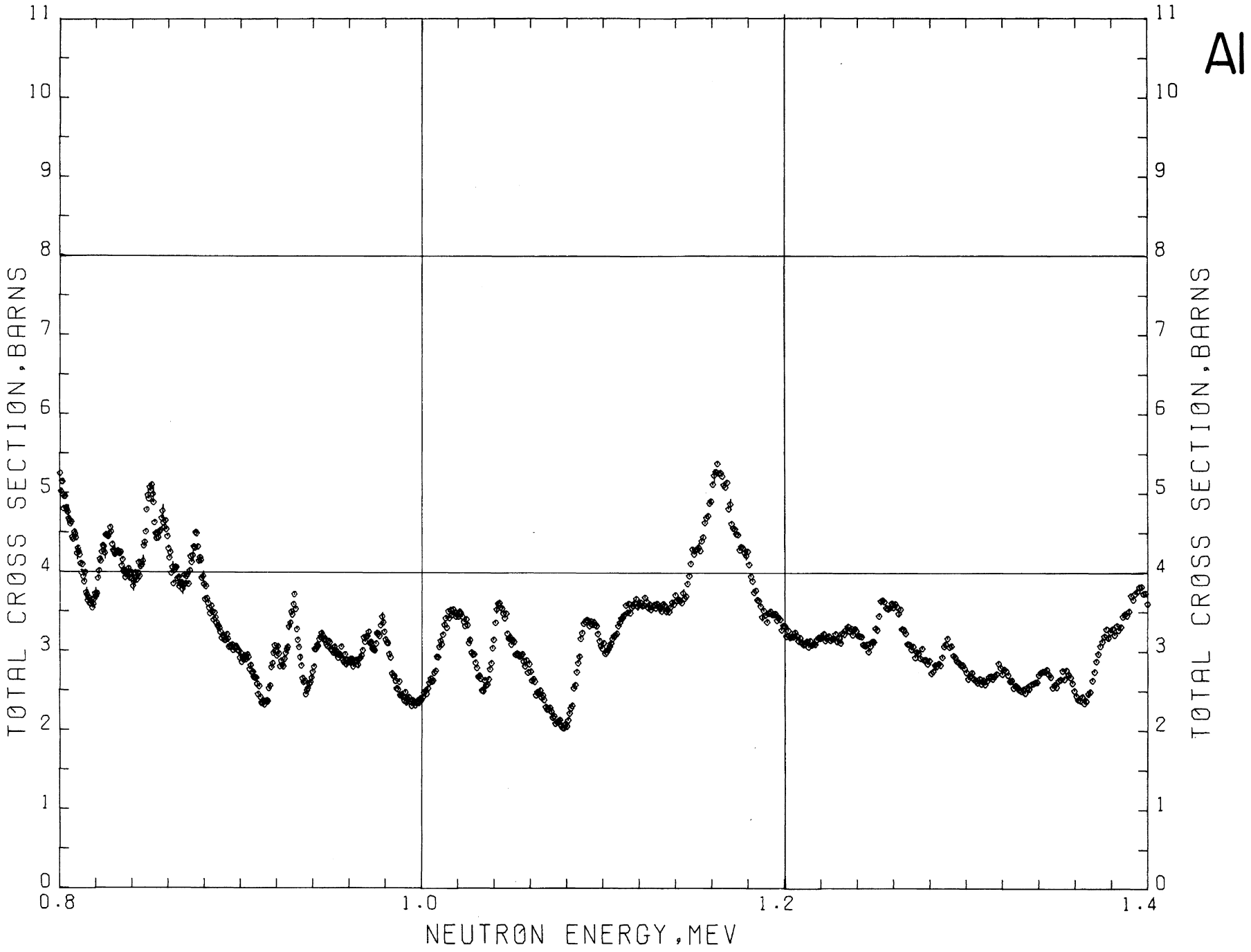
Al
TOTAL CROSS SECTION, BARNS
NEUTRON ENERGY, MEV
0
1
2
3
4
5
6
7
8
9
10
11
0.8
1.0
1.2
1.4

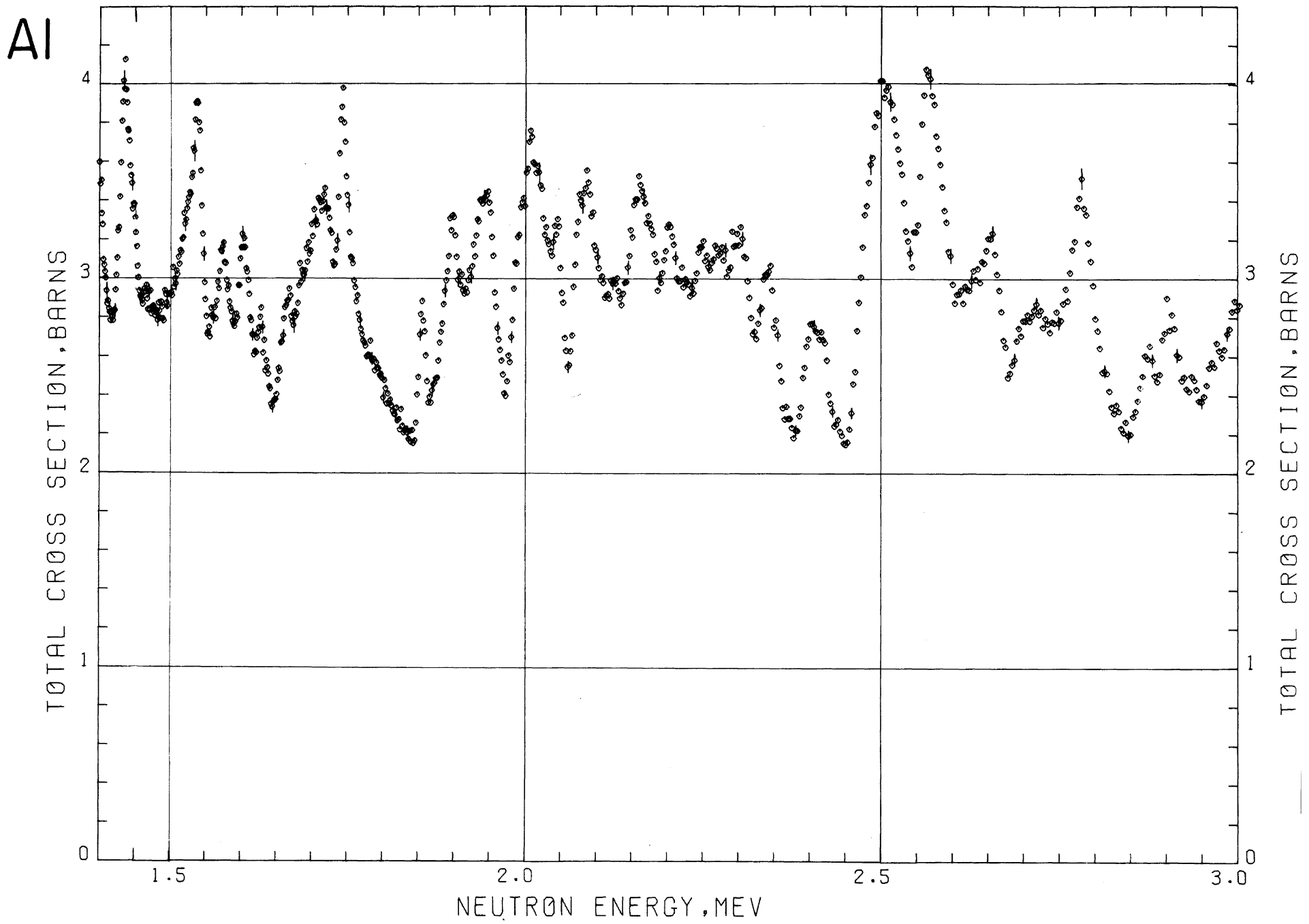
Al
TOTAL CROSS SECTION, BARNS
NEUTRON ENERGY, MEV
0
1
2
3
4
1.5
2.0
2.5
3.0

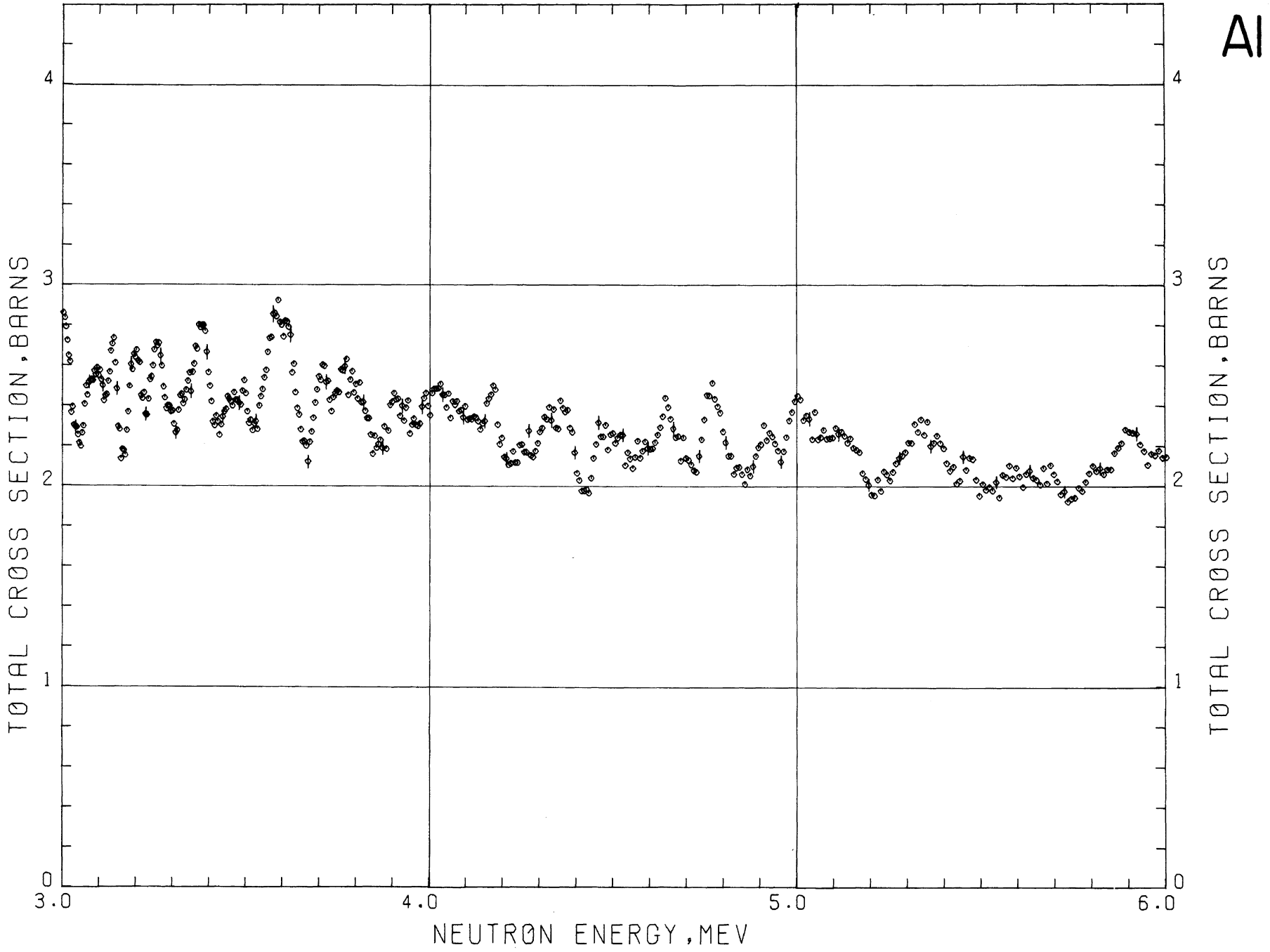
Al
TOTAL CROSS SECTION, BARNS
TOTAL CROSS SECTION, BARNS
0
1
2
3
4
3.0
4.0
5.0
6.0
NEUTRON ENERGY, MEV

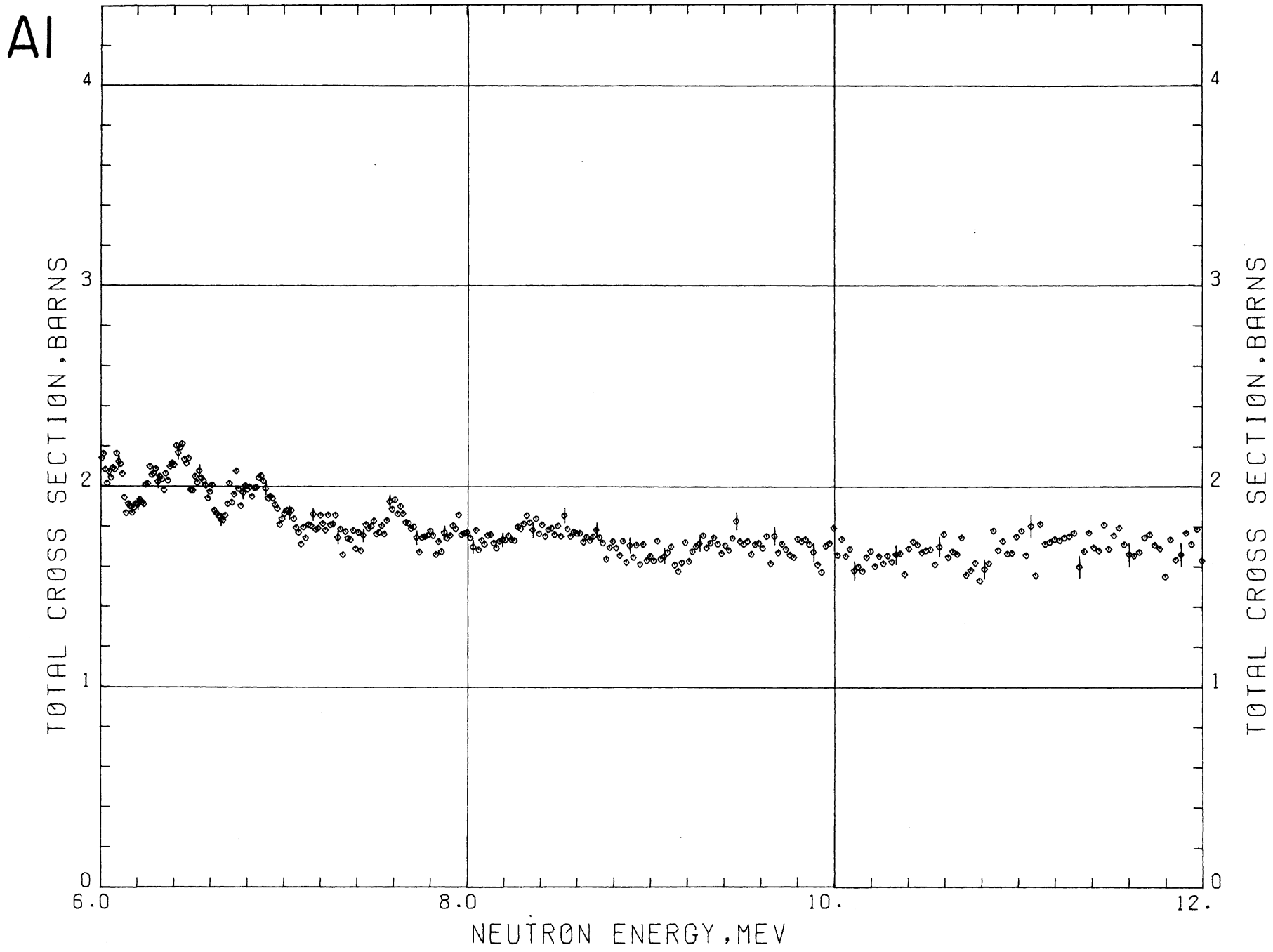
Al
TOTAL CROSS SECTION, BARNS
NEUTRON ENERGY, MEV
0
1
2
3
4
6.0
8.0
10.
12.

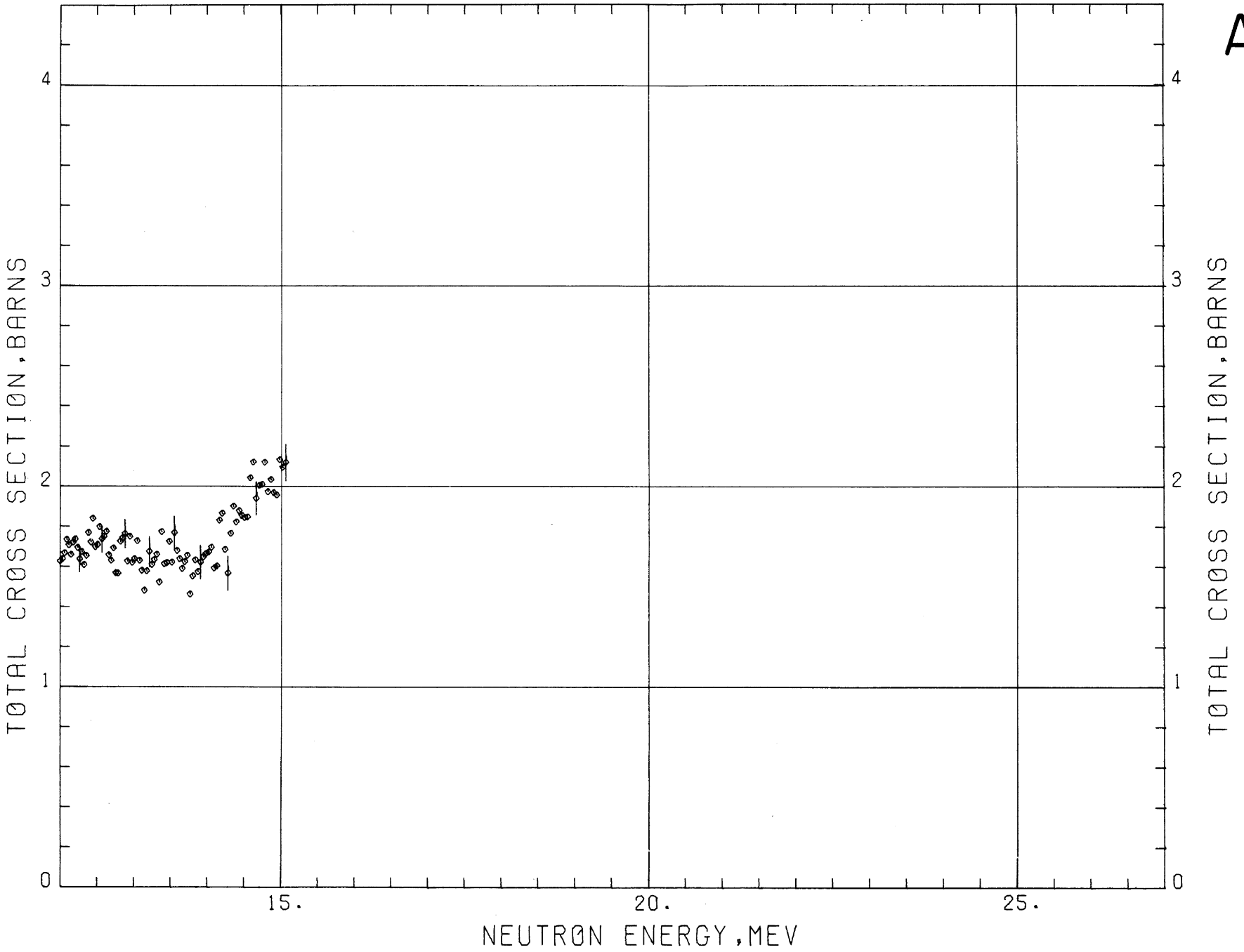
Al
TOTAL CROSS SECTION, BARNS
TOTAL CROSS SECTION, BARNS
0
1
2
3
4
15.
20.
25.
NEUTRON ENERGY, MEV

SILICON

Sample Material: polycrystalline silicon bar

Sample Diameter: 5.08 cm

Sample Thickness: 4.6 cm, $n = 0.2294$ atoms/barn

17.9 cm, $n = 0.8957$ atoms/barn

Literature Reference: R. A. Schrack, R. B. Schwartz, and H. T. Heaton II, Bull. Am. Phys. Soc. **16,** 495 (1971).

Comments: The samples were semiconductor grade silicon having impurity levels $< 10^{-6}$.

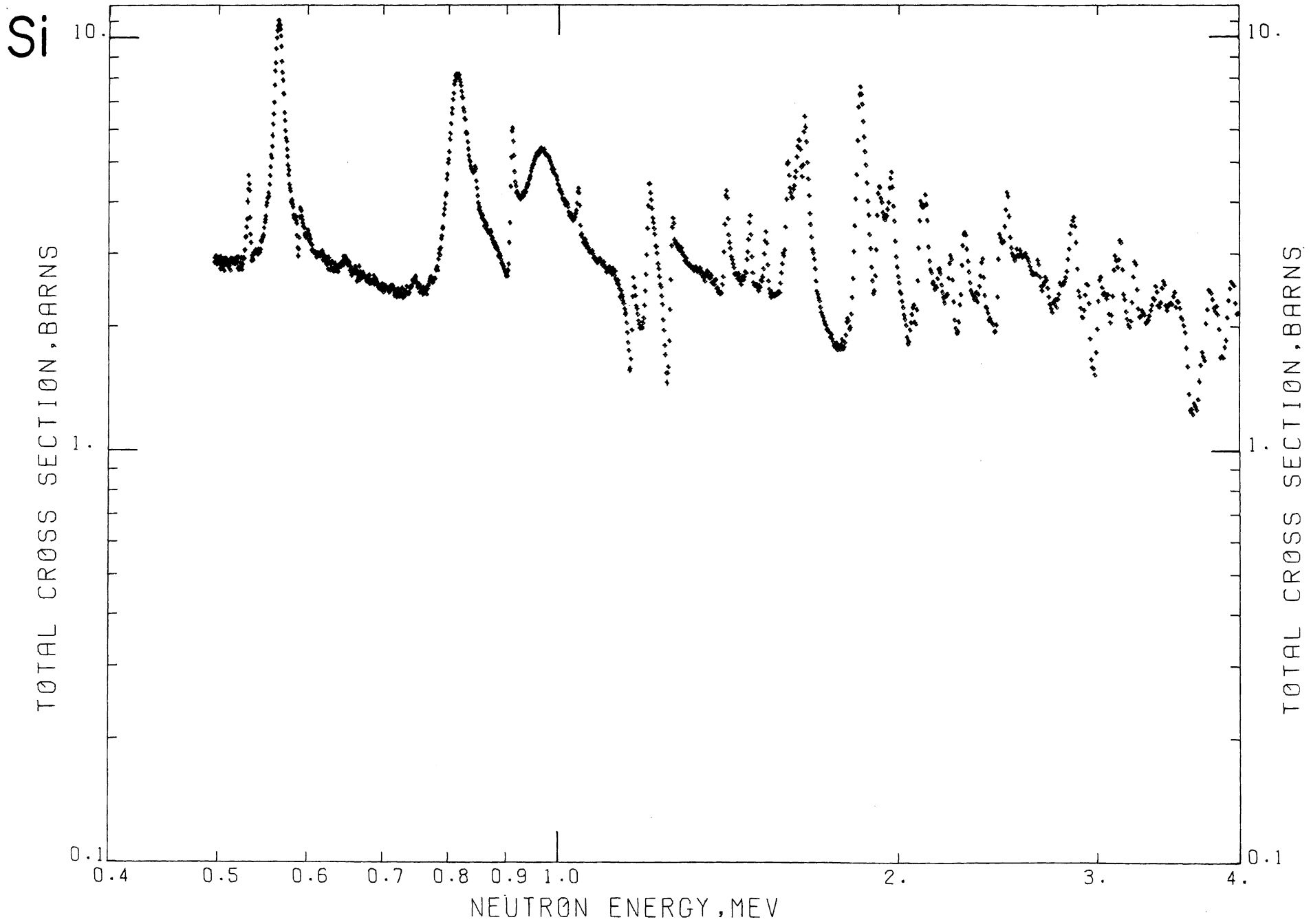
Si
10.
1.
0.1
TOTAL CROSS SECTION, BARNS
0.4
0.5
0.6
0.7
0.8
0.9
1.0
2.
3.
4.
NEUTRON ENERGY, MEV

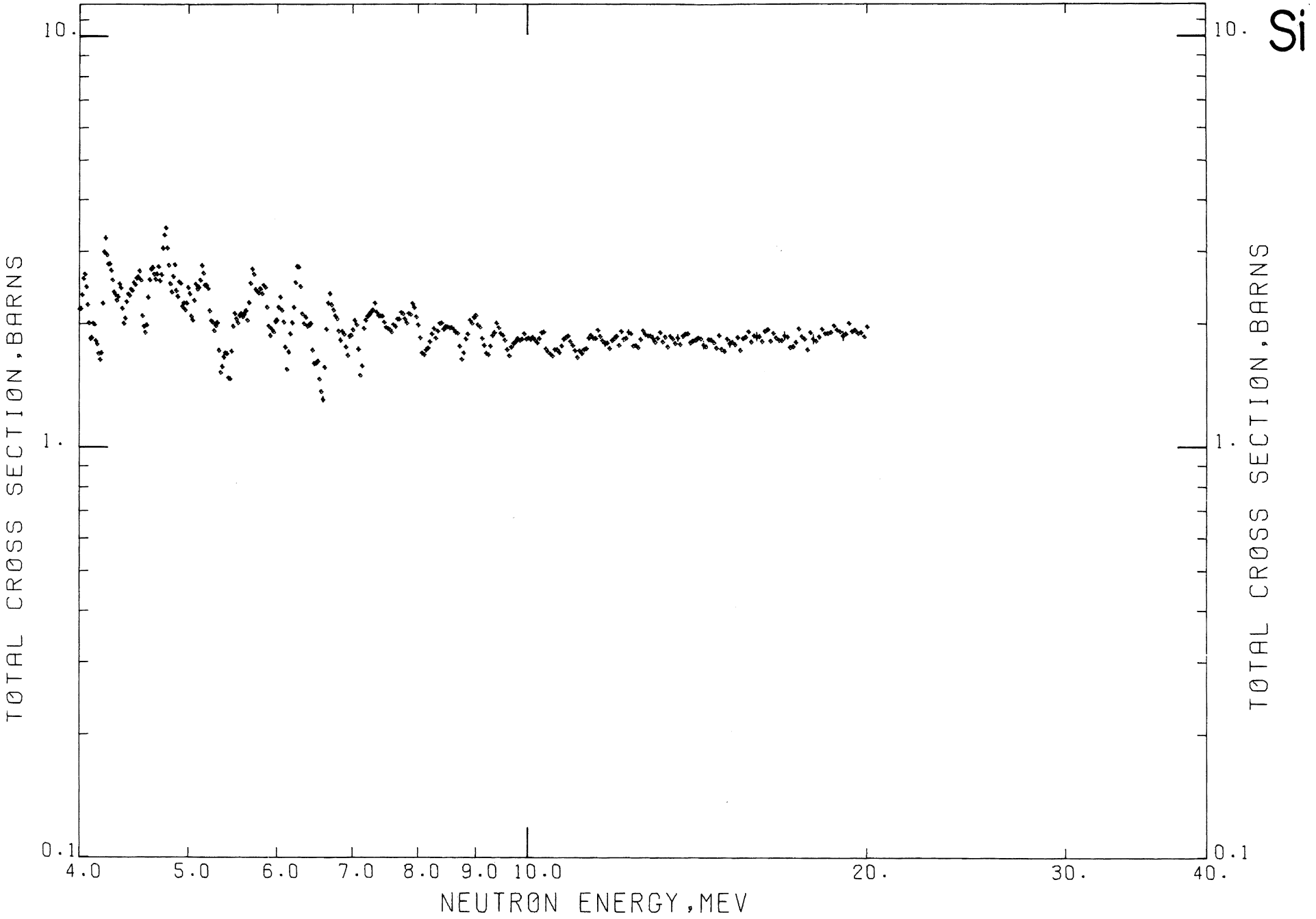
Si
TOTAL CROSS SECTION, BARNS
10.
1.
0.1
4.0
5.0
6.0
7.0
8.0
9.0
10.0
20.
30.
40.
NEUTRON ENERGY, MEV

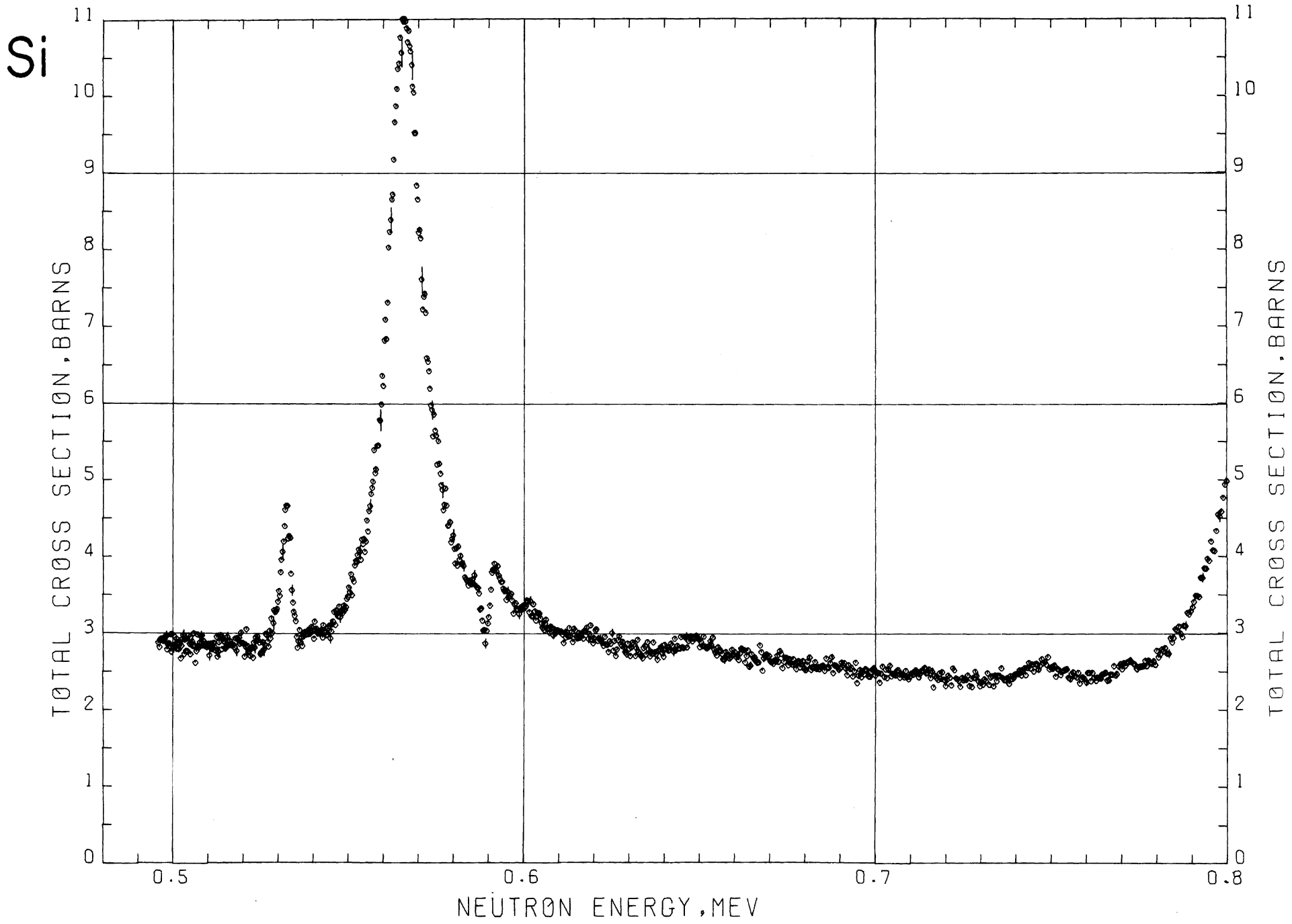
Si
TØTAL CRØSS SECTIØN, BARNS
NEUTRØN ENERGY, MEV
0
1
2
3
4
5
6
7
8
9
10
11
0.5
0.6
0.7
0.8

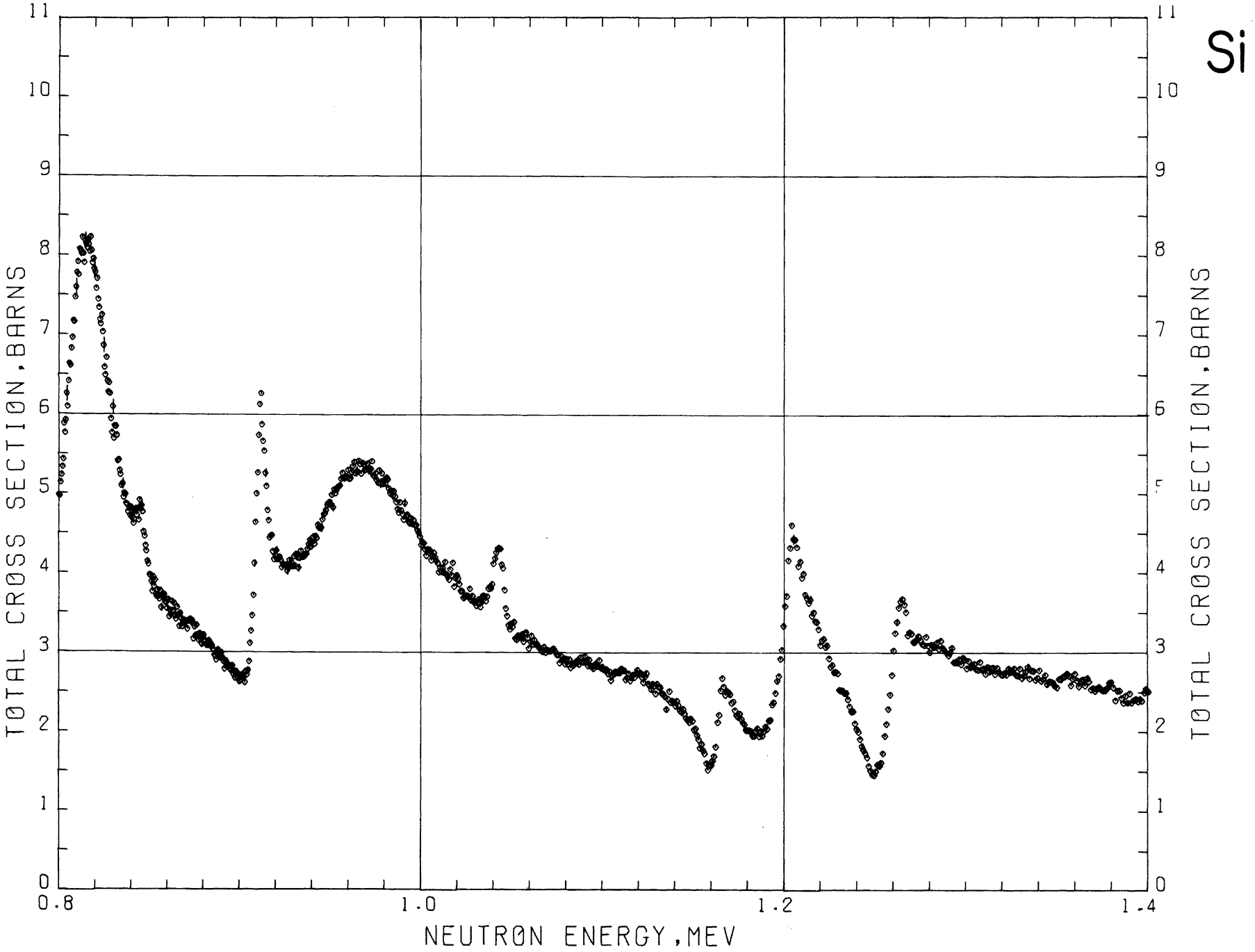
Si
TOTAL CROSS SECTION, BARNS
NEUTRON ENERGY, MEV
0.8
1.0
1.2
1.4
0
1
2
3
4
5
6
7
8
9
10
11

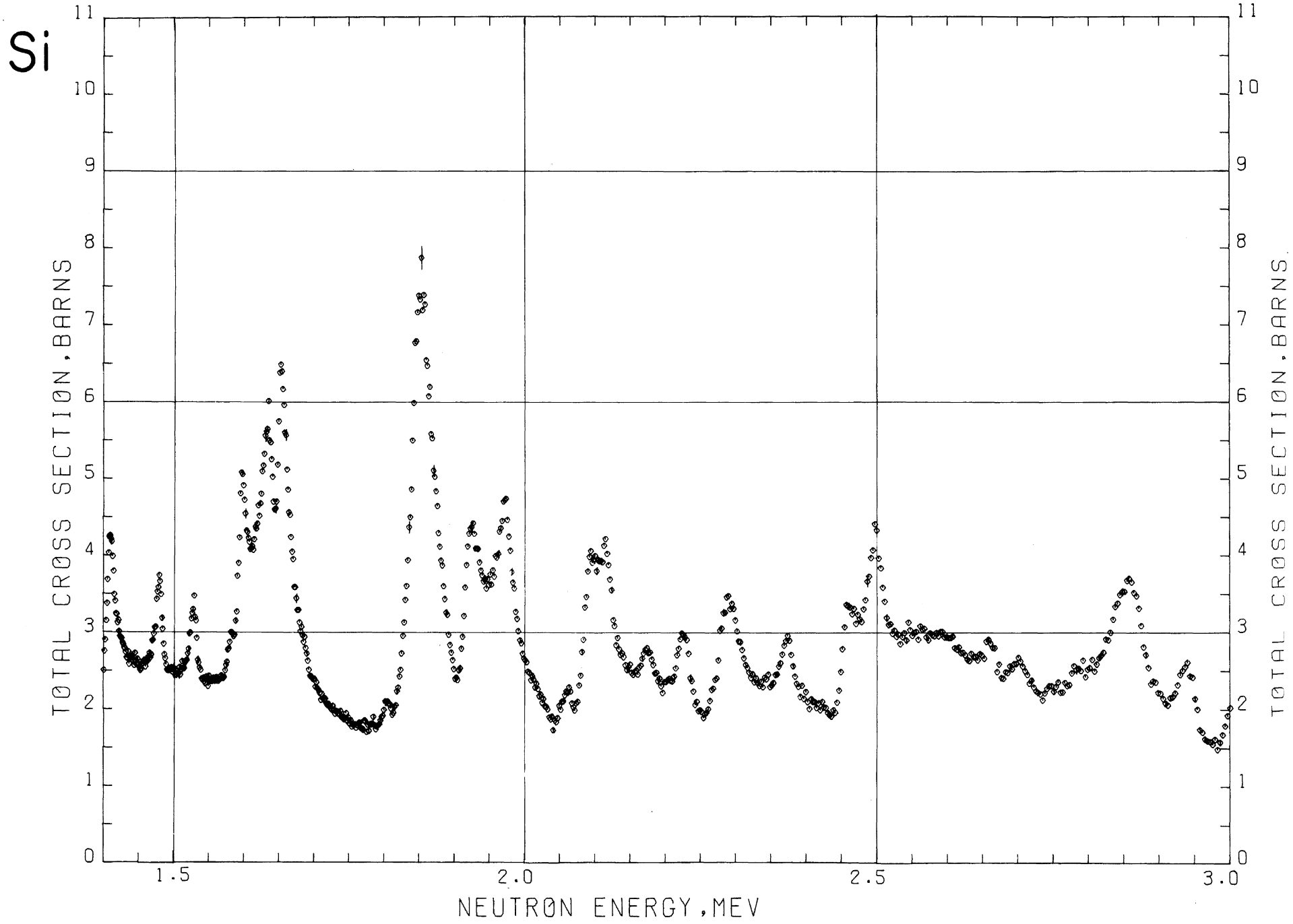
Si
TOTAL CROSS SECTION, BARNS
NEUTRON ENERGY, MEV
0
1
2
3
4
5
6
7
8
9
10
11
1.5
2.0
2.5
3.0

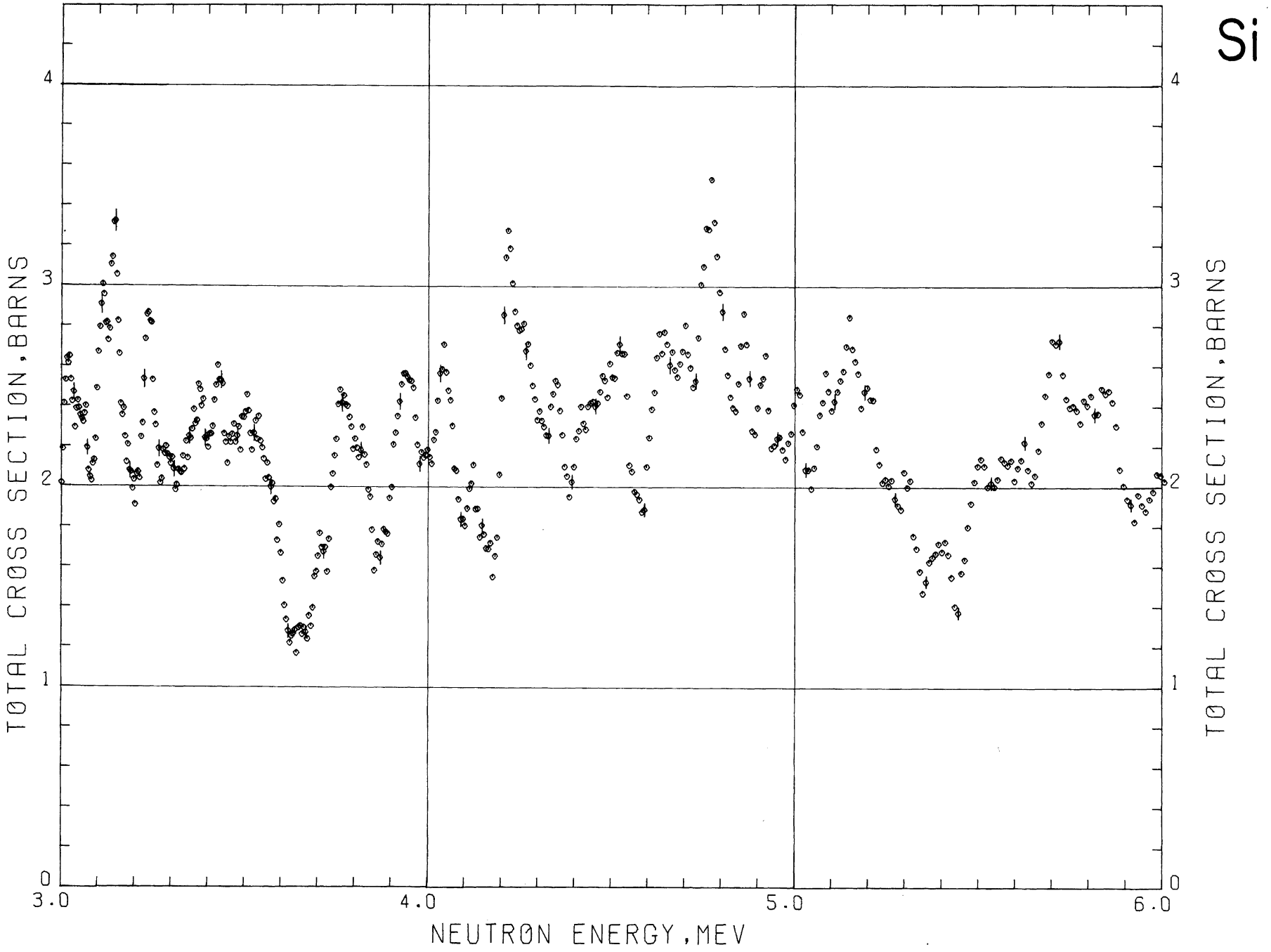
Si
TOTAL CROSS SECTION, BARNS
NEUTRON ENERGY, MEV
0
1
2
3
4
3.0
4.0
5.0
6.0

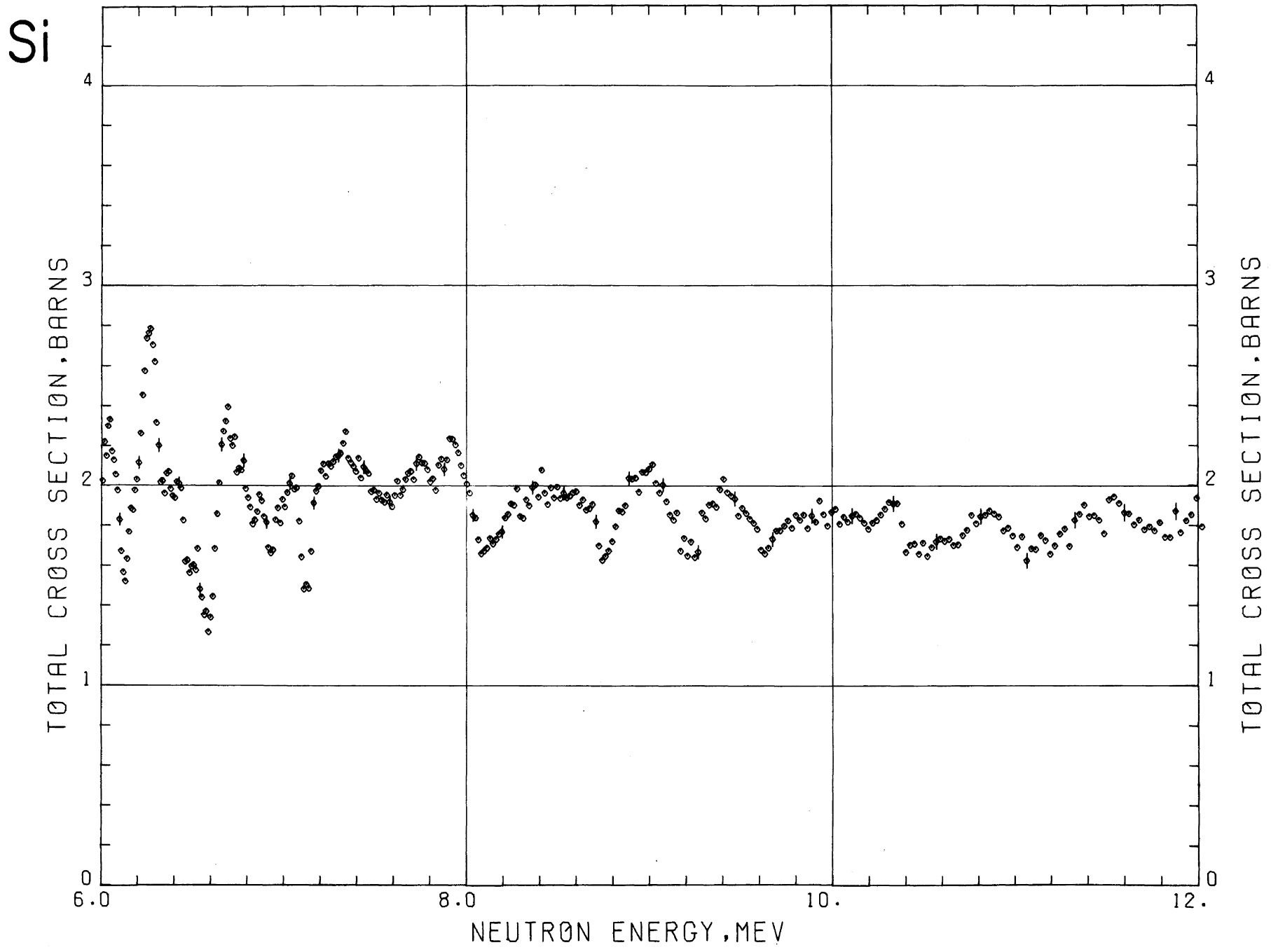
Si
TOTAL CROSS SECTION, BARNS
NEUTRON ENERGY, MEV
0
1
2
3
4
6.0
8.0
10.
12.

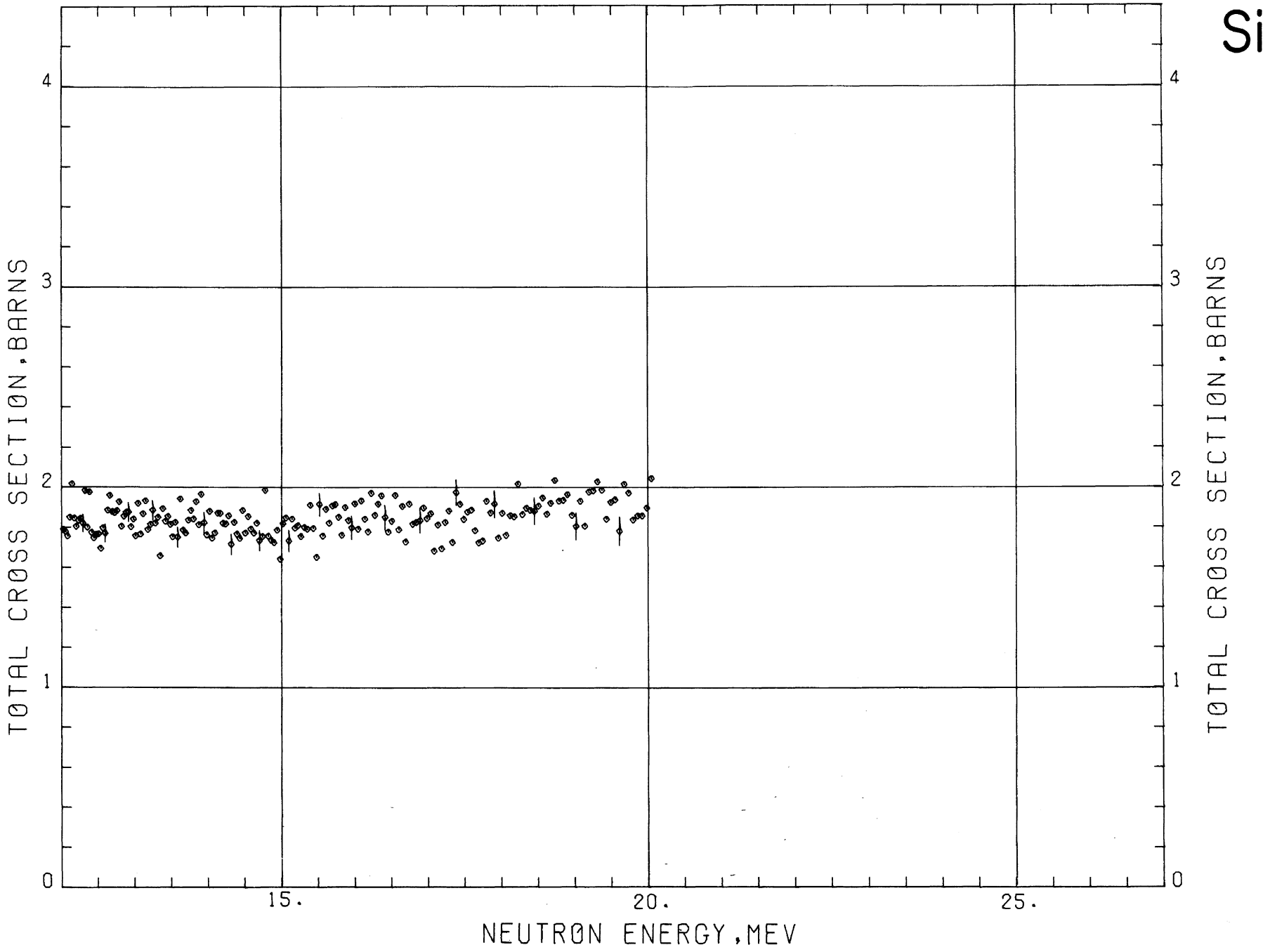
Si
TOTAL CROSS SECTION, BARNS
TOTAL CROSS SECTION, BARNS
0
1
2
3
4
15.
20.
25.
NEUTRON ENERGY, MEV

CALCIUM

Sample Material: metallic calcium

Sample Diameter: 12.7 cm

Sample Thickness: 14.5 cm, $n = 0.3331$ atoms/barn
44.7 cm, $n = 1.027$ atoms/barn

Analysis: The samples were fabricated from 99 percent purity metal and placed in metal containers to prevent excessive oxidation. A qualitative spectrographic analysis of the samples disclosed the impurities of largest concentration were magnesium and strontium, both present in concentrations greater than 0.1 percent but less than 1 percent.

Literature Reference: R. A. Schrack, R. B. Schwartz, and H. T. Heaton II, Bull. Am. Phys. Soc. **17**, 555 (1972).

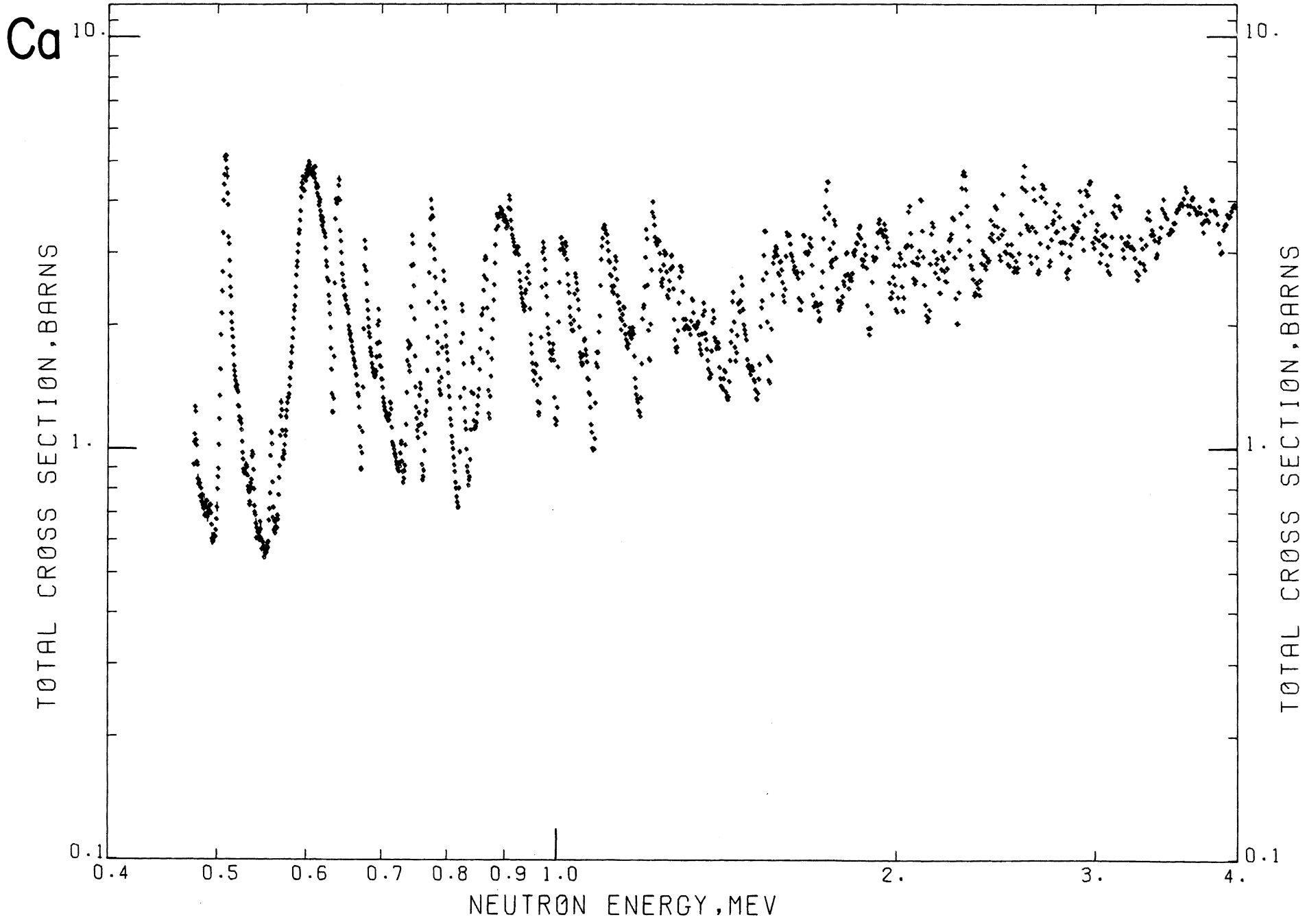
Ca
10.
1.
0.1
TØTAL CRØSS SECTIØN, BARNS
0.4
0.5
0.6
0.7
0.8
0.9
1.0
2.
3.
4.
NEUTRØN ENERGY, MEV

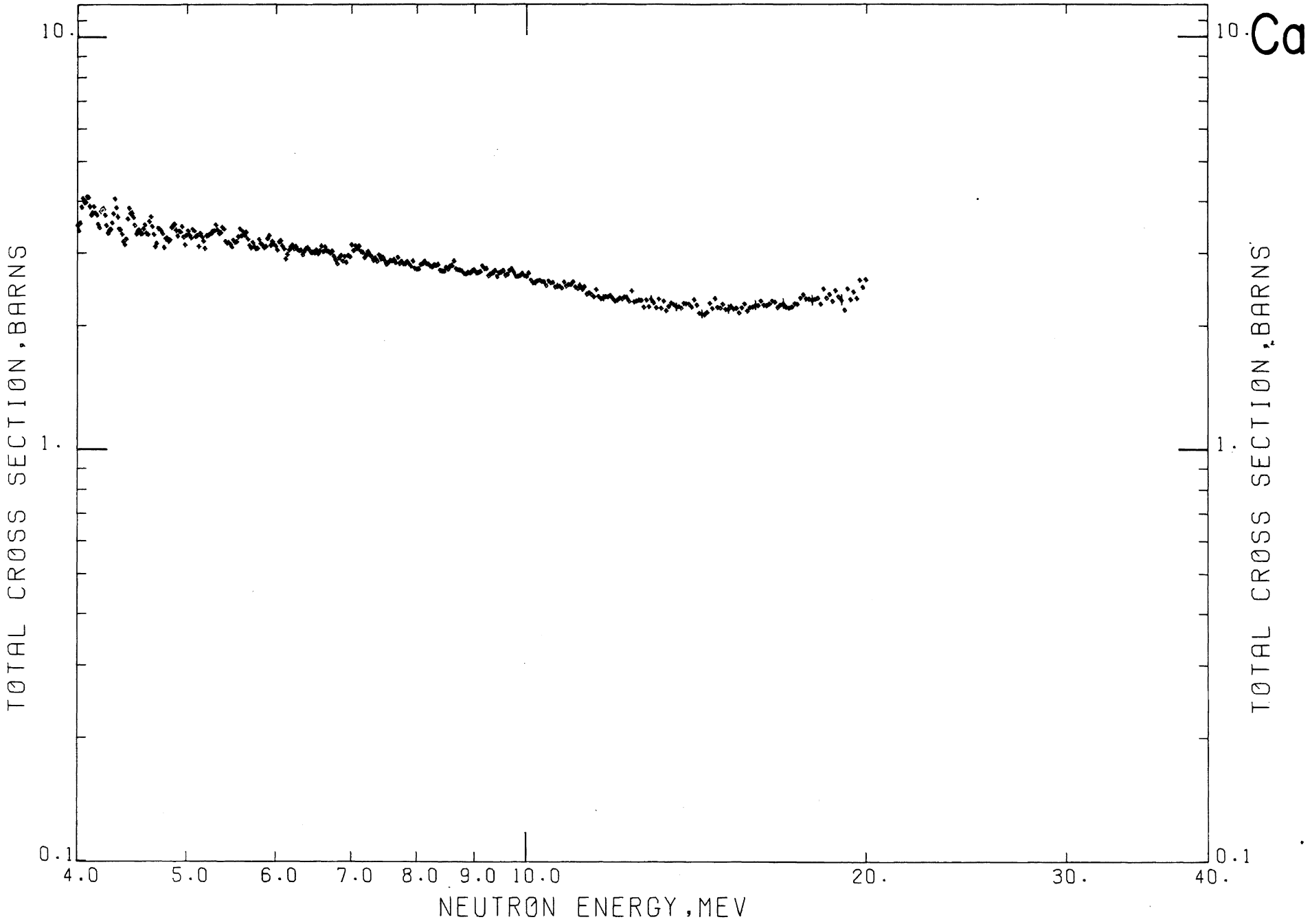
Ca
TØTAL CRØSS SECTIØN, BARNS
NEUTRØN ENERGY, MEV
10.
1.
0.1
4.0
5.0
6.0
7.0
8.0
9.0
10.0
20.
30.
40.

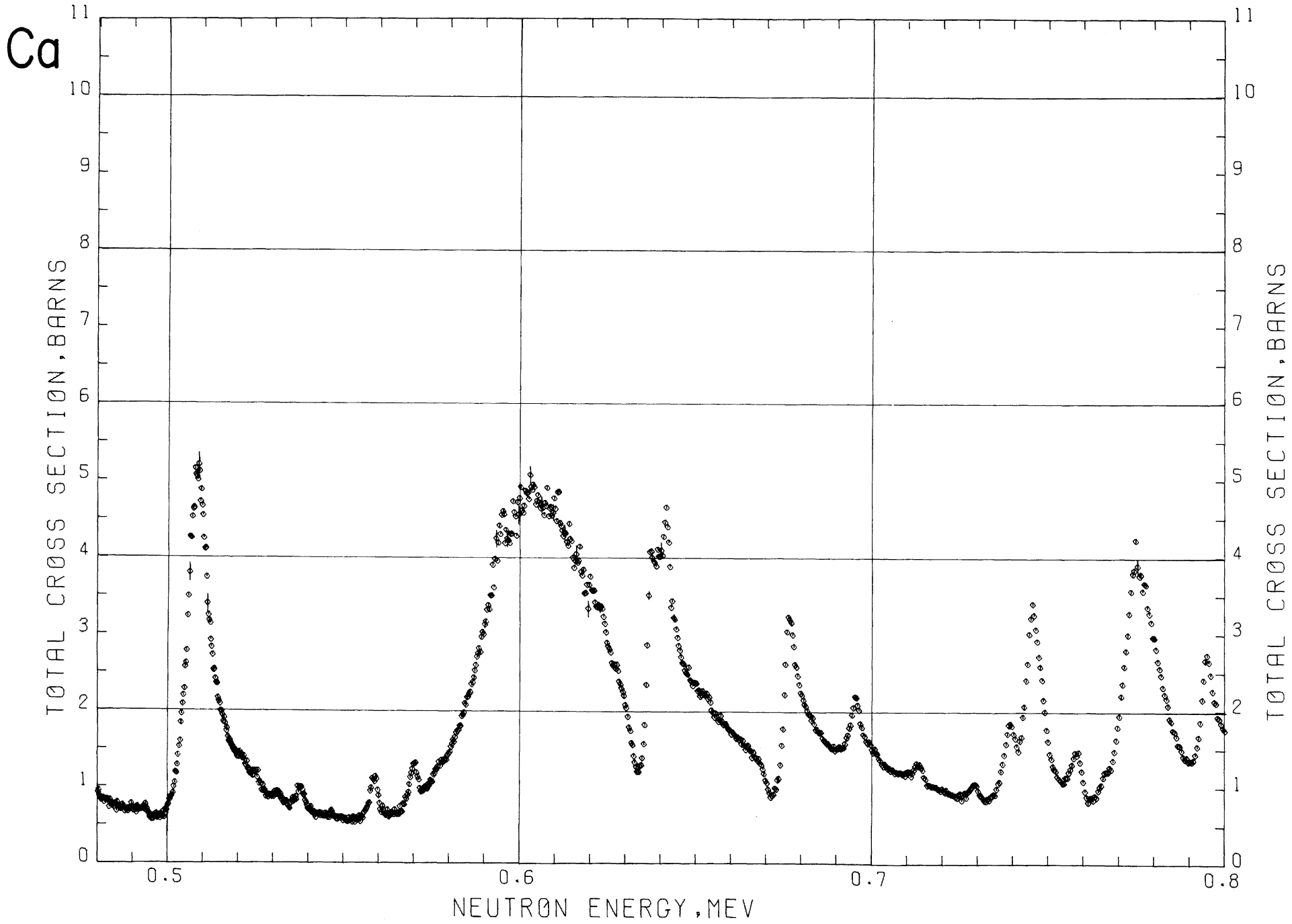
Ca
TØTAL CRØSS SECTIØN, BARNS
NEUTRØN ENERGY, MEV
0
1
2
3
4
5
6
7
8
9
10
11
0.5
0.6
0.7
0.8

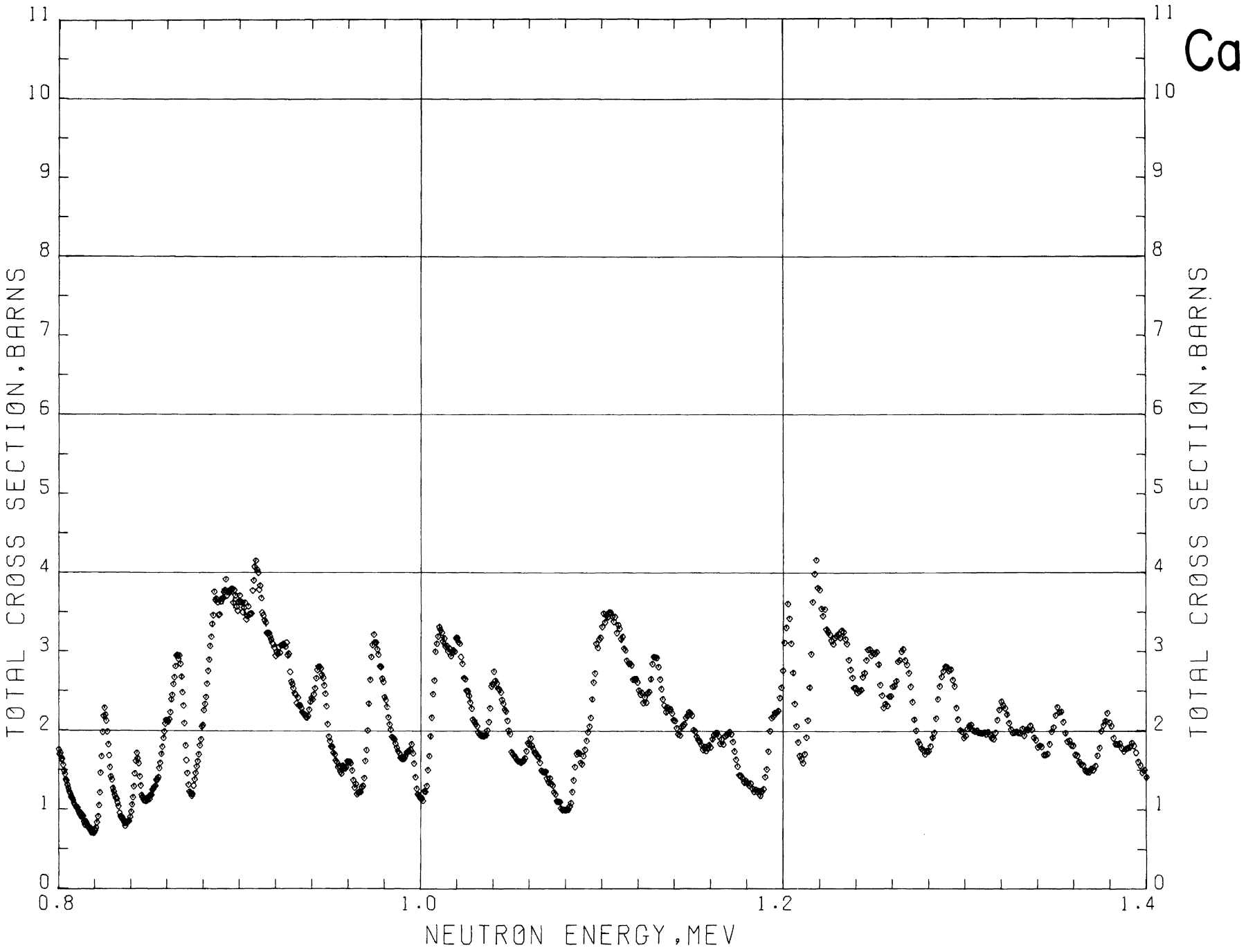
Ca
TOTAL CROSS SECTION, BARNS
NEUTRON ENERGY, MEV
0.8
1.0
1.2
1.4
0
1
2
3
4
5
6
7
8
9
10
11

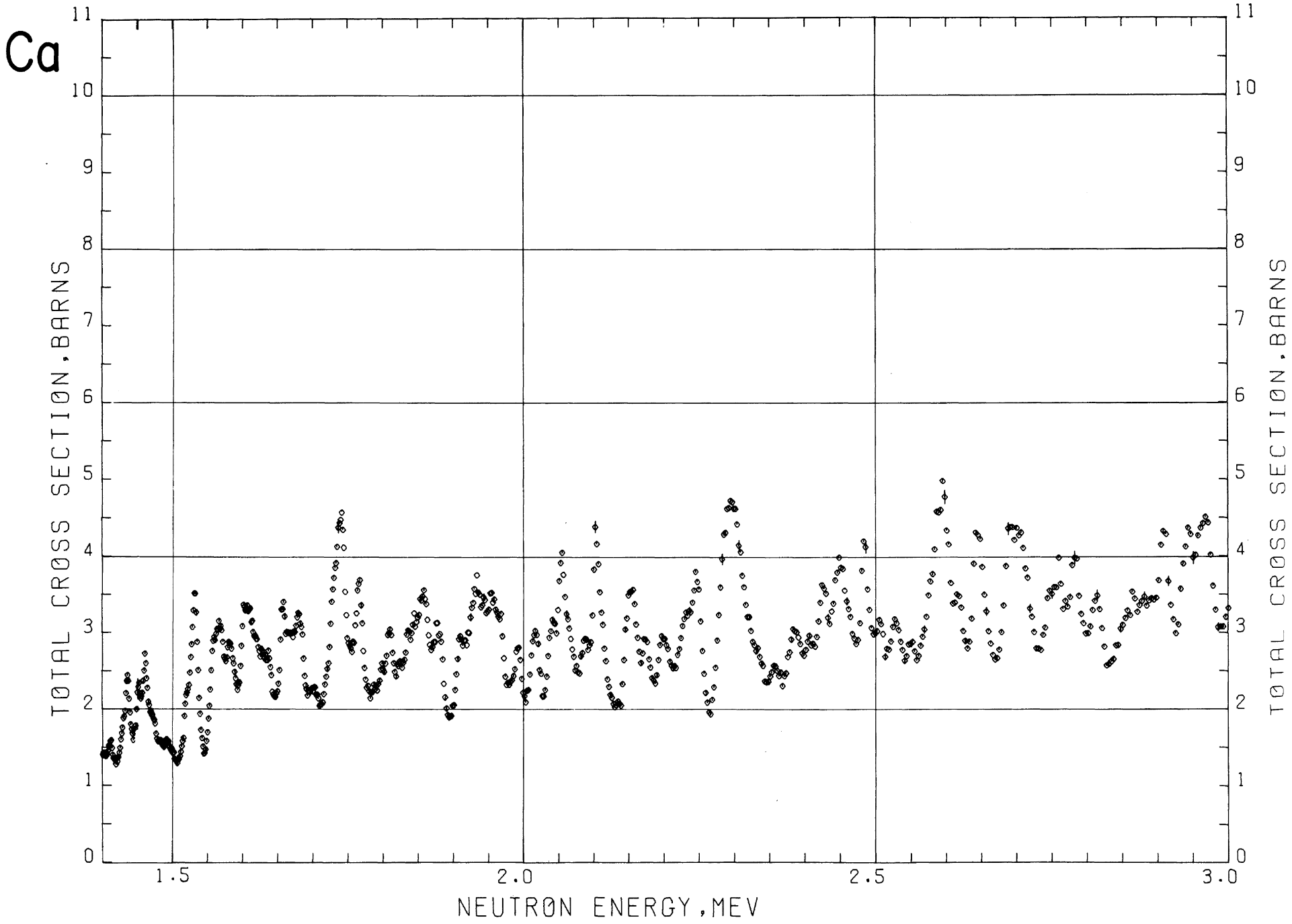
Ca
TOTAL CROSS SECTION, BARNS
NEUTRON ENERGY, MEV
0
1
2
3
4
5
6
7
8
9
10
11
1.5
2.0
2.5
3.0

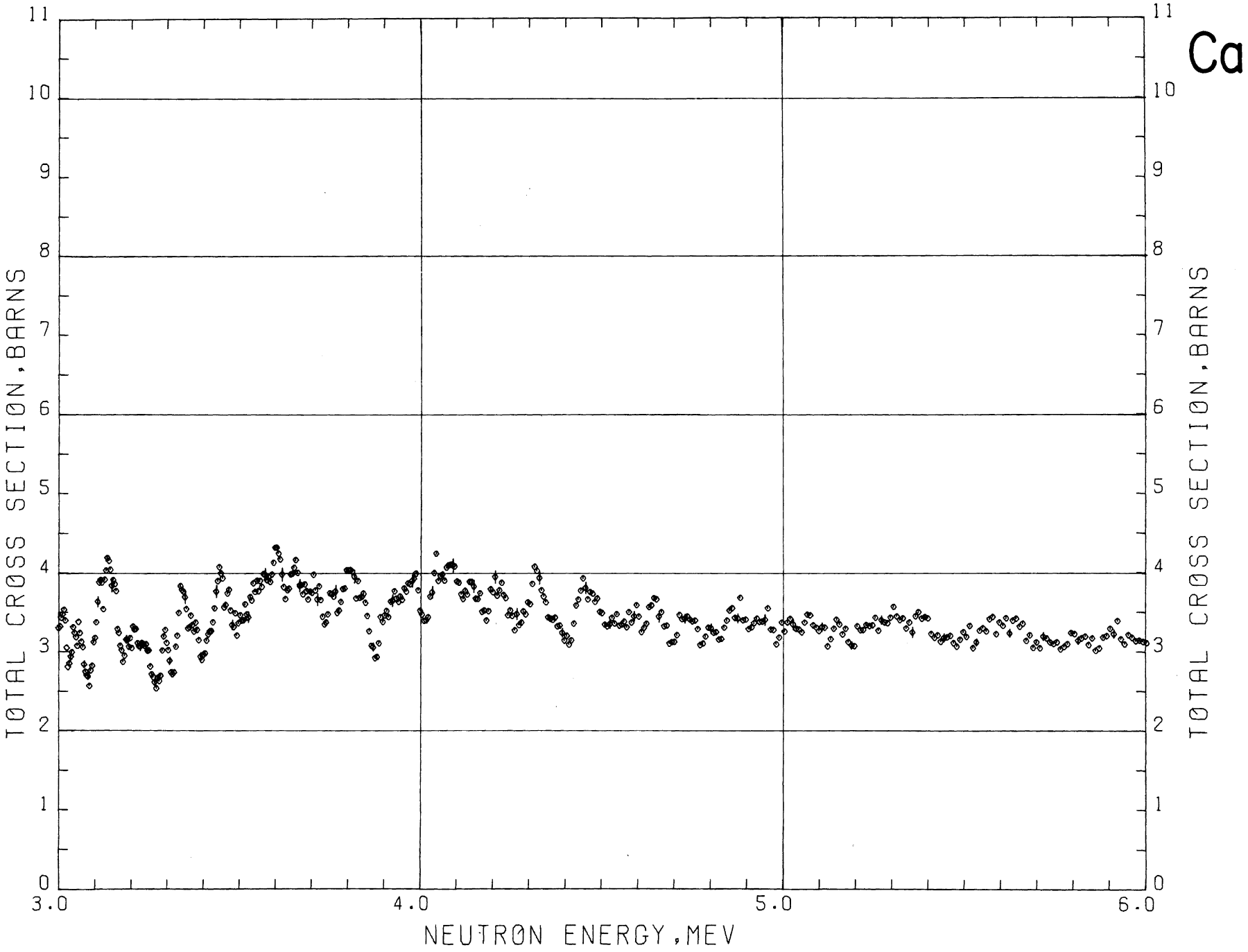
Ca
TOTAL CROSS SECTION, BARNS
NEUTRON ENERGY, MEV
0
1
2
3
4
5
6
7
8
9
10
11
3.0
4.0
5.0
6.0

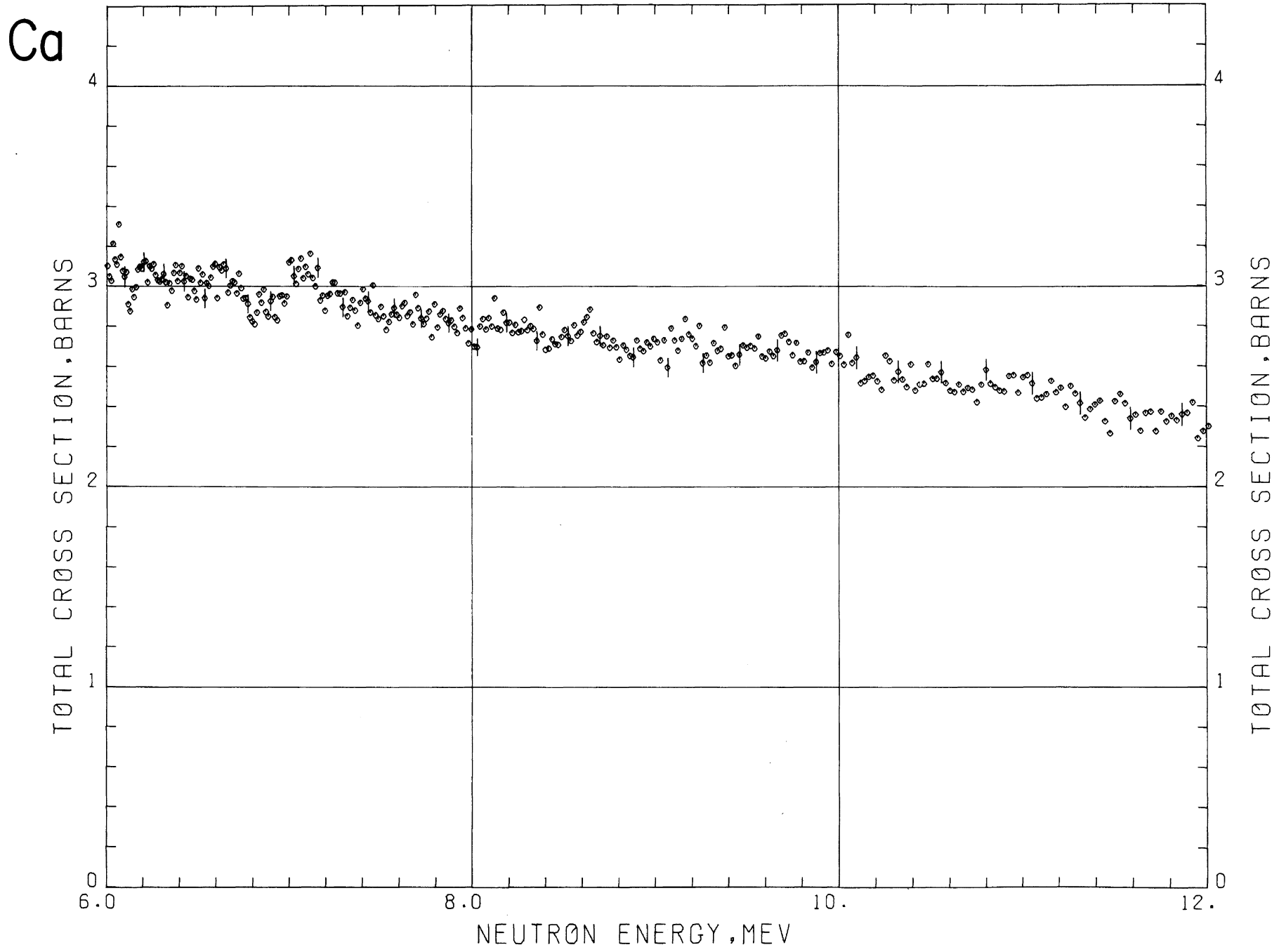
Ca
TOTAL CROSS SECTION, BARNS
NEUTRON ENERGY, MEV
6.0
8.0
10.
12.
0
1
2
3
4

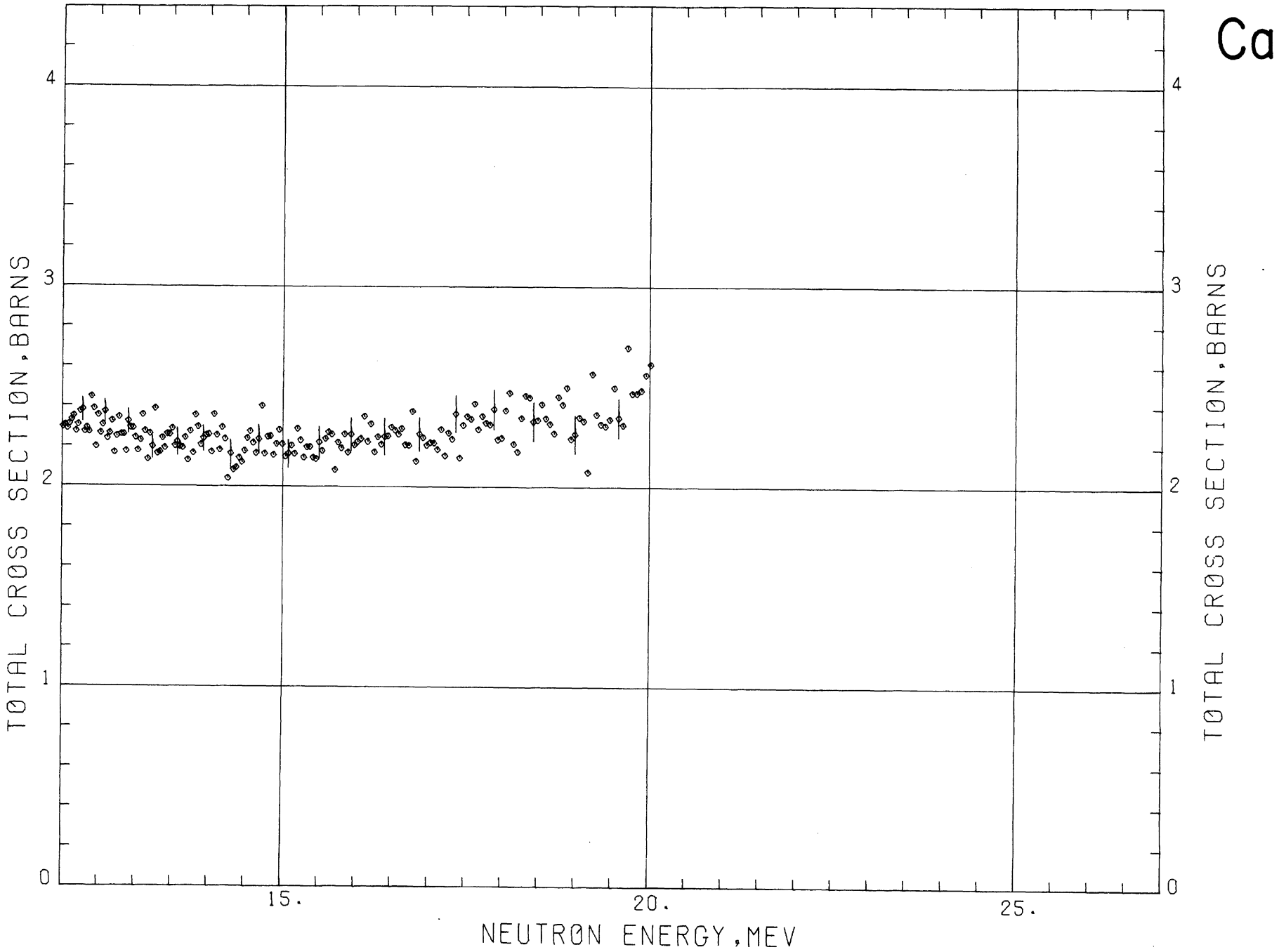
Ca
TOTAL CROSS SECTION, BARNS
TOTAL CROSS SECTION, BARNS
0
1
2
3
4
15.
20.
25.
NEUTRON ENERGY, MEV

TITANIUM

Sample Material: metallic titanium bar

Sample Diameter: 12.7 cm

Sample Thickness: 10.7 cm, $n = 0.6368$ atoms/barn

Literature Reference: R. B. Schwartz, R. A. Schrack, and H. T. Heaton II, Bull. Am. Phys. Soc. **14**, 494 (1969).

Analysis: A qualitative spectrographic analysis of the sample showed no impurities at levels greater than 0.1 percent.

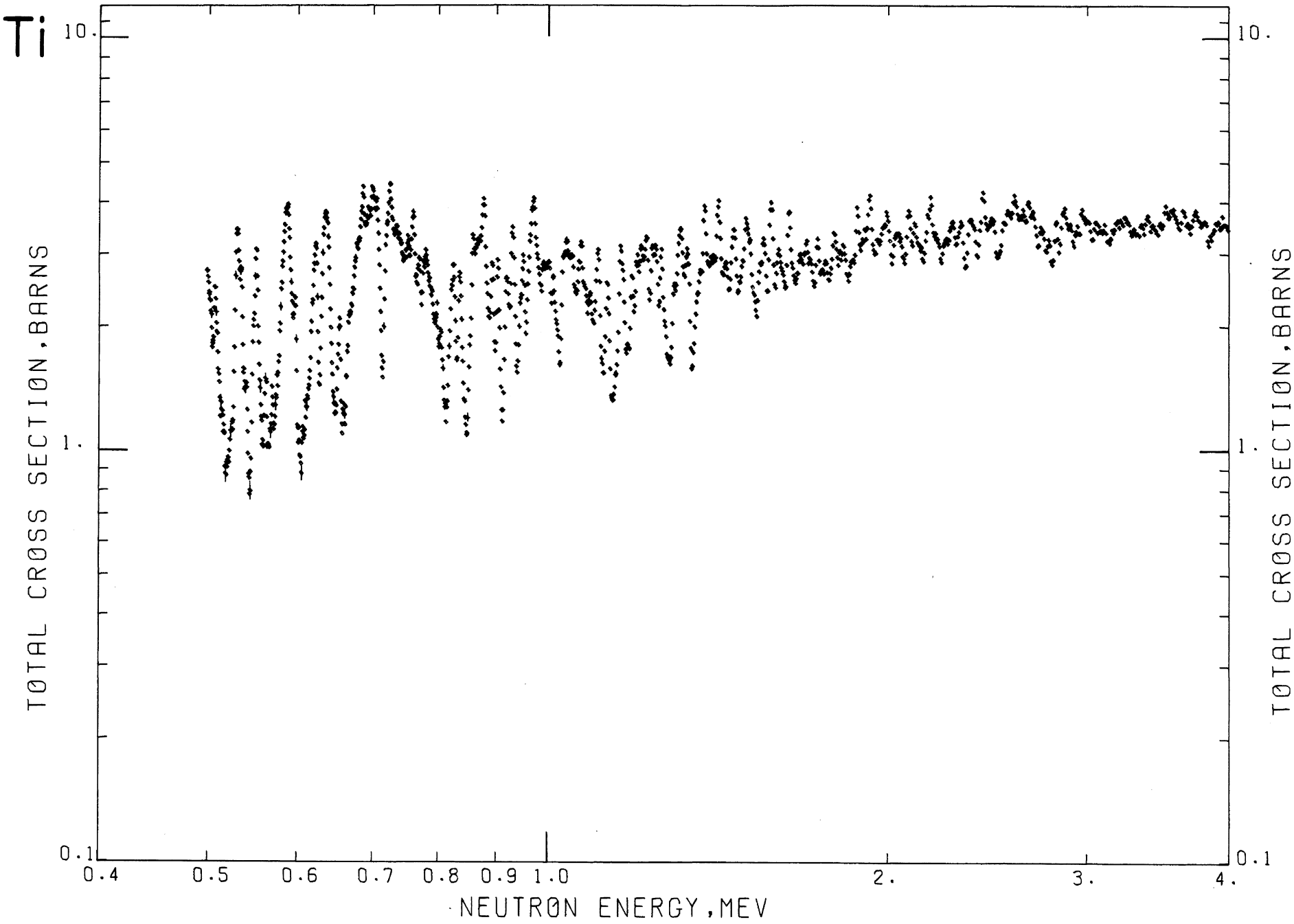
Ti
10.
1.
0.1
TØTAL CRØSS SECTIØN,BARNS
0.4
0.5
0.6
0.7
0.8
0.9
1.0
2.
3.
4.
NEUTRØN ENERGY,MEV

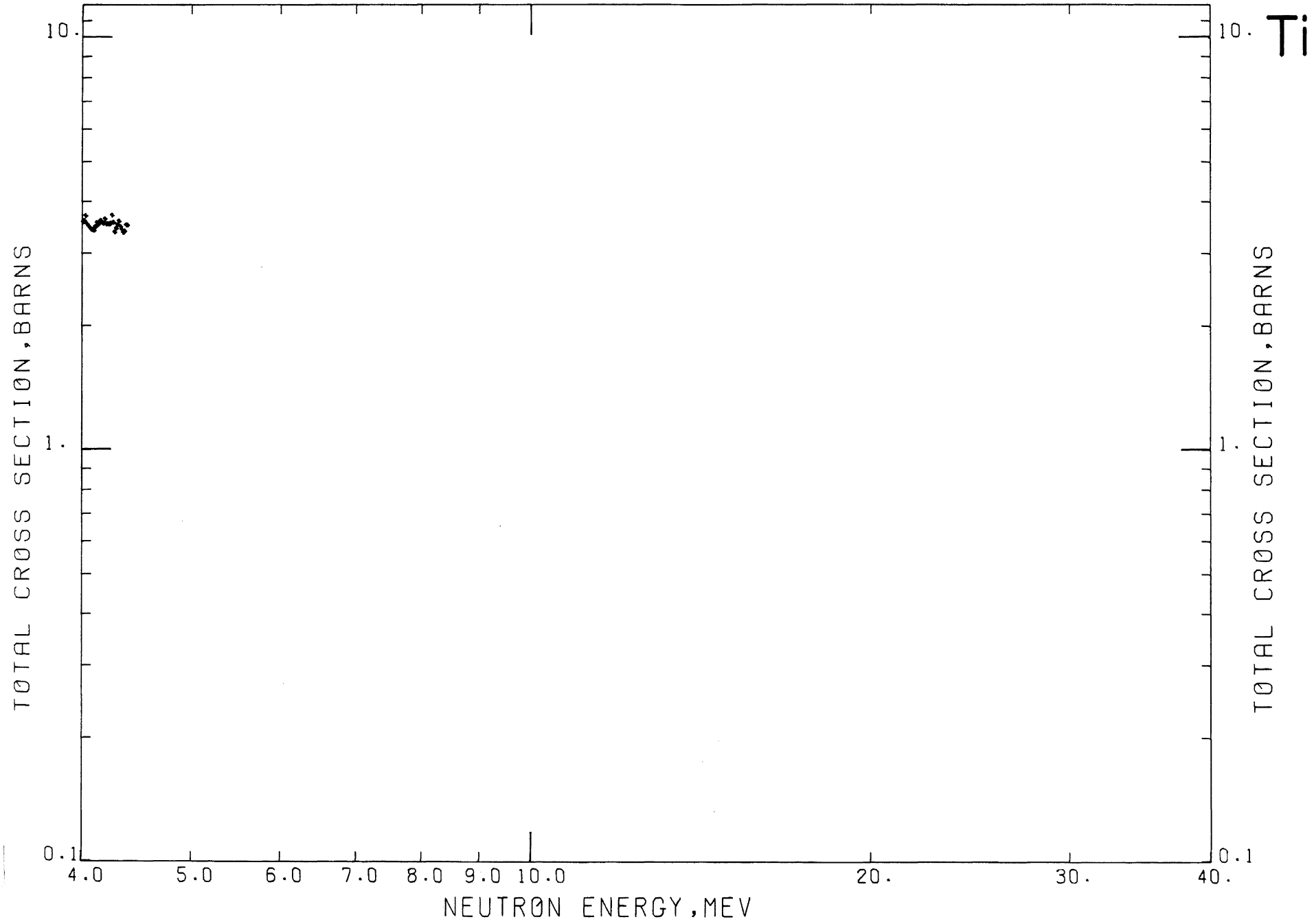
Ti
TOTAL CROSS SECTION, BARNS
10.
1.
0.1
4.0
5.0
6.0
7.0
8.0
9.0
10.0
20.
30.
40.
NEUTRON ENERGY, MEV

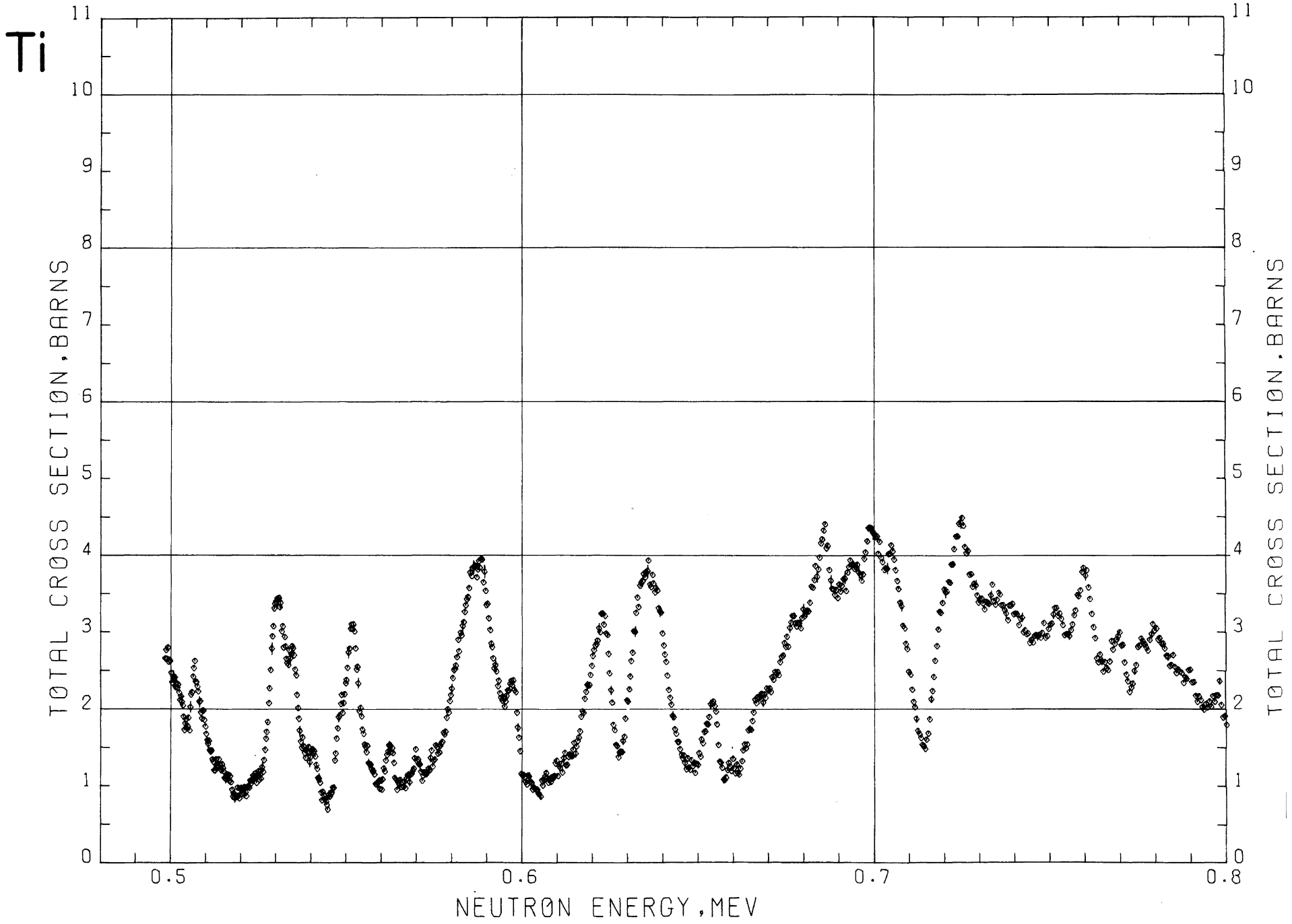
Ti
TOTAL CROSS SECTION, BARNS
NEUTRON ENERGY, MEV
0.5
0.6
0.7
0.8
0
1
2
3
4
5
6
7
8
9
10
11

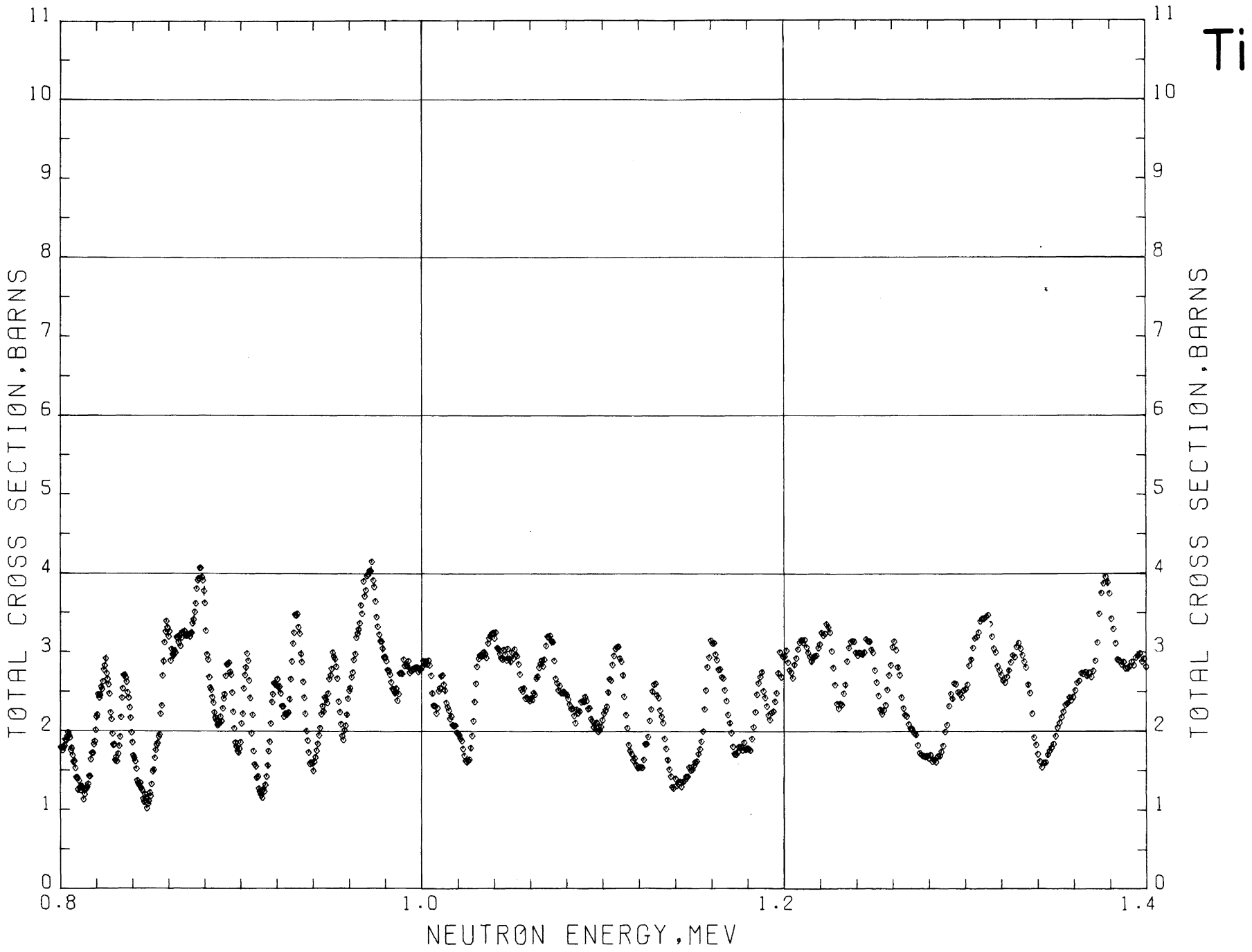
Ti
TOTAL CROSS SECTION, BARNS
NEUTRON ENERGY, MEV
0.8
1.0
1.2
1.4
0
1
2
3
4
5
6
7
8
9
10
11

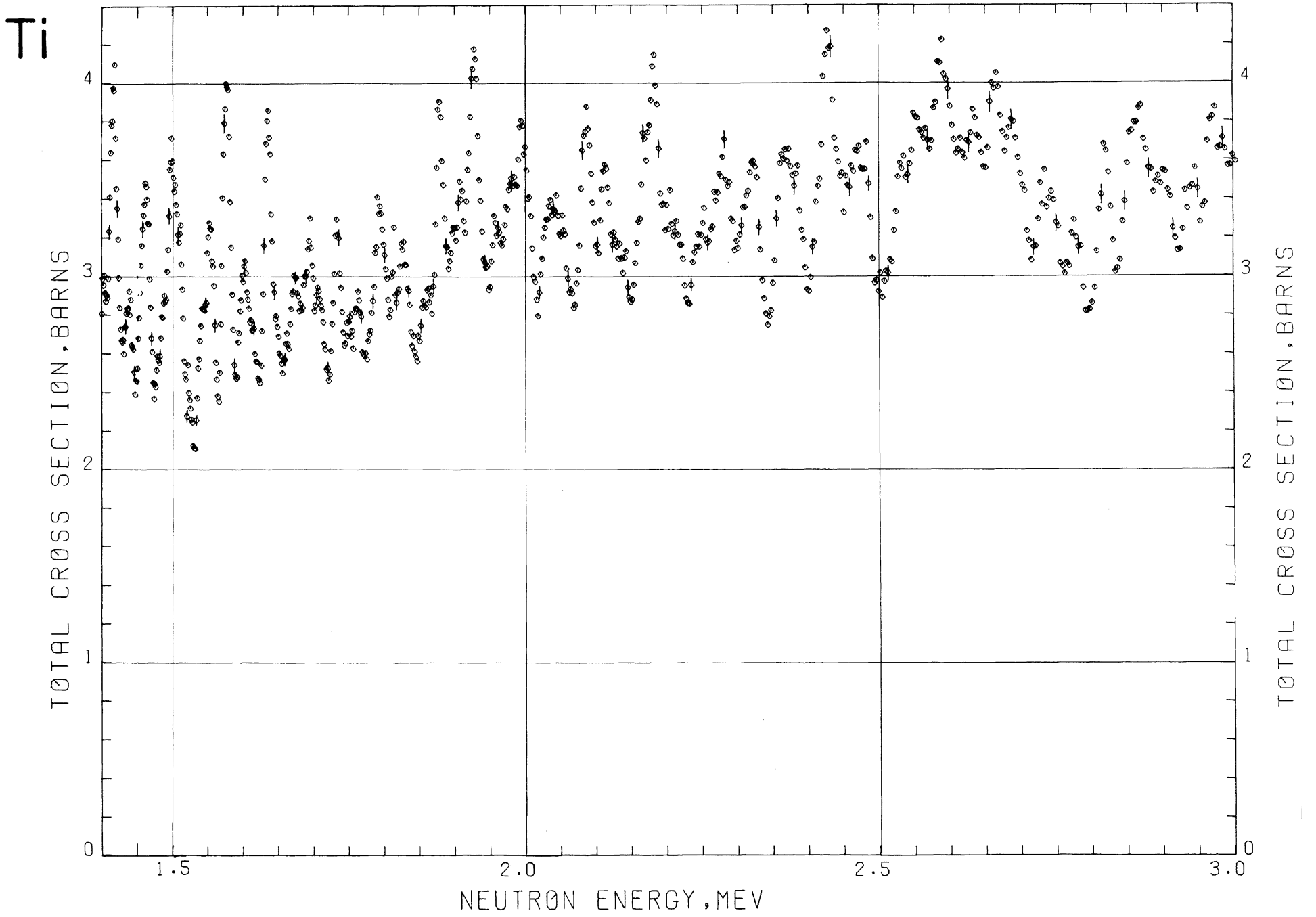
Ti
TØTAL CRØSS SECTIØN, BARNS
NEUTRØN ENERGY, MEV
0
1
2
3
4
1.5
2.0
2.5
3.0

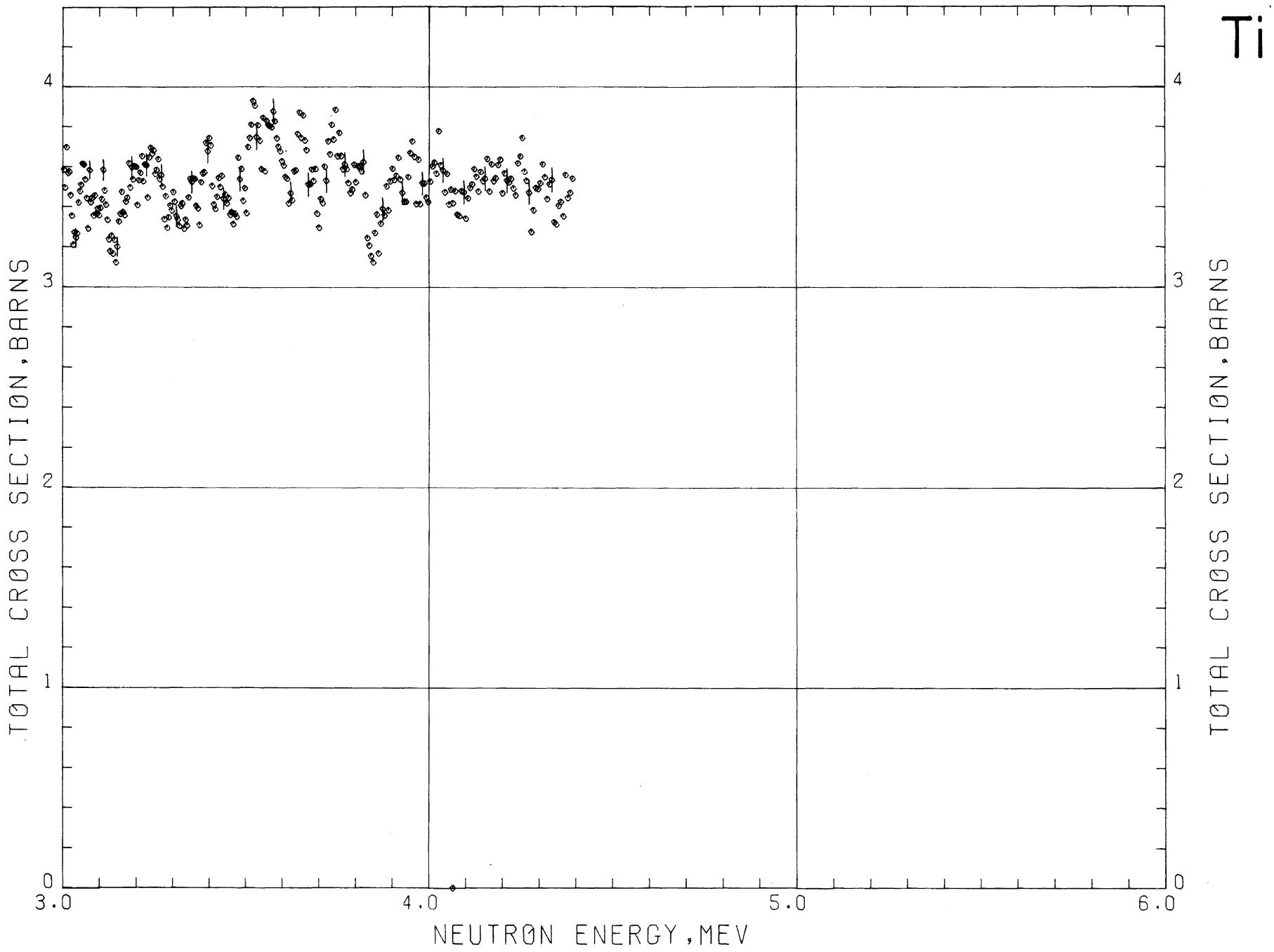
Ti
TOTAL CROSS SECTION, BARNS
NEUTRON ENERGY, MEV
0
1
2
3
4
3.0
4.0
5.0
6.0

IRON

Sample Material: metallic iron

Sample Diameter: 12.7 cm

Sample Thickness: 2.94 cm, $n = 0.2490$ atoms/barn

11.8 cm, $n = 0.9997$ atoms/barn

Analysis: The samples were fabricated of SAE 1017 steel containing 0.9 percent manganese. The presence of the manganese may, at worst, introduce spurious fluctuations of up to 3 percent in amplitude in the energy region where there are sharp resonances ($\leq$ 2 MeV) and should have negligible effect at higher energies.

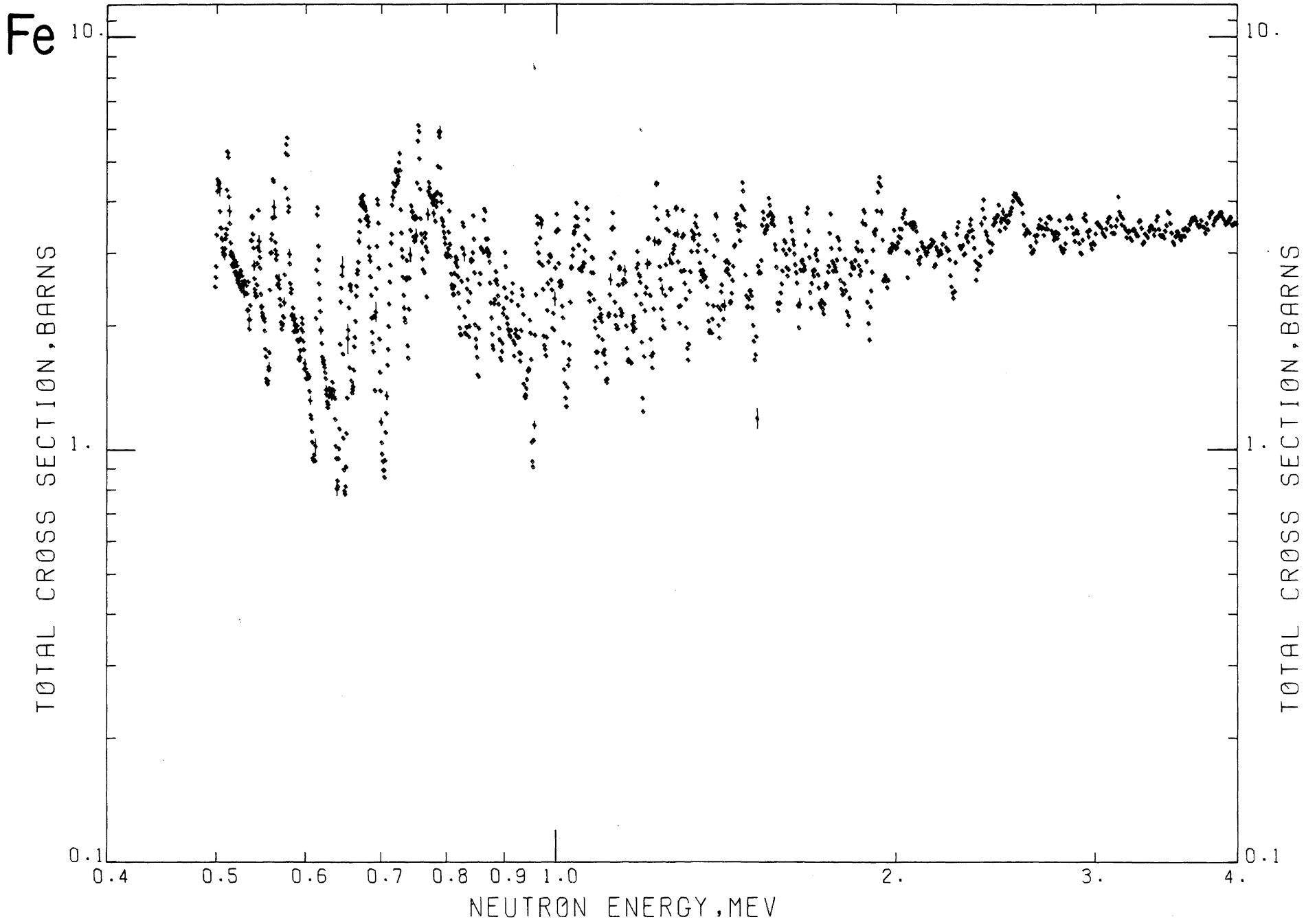
Fe
10.
1.
0.1
TOTAL CROSS SECTION, BARNS
0.4
0.5
0.6
0.7
0.8
0.9
1.0
2.
3.
4.
NEUTRON ENERGY, MEV

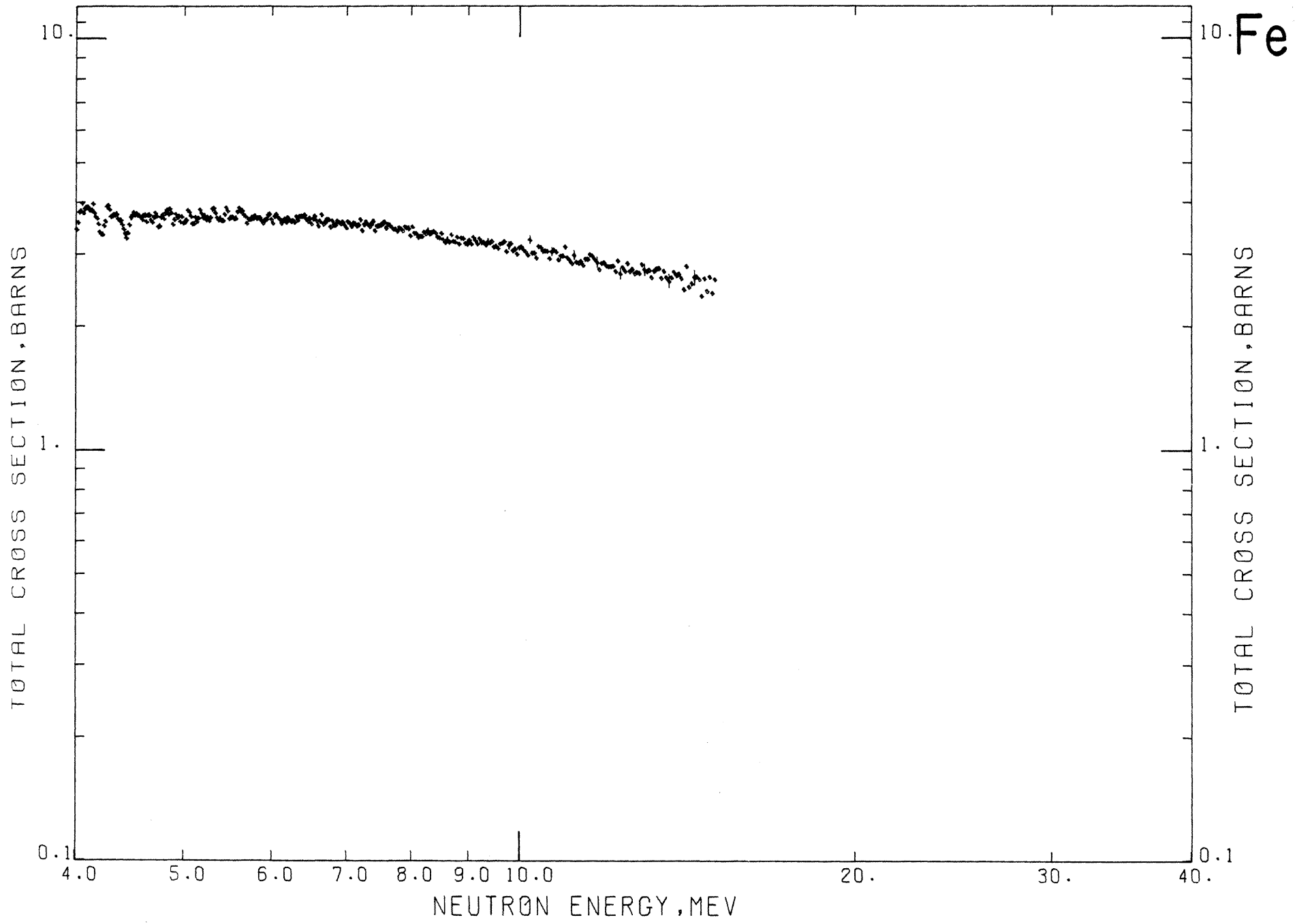
Fe
TOTAL CROSS SECTION, BARNS
10.
1.
0.1
4.0
5.0
6.0
7.0
8.0
9.0
10.0
20.
30.
40.
NEUTRON ENERGY, MEV

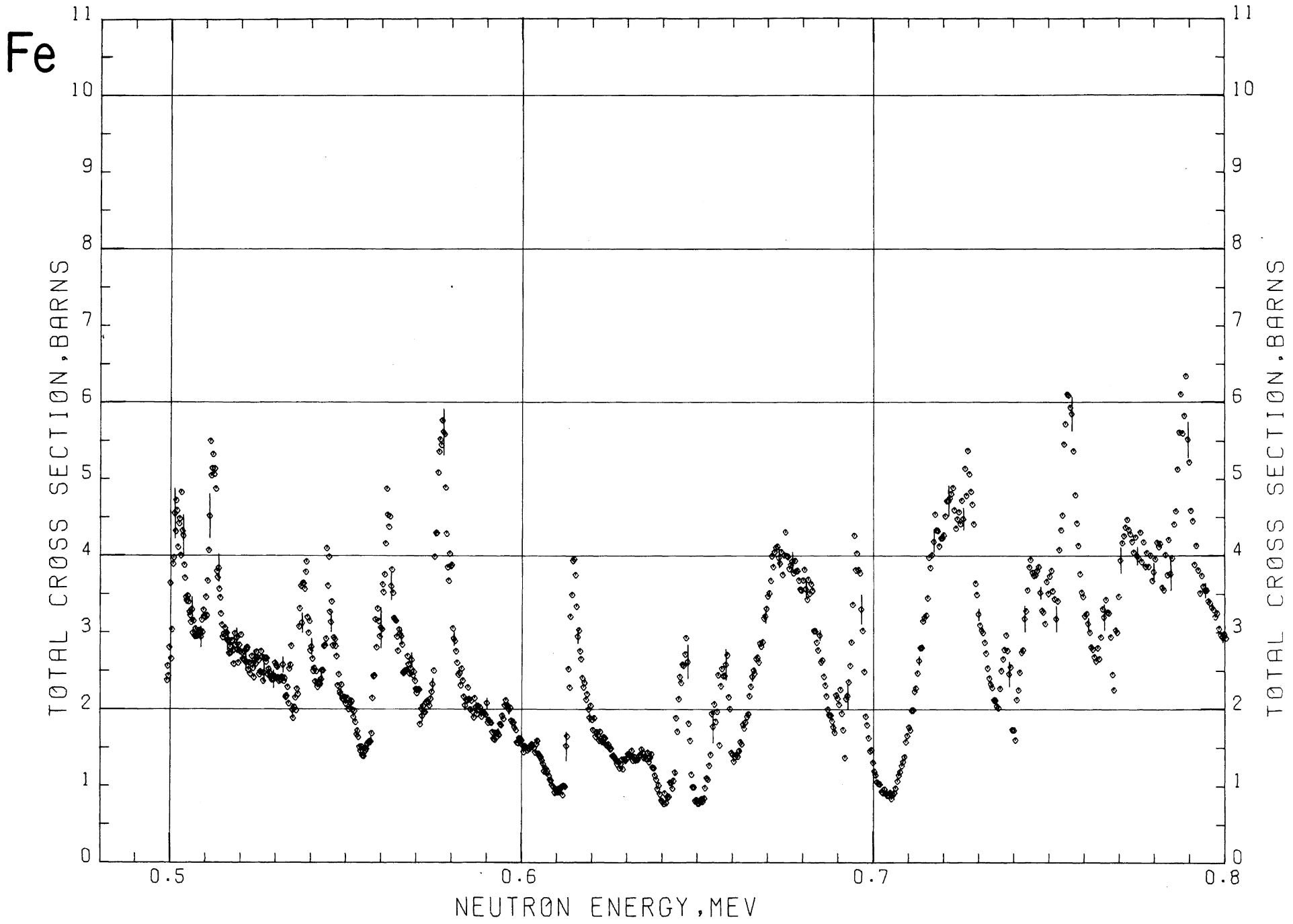
Fe
TOTAL CROSS SECTION, BARNS
NEUTRON ENERGY, MEV
0
1
2
3
4
5
6
7
8
9
10
11
0.5
0.6
0.7
0.8

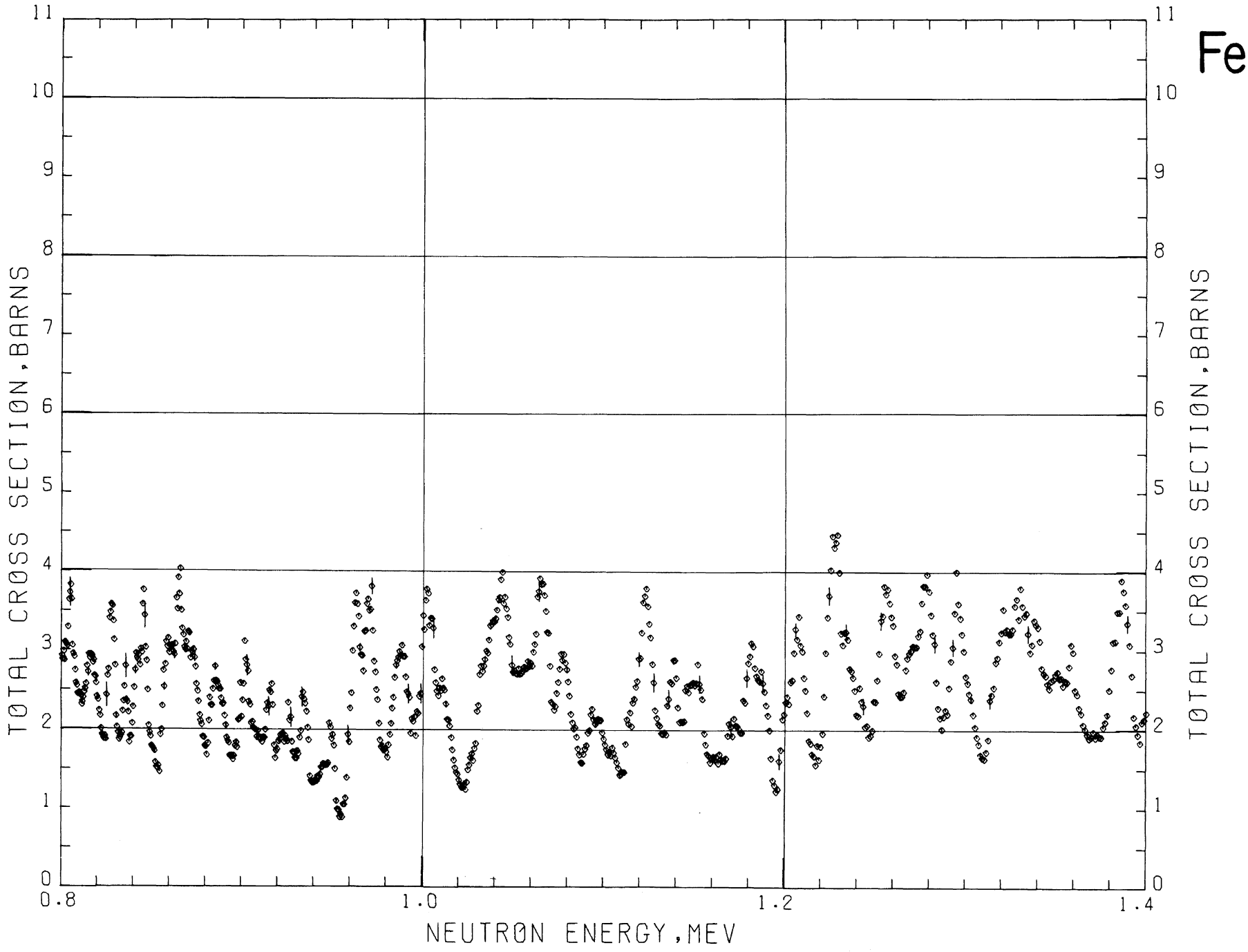
Fe
TOTAL CROSS SECTION, BARNS
NEUTRON ENERGY, MEV
0.8
1.0
1.2
1.4
0
1
2
3
4
5
6
7
8
9
10
11

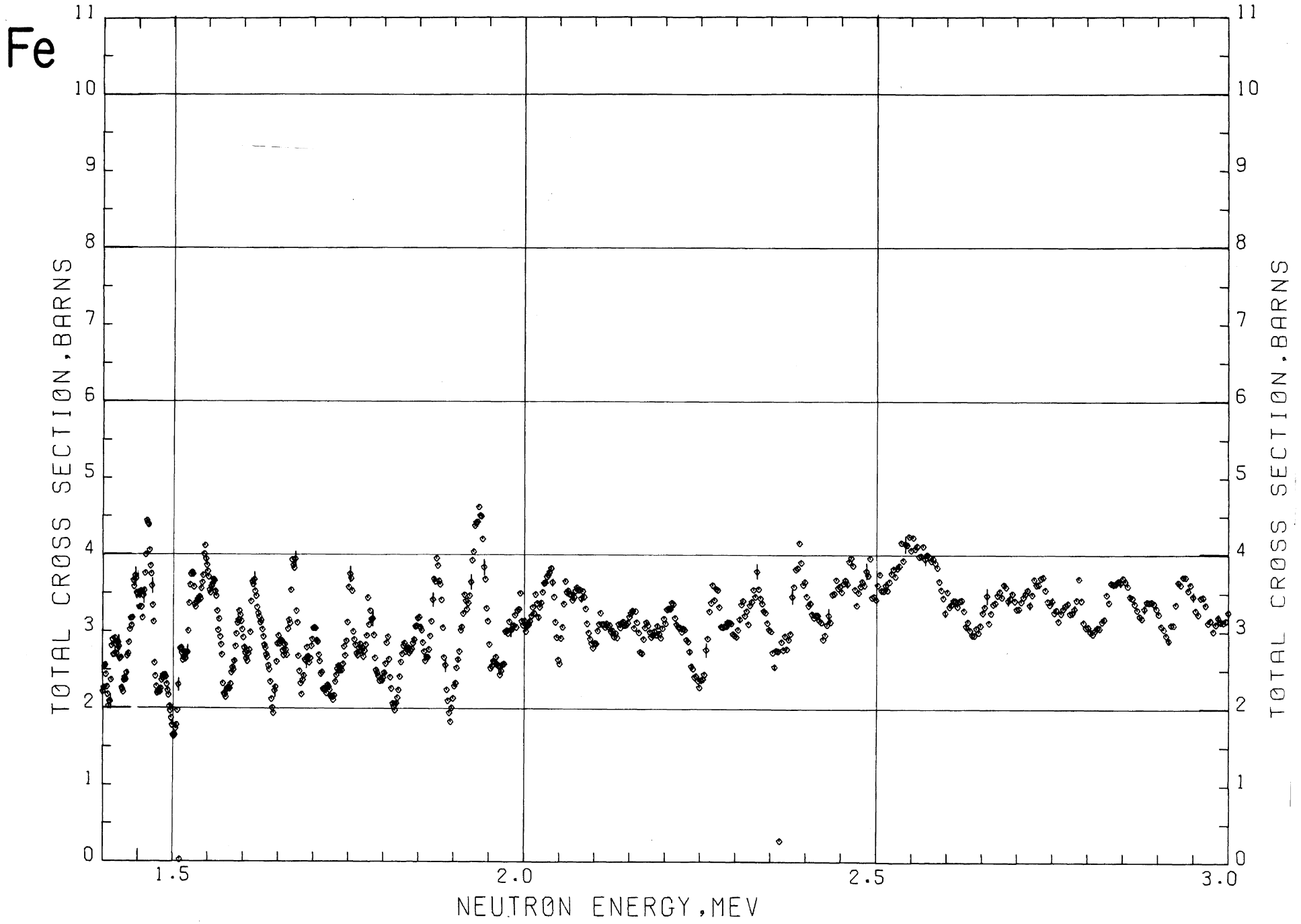
Fe
TØTAL CRØSS SECTIØN, BARNS
NEUTRØN ENERGY, MEV
0
1
2
3
4
5
6
7
8
9
10
11
1.5
2.0
2.5
3.0

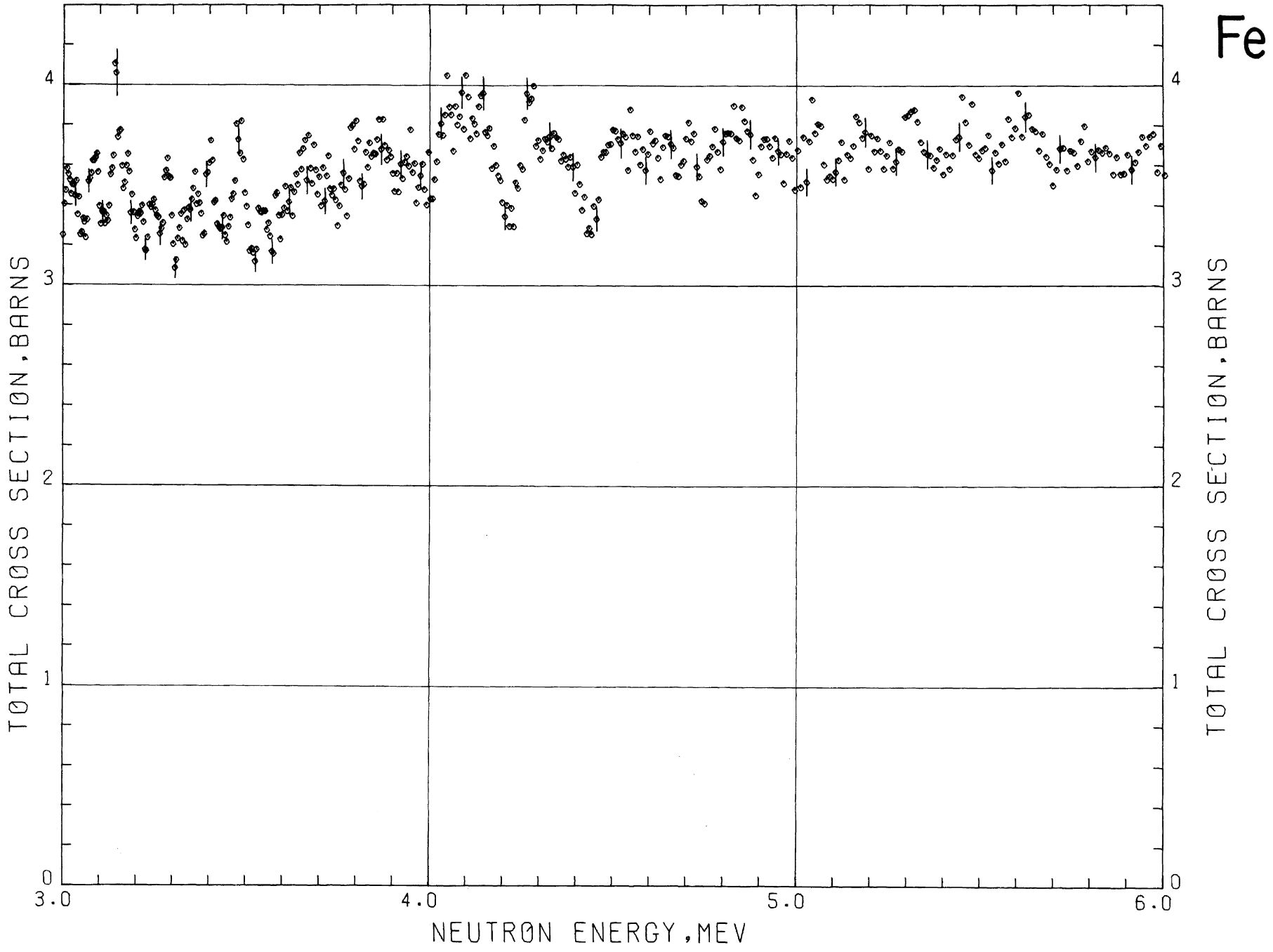
Fe
TOTAL CROSS SECTION, BARNS
TOTAL CROSS SECTION, BARNS
0
1
2
3
4
3.0
4.0
5.0
6.0
NEUTRON ENERGY, MEV

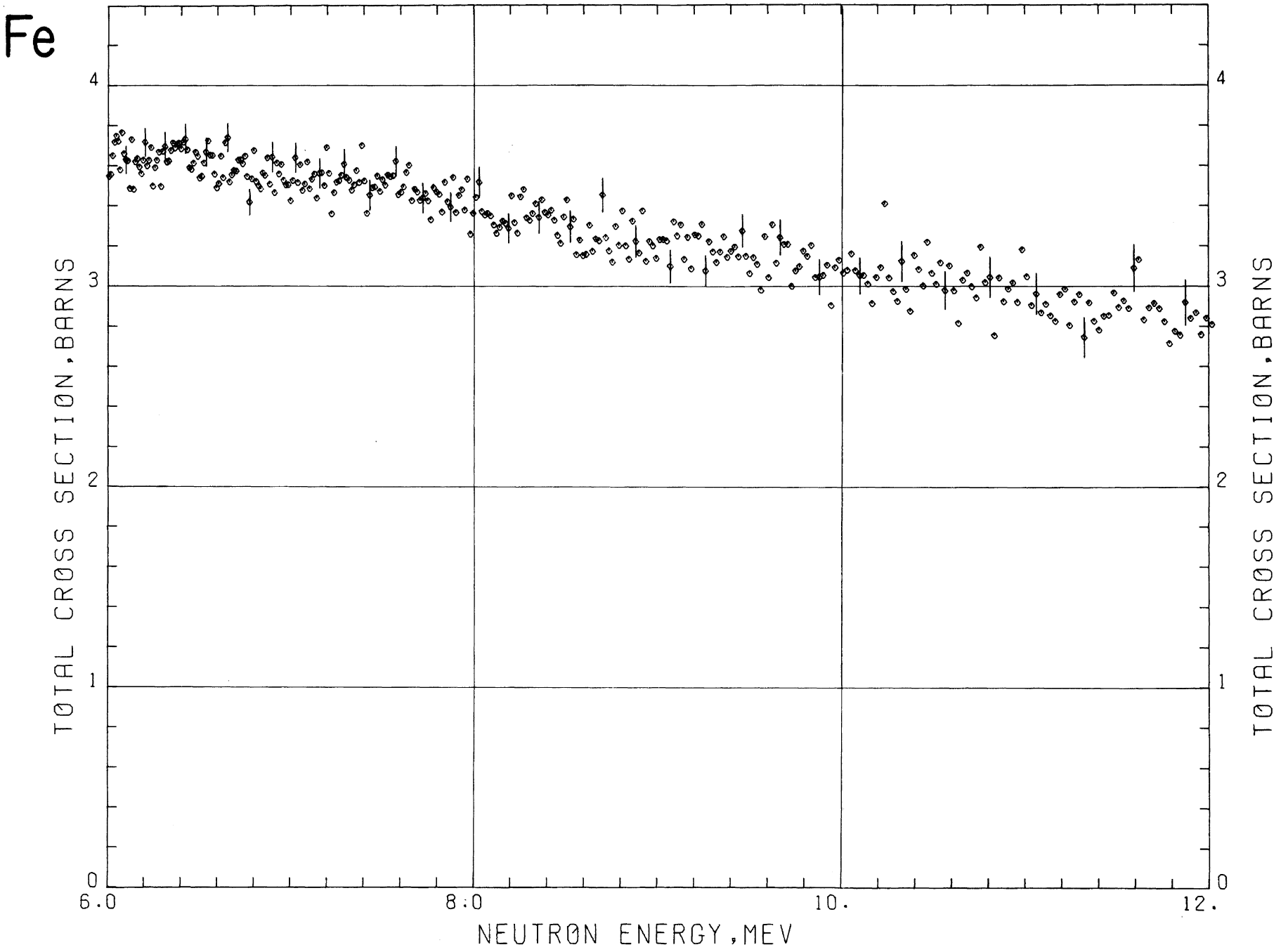
Fe
TOTAL CROSS SECTION, BARNS
NEUTRON ENERGY, MEV
0
1
2
3
4
6.0
8.0
10.
12.

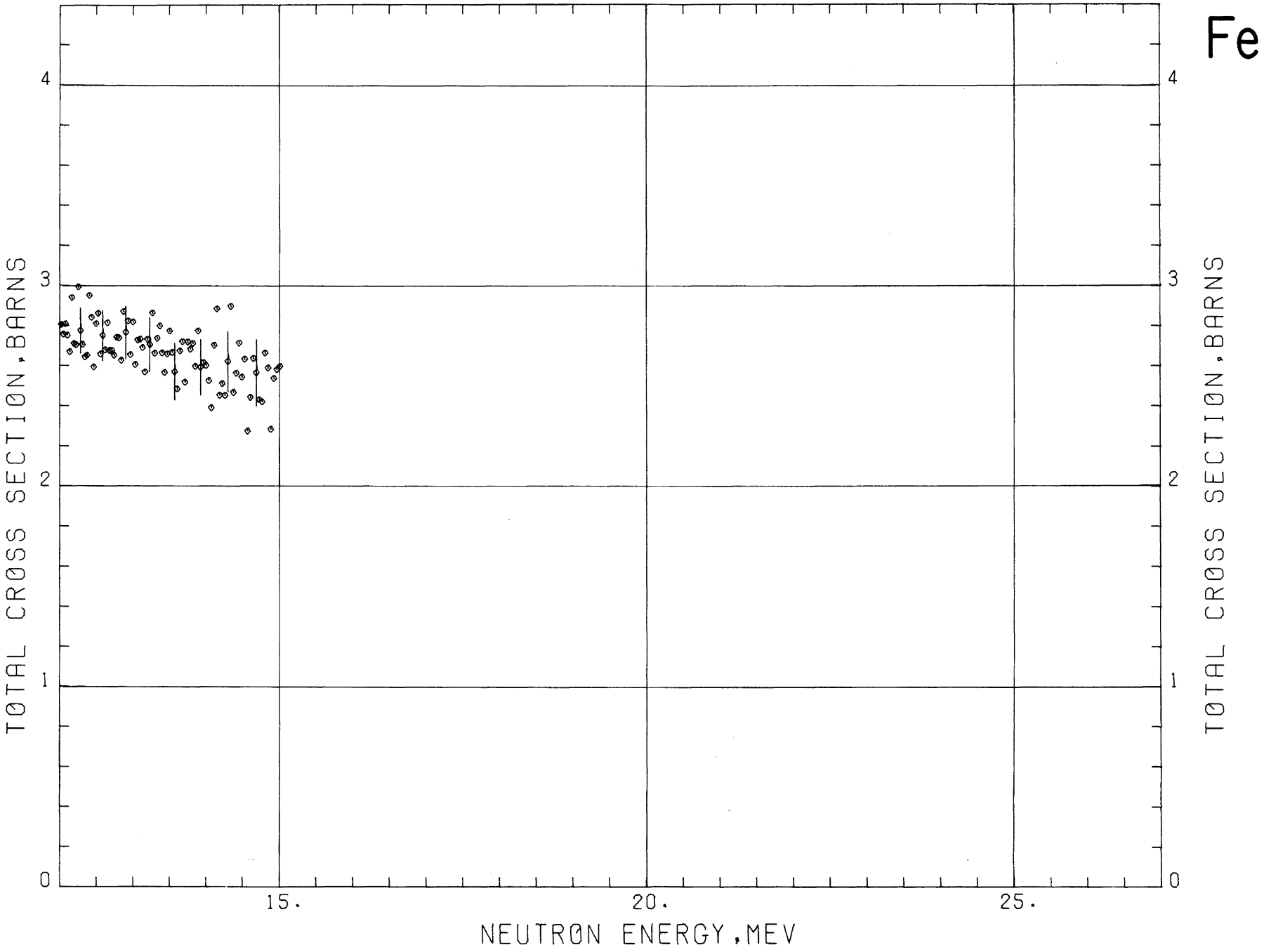
Fe
TOTAL CROSS SECTION, BARNS
TOTAL CROSS SECTION, BARNS
0
1
2
3
4
15.
20.
25.
NEUTRON ENERGY, MEV

NICKEL

Sample Material: nickel 200 cold drawn rod

Sample Diameter: 5.08 cm

Sample Thickness: 4.46 cm, $n = 0.4047$

11.37 cm, $n = 1.032$

Analysis: Qualitative spectrographic analysis of the sample showed no impurities greater than 0.1 percent.

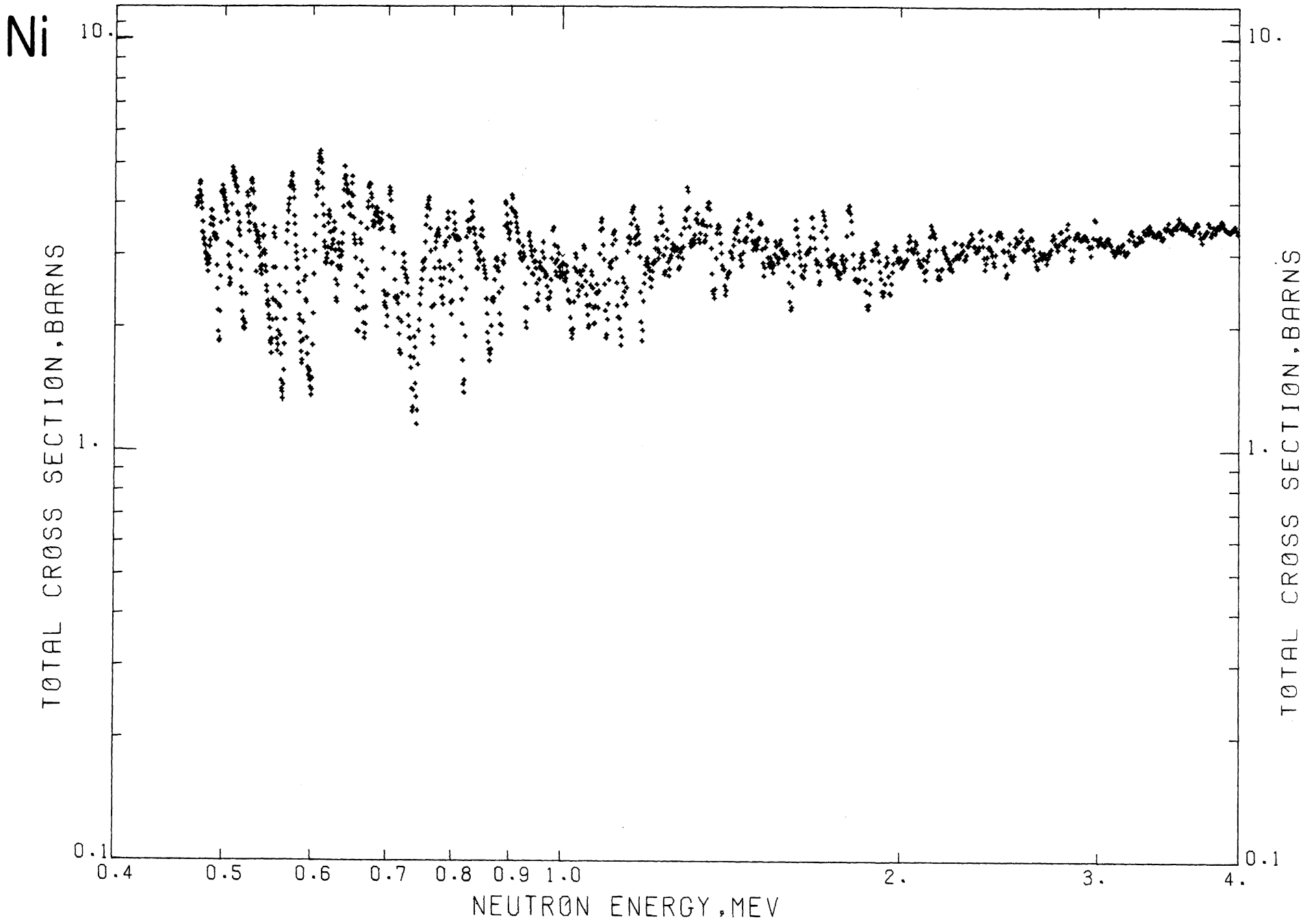
Ni
10.
1.
0.1
TOTAL CROSS SECTION, BARNS
0.4
0.5
0.6
0.7
0.8
0.9
1.0
2.
3.
4.
NEUTRON ENERGY, MEV

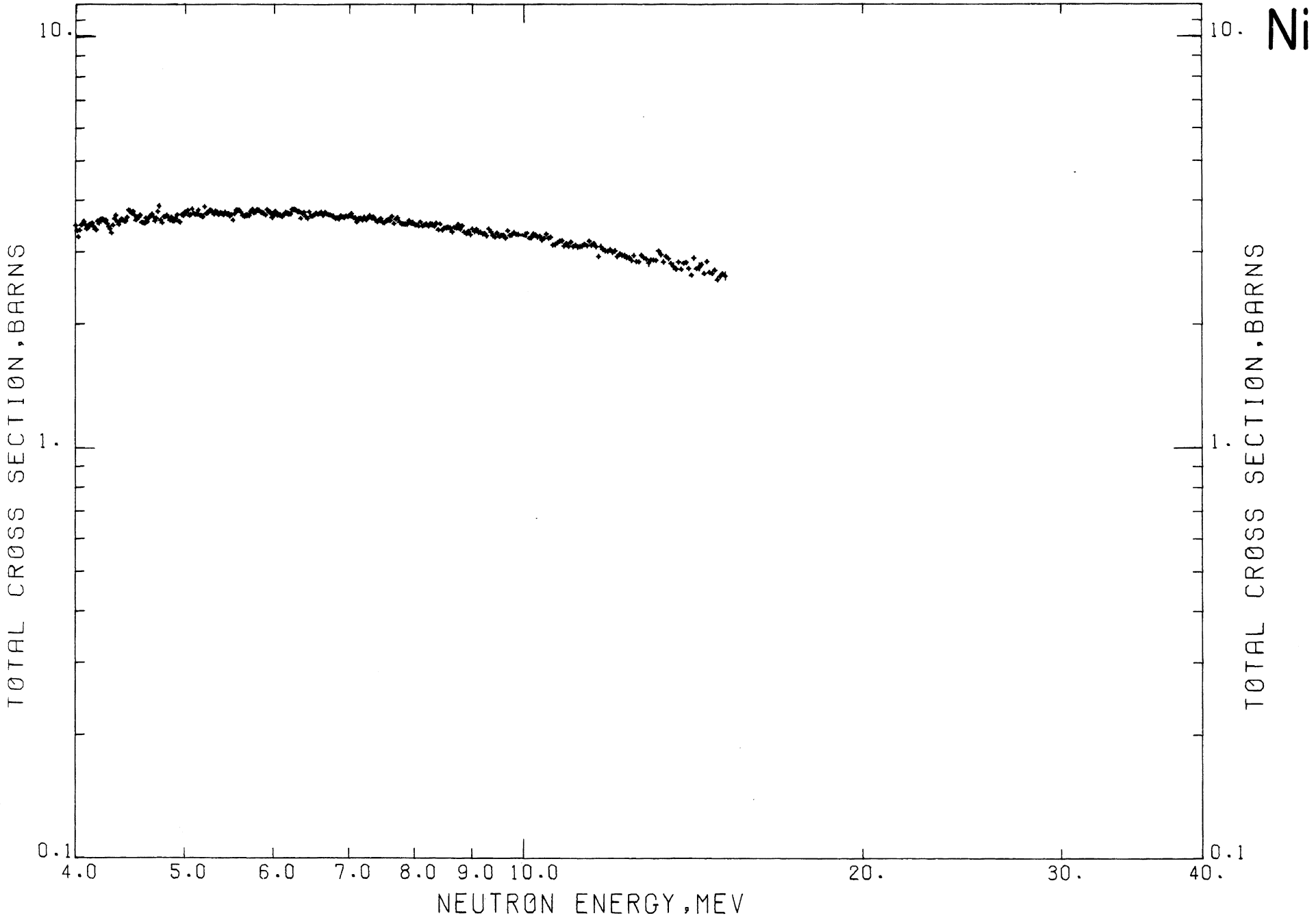
Ni
10.
1.
0.1
TOTAL CROSS SECTION, BARNS
4.0
5.0
6.0
7.0
8.0
9.0
10.0
20.
30.
40.
NEUTRON ENERGY, MEV

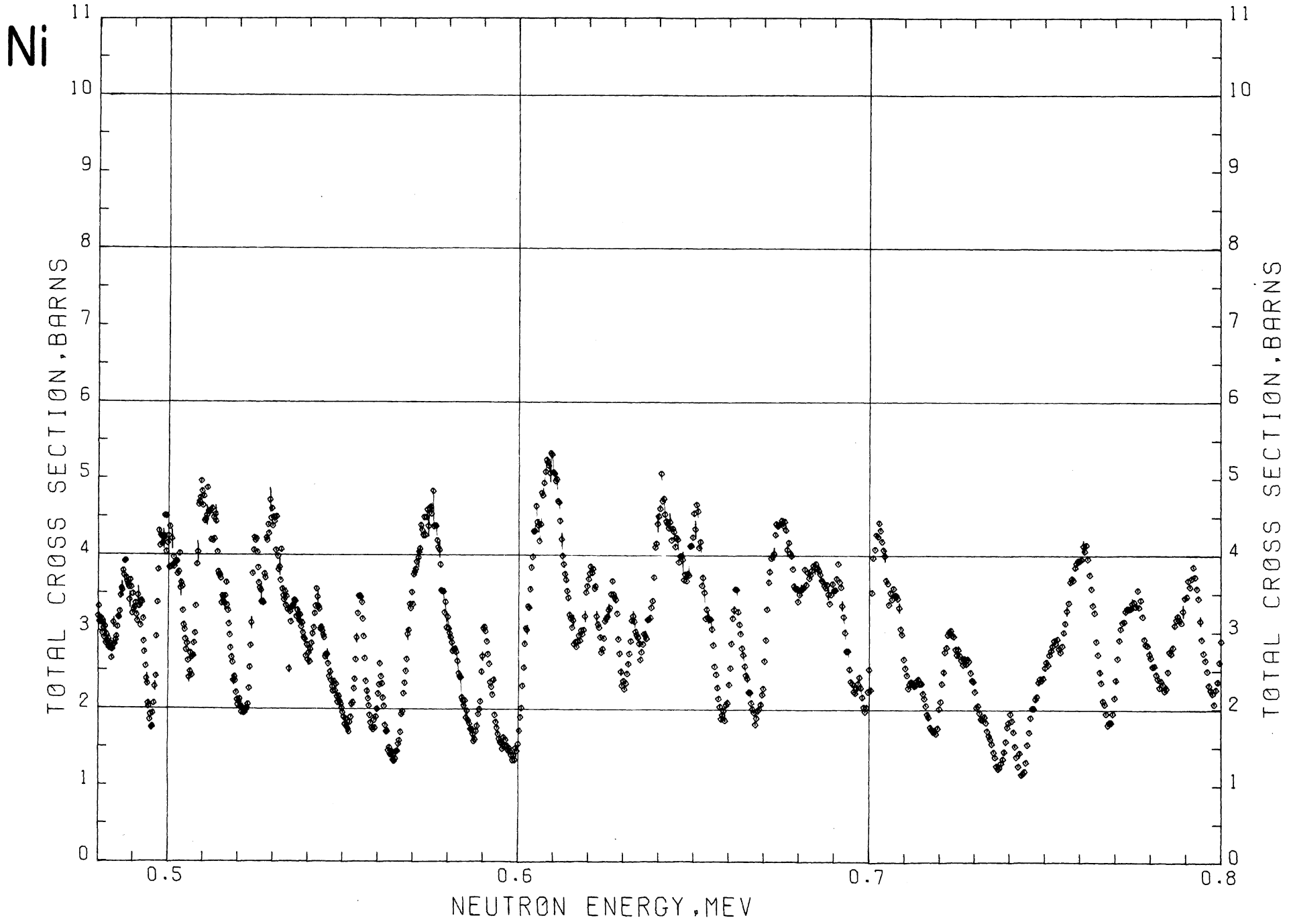
Ni
TOTAL CROSS SECTION, BARNS
NEUTRON ENERGY, MEV
0.5
0.6
0.7
0.8
0
1
2
3
4
5
6
7
8
9
10
11

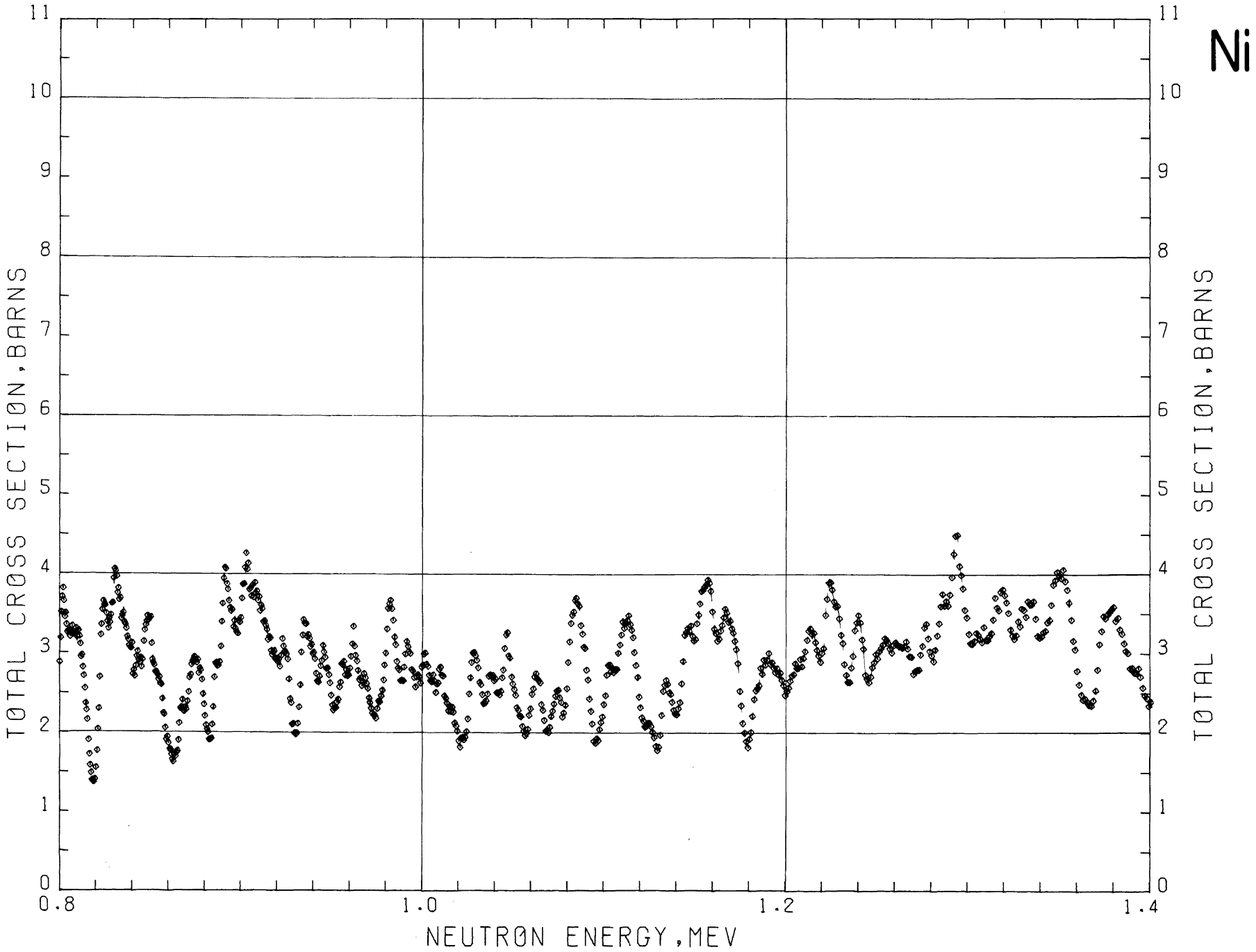
Ni
TOTAL CROSS SECTION, BARNS
NEUTRON ENERGY, MEV
0.8
1.0
1.2
1.4
0
1
2
3
4
5
6
7
8
9
10
11

Ni

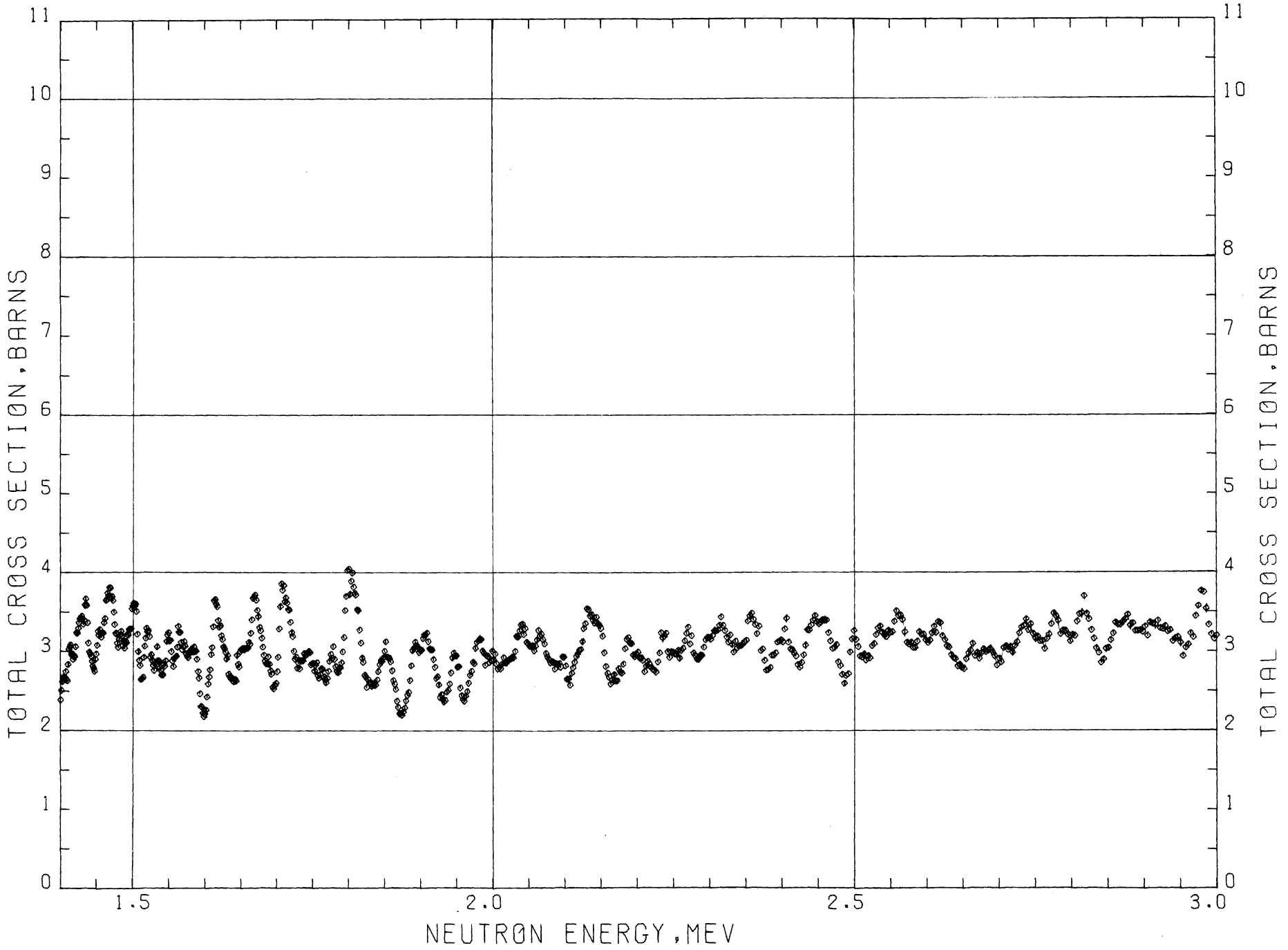
TOTAL CROSS SECTION, BARNS
NEUTRON ENERGY, MEV
0
1
2
3
4
5
6
7
8
9
10
11
1.5
2.0
2.5
3.0

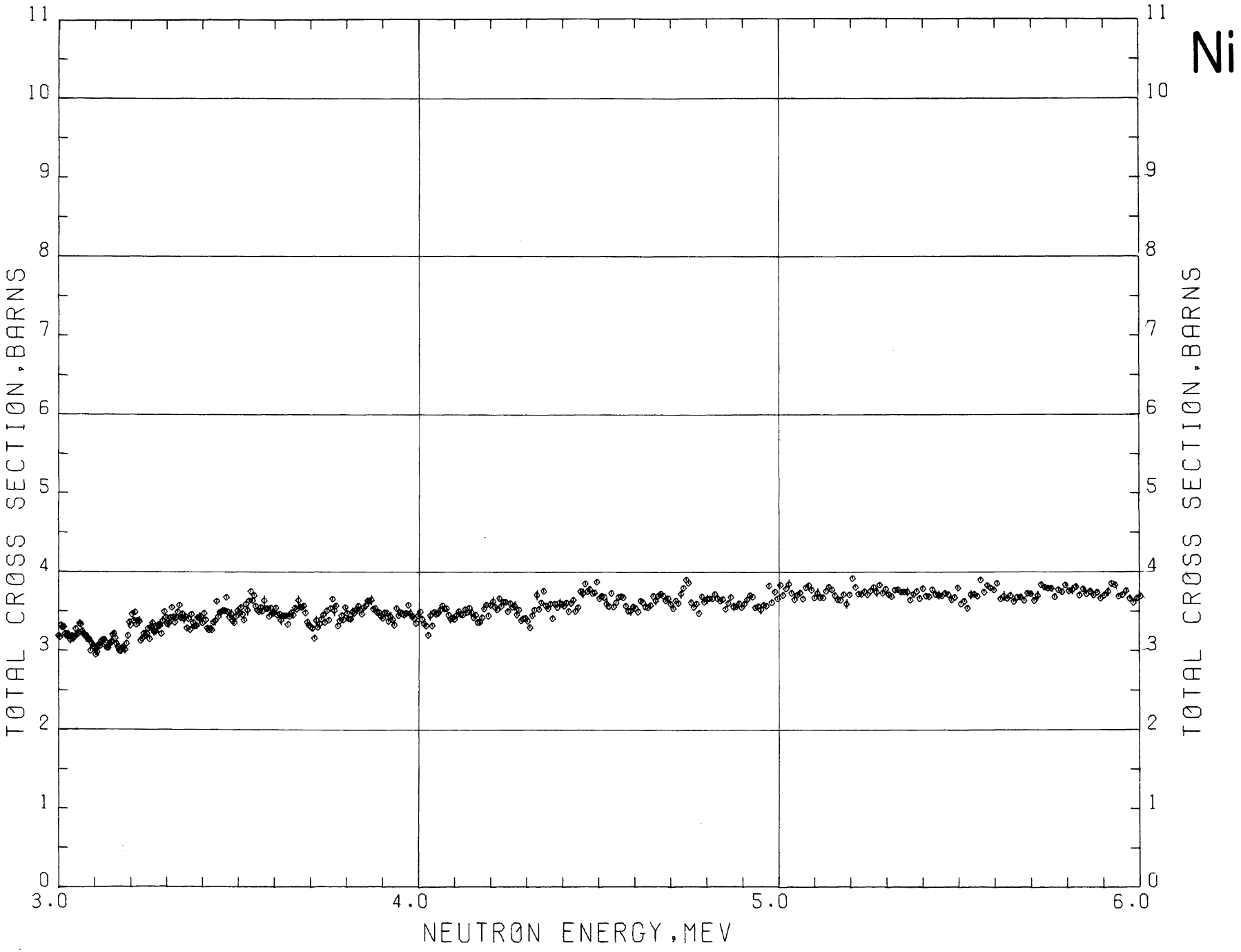
Ni
TOTAL CROSS SECTION, BARNS
NEUTRON ENERGY, MEV
0
1
2
3
4
5
6
7
8
9
10
11
3.0
4.0
5.0
6.0

Ni

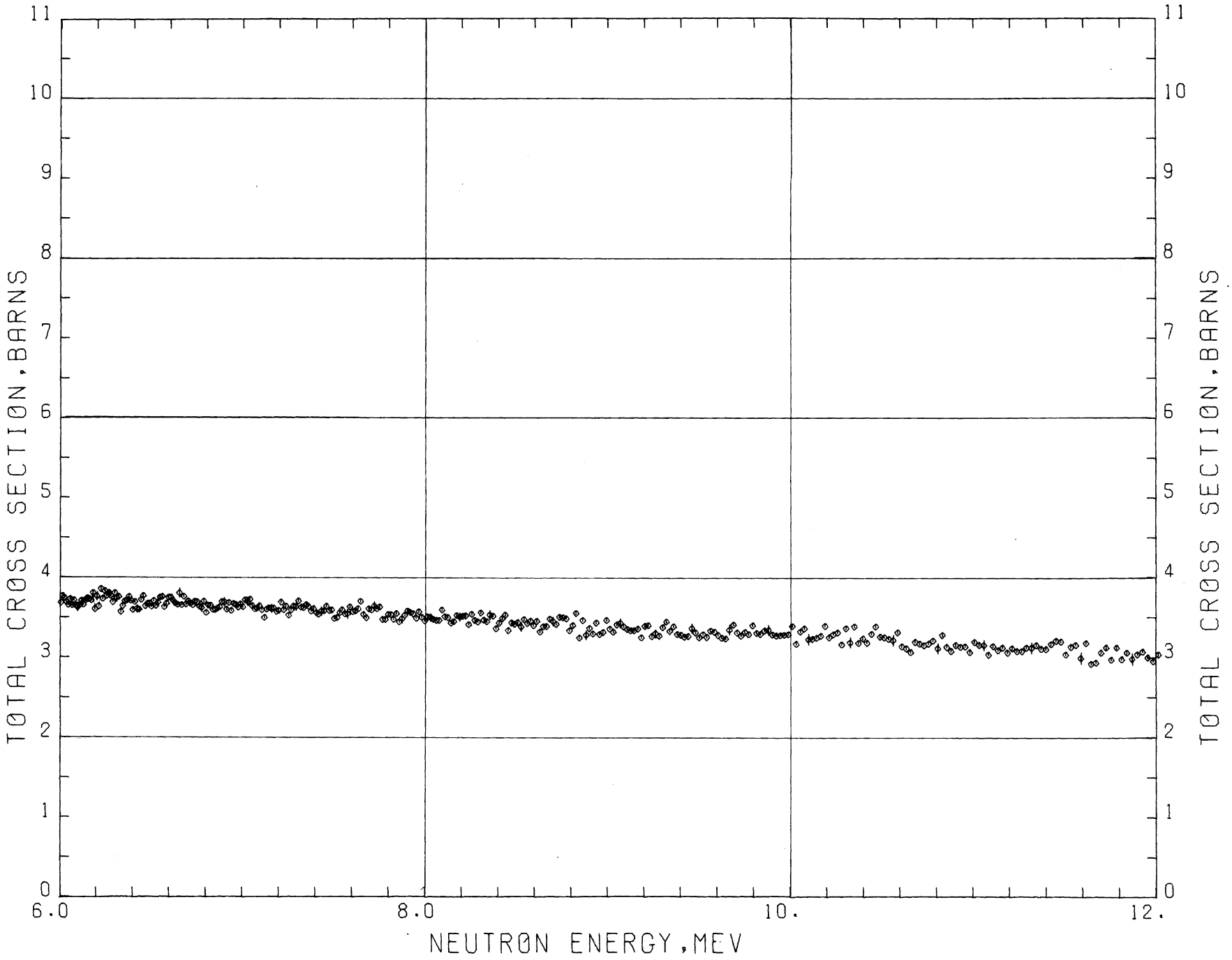
TOTAL CROSS SECTION, BARNS
NEUTRON ENERGY, MEV
0
1
2
3
4
5
6
7
8
9
10
11
6.0
8.0
10.
12.

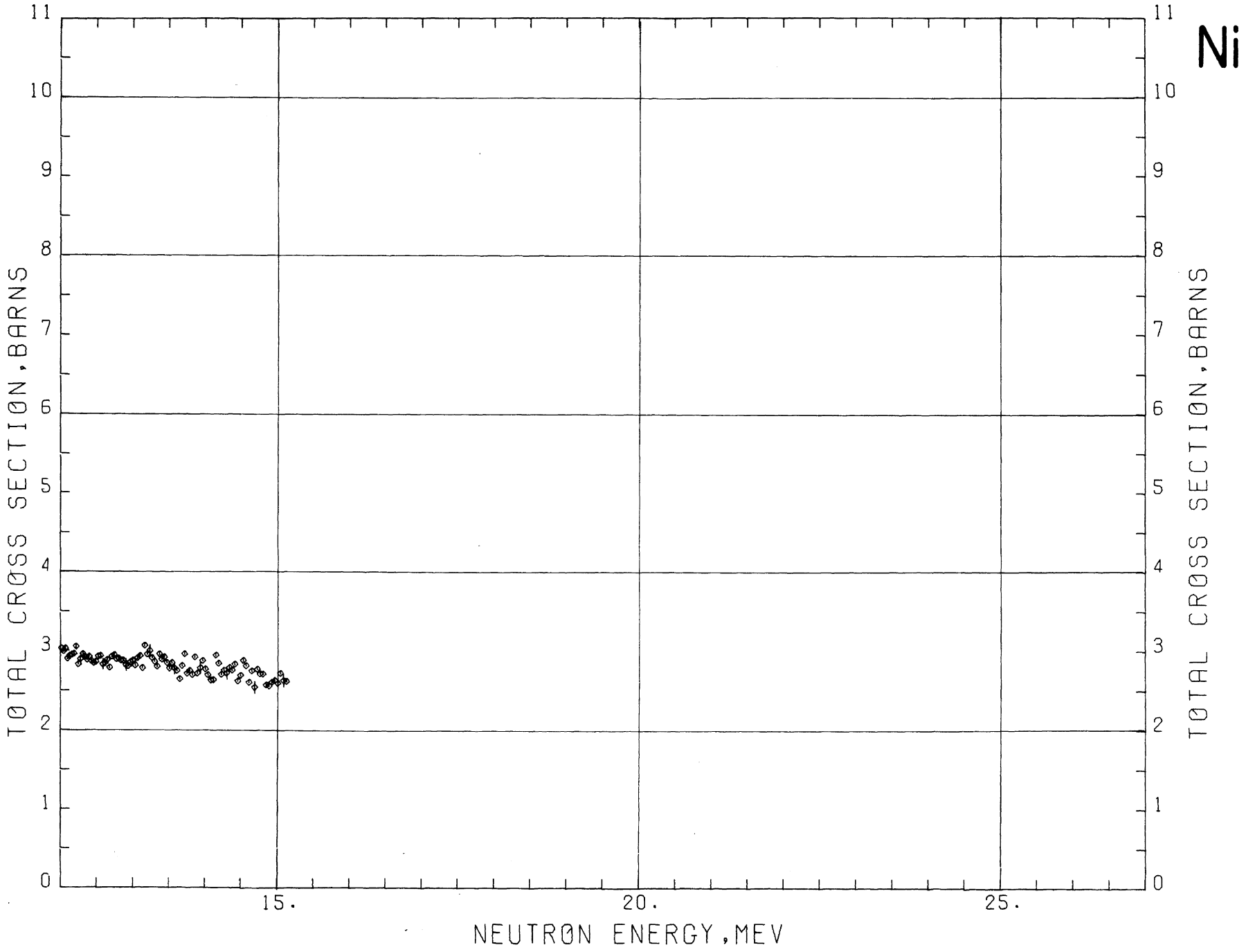
Ni
TOTAL CROSS SECTION, BARNS
NEUTRON ENERGY, MEV
0
1
2
3
4
5
6
7
8
9
10
11
15.
20.
25.

LEAD

Sample Material: metallic lead sheet

Sample Diameter: 12.7 cm

Sample Thickness: 7.6 cm, $n = 0.2614$ atoms/barn

Analysis: A qualitative spectrographic analysis was made on the sample; the principal impurity was copper, present to less than 0.1 percent. All other impurities were less than 0.01 percent.

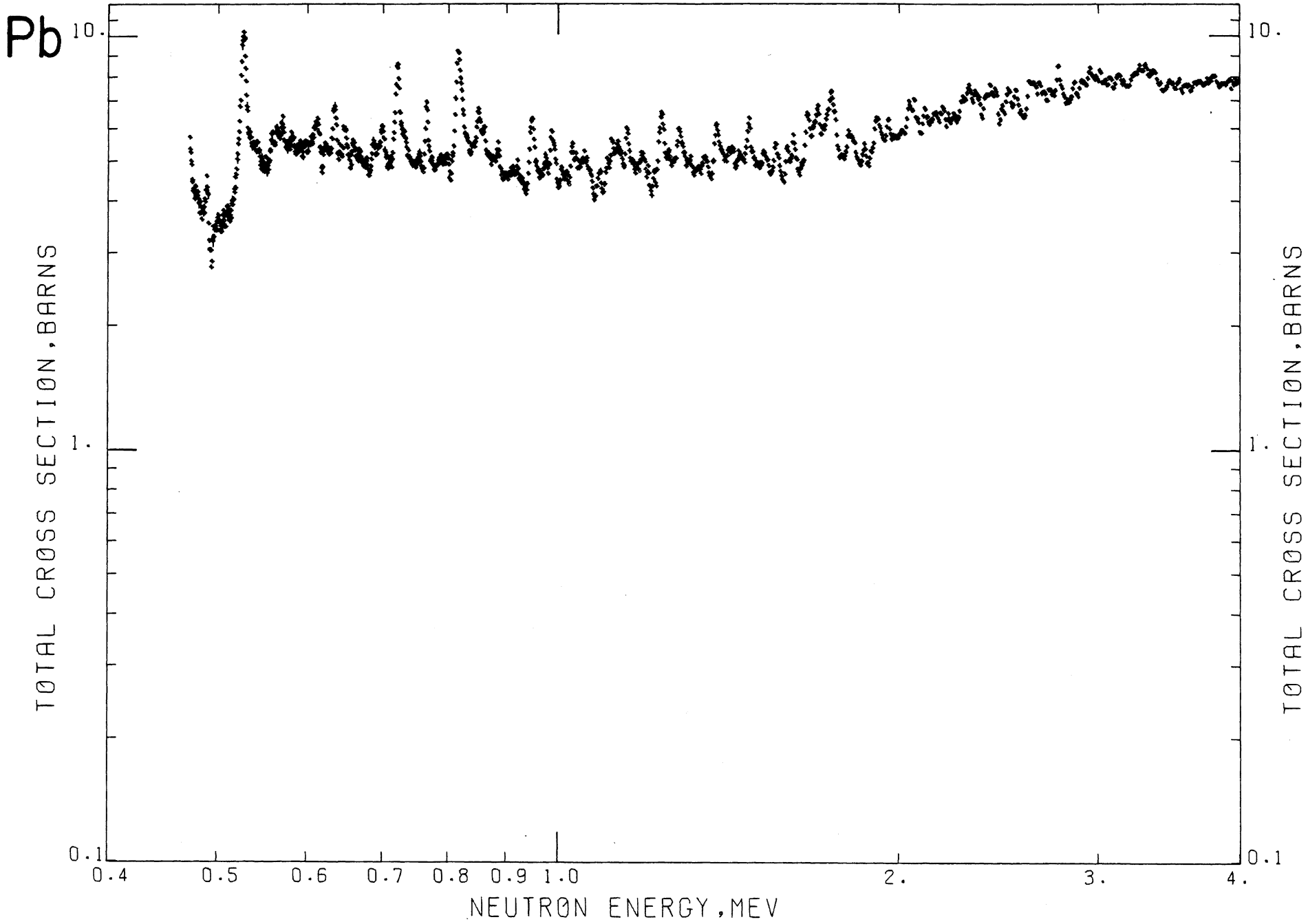
Pb
10.
1.
0.1
TOTAL CROSS SECTION, BARNS
0.4
0.5
0.6
0.7
0.8
0.9
1.0
2.
3.
4.
NEUTRON ENERGY, MEV

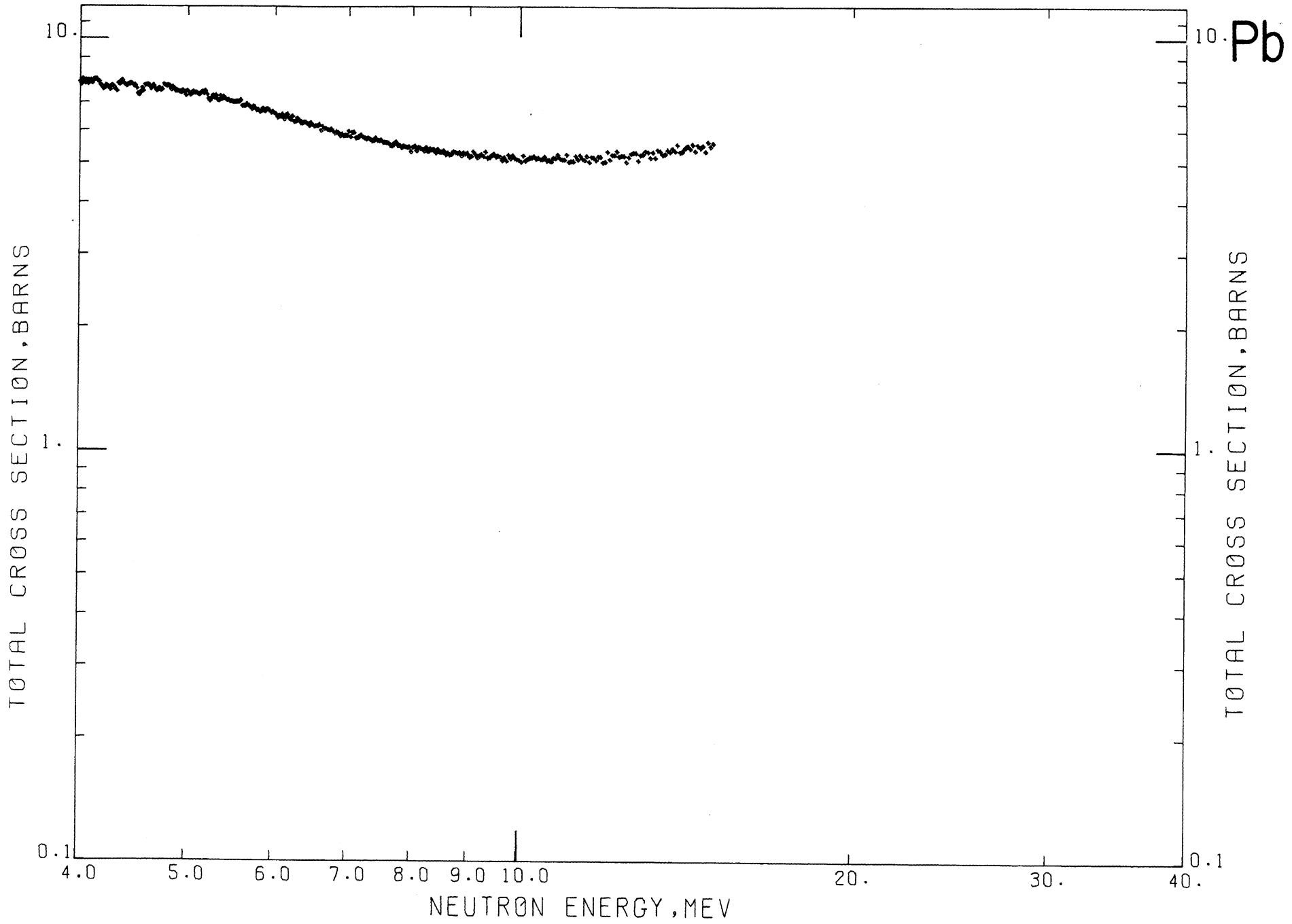
Pb
TOTAL CROSS SECTION, BARNS
NEUTRON ENERGY, MEV
10.
1.
0.1
4.0
5.0
6.0
7.0
8.0
9.0
10.0
20.
30.
40.

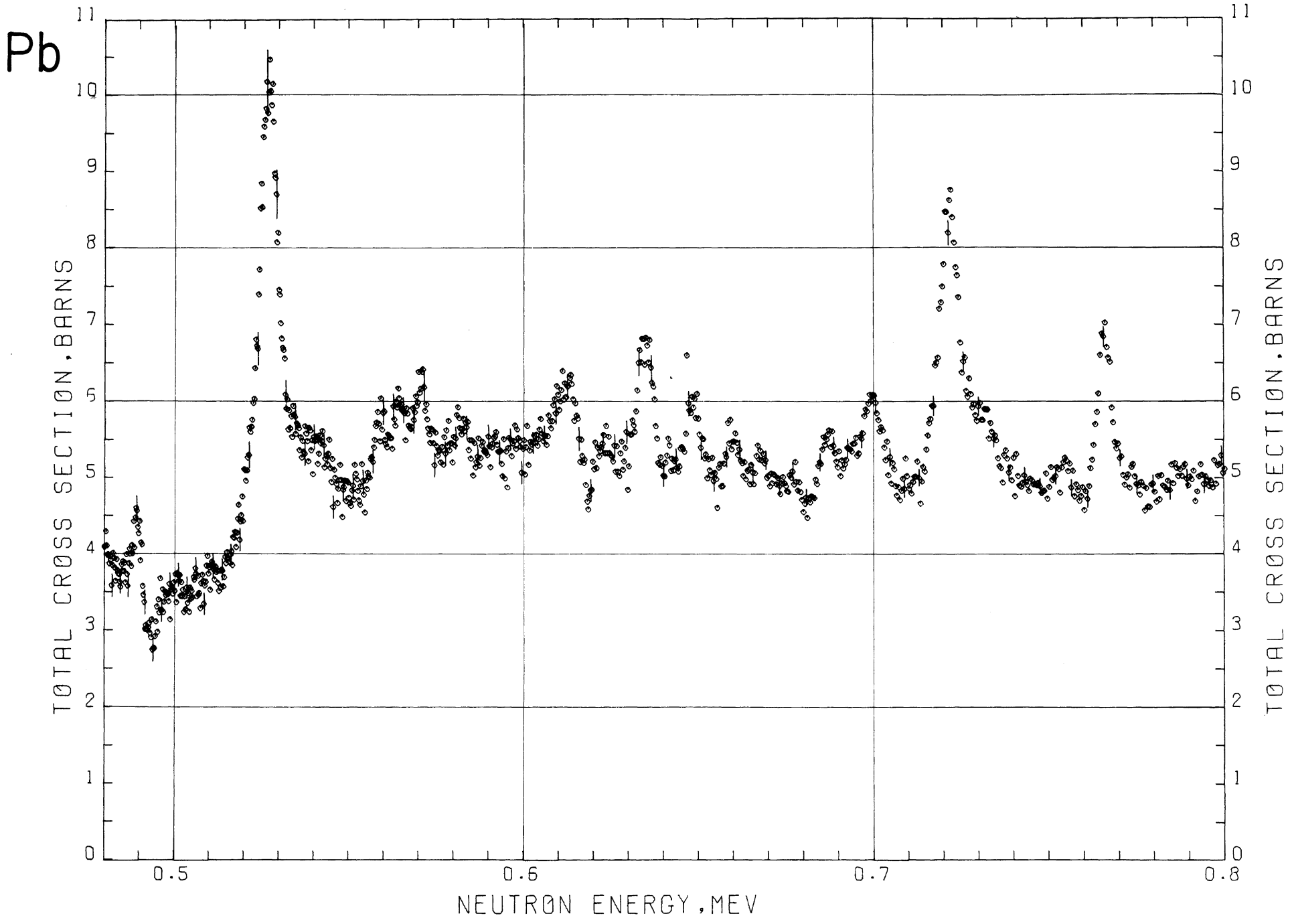
Pb
TOTAL CROSS SECTION, BARNS
NEUTRON ENERGY, MEV
0.5
0.6
0.7
0.8
0
1
2
3
4
5
6
7
8
9
10
11

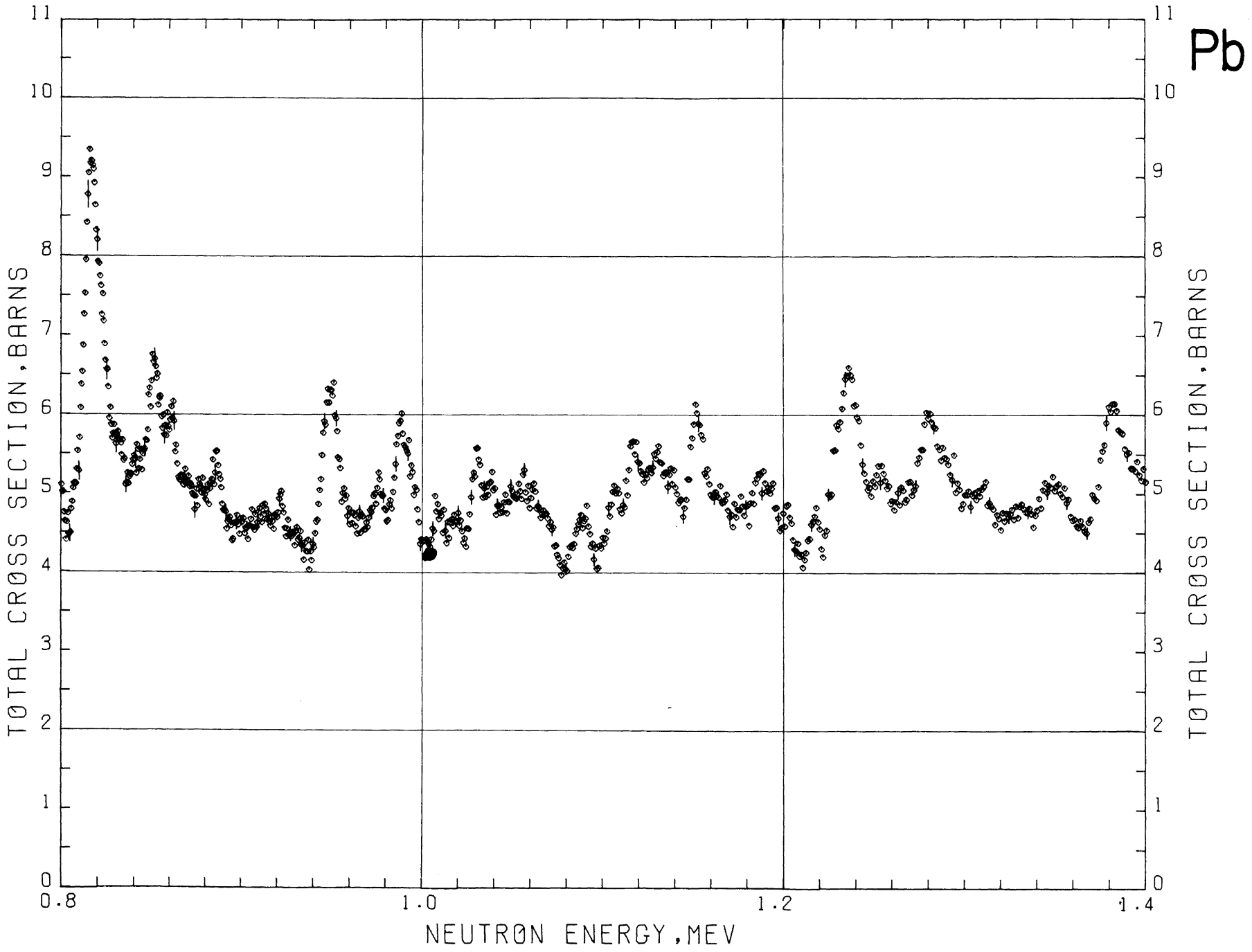
Pb
TOTAL CROSS SECTION, BARNS
NEUTRON ENERGY, MEV
0.8
1.0
1.2
1.4
0
1
2
3
4
5
6
7
8
9
10
11

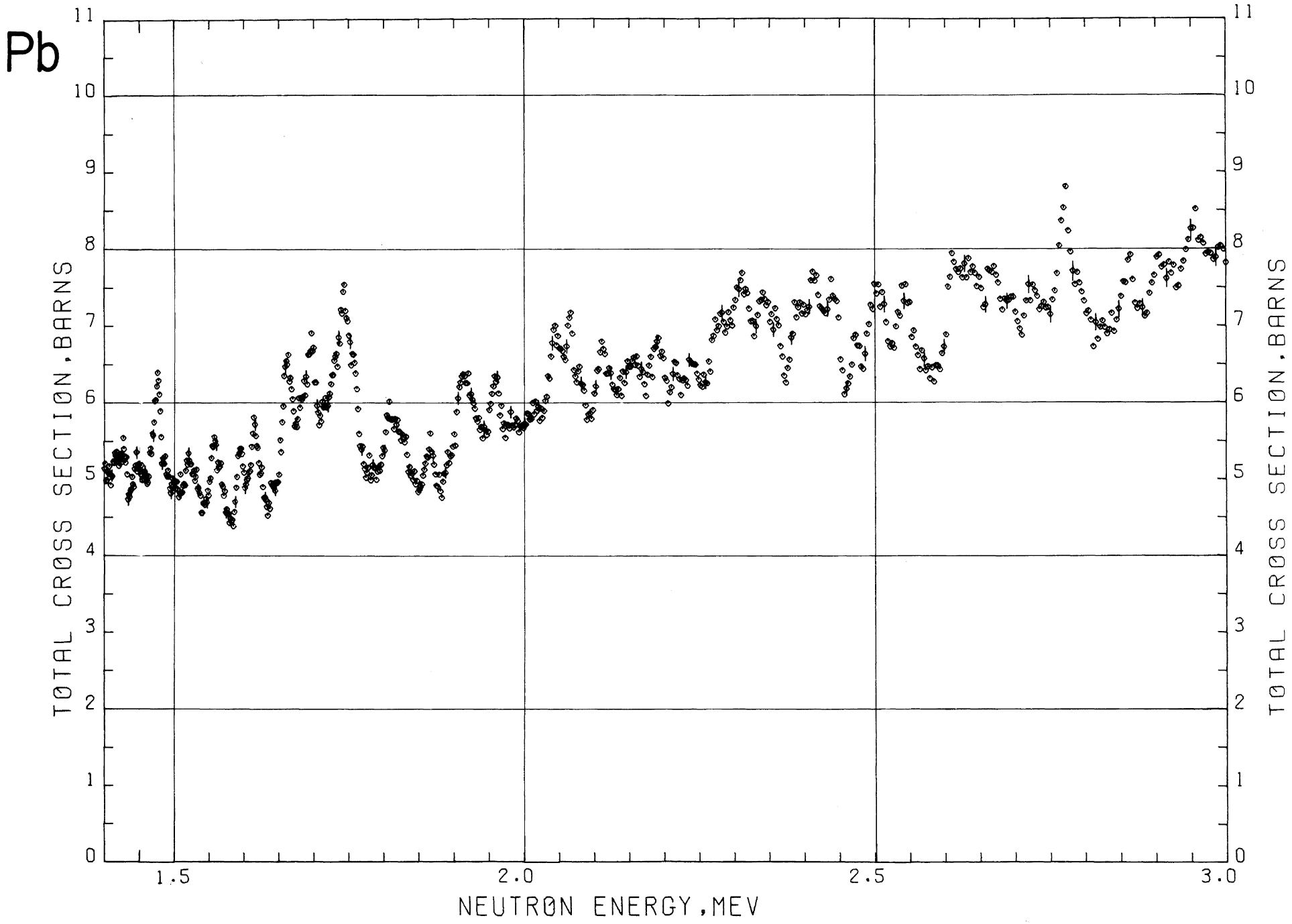
Pb
TOTAL CROSS SECTION, BARNS
NEUTRON ENERGY, MEV
0
1
2
3
4
5
6
7
8
9
10
11
1.5
2.0
2.5
3.0

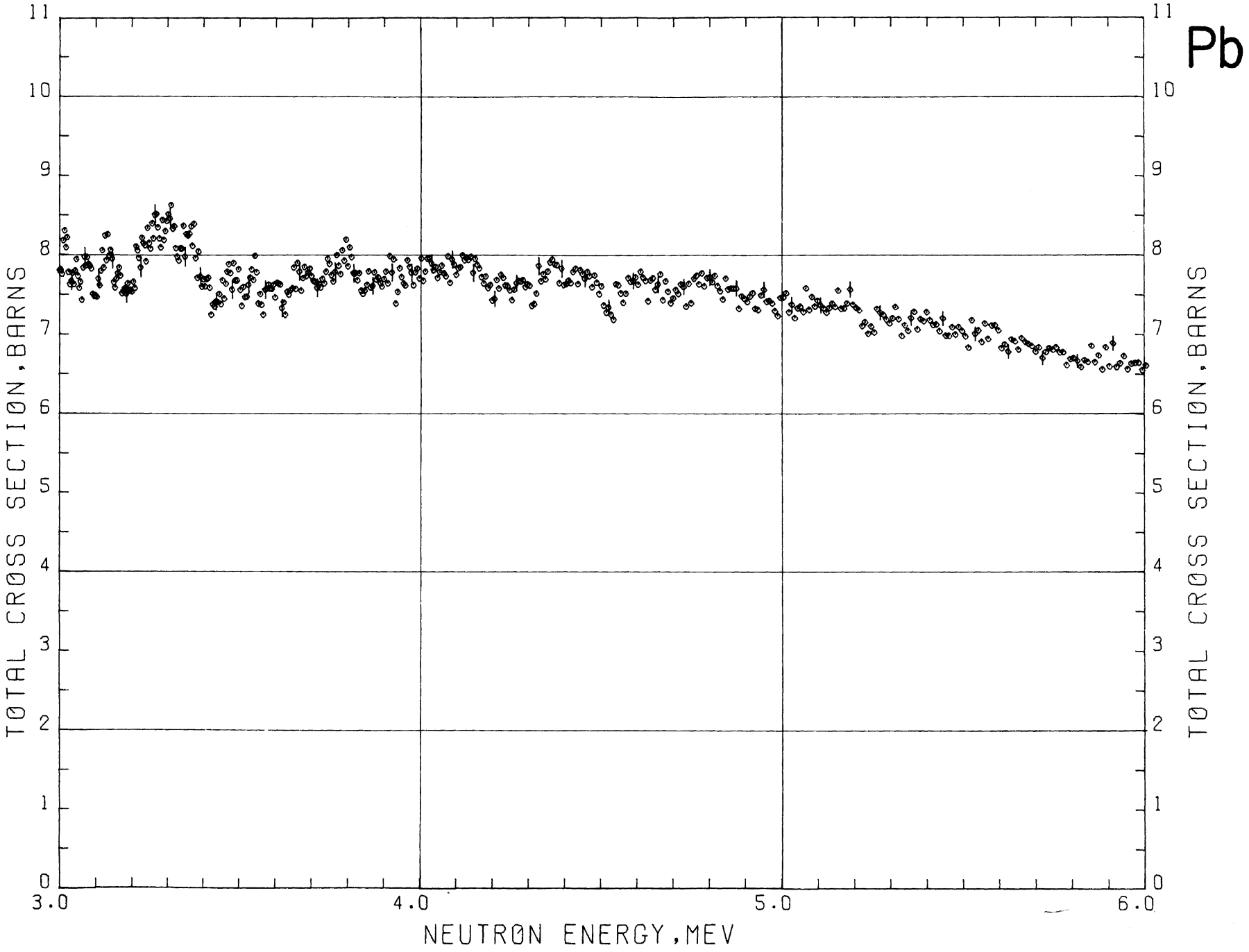
Pb
TOTAL CROSS SECTION, BARNS
NEUTRON ENERGY, MEV
0
1
2
3
4
5
6
7
8
9
10
11
3.0
4.0
5.0
6.0

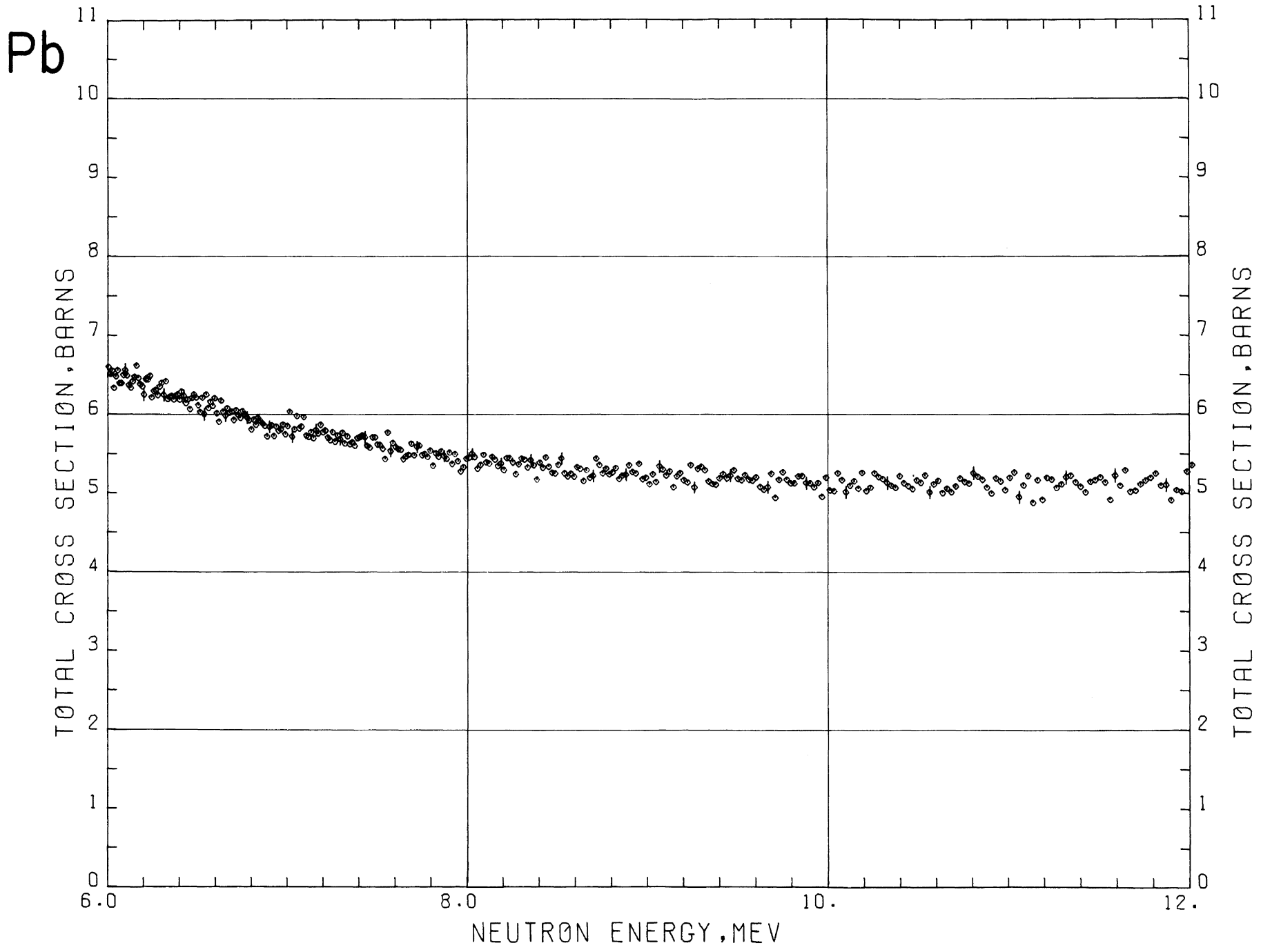
Pb
TOTAL CROSS SECTION, BARNS
NEUTRON ENERGY, MEV
6.0
8.0
10.
12.
0
1
2
3
4
5
6
7
8
9
10
11

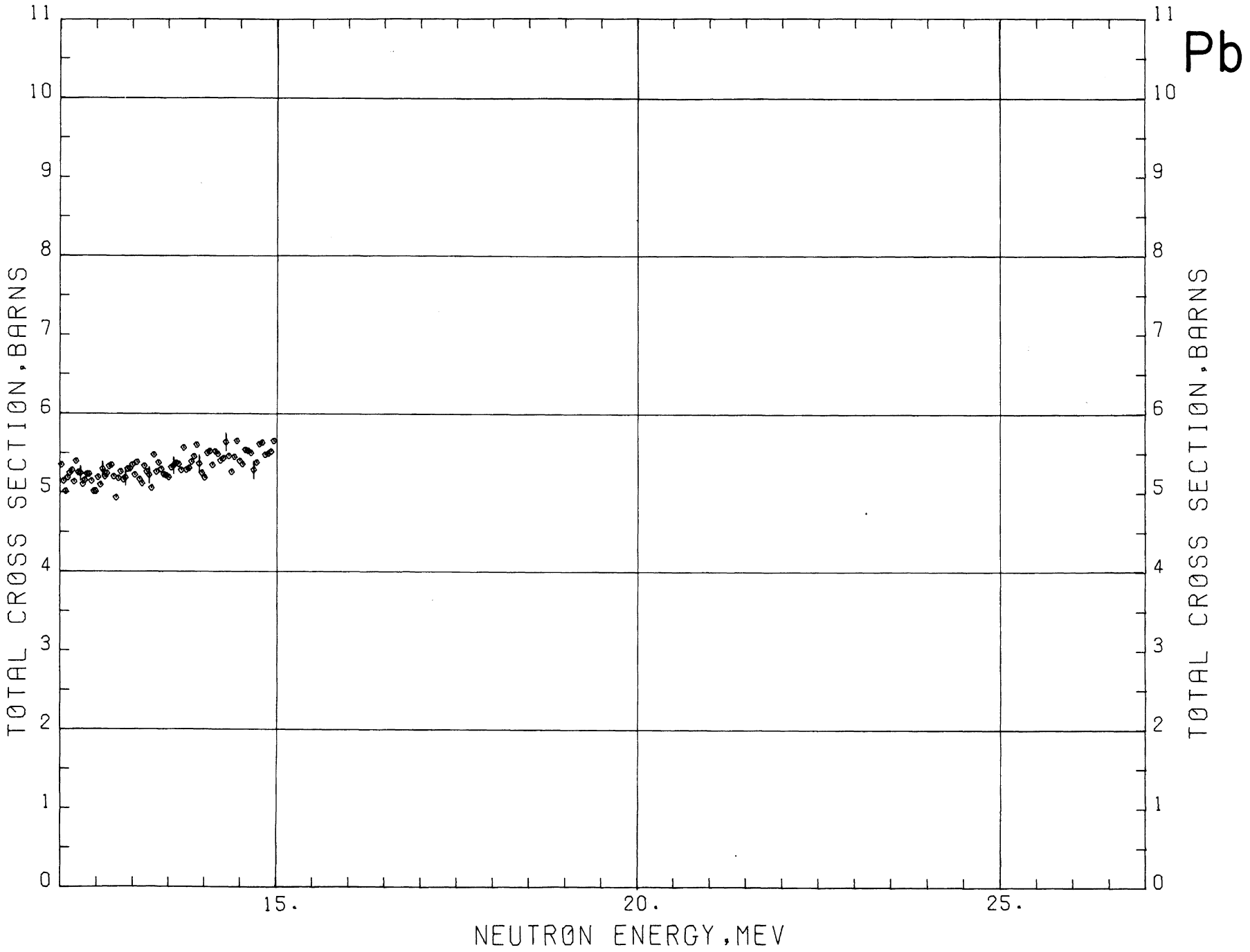
Pb
TOTAL CROSS SECTION, BARNS
TOTAL CROSS SECTION, BARNS
NEUTRON ENERGY, MEV
0
1
2
3
4
5
6
7
8
9
10
11
15.
20.
25.

^{235}URANIUM

Sample Material: enriched metallic uranium

Sample Diameter: 1.91 cm

Sample Thickness: 4.45 cm, $n = 0.2136$ atoms/barn

Analysis:

^{234}U:	1.00 percent	C:	200 ppm by weight
^{235}U:	93.22	Si:	200
^{236}U:	0.38	Fe:	200
^{238}U:	5.39	O:	80
		P:	50
		Ni:	30
		Al:	20

Literature Reference: R. B. Schwartz, H. T. Heaton II, J. Menke, and R. A. Schrack, Bull. Am. Phys. Soc. 18 (1973) 539.

Comments: The measured cross section has been corrected for the ^{238}U and carbon content, using our previously measured values of these cross sections. Since the maximum correction was 0.4 percent, any errors in the corrections would introduce a totally negligible error in the final cross section. Systematic errors in the final corrected cross sections due to the remaining impurities are < 0.1 percent.

Acknowledgment: We should like to thank the Los Alamos Scientific Laboratory for providing us with the sample, and for doing the chemical and isotopic analysis.

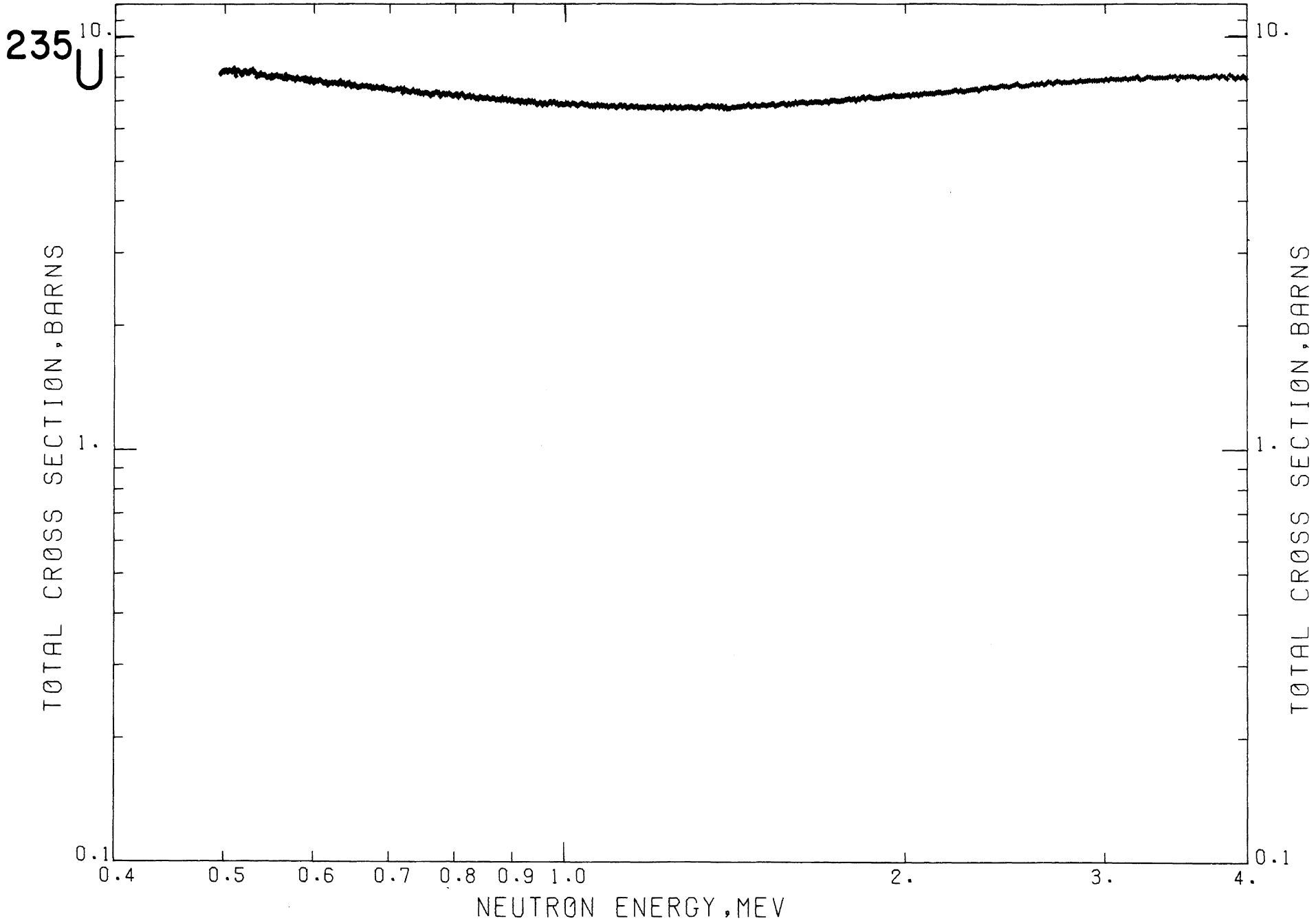
235U
10.
1.
0.1
TOTAL CROSS SECTION, BARNS
0.4
0.5
0.6
0.7
0.8
0.9
1.0
2.
3.
4.
NEUTRON ENERGY, MEV

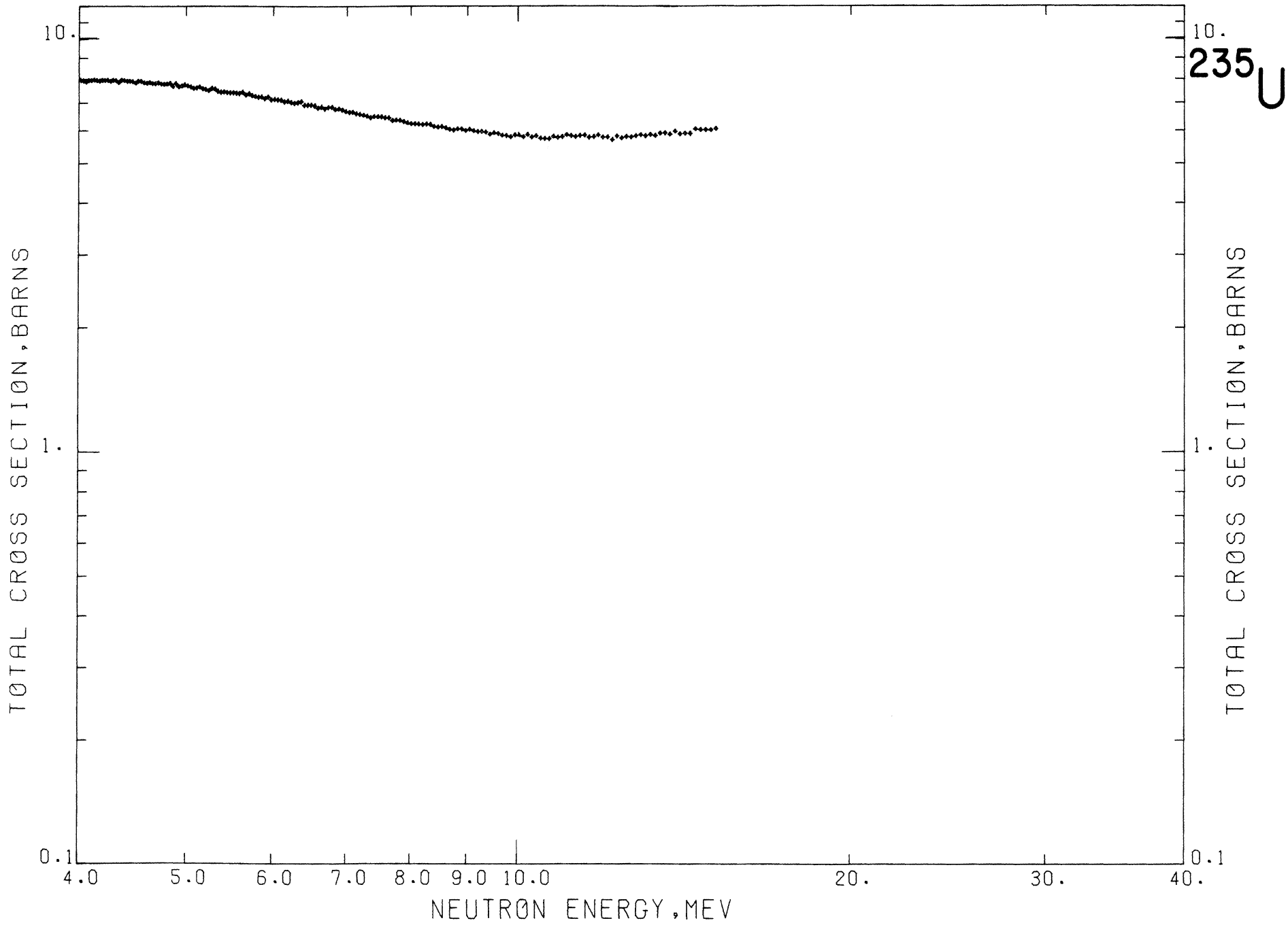
10.
1.
0.1
TOTAL CROSS SECTION, BARNS
4.0
5.0
6.0
7.0
8.0
9.0
10.0
20.
30.
40.
NEUTRON ENERGY, MEV
235U

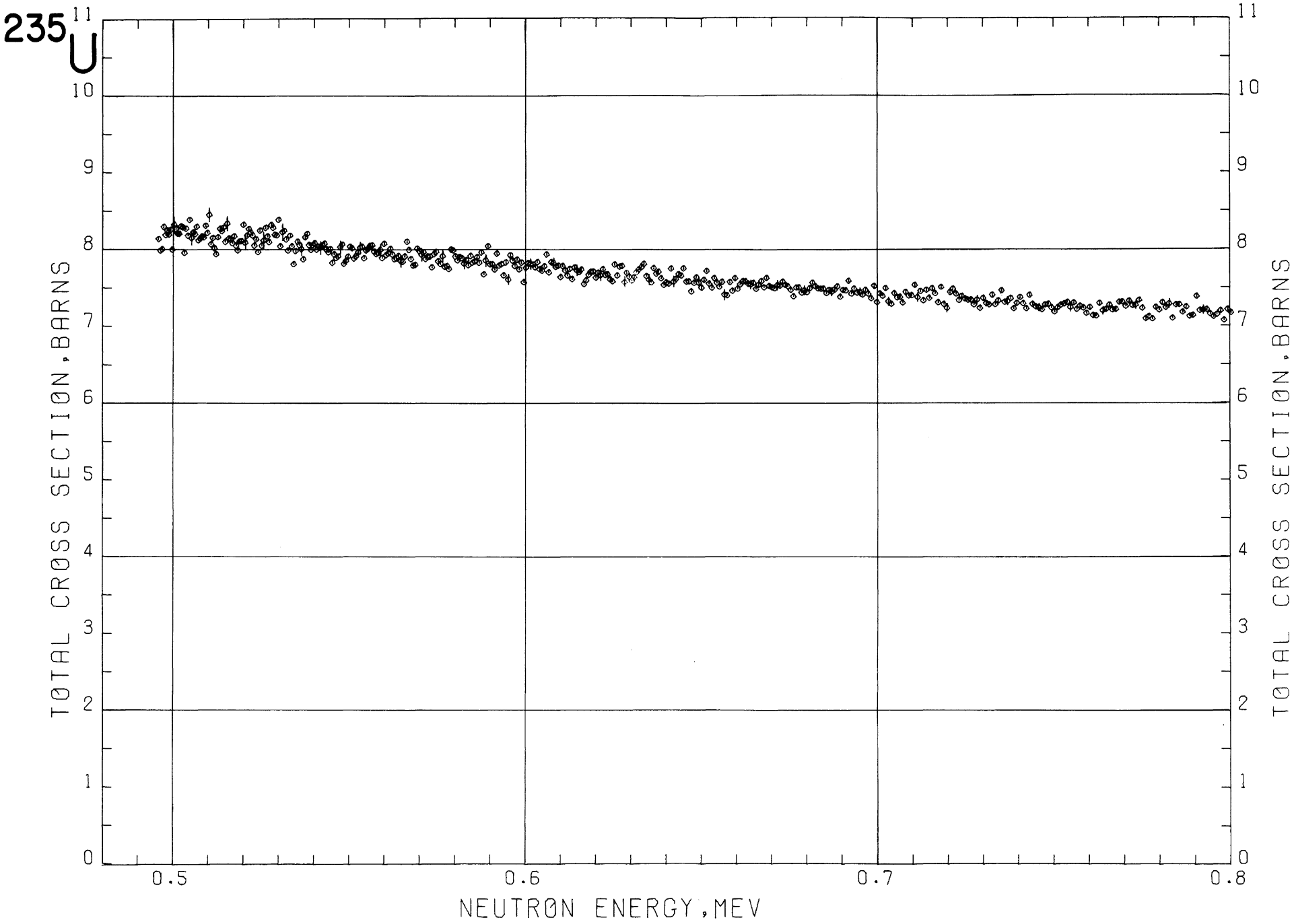
235U
TOTAL CROSS SECTION, BARNS
NEUTRON ENERGY, MEV
0.5
0.6
0.7
0.8
0
1
2
3
4
5
6
7
8
9
10
11

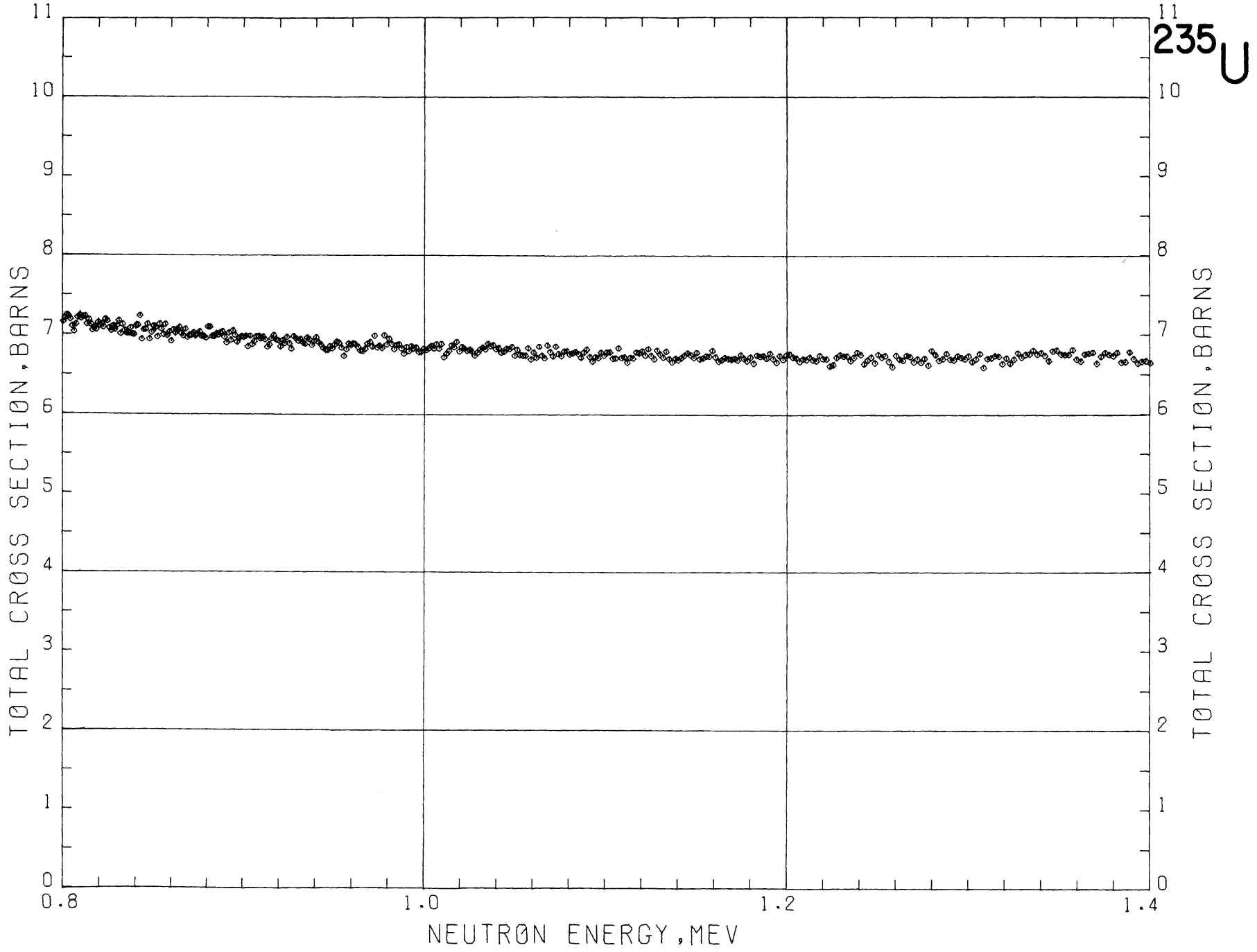
235U
TOTAL CROSS SECTION, BARNS
NEUTRON ENERGY, MEV
0.8
1.0
1.2
1.4
0
1
2
3
4
5
6
7
8
9
10
11

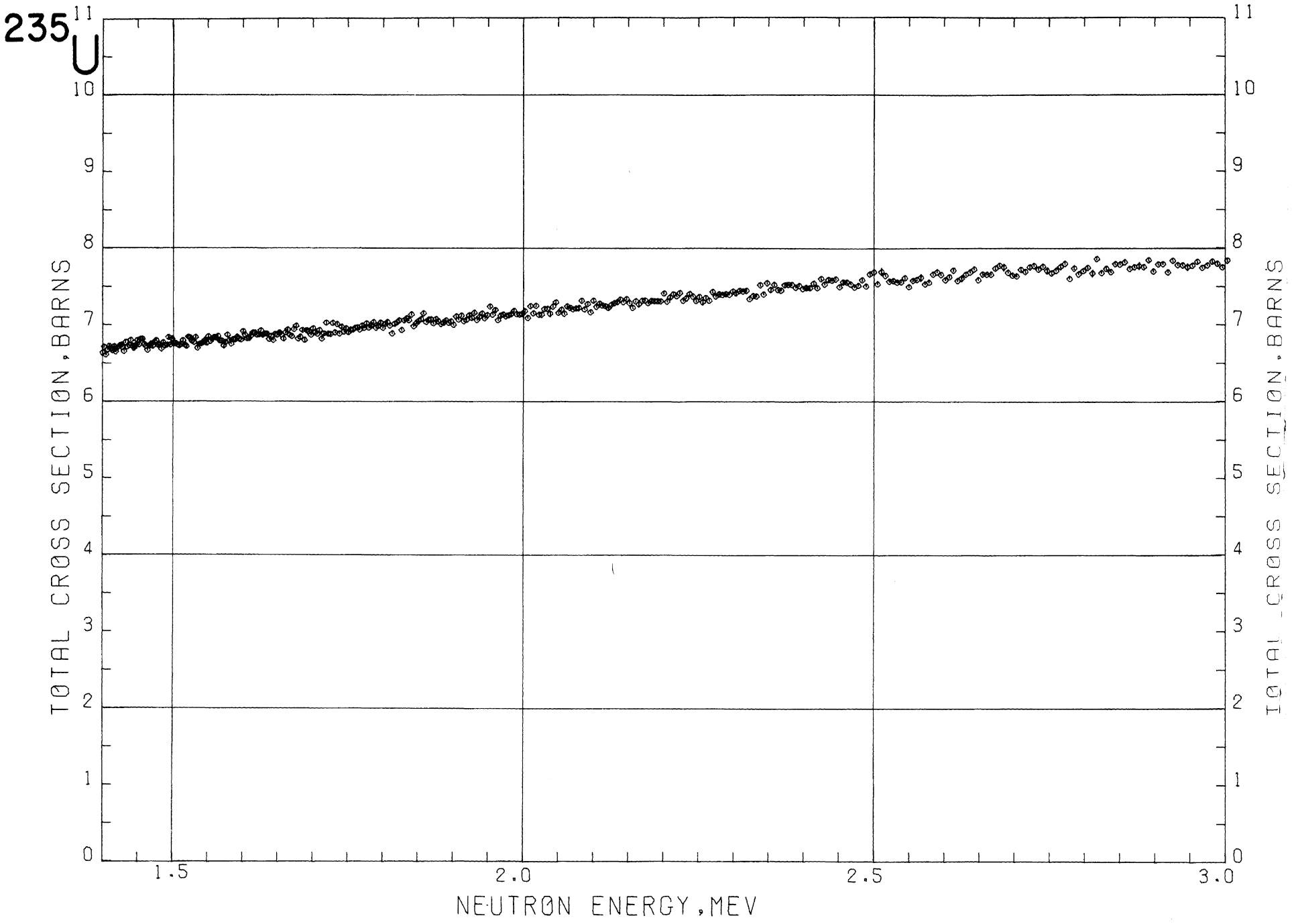
235U
TOTAL CROSS SECTION, BARNS
NEUTRON ENERGY, MEV
0
1
2
3
4
5
6
7
8
9
10
11
1.5
2.0
2.5
3.0

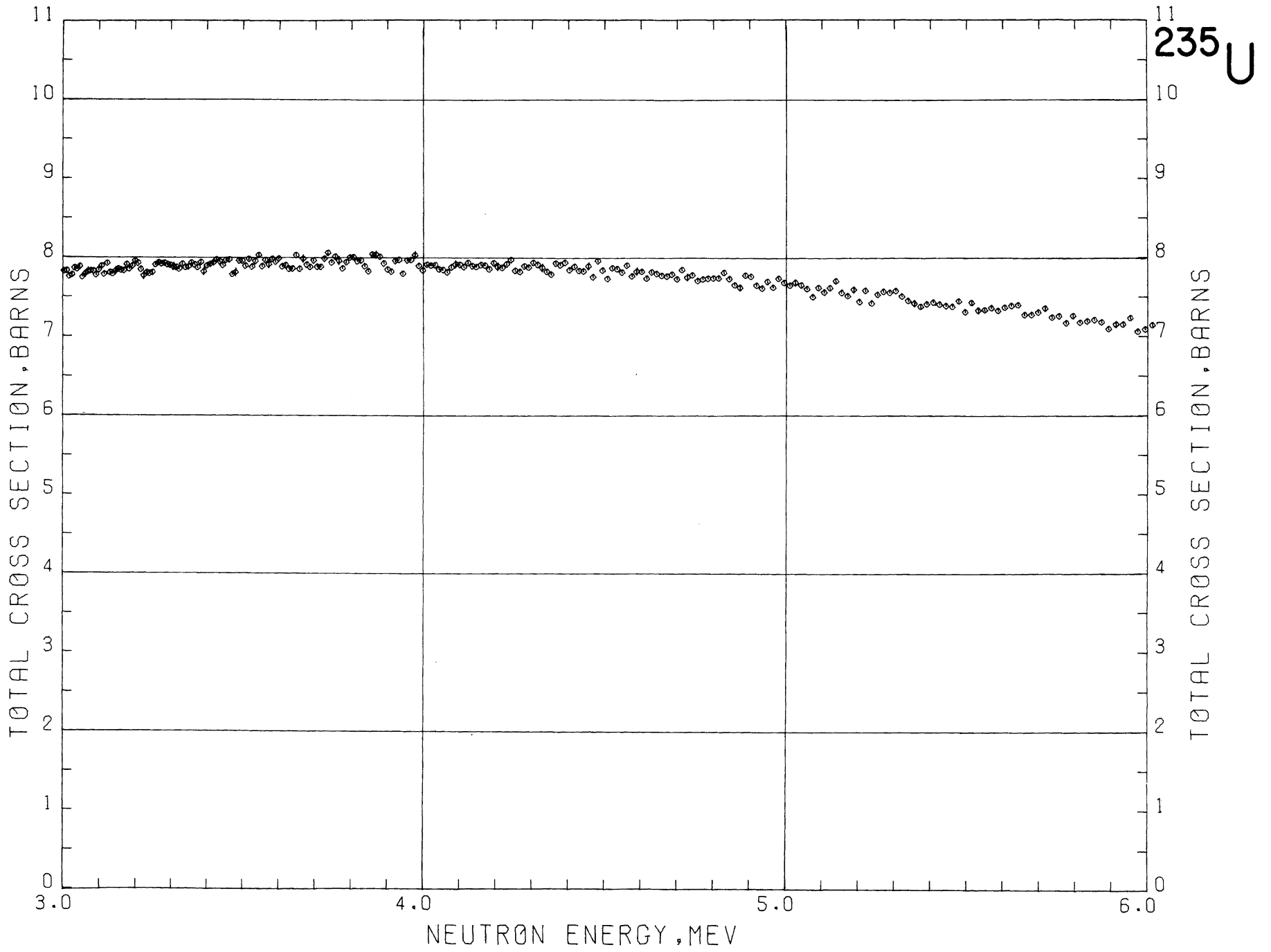
235U
TOTAL CROSS SECTION, BARNS
NEUTRON ENERGY, MEV
0
1
2
3
4
5
6
7
8
9
10
11
3.0
4.0
5.0
6.0

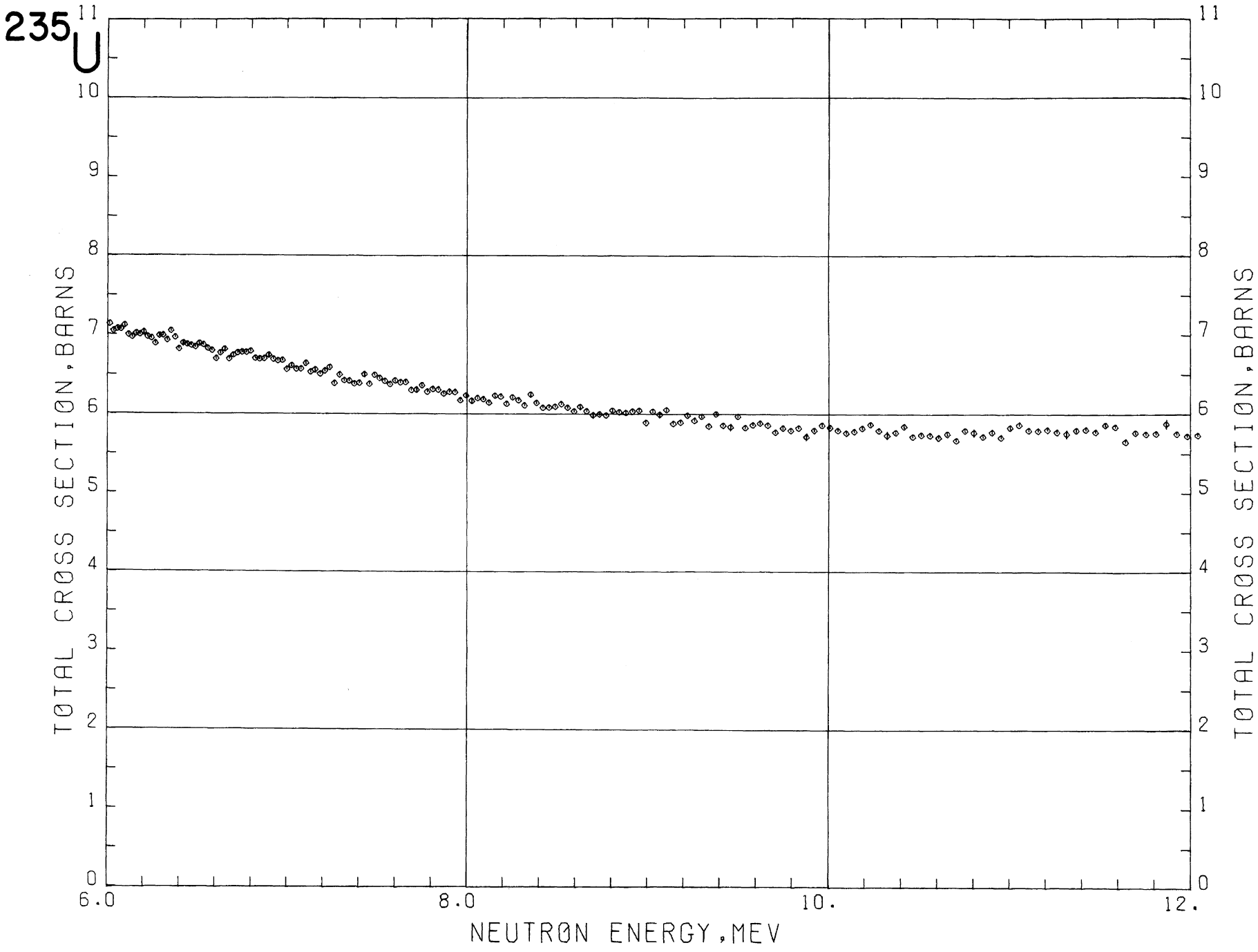
235U
TOTAL CROSS SECTION, BARNS
NEUTRON ENERGY, MEV
6.0
8.0
10.
12.
0
1
2
3
4
5
6
7
8
9
10
11

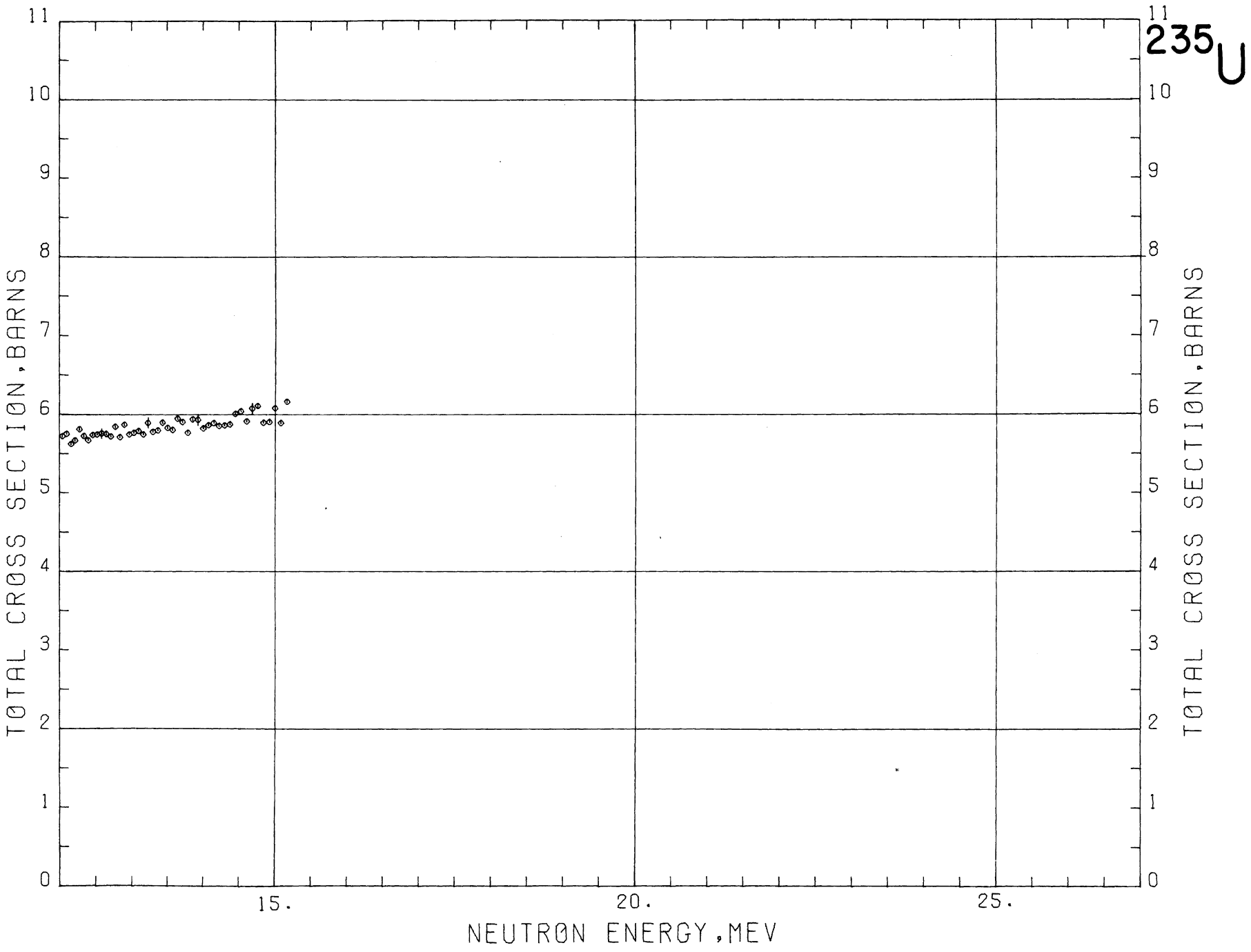
235U
TOTAL CROSS SECTION, BARNS
NEUTRON ENERGY, MEV
0
1
2
3
4
5
6
7
8
9
10
11
15.
20.
25.

^{238}URANIUM

Sample Material: depleted uranium metal

Sample Sizes: 5.08 cm diam; 1.91 cm thick; $n = 0.0914$
5.08 cm diam; 4.45 cm thick; $n = 0.2128$
1.91 cm diam; 4.45 cm thick; $n = 0.2132$

Analysis:

^{235}U:	0.19 percent	C:	350 ppm by weight
^{238}U:	99.80	Si:	400
		Fe:	100
		O:	85
		Ni:	30
		Al:	15

Literature Reference: R. B. Schwartz, H. T. Heaton II, J. Menke, and R. A. Schrack, Bull. Ann. Phys. Soc. 18 (1973) 539.

Comments: The measured cross sections have been corrected for the carbon and silicon content, using our previously measured values for these cross sections. Since the magnitude of the corrections is < ½ percent, any errors in the corrections would introduce a totally negligible in the final cross section. Systematic errors in the final, corrected, cross section due to the remaining impurities are < 0.1 percent.

Acknowledgment: We should like to thank the Los Alamos Scientific Laboratory for providing us with the samples, and for performing the chemical and isotopic analysis.

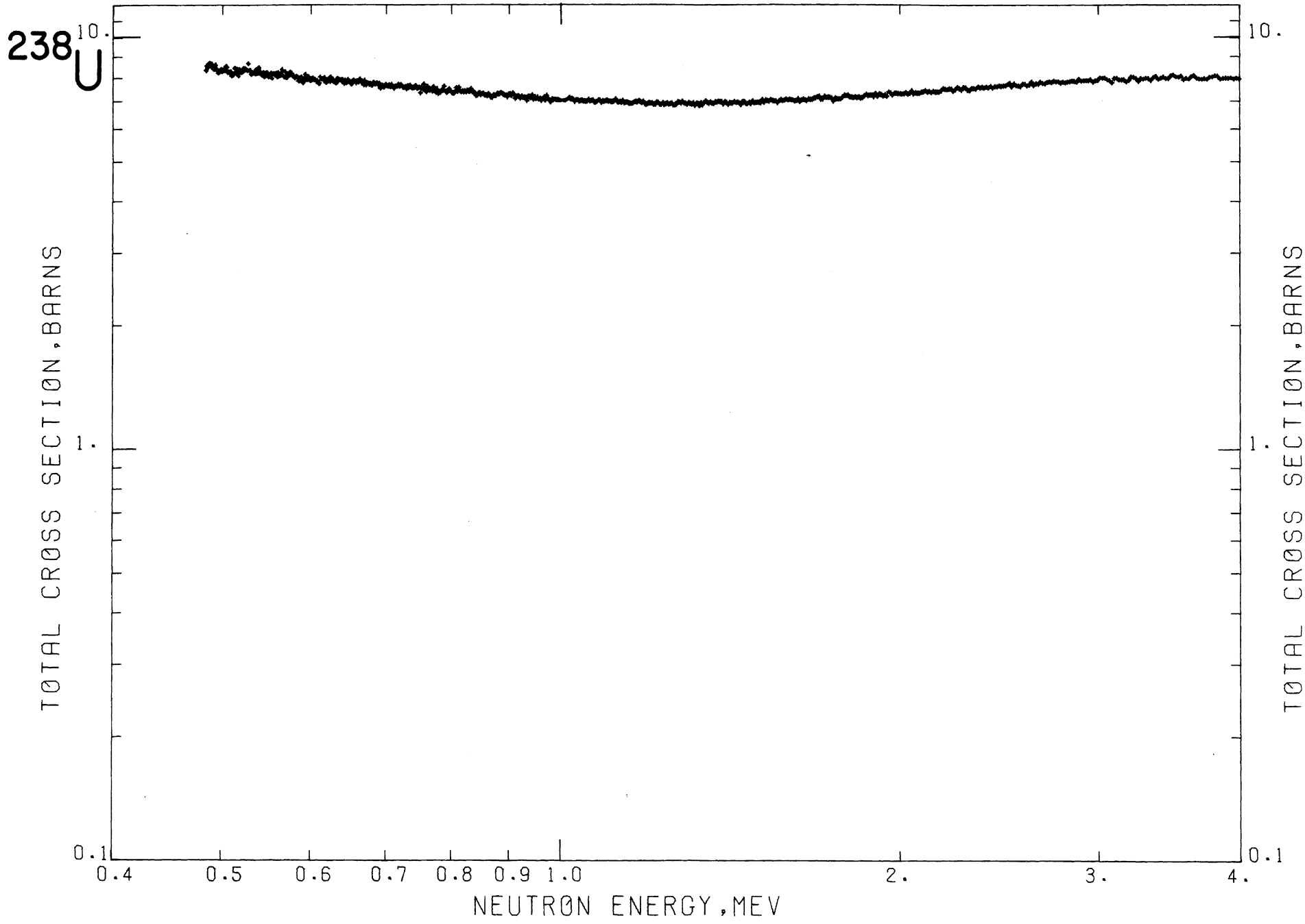
238U
10.
1.
0.1
TOTAL CROSS SECTION, BARNS
0.4
0.5
0.6
0.7
0.8
0.9
1.0
2.
3.
4.
NEUTRON ENERGY, MEV

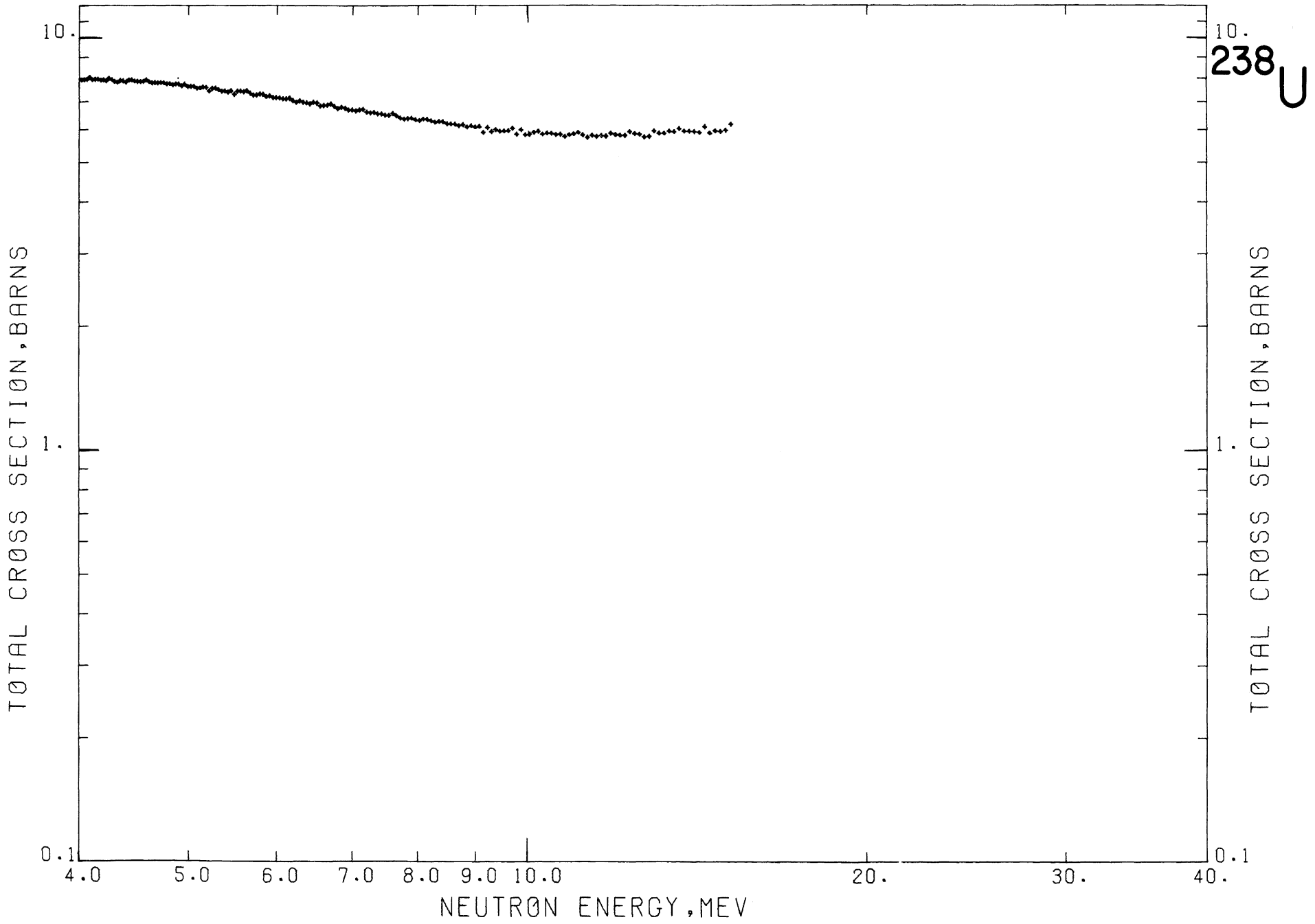
238U
TOTAL CROSS SECTION, BARNS
NEUTRON ENERGY, MEV
10.
1.
0.1
4.0
5.0
6.0
7.0
8.0
9.0
10.0
20.
30.
40.

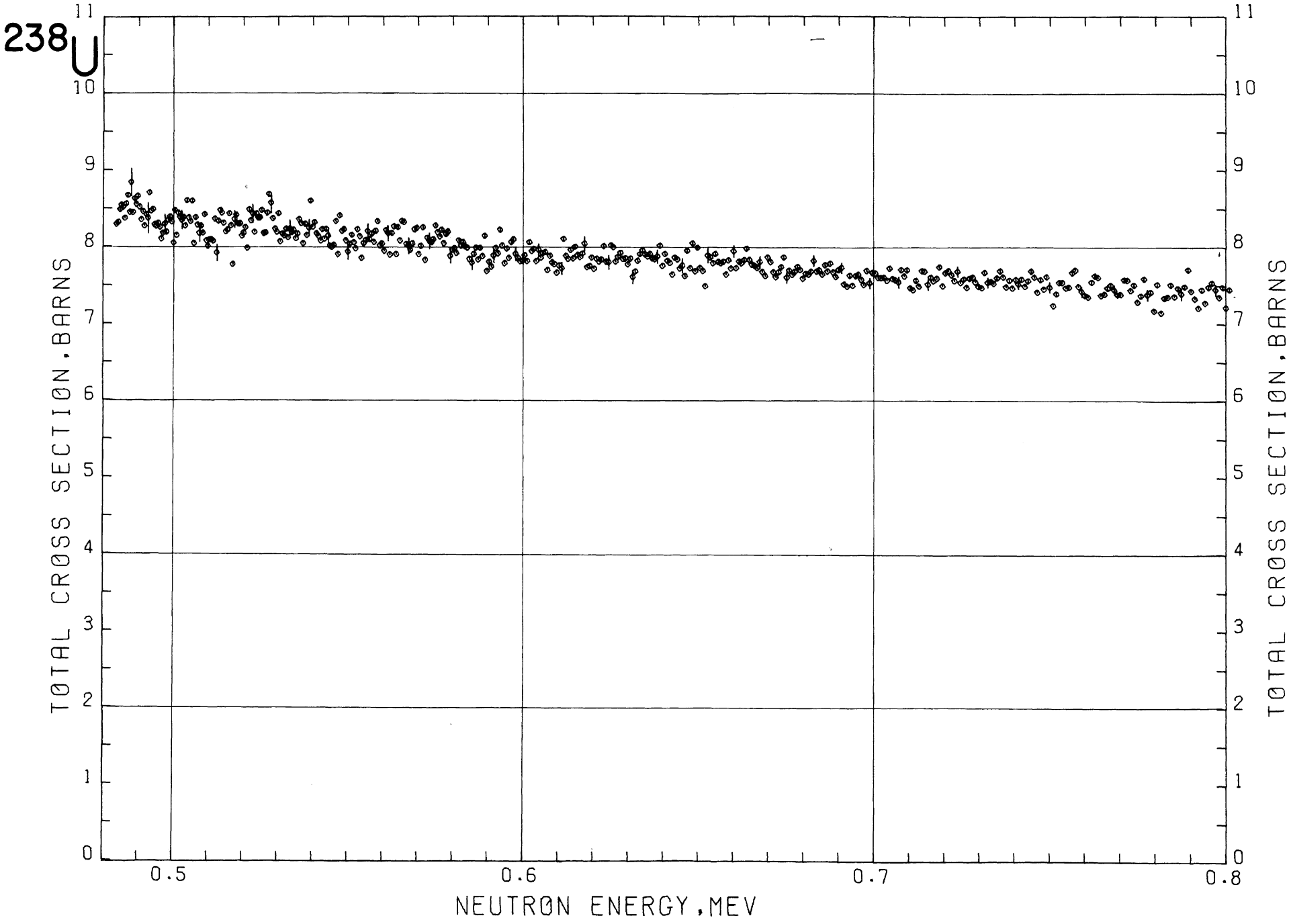
238U
TOTAL CROSS SECTION, BARNS
NEUTRON ENERGY, MEV
0.5
0.6
0.7
0.8
0
1
2
3
4
5
6
7
8
9
10
11

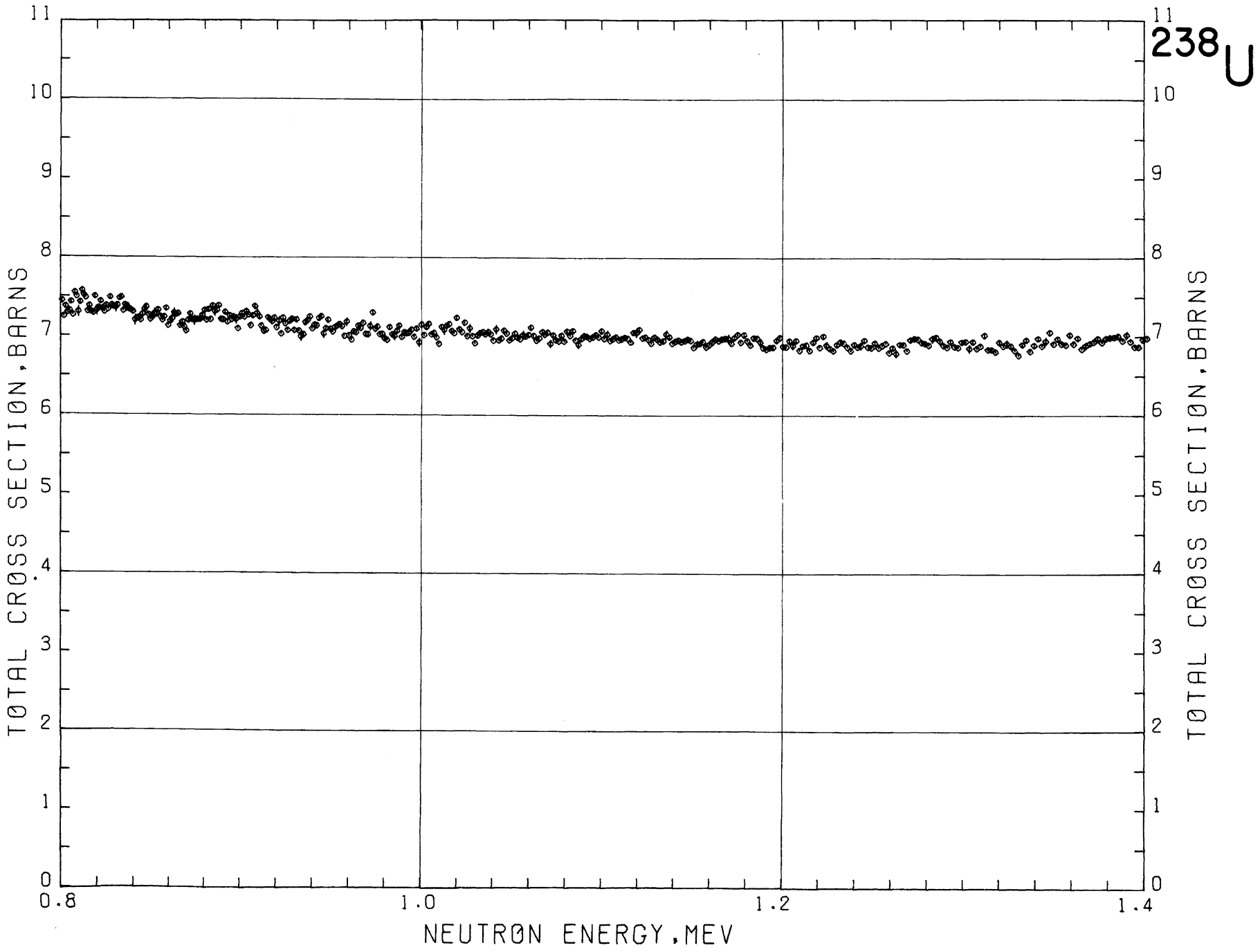
238U
TOTAL CROSS SECTION, BARNS
NEUTRON ENERGY, MEV
0.8
1.0
1.2
1.4
0
1
2
3
4
5
6
7
8
9
10
11

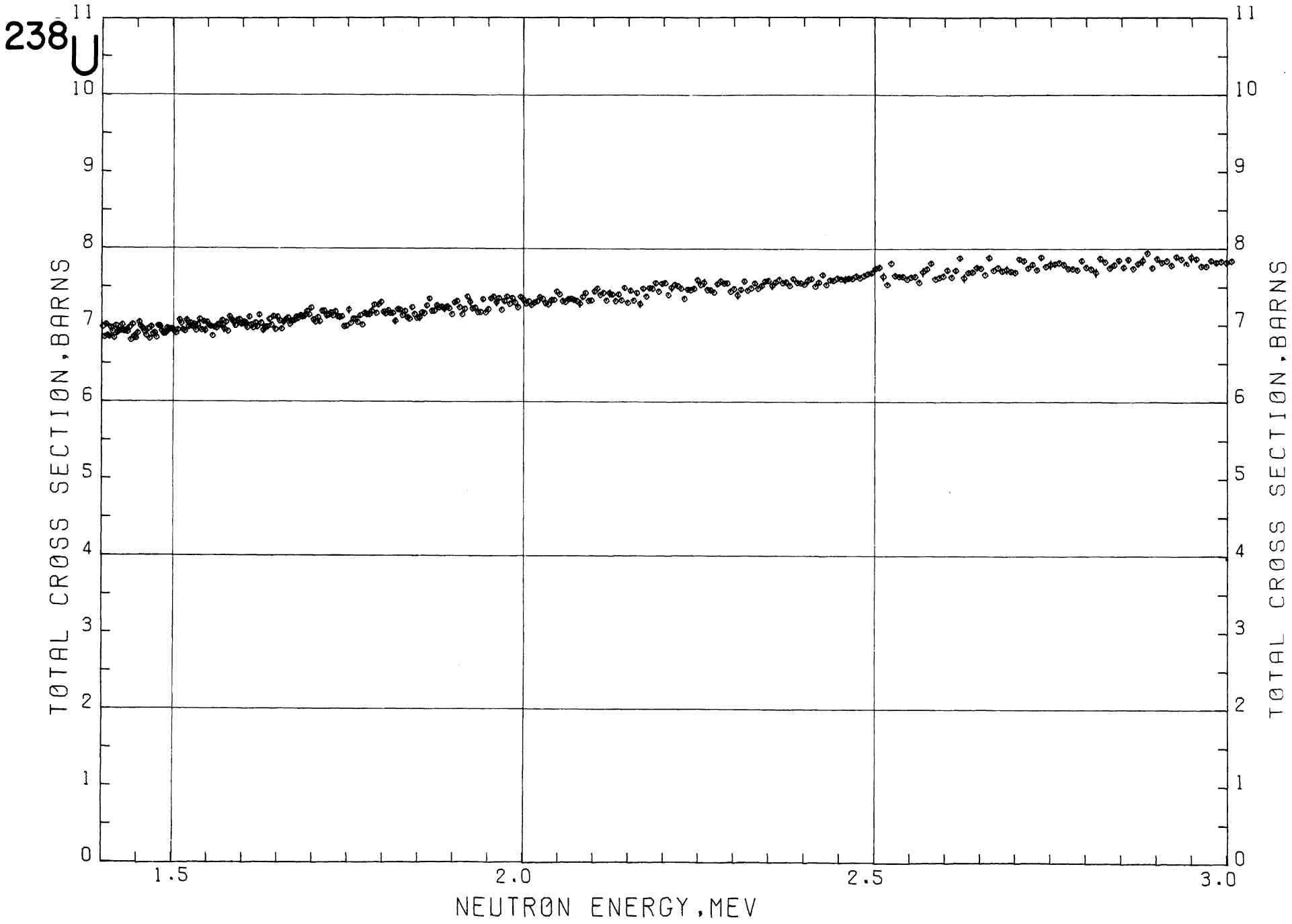
238U
TOTAL CROSS SECTION, BARNS
NEUTRON ENERGY, MEV
0
1
2
3
4
5
6
7
8
9
10
11
1.5
2.0
2.5
3.0

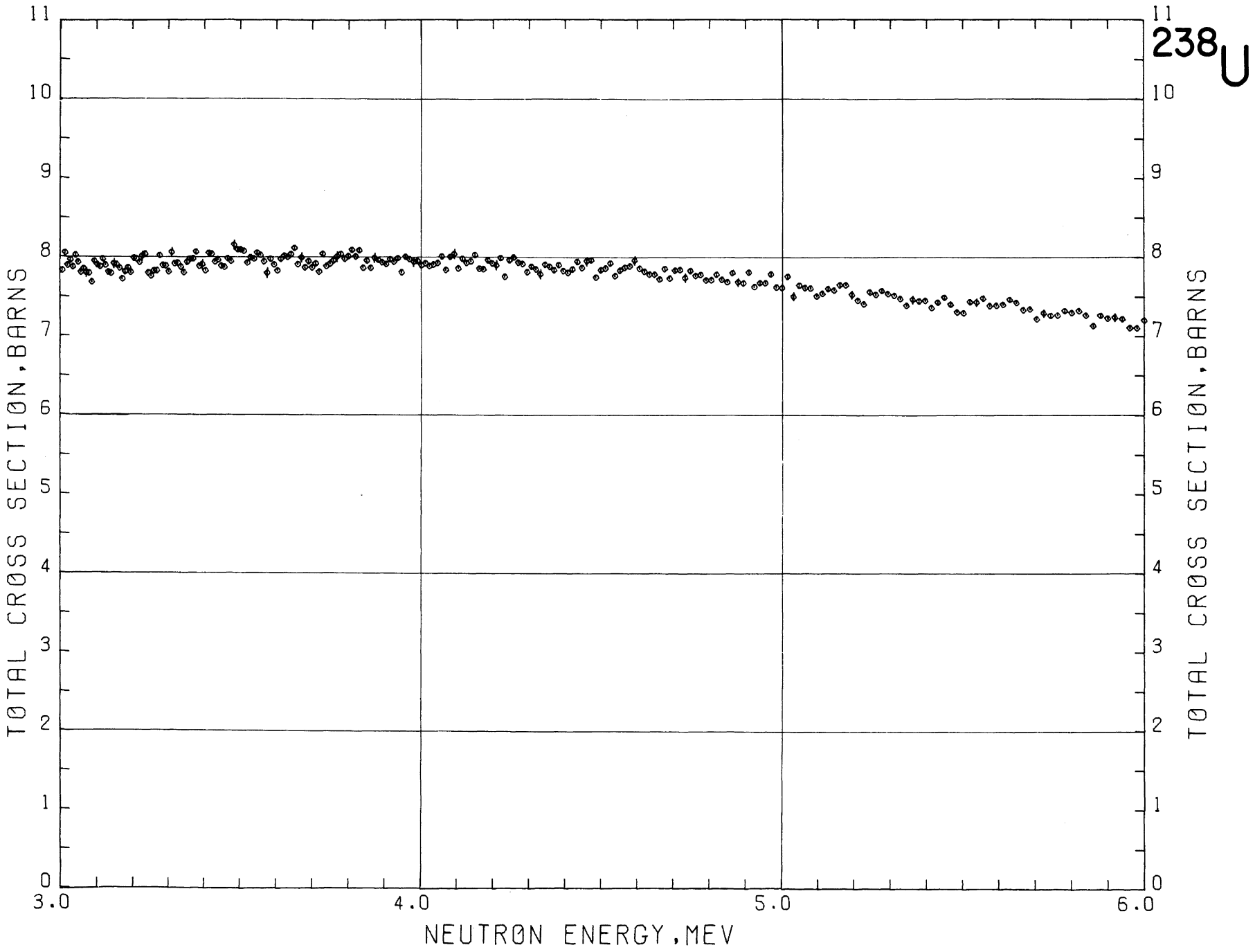
238U
TOTAL CROSS SECTION, BARNS
NEUTRON ENERGY, MEV
11
10
9
8
7
6
5
4
3
2
1
0
3.0
4.0
5.0
6.0

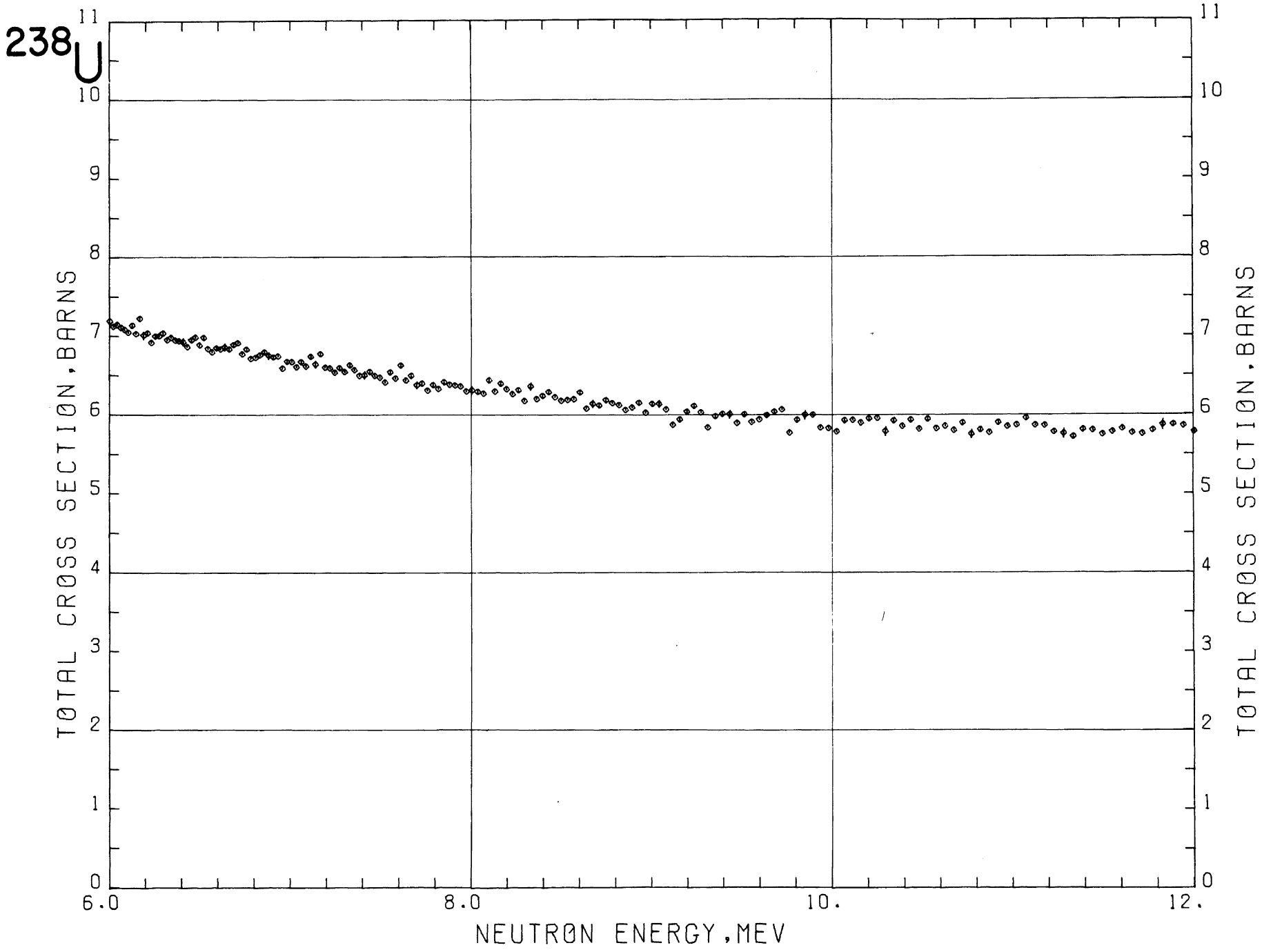
238U
TOTAL CROSS SECTION, BARNS
NEUTRON ENERGY, MEV
6.0
8.0
10.
12.
0
1
2
3
4
5
6
7
8
9
10
11

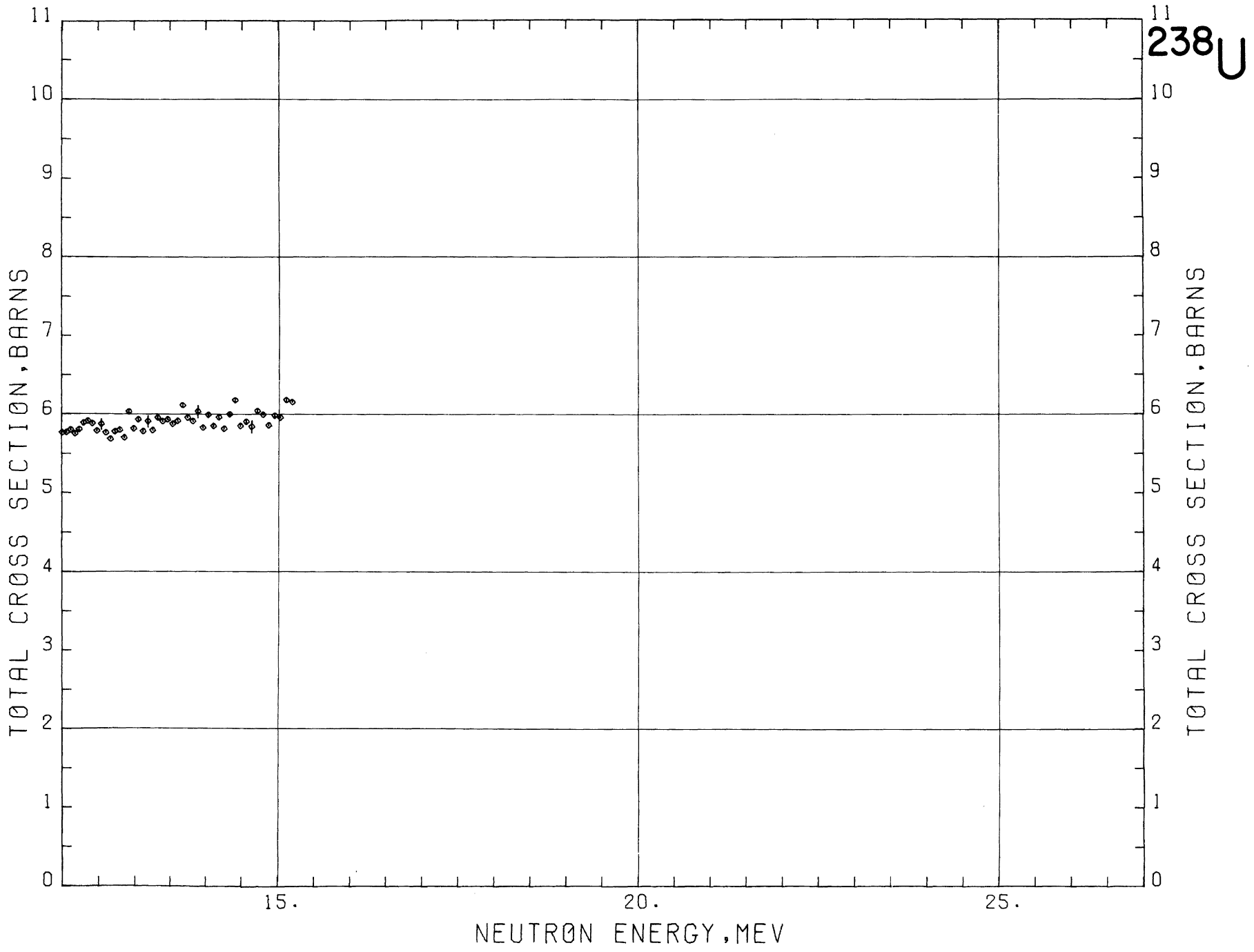
238U
TOTAL CROSS SECTION, BARNS
NEUTRON ENERGY, MEV
0
1
2
3
4
5
6
7
8
9
10
11
15.
20.
25.

^{239}PLUTONIUM

Sample Material: plutonium metal

Sample Diameter: 1.91 cm

Sample Thickness: 4.45 cm, $n = 0.2207$ atoms/gram

Analysis:

^{238}Pu:	0.01 percent	O:	260 ppm by weight
^{239}Pu:	93.94	Al:	15
^{240}Pu:	5.66	C:	15
^{241}Pu:	0.37	H:	10
^{242}Pu:	0.02		

Literature Reference: R. B. Schwartz, H. T. Heaton II, J. Menke, and R. A. Schrack, Bull. Am. Phys. Soc. 18 (1973) 539.

Comments: The measured cross section has been corrected for the oxygen in the sample, using our previously measured value of the cross section. Since the magnitude of the correction is $< \frac{1}{2}$ percent, any error in the correction would introduce a totally negligible error in the final cross section. We are not able to correct for the ^{240}Pu content of the sample since we do not have accurate measurements of the ^{240}Pu cross section in this energy range. It is very likely, however, that the ^{240}Pu cross section will be very similar to that of ^{239}Pu, and that therefore the ^{240}Pu introduces only a very small error.

Acknowledgment: We should like to thank the Los Alamos Scientific Laboratory for providing us with the sample, and for doing the chemical and isotopic analysis.

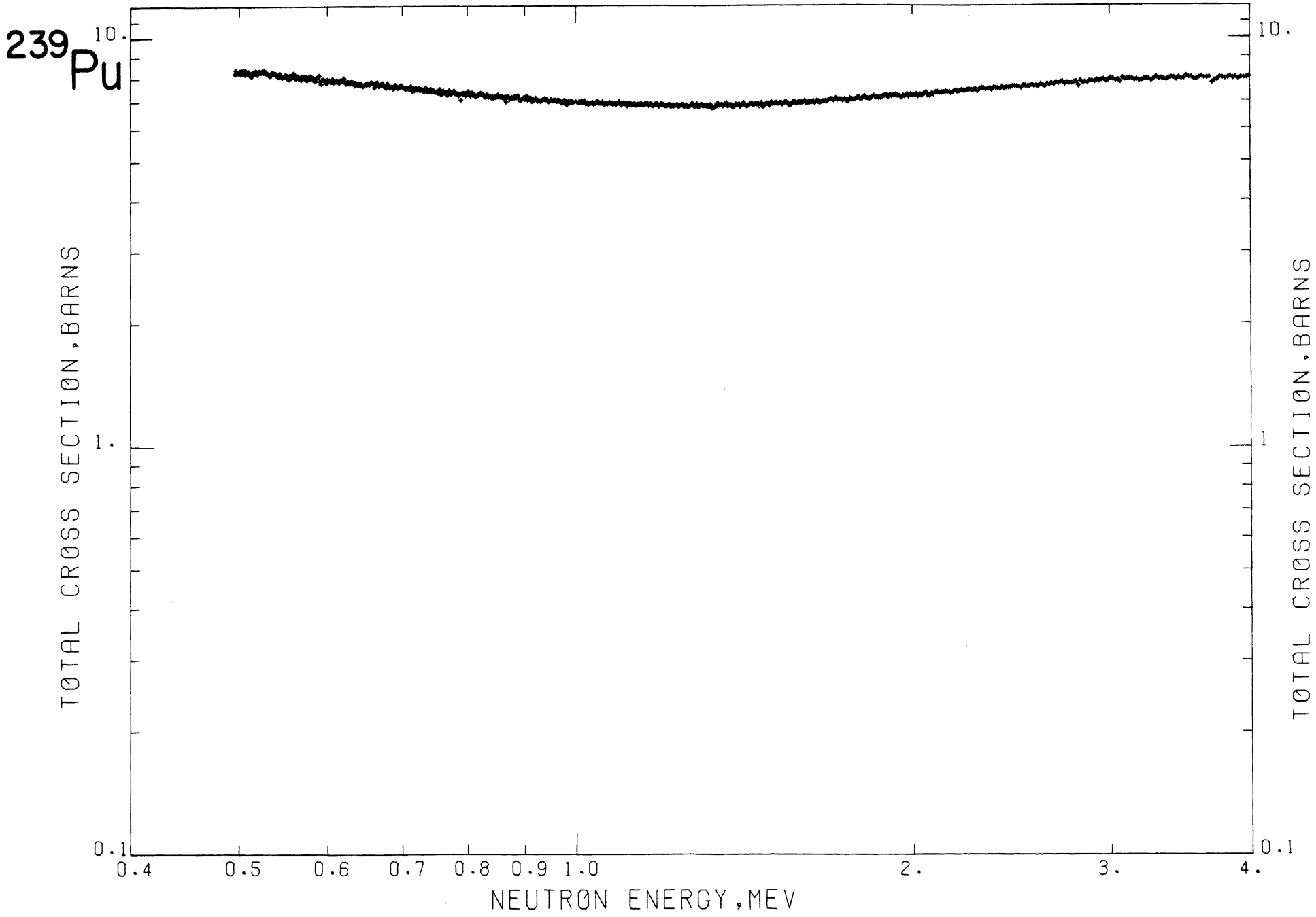
239Pu
10.
1.
0.1
TOTAL CROSS SECTION, BARNS
0.4
0.5
0.6
0.7
0.8
0.9
1.0
2.
3.
4.
NEUTRON ENERGY, MEV

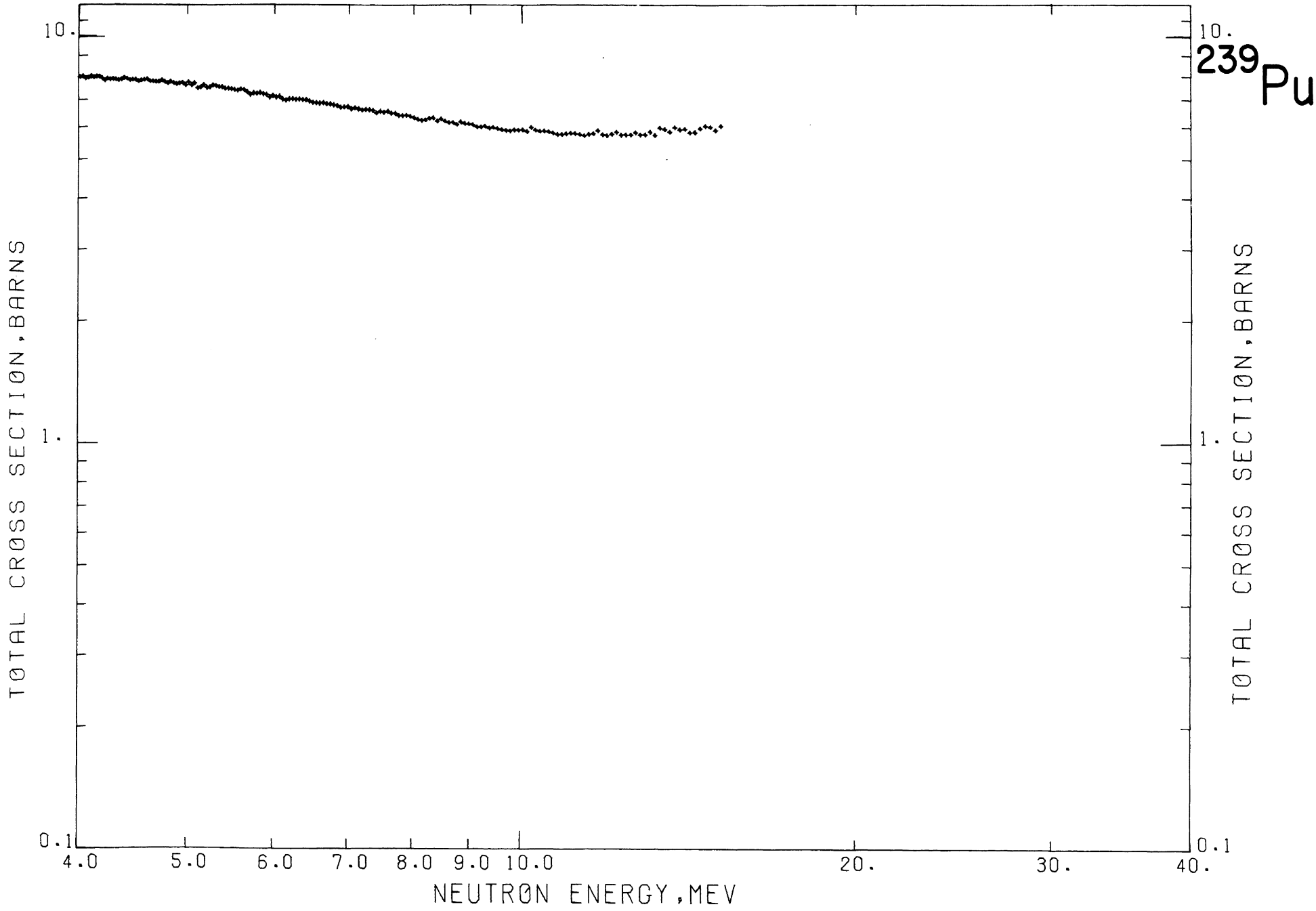
239Pu
TOTAL CROSS SECTION, BARNS
10.
1.
0.1
4.0
5.0
6.0
7.0
8.0
9.0
10.0
20.
30.
40.
NEUTRON ENERGY, MEV

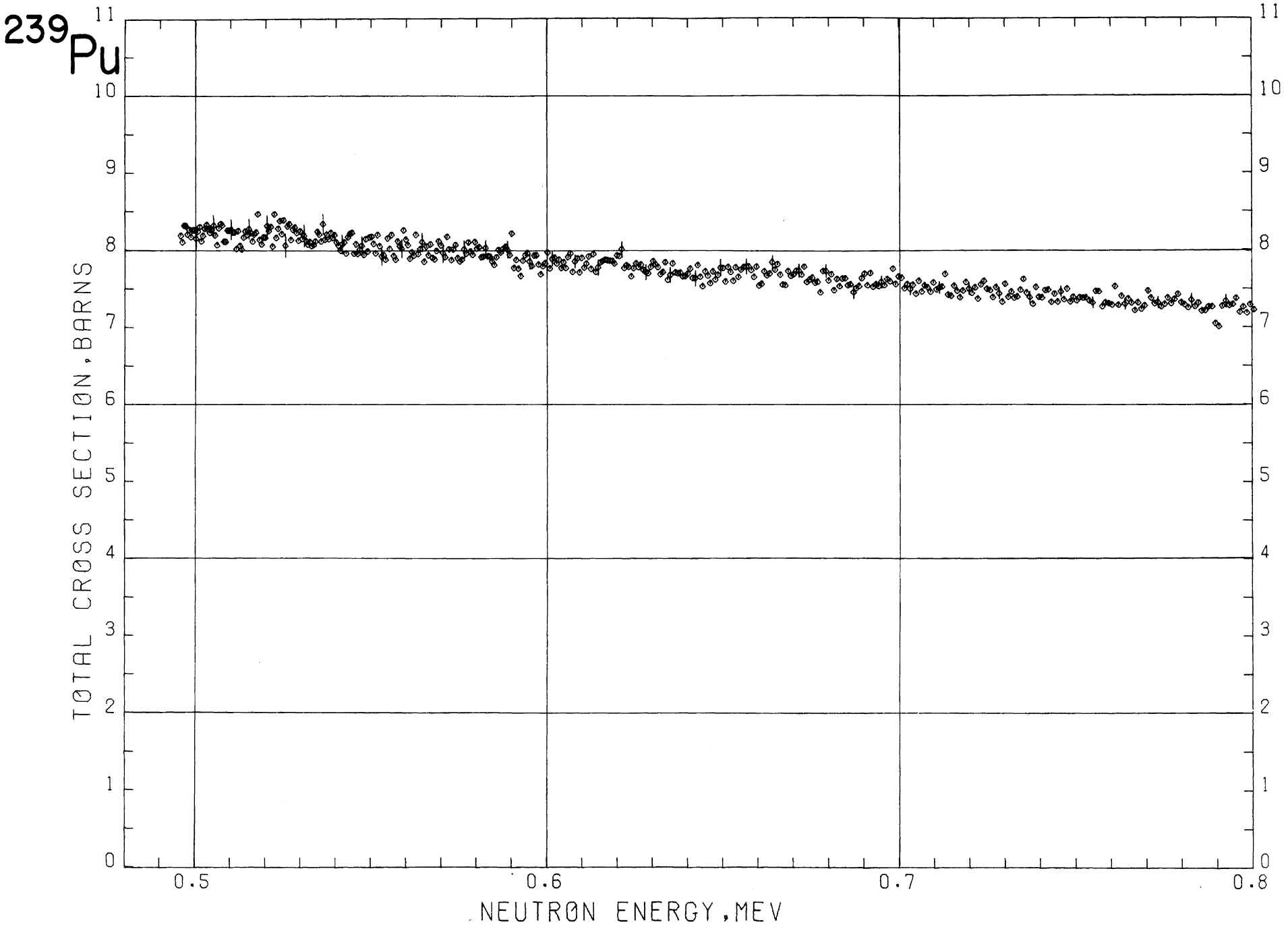
239Pu
TOTAL CROSS SECTION, BARNS
NEUTRON ENERGY, MEV
0
1
2
3
4
5
6
7
8
9
10
11
0.5
0.6
0.7
0.8

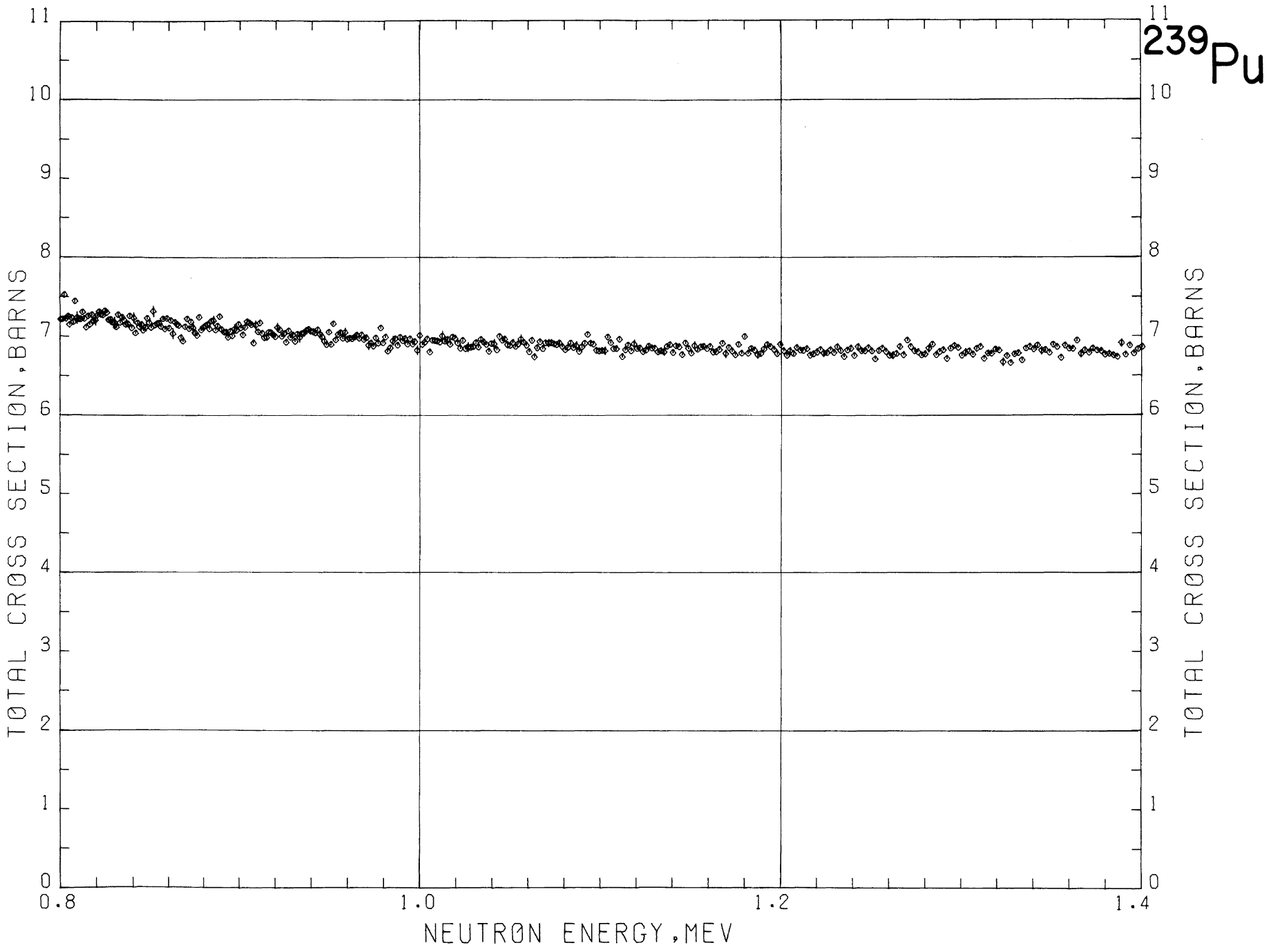
239Pu
TOTAL CROSS SECTION, BARNS
NEUTRON ENERGY, MEV
0.8
1.0
1.2
1.4
0
1
2
3
4
5
6
7
8
9
10
11

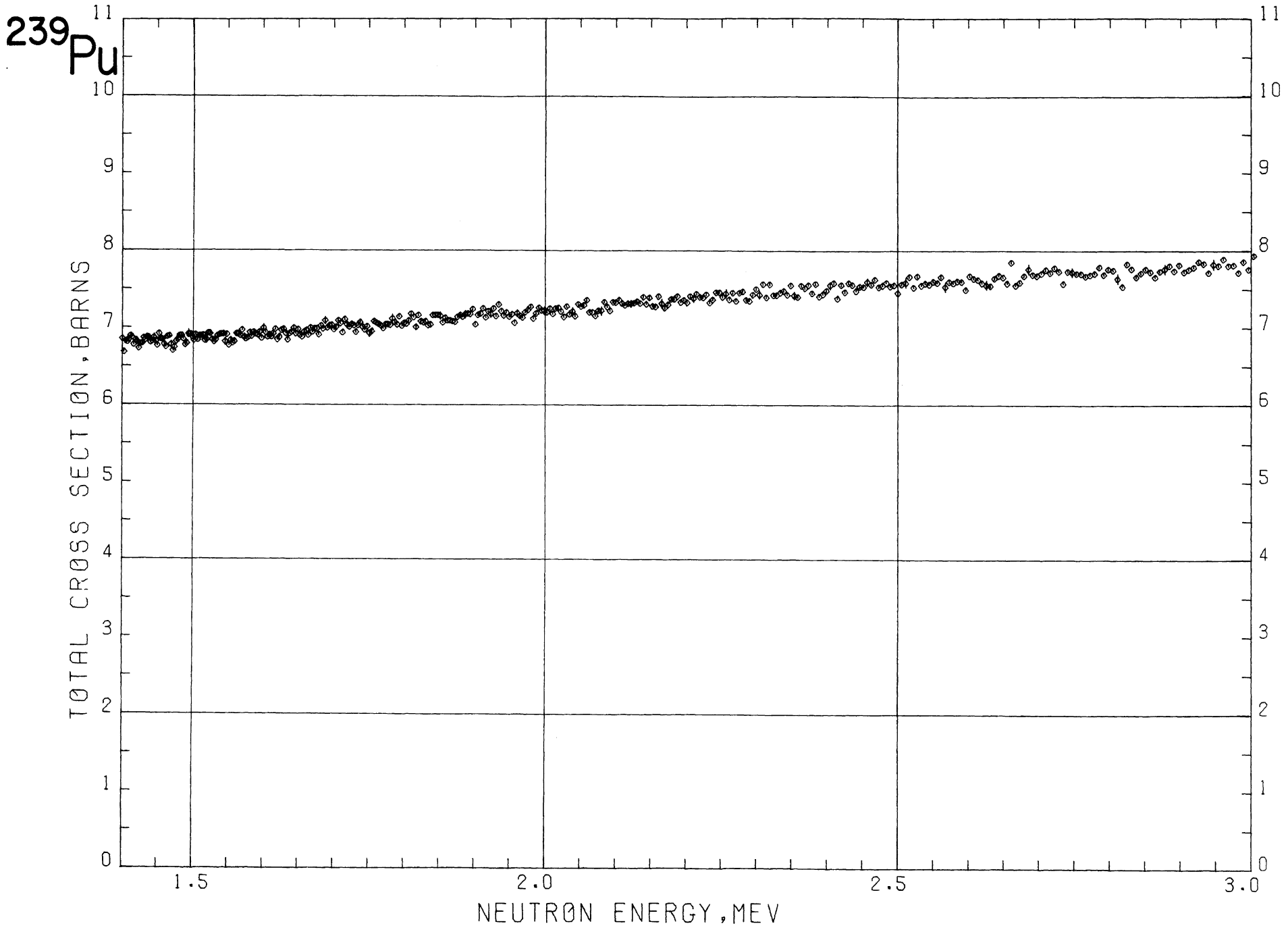
239Pu
TOTAL CROSS SECTION, BARNS
NEUTRON ENERGY, MEV
0
1
2
3
4
5
6
7
8
9
10
11
1.5
2.0
2.5
3.0

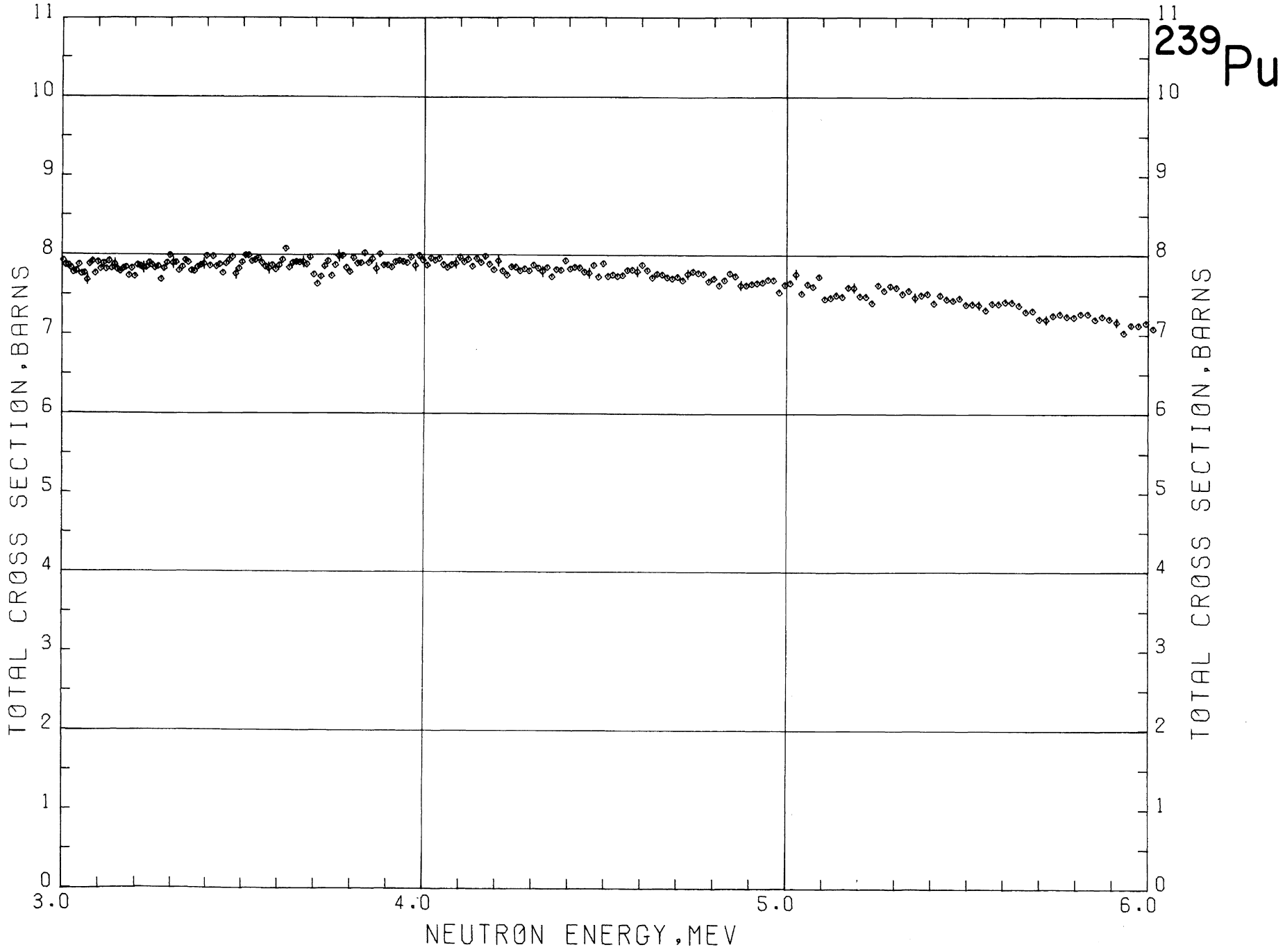
239Pu
TOTAL CROSS SECTION, BARNS
NEUTRON ENERGY, MEV
0
1
2
3
4
5
6
7
8
9
10
11
3.0
4.0
5.0
6.0

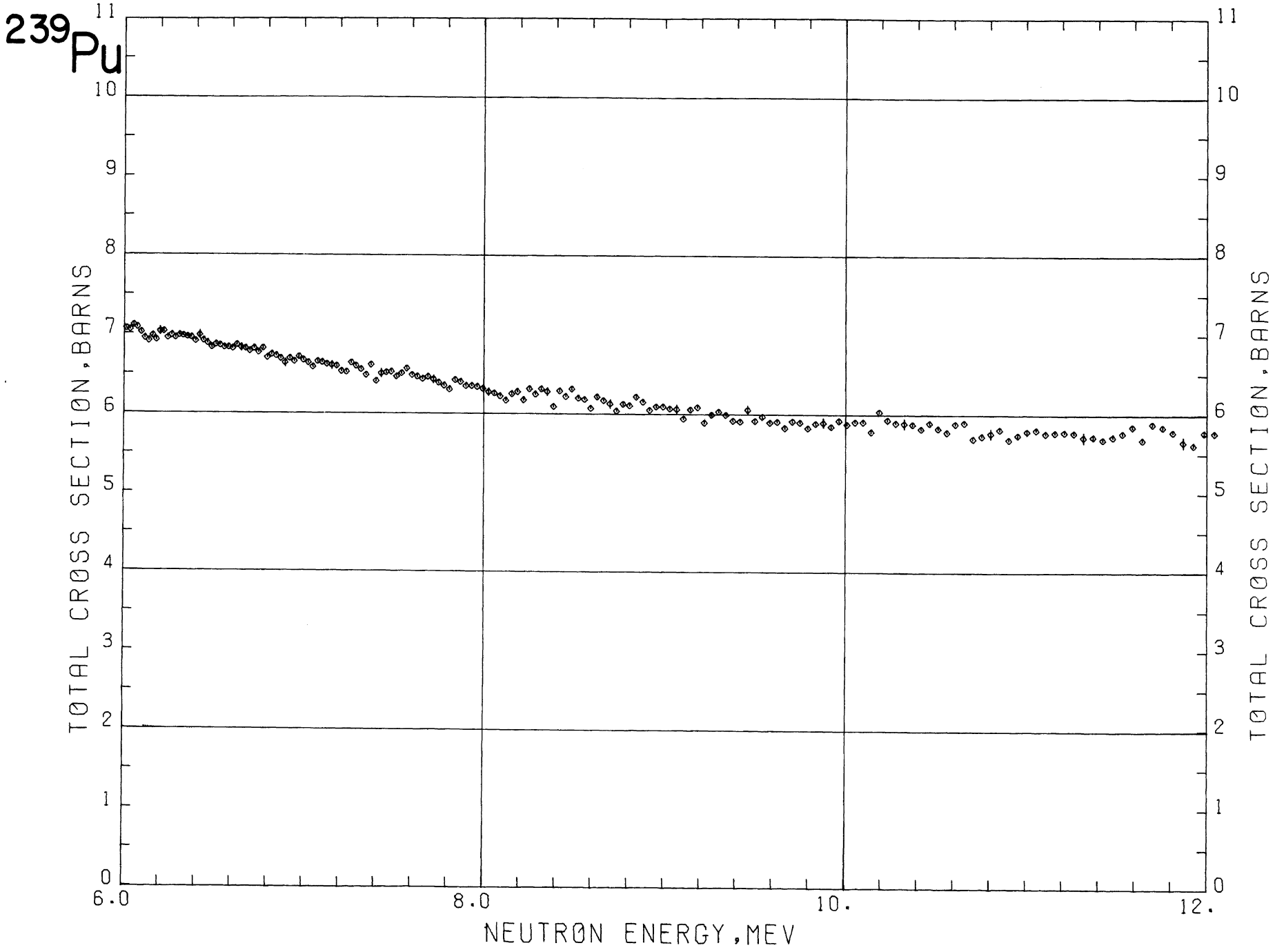
239Pu
TOTAL CROSS SECTION, BARNS
NEUTRON ENERGY, MEV
6.0
8.0
10.
12.
0
1
2
3
4
5
6
7
8
9
10
11

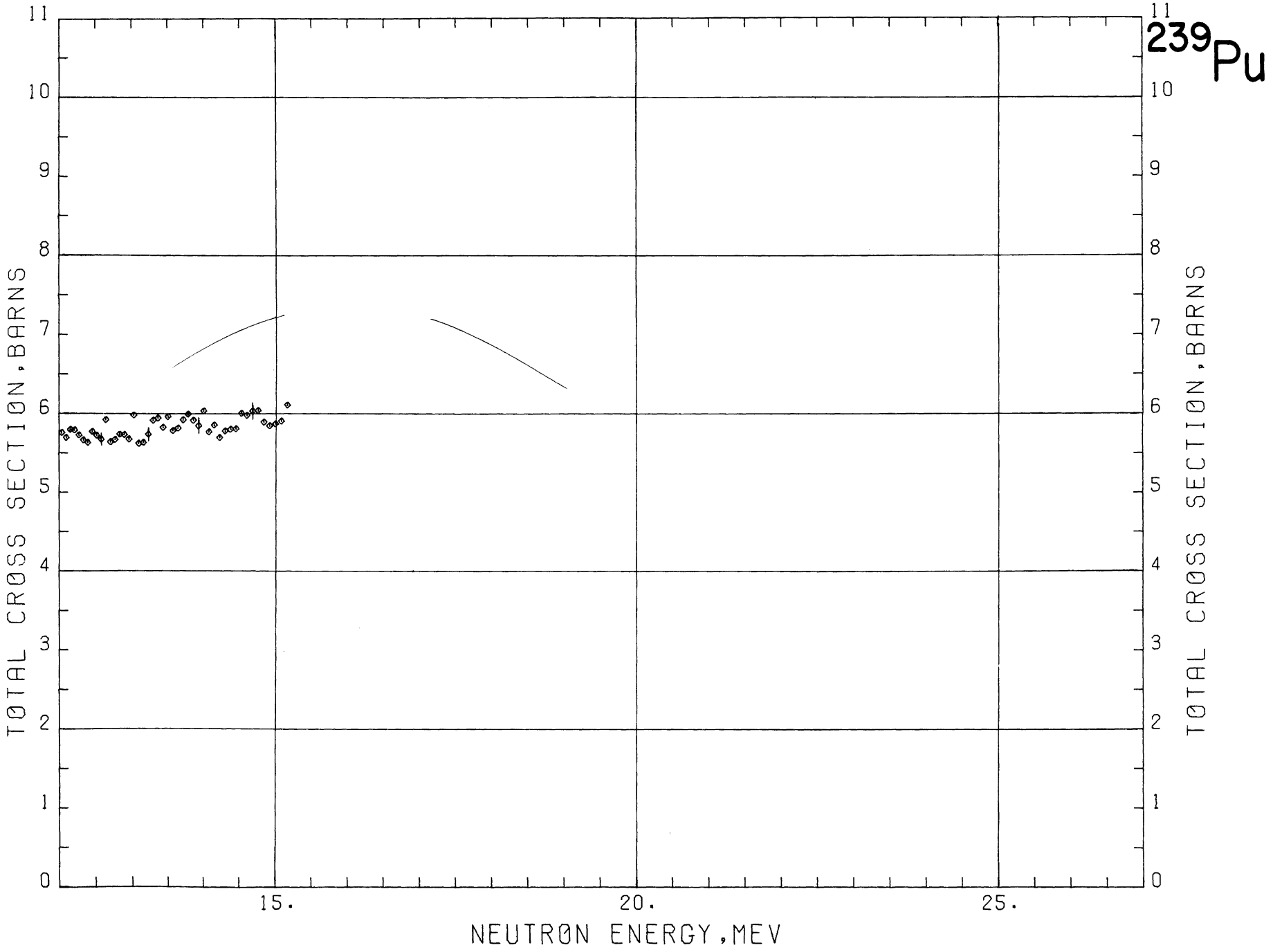
239Pu
TOTAL CROSS SECTION, BARNS
NEUTRON ENERGY, MEV
0
1
2
3
4
5
6
7
8
9
10
11
15.
20.
25.

Appendix–Experimental Techniques

A brief account of our experiment has been given earlier [1][1]. This will be expanded and brought up-to-date here.

A1. Experimental Arrangement

Figure 1 is a bird's eye view of our target area. We use the pulsed beam of the NBS electron linear accelerator as a source of neutrons. The beam enters from the bottom of the picture, and passes through a secondary emission monitor, which is our first monitor. Since this setup was designed for both photoneutron spectroscopy as well as neutron cross section measurements, our equipment also includes a dumping magnet. For cross section measurements, the magnet is simply turned off and serves no function. The electron beam emerges from the magnet vacuum chamber into air, and hits our neutron producing target.

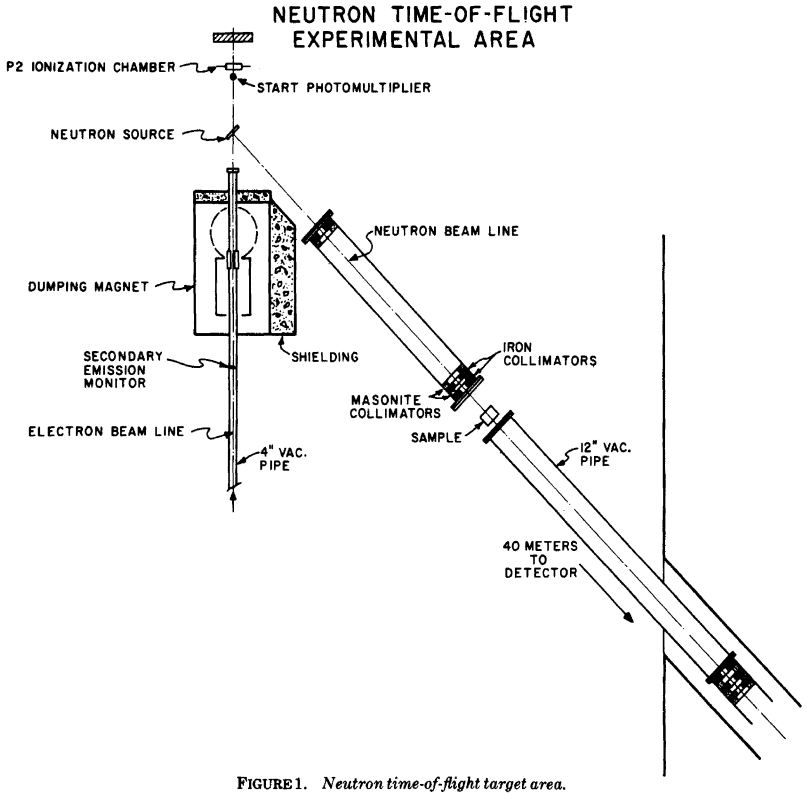

FIGURE 1. *Neutron time-of-flight target area.*

[1] Figures in brackets indicate the literature references at the end of the appendix.

The resulting neutrons are observed at 135° over a 40 m evacuated flight path. The transmission samples are placed three meters from the neutron source.

A2. Electron Linear Accelerator

The NBS electron linear accelerator has been described previously [2], and hence only the characteristics of particular importance to the time-of-flight experiments will be mentioned here.

For neutron total cross section measurements the linac is generally run at about 60 MeV. The exact energy is, of course, rather arbitrary, as long as it is considerably higher than the highest energy neutrons to be measured. On the other hand, once the energy is chosen, it must remain stable over the course of a measurement (several days) in order that the high-energy part of the neutron spectrum remains the same. The beam is therefore energy analyzed through 2 percent energy slits before hitting the neutron producing target.

Since the electronics for this system can only process one count per beam burst, and since the yield of neutrons is fairly high, only very low beam currents are required, average currents being of the order of 100 nA. Approximately ten times more current is available in a 2 ns wide pulse.

The linac injector has a fairly conventional triode gun,[2] driven by a special pulser which allows a wide range of pulse widths: from several microseconds down to less than 2 ns. We normally run with a 1½ to 2 ns wide pulse, at a repetition rate of 720 pulses per second.

The average dark current is generally held to 0.01 percent of the average beam current, and hence causes no problem.

The beam spot size is ~ 3 mm in diameter.

Once tuned up, the linac is generally quite stable in operation. Specifically, the beam spot is stable in size and position, the beam current fluctuates by less than 10 percent, the energy remains within the 2 percent limits and the pulse shape remains constant over many hours. This high stability is very important for accurate data taking.

A3. Neutron Producing Target

To some extent, it is possible to "tailor" the neutron spectrum by the choice of neutron producing target. Very generally, in the MeV energy range, higher Z targets produce more neutrons, but of low energy and lower Z materials will give fewer neutrons, but of higher energy. The *observed* spectrum will, of course, be modified by the variation in the detector efficiency as a function of energy. In our early measurements (which only went to ~ 5 MeV neutron energy), cadmium targets 1 to 2 cm thick were used. The yield from cadmium falls off sharply above about 6 MeV, however, so a combination of ~ 0.1 cm tungsten, backed by ~ 3 cm beryllium is now used. The tungsten provides the low energy neutrons and also acts as an efficient bremsstrahlung radiator

[2] Applied Radiation Corporation Model 10. (This particular piece of equipment, and certain other commercial equipment, instruments and materials are identified in this Monograph in order to adequately specify the experimental procedure. In no case does such identification imply recommendation or endorsement by the National Bureau of Standards, nor does it imply that the material or equipment identified is necessarily the best available for the purpose.)

for the beryllium which, in turn, supplies the higher energy neutrons. The difference in thickness between the W and the Be is typical of the difference in yields between high Z and low Z materials. The use of a target which is mainly low-Z is also important in solving some of the problems associated with the gamma flash, as will be discussed in section A4.3.

A4. Instrumentation

A4.1. Detector and Fast Timing Electronics

The main function of the fast electronics is simply to provide a "start" signal, related in time to the production of the neutrons, and a "stop" signal, similarly related in time to the detection of a neutron at the end of the flight path. These signals are then analyzed and encoded by a Time Interval Counter. (sec. A4.3)

A block diagram of the electronics is shown in figure 2. Not included are such ancillary units as fanouts, pulse shapers, and delay cables, nor do we show the slow electronics necessary to produce the logic signals for the on-line data handling system.

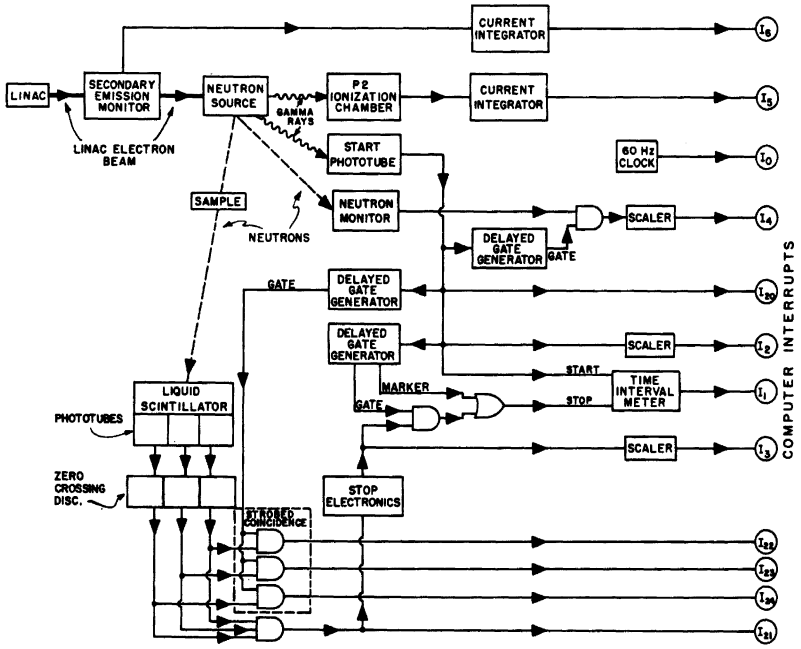

FIGURE 2. *Block diagram of electronics.*

The shower developed when the electron beam strikes the neutron producing target impinges upon a bare RCA 931A phototube (i.e., no scintillator is used). The phototube anode signal is fed to a zero crossing discriminator [3] whose output furnishes the "start" signal. The start signal performs several functions. It is fed to the Time Interval Counter, initiates delayed gates and a marker generator, and is scaled by the computer.

The neutron ("stop") detector is a 13 in. diam. by 5 in thick NE 211[3] liquid scintillator, viewed by 3 Amperex type 58AVP photomultipliers. The anode signals are fed to zero cross-over discriminators [3]. The outputs of the zero crossing discriminators go to a Two-Out-of-Three [4] coincidence gate and an OR gate.

The Two-Out-of-Three coincidence requirement reduces the noise counts.

The actual "stop" timing is derived from the output of the OR circuit. Before each run, the delays among the three phototubes and zero crossing discriminators are carefully matched so that the centroids of the timing distributions for the three tubes are exactly coincident in time (i.e., total spread less than 200 ps) at the input to the OR circuit. For each individual event, however, there will generally be some spread in the time of arrival of the three pulses. Since the Time Interval Counter is triggered by the leading edge of its input pulse, timing from the output of the OR circuit means that the timing is actually determined by whichever of the (nominally coincident) pulses arrives first. This procedure makes the best use of the timing information from the scintillator.

Signals from dynode 14 of each phototube are summed in a fast adder-discriminator. Since the gains of the phototubes are carefully matched, this provides a convenient method for setting the overall bias level, which is usually set at about 160 keV energy neutrons.

The outputs of the Two-Out-of-Three coincidence, the "OR" and the fast adder-discriminator are suitably shaped and delayed, and applied to the inputs of an AND circuit, along with the output of a delayed gate generator which is used to define the timing range and hence the energy range. If no neutron is detected during the time the delayed gate is open, the marker pulse generator provides an artificial stop pulse which resets the Time Interval Counter.

A4.2. System Response Function

We have used two approaches in determining the response function of our system: synthesis and analysis. In the synthesis approach, we fold all the known contributions to the response function to obtain the final overall response function. We have used contributions from the following sources:

1. Electronic response function
2. Neutron detector thickness
3. Neutron source thickness
4. Electron beam pulse width
5. Timing channel bin width

The electronic response function was determined by a coincidence technique using ^{22}Na γ rays. For γ rays whose pulse height was approximately equal to that of 0.5 MeV neutrons, the response function was 3.5 ns FWHM. The detector and source response functions are truncated exponentials determined by the mean free path of the neutrons and their flight time in the medium. The electron beam pulse shape was assumed to be a 2 ns wide Gaussian, as determined from measurements of the gamma flash shape through thick absorbers.

[3] Manufactured by Nuclear Enterprises, Inc.

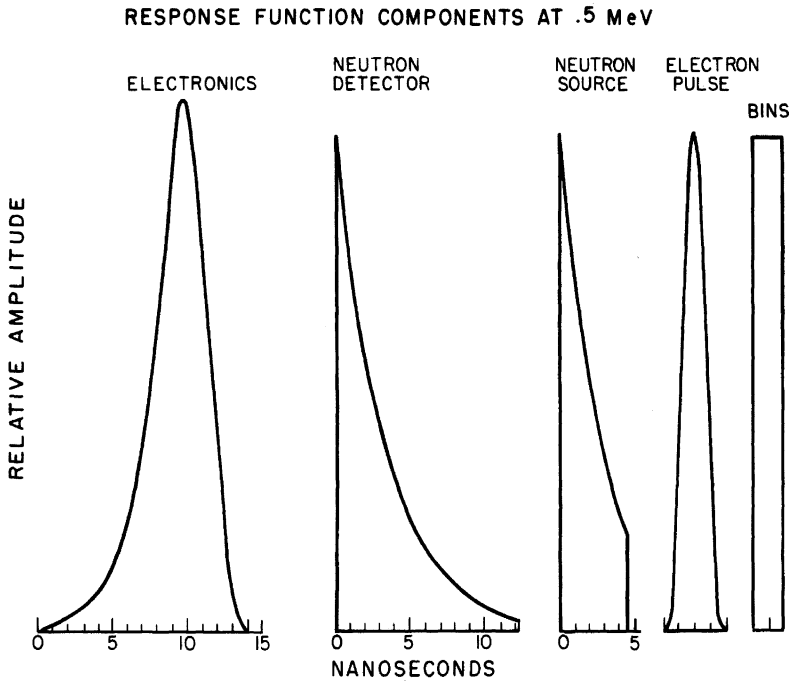

FIGURE 3. *Elements of response function, evaluated at ~ 500 keV.*

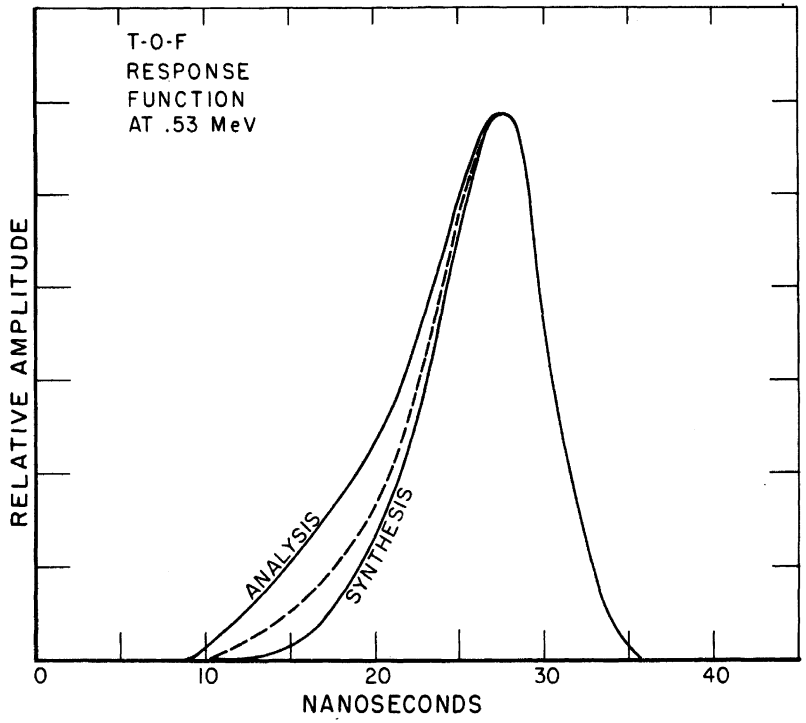

FIGURE 4. *Time-of-flight response function at 530 keV.*

All of these contributions, evaluated at approximately 500 keV neutron energy, are shown in figure 3. The synthesized overall response function is shown in figure 4 and has a width of 8 ns or 2.2 keV at 530 keV.

The response function was also determined by analysis of the 534 keV line in Si. The natural width of this line is considerably less than the response function of the system so that the shape of the transmission line is a good indication of the response function shape. To improve the analysis, the natural Breit-Wigner shape (determined by area analysis of the transmission) was unfolded from the transmission. The response function thus obtained has a width of 2.4 kilovolts or 9 ns. The response function used at 530 kilovolts is the compromise shown by the dashed line in figure 4.

It should be noted that the response function improves rapidly above about 600 keV neutron energy, since the electronic response function as well as effects due to source and detector thicknesses all improve at higher energies. The measured (analyzed) response function is about 5.5 ns (11 keV) at 2.1 MeV and about 3.4 ns (120 keV) at 14 MeV. Figure 5 shows the width of the response function as a function of neutron energy. The points are from analyses of narrow resonances. (The point at 14 MeV is the measured direct response to 14 MeV neutrons generated by the NBS Van de Graaff.)

A4.3. Gamma Flash

When the linac electron beam strikes the neutron-producing target, an intense burst of gamma rays (the "gamma flash") is produced. The gamma flash produces three undesirable effects in the detector:

1. A very large primary pulse, which may cause over-load and baseline shift problems;
2. An after-pulse, occurring approximately 600 ns after the main pulse; and
3. An enormous increase in phototube noise for approximately 750 ns after the gamma flash pulse.

The after-pulse is caused by the photoelectrons from the gamma-flash pulse ionizing the residual gas in the region between the photocathode and the first dynode in the phototube [5]. The ions are isochronously accelerated back to the photocathode, causing the observed after-pulse.

Since the problem occurs in the "front end" of the phototube before the photoelectrons even reach the first dynode, pulsing off the phototube in the usual way, i.e., pulsing off the first few dynodes, will not help. It was pointed out by Farinelli and Malvano [6], however, that a phototube can be just as well turned off by pulsing its

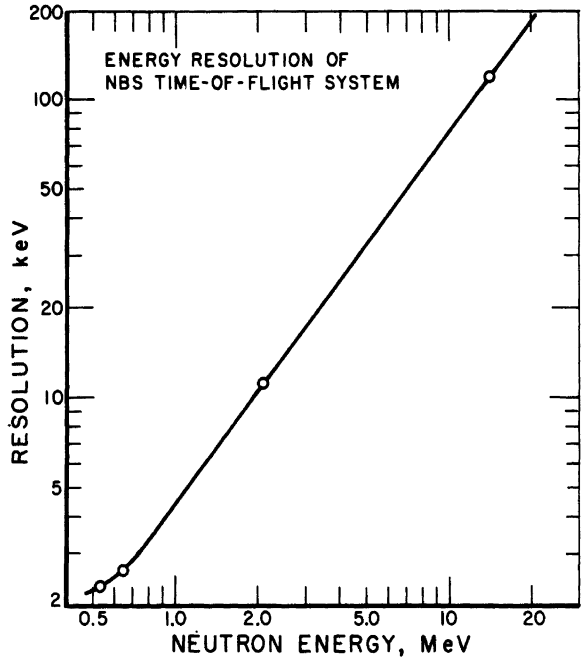

FIGURE 5. *Time-of-flight energy resolution as a function of energy.*

focus electrode. In our case, we are not really concerned with turning off the phototube per se: our object is specifically to reverse the electrostatic field near the photocathode so that the enormous number of photoelectrons generated by the gamma flash are not accelerated down the photocathode-first dynode space. We do this by applying a 600 volt negative pulse to the focus electrode of the 58AVP during the gamma flash.

Figure 6 shows the electrostatic field lines in the front end of a 58AVP as mapped out on an analog electrostatic field plotter. (For clarity, we show the field lines which would exist with the photocathode at ground and +2600 volts on the anode; in actual practice the anode is at ground and −2600 volts is applied to the cathode.) Figure 6a shows the field lines during normal operation; figure 6b shows the field lines with −600 volts applied to the focus. Note the reversal of the field at the photocathode, so that photoelectrons are not accelerated down to the first dynode.

After the applied pulse, the photomultiplier gain recovers as rapidly as the pulse decays, which in our case is about 100 ns (caused mainly by the stray capacity of the leads and the phototubes.)

This method of eliminating the after-pulse also, of course, essentially eliminates most of the primary gamma flash pulse itself. Further details of the phototube pulsing as well as a circuit diagram of the pulser, have already been published [7].

While the phototube becomes rather noisy for several microseconds after the applied pulse, the Two-out-of-Three coincidence requirement eliminates this as a

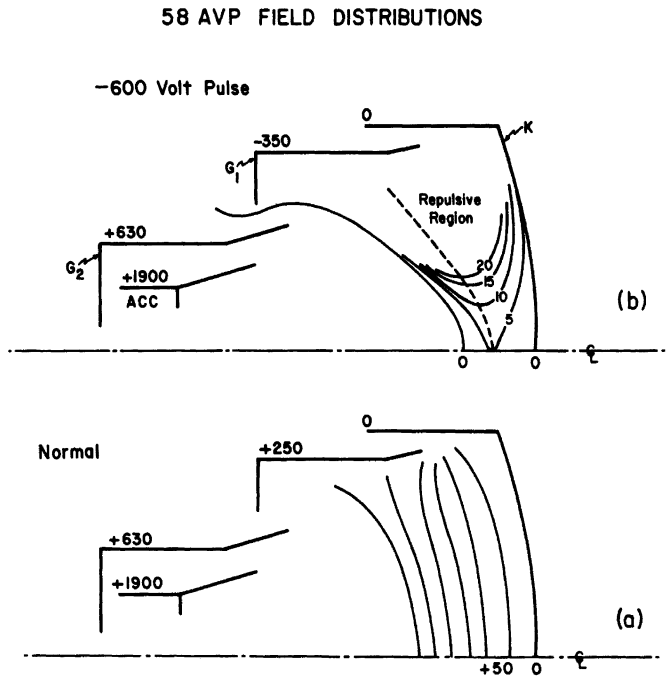

FIGURE 6. *Electrostatic field lines in the type 58AVP photomultiplier.*

The upper part of the figure shows the field lines when the −600 volt pulse is applied to the focus electrode, G_1. The lower part of the figure shows the applied voltages and resultant field lines during normal operation. For clarity, the voltages shown are those which would exist with the photocathode at ground and +2600 volts on the anode. In actual use, the anode is run at dc ground and −2600 volts is applied to the cathode. The field lines are, of course, the same in either case.

problem. A much more serious noise problem is caused by the gamma flash itself. While the noise from the gamma flash pulse decays after about 750 ns, it is so intense during this period that a significant number of accidental coincidences are recorded. Requiring a three-fold (rather than 2/3) coincidence helps, but results in an appreciable loss of smaller pulses. In addition to pulsing off the phototube, it was also found necessary to reduce the intensity of the gamma flash by using a 1 inch thick tungsten filter in the beam *and* by using a neutron-producing target consisting largely of low-Z material (see sec. A3). In this way, we are able to make accurate measurements out to about 20 MeV, or 500 ns after the gamma flash pulse.

A4.4. Time Interval Counter

As indicated earlier, the "start" and "stop" signals are analyzed by the Time Interval Counter. This is a commercial digital timing device[4] with one nanosecond

[4] Manufactured by Eldorado Electrodata Corporation.

resolution and accuracy. The integral linearity of the device is easily checked by means of an accurate frequency standard or a marker generator based on such a standard, and is within one ns.

The differential linearity is checked in the usual way: The Time Interval Counter is started by a pulse generator, and stopped with random pulses from a gamma ray source. When properly adjusted the differential nonlinearity is $\lesssim 3$ percent, most of which cancels out in a transmission measurement.

A4.5. Energy Calibration

Our system allows convenient, absolute energy calibration. (By "absolute" we mean that the energy scale is determined in terms of measured distances and times, rather than by comparison with other measurements.) The procedure is simply to record the position of the γ-flash using the Time Interval Counter, and then correct back for the flight time of the gamma rays down the 40 m flight path. This accurately determines the time of arrival of the electron pulse at the neutron producing target, relative to some (arbitrary) zero time on the Time Counter. The neutron times-of-flight are then measured using exactly the same electronics in exactly the same physical location, and hence are measured with respect to the same (arbitrary) zero. Since the widths of the timing channels on the counter are known, this gives an absolute measurement of the neutron time-of-flight. A measurement of the path length then gives a direct measurement of the neutron energy.

The uncertainty in the energy scale determination arises primarily from uncertainties in the timing measurements. These include nonlinearities of the Time Counter, long-term (i.e., a few days) drifts in the timing, and systematic timing differences between neutrons and gamma rays. The non-linearities and long term drifts have both been carefully checked, and are less than 1 ns and ½ ns, respectively. While it is difficult to measure directly the difference in the timing response of the scintillator-phototubes-discriminators between neutrons and gammas, it is known that NE 211 does not show any difference in response between neutrons and gammas. The slewing between small pulses (due to low energy neutrons) and large pulses (from the gamma flash) is approximately 1 ns.

The path length has been measured with a geodimeter[5] to an accuracy of 0.02 percent; this contributes a negligible error to the energy scale uncertainty. A minor problem arises due to the detector thickness. The detector is approximately 4 mean free paths thick at 0.5 MeV, and 0.3 mean free paths at 20 MeV. Therefore, the low energy neutrons effectively stop near the front face of the scintillator, whereas, on the average, the high energy neutrons stop nearer the center. Thus, the effective path length is greater for high-energy than for low energy neutrons. This difference in path length (amounting to almost 0.1%) can, however, easily be calculated and is corrected for.

The final energies are all calculated relativistically.

Taking all the above factors into consideration, the over-all uncertainty in the energy scale determination is 0.04 ns/m (e.g., $\pm$ 3 keV at a neutron energy of 2 MeV).

Below about 2 MeV this compares very favorably with the best work reported from Van de Graaff accelerators. At higher energies, some high-accuracy Van de Graaff experiments [8] have smaller errors, but, in any case, the time-of-flight method has the great virtue of allowing a direct measurement. It is worth noting that there is excellent agreement, even at the higher energies, between our energy scale and that reported by the Wisconsin group [8] (i.e., agreement within ~ 8 keV at 6 MeV neutron energy).

[5] We are grateful to Mr. George Lesley of the U.S. Coast and Geodetic Survey for making this measurement.

A4.6. Data Handling

The data from the Time Interval Counter, as well as the counts from the monitors, various scalers, clocks, etc. are all handled by the NBS on-line data handling system. The general features of this system have been described previously [9], and a detailed report of our use of the system has been published [10]; hence, only the major features will be reviewed here.

The on-line data handling system has been constructed around an XDS 920 computer. (16K core memory, 24 bit word, and 8μs cycle time). The modular concept has been applied to both the software and hardware design of the system. Associated with the 80 levels of priority interrupts are programs used to record the experimental data. The priority hierachy insures that the most important data will be recorded first, after which time the computer can do more routine functions, such as present a CRT display, output the data etc.

A5. Monitoring

Two monitors are used: a secondary emission monitor (SEM) to monitor the electron beam, and an NBS P2 ionization chamber [11] which monitors the shower created in the neutron producing target. The ratios among the monitor counts and the total neutron counts are printed out periodically during an experiment. The constancy of these ratios during the course of the experiment is a measure of the overall stability.

It is important to note, however, that the spread in value of these ratios only represents an *upper* limit to the error caused by any errors in monitoring. This is because in our transmission measurements the samples are cycled in and out every twenty minutes. Hence drifts, with time constants long compared to twenty minutes, will cancel out.

A5.1. Secondary Emission Monitor

The secondary emission monitor (SEM) consists of three aluminum foils, each approximately 1 mg/cm^2 thick. A thin layer of platinum (~ 25 μg/cm^2) is evaporated on the aluminum surfaces to reduce ageing effects. Although work in this laboratory indicates that an SEM may not give very reproducible results for high ($\gtrsim$ 20 μA) electron beam currents, the SEM is satisfactory for the low currents (~ 100 nanoamps) used in this experiment. The ratio of neutron counts to SEM readings show RMS fluctuations of ~ 1½ percent during the course of an experiment (i.e., two to three days).

A5.2. Ionization Chamber

The more stable of our two monitors is a conventional NBS P2 ionization chamber [11]. The P2 is placed immediately behind the neutron producing target, and hence effectively monitors the shower produced in this target. Although the P2 may overload (due to recombination effects) at high currents, again, as in the case of the SEM, at the low currents used in these experiments there is no sign of overloading. The neutron-to-P2 ratios fluctuate by $\pm$ ½ percent during the course of an experiment.

A6. Sample Thickness Considerations

It had been customary to use fairly thin samples—50 percent to 70 percent average transmission—in total cross section measurements. In a low background situation, however, there are two factors which argue for the use of thicker samples—say, $\lesssim 15$ percent transmission.

First, Rose and Shapiro [13] long ago showed that where the background is low, the optimum sample for minimum statistical error is approximately two mean free paths thick; i.e., transmission ~ 15 percent.

Secondly, the over-all cross-section *accuracy* (as opposed to the statistical *precision*) may be improved by the use of a thick sample. This is easily seen: since $T = e^{-n\sigma}$, where T is the measured transmission, n is the areal density of the sample (in units, of, say, atoms/barn) and σ is the total cross section,

$$\frac{d\sigma}{\sigma} = \frac{1}{n\sigma}\frac{dT}{T}. \tag{1}$$

(We call the dimensionless quantity $n\sigma$ the "sample thickness.")

Thus, for example, an error in normalization will give a constant fractional error in the *transmission*. Equation (1) shows that for this case, the resultant error in the cross section may be reduced by simply running a thick sample. Equation (1) also explains why a particular cross section measurement may be accurate where the cross section σ is high, but have large fractional errors where σ is low.

On the other hand, eq (1) does not, of course, mean that one can achieve arbitrarily small errors in the final measured cross section by using arbitrarily thick samples. In addition to losing statistical precision for samples whose thickness is far from optimum, for very thick samples ($n\sigma \gtrsim 5$; $T < 1\%$) the in-scattering correction (see sec. A7.3) becomes large and difficult to calculate, even in good geometry. More important, for thick samples, the background correction becomes large, and the ever-present uncertainties in the background can become the dominant error.

In addition, if the instrumental resolution width is wider than the natural width of any structure to be measured, the observed peak cross sections will be higher for thinner samples. In other words, a thick sample worsens the apparent resolution. This is sometimes referred to as a "beam hardening" effect.

A final complication derives from the simple fact that cross sections vary with energy, hence a particular sample which is "thick" at one energy may be very "thin" at another energy.

Thus, while it is clear that the sample thickness has an important function in determining the quality of a total cross section measurement, the procedure for choosing the "n" value of the sample is much less clear. Careful consideration must be given to all the sources of error in a particular experiment, as well as the use to which the final data will be put, before the optimum sample thickness can be sensibly chosen. In our case, the background is very low and well-behaved (see sec. A7.1). In addition, an important use of our data was to be as input in neutron transport calculations; for deep-penetration calculations the *minima* in the cross section are most important. Thus, relatively large "n" values seem to be called for. Such samples might, however, be too thick to give any useful information in regions where the cross section is high; hence we generally ran with two different samples. The "n" value for the thicker sample was commonly $\gtrsim 1$; "n" for the thinner sample was a factor of 2 to 4 less.

We thus had samples appropriate to cover a wide range of cross section values and, in addition, the data from the two samples provided an important check on internal consistency. (The exact "n" values used are listed for each element in the main body of this report. It will be seen that even the "thin" samples are rather thicker than has been customary in this type of measurement.)

A7. Corrections to the Data

A7.1. Background

The background is measured by simply inserting a "shadow bar" (32 cm of copper plus 15 cm of polyethylene) in place of the transmission sample. The background counting rate is generally less than 0.3 percent of the open beam counting rate. About half of the background is due to cosmic rays and natural room background, and the other half is associated with the linac beam. The background is flat and structureless, and quite constant during the course of a run.

We have investigated the question of whether the true background is adequately determined by this simple shadow-bar measurement. We have, for example, measured counting rates with the detector off-axis, at "long" times-of-flight between machine bursts, with the beam purposely missteered, with various combinations of shielding and beam stops, etc. We find no significant background beyond that measured with the shadow bar technique. We note that our cross section measurements tend to be rather immune to background caused by neutrons which scatter off the walls of the measurement room and return to the detector, since such an event must occur within 4 μs of the beam burst (at which time our gate closes) and must give a pulse larger than a 160 keV recoil proton.

The "black resonance" technique commonly used to measure backgrounds in the eV and keV regions can not be used in the same way in the MeV region, simply because the peak heights are so much lower. Nevertheless, a measurement with black (or almost black) resonances does provide a valuable check on backgrounds determined from shadow bar measurements. This was generally the case in our "thick" sample measurements and the results (albeit often with rather poor statistics) were consistent with our assumed background. The 2.95 MeV resonance in carbon, for example, was studied with a quite thick sample ($n = 1.2$) for which the transmission T was 2.4 percent, and with a thinner sample ($n = 0.48$) with $T = 23$ percent. The final value for the peak cross section was the same for the two samples, despite the factor of ten difference in transmission, indicating that the background was accurately known.

A7.2. Dead Time

With a low duty cycle machine (maximum rep. rate = 720 pulses per second) and an electronic system which will only record one count per pulse, it is difficult to obtain good counting statistics in each of several thousand channels in a reasonable amount of running time. In addition to optimizing the sample thickness (sec. A6), it is also necessary to run at high counting rates, which unfortunately, means that large dead time corrections are required. In practice we select a beam current such that during the "open" runs, an average of one neutron per burst is *detected* by the "stop" detector. For this case, Poisson statistics show that the average number of neutrons actually *recorded* by the electronics is $(1-1/e)$ per burst, and in the last timing channel (lowest energy neutrons) the ratio of true counts to recorded counts is equal to e.

For a "one-shot" electronic system which completely recovers between pulses, it has been shown, [14] however, that to first order the dead-time correction is a sim-

ple, exact, analytical function which only involves explicitly measured quantities. Specifically,

$$T_i = \frac{R_i}{1 - \left[\sum_{c=1}^{i-1} R_c/S + R_i/2S\right]}$$

where T_i is the true number of counts in channel i; R_i is the number of recorded counts in channel i; S is the total number of start counts; and ΣR_c is the sum of all the recorded counts from channel 1 to channel $(i-1)$.

This is, however, only a first-order correction and is exact only to the extent that the counting rate remains constant during the course of a run. (A "run" is generally 20 minutes, as noted in section A5.) If the counting rate fluctuates, there is a second-order correction which must be made numerically. The second order correction is minimized by taking data only when the beam current (and hence the counting rate) is within ± 10 percent of a predetermined value. This is accomplished by driving a meter-relay from the integrated output of the ionization chamber beam monitor. If the beam current varies from its original value by more than 10 percent, the meter relay turns off the counting equipment. In practice, the linac beam current is generally stable enough in intensity so that it remains well within the ± 10 percent limits. Under these conditions, the second-order dead time correction is negligible.

We have verified these expectations experimentally, primarily by running at different neutron counting rates and by recording "flat" timing spectra from radioactive sources at counting rates equivalent to those obtained under actual running conditions. We find that these large corrections can be made very accurately and introduce negligibly small errors in the final result. This is further verified by the good agreement between thick and thin sample measurements.

By using thick samples and counting at relatively high rates, in ~ 50 hours of running time the statistical errors are approximately 2 percent over most of the 3500 channels.

A7.3. Inscattering

The good geometry which is intrinsic in a time-of-flight experiment almost automatically insures that the inscattering correction will be small.

The fractional change in the total cross section, $\frac{\Delta\sigma_t}{\sigma_t}$, due to inscattering is given by [15]:

$$\frac{\Delta\sigma_t}{\sigma_t} = \left[\frac{r_1 r_2}{r_3}\right]\left[\frac{\sigma(0)}{\sigma_t}\right][f(n\sigma)]$$

where

r_1 is the sample-to-source solid angle,
r_2 is the detector-to-sample solid angle,
r_3 is the detector-to-source solid angle,
$\sigma(0)$ is the scattering cross section at 0°, in b/sr.

In our case, the first term in brackets (called the "inscattering index" by Foster and Glasgow [16]) equals 2×10^{-4} for our 5-cm diameter samples. The second term is generally 0.5 or less. The last term, which is essentially a multiple scattering correction to the in-scattering varies between 1 and 3 for the sample thicknesses used in these measurements. Hence, the overall in-scattering correction would be approximately 10^{-4}, and is, therefore, generally ignored.

A8. Summary

In the appendix we have described the NBS system for making accurate total cross section measurements in the MeV energy region, the main body of this Monograph consisting of detailed curves of the cross sections measured with this system. In future publications we will discuss some of these measurements in detail, and make comparisons with results from other laboratories.

We should like to thank Julian Whittaker for his inestimable contributions to the electronics and instrumentation. It is very doubtful that this program would have succeeded without his active assistance.

A9. References

[1] Schwartz, R. B., Schrack, R. A., and Heaton, H. T., II, Proc. Symp. Neutron Standards and Flux Normalization, AEC CONF-701002, Argonne, Illinois, p. 377 (Oct. 21, 1970).
[2] Leiss, J. E., Proc. 1966 Linear Accelerator Conf., Los Alamos, New Mexico, p. 20 (Sept. 1966).
[3] Whittaker, J. K., IEEE Trans. on Nuclear Science NS-13, No. 1, 399 (1966).
[4] Whittaker, J. K., Nucl. Instr. and Meth. 45, 138 (1966).
[5] Morton, G. A., Smith, H. M., and Wasserman, R., IEEE Trans. Nucl. Sci. NS-14, No. 1, 443 (1967); Shin, Y. M., Ku, S. H., Glavina, C., and Rawlins, J. A., Nucl. Instr. and Meth. 58, 353 (1968).
[6] Farinelli, U., and Malvano, R., Rev. Sci. Instr. 29, 699 (1958).
[7] Schrack, R. A., Heaton, H.T. II, and Schwartz, R. B., Nucl. Instr. and Meth. 77, 175 (1970).
[8] Davis, J. C., and Noda, F. T., Nucl. Phys. A134, 361 (1969).
[9] Broberg, J. B., IEEE Trans. Nucl. Sci. NS-13, No. 1, 192 (1966); Wyckoff, J. M., loc. cit. 199.
[10] Heaton, H. T., II, Nat. Bur. Stand. (U.S.) Tech. Note 515, 31 pages (Jan. 1970).
[11] Pruitt, J. S., and Domen, S. R., Nat. Bur. Stand. (U.S.) Monogr. 48, 18 pages (June 1952).
[12] Miller, D. W., Fast Neutron Physics, Part II, Chapter V. A., p. 985, J. B. Marion and J. L. Fowler, Eds. (Interscience Publishers, New York, 1963).
[13] Rose, M. E., and Shapiro, M. M., Phys. Rev. 74, 1853 (1948).
[14] Bollinger, L. M., and Thomas, G. E., Rev. Sci. Instr. B2, 1044 (1961); Kirkbride, J., Yates, E. C., and Crandall, D. G., Nucl. Instr. and Meth. 52, 293 (1967).
[15] Bratenahl, A., Peterson, J. M., and Stoering, J. P., Phys. Rev. 110, 927 (1957).
[16] Foster, D. G., Jr., and Glasgow, D. W., Phys. Rev. C3, 576 (1971).

FORM NBS-114A (1-71)

U.S. DEPT. OF COMM. BIBLIOGRAPHIC DATA SHEET	1. PUBLICATION OR REPORT NO. NBS MN-138	2. Gov't Accession No.	3. Recipient's Accession No.

4. TITLE AND SUBTITLE

MeV Total Neutron Cross Sections

5. Publication Date
January 1974

6. Performing Organization Code

7. AUTHOR(S)
R.B. Schwartz, R.A. Schrack, and H.T. Heaton II

8. Performing Organization

9. PERFORMING ORGANIZATION NAME AND ADDRESS

NATIONAL BUREAU OF STANDARDS
DEPARTMENT OF COMMERCE
WASHINGTON, D.C. 20234

10. Project/Task/Work Unit No.
2410222

11. Contract/Grant No.

12. Sponsoring Organization Name and Address

Same as No. 9.

13. Type of Report & Period Covered
Final

14. Sponsoring Agency Code

15. SUPPLEMENTARY NOTES

16. ABSTRACT (A 200-word or less factual summary of most significant information. If document includes a significant bibliography or literature survey, mention it here.)

This report is a compilation of the MeV neutron total cross section data measured at the National Bureau of Standards over the past several years. The measurements generally span the energy interval from 0.5 to 15 or 20 MeV; data are prosented in graphical form for twelve normally occurring elements, plus the separated isotopes ^{235}U, ^{238}U, and ^{239}Pu. An appendix is included which gives complete details of the experimental technique.

17. KEY WORDS (Alphabetical order, separated by semicolons)

Mev neutrons; neutron time-of-flight; neutron total cross sections.

18. AVAILABILITY STATEMENT

[X] UNLIMITED.

[ ] FOR OFFICIAL DISTRIBUTION. DO NOT RELEASE TO NTIS.

19. SECURITY CLASS (THIS REPORT)
UNCLASSIFIED

20. SECURITY CLASS (THIS PAGE)
UNCLASSIFIED

21. NO. OF PAGES
160

22. Price
$3.60

USCOMM-DC 66244-P71

NBS TECHNICAL PUBLICATIONS

PERIODICALS

JOURNAL OF RESEARCH reports National Bureau of Standards research and development in physics, mathematics, and chemistry. Comprehensive scientific papers give complete details of the work, including laboratory data, experimental procedures, and theoretical and mathematical analyses. Illustrated with photographs, drawings, and charts. Includes listings of other NBS papers as issued.

Published in two sections, available separately:

- **Physics and Chemistry (Section A)**

Papers of interest primarily to scientists working in these fields. This section covers a broad range of physical and chemical research, with major emphasis on standards of physical measurement, fundamental constants, and properties of matter. Issued six times a year. Annual subscription: Domestic, $17.00; Foreign, $21.25.

- **Matnematical Sciences (Section B)**

Studies and compilations designed mainly for the mathematician and theoretical physicist. Topics in mathematical statistics, theory of experiment design, numerical analysis, theoretical physics and chemistry, logical design and programming of computers and computer systems. Short numerical tables. Issued quarterly. Annual subscription: Domestic, $9.00; Foreign, $11.25.

DIMENSIONS, NBS

The best single source of information concerning the Bureau's measurement, research, developmental, cooperative, and publication activities, this monthly publication is designed for the layman and also for the industry-oriented individual whose daily work involves intimate contact with science and technology —*for engineers, chemists, physicists, research managers, product-development managers, and company executives.* Annual subscription: Domestic, $6.50; Foreign, $8.25.

NONPERIODICALS

Applied Mathematics Series. Mathematical tables, manuals, and studies.

Building Science Series. Research results, test methods, and performance criteria of building materials, components, systems, and structures.

Handbooks. Recommended codes of engineering and industrial practice (including safety codes) developed in cooperation with interested industries, professional organizations, and regulatory bodies.

Special Publications. Proceedings of NBS conferences, bibliographies, annual reports, wall charts, pamphlets, etc.

Monographs. Major contributions to the technical literature on various subjects related to the Bureau's scientific and technical activities.

National Standard Reference Data Series. NSRDS provides quantitative data on the physical and chemical properties of materials, compiled from the world's literature and critically evaluated.

Product Standards. Provide requirements for sizes, types, quality, and methods for testing various industrial products. These standards are developed cooperatively with interested Government and industry groups and provide the basis for common understanding of product characteristics for both buyers and sellers. Their use is voluntary.

Technical Notes. This series consists of communications and reports (covering both other-agency and NBS-sponsored work) of limited or transitory interest.

Federal Information Processing Standards Publications. This series is the official publication within the Federal Government for information on standards adopted and promulgated under the Public Law 89–306, and Bureau of the Budget Circular A–86 entitled, Standardization of Data Elements and Codes in Data Systems.

Consumer Information Series. Practical information, based on NBS research and experience, covering areas of interest to the consumer. Easily understandable language and illustrations provide useful background knowledge for shopping in today's technological marketplace.

BIBLIOGRAPHIC SUBSCRIPTION SERVICES

The following current-awareness and literature-survey bibliographies are issued periodically by the Bureau:

Cryogenic Data Center Current Awareness Service (Publications and Reports of Interest in Cryogenics). A literature survey issued weekly. Annual subscription: Domestic, $20.00; foreign, $25.00.

Liquified Natural Gas. A literature survey issued quarterly. Annual subscription: $20.00.

Superconducting Devices and Materials. A literature survey issued quarterly. Annual subscription: $20.00. Send subscription orders and remittances for the preceding bibliographic services to the U.S. Department of Commerce, National Technical Information Service, Springfield, Va. 22151.

Electromagnetic Metrology Current Awareness Service (Abstracts of Selected Articles on Measurement Techniques and Standards of Electromagnetic Quantities from D-C to Millimeter-Wave Frequencies). Issued monthly. Annual subscription: $100.00 (Special rates for multi-subscription). Send subscription order and remittance to the Electromagnetic Metrology Information Center, Electromagnetics Division, National Bureau of Standards, Boulder, Colo. 80302.

Order NBS publications (except Bibliographic Subscription Services) from: Superintendent of Documents, Government Printing Office, Washington, D.C. 20402.

U.S. DEPARTMENT OF COMMERCE
National Bureau of Standards
Washington, D.C. 20234

OFFICIAL BUSINESS

Penalty for Private Use, $300

POSTAGE AND FEES PAID
U.S. DEPARTMENT OF COMMERCE
COM-215